

ABSTRACT

Title of Document: SMALL MOLECULE ACTIVATION AND
ATOM AND GROUP TRANSFER
REACTIONS MEDIATED BY MID VALENT
GROUP 6 'CPAM' COMPOUNDS

Wesley Scott Farrell, Doctor of Philosophy,
2015

Directed By: Professor Lawrence R. Sita, Department of
Chemistry and Biochemistry

The use of organometallic compounds to activate small molecules (e.g. CO₂, N₂, N₂O, O₂, etc.) has long been of significant scientific interest. Described here is the synthesis and characterization of mid valent group 6 compounds supported by the pentamethylcyclopentadienyl, amidinate (CpAm) ligand framework, along with their ability to not only activate small molecules that are inexpensive, abundant, and/or hazardous, but use them to generate many value added products under mild conditions. Sulfur atom transfer (SAT) was employed to catalytically prepare carbonyl sulfide and isothiocyanates from elemental sulfur. In the case of carbonyl sulfide, this process was able to be performed in the presence of primary amines, allowing for the isolation of symmetric ureas, and in the case of isothiocyanates, the reaction was successful in the presence of benzhydrazide to allow for the isolation of aroylthiosemicarbazides in good yields. Molecular oxygen was found to afford high valent dioxo species which were

inactive towards oxygen atom transfer (OAT). However, OAT was achieved for the catalytic deoxygenation of sulfoxides. Dinitrogen fixation has previously been discovered by our group to afford -ER_3 ($\text{E} = \text{C}, \text{Si}, \text{Ge}$) derivatized isocyanates through [2+1] cycloaddition of CO. Reported here is an extension of this work to include N_2 fixation with concomitant reduction of the greenhouse gas CO_2 to prepare the same isocyanates *via* [2+2] cycloaddition of CO_2 . Furthermore, the completion of several efficient N_2 fixation synthetic cycles through two distinct pathways is discussed. Additionally, given the tremendous impact of high valent group 6 alkylidene compounds to catalyze olefin metathesis reactions, the synthesis of mid valent CpAm group 6 alkylidenes was a challenging, yet attractive target. Attempts to isolate such compounds are presented, along with descriptions of the products obtained and their reactivity towards small molecules.

SMALL MOLECULE ACTIVATION AND ATOM AND GROUP TRANSFER
REACTIONS MEDIATED BY MID VALENT GROUP 6 ‘CPAM’ COMPOUNDS

By

Wesley Scott Farrell

Thesis submitted to the Faculty of the Graduate School of the
University of Maryland, College Park, in partial fulfillment
of the requirements for the degree of
Doctor of Philosophy
2015

Advisory Committee:

Professor Lawrence R. Sita, Chair

Professor Bryan W. Eichhorn

Professor Andrei N. Vedernikov

Professor Timothy H. Warren

Professor Ichiro Takeuchi, Dean’s Representative

© Copyright by
Wesley Scott Farrell
2015

Dedicated to my beautiful wife, Elise, without whom the completion of the writing of this thesis, and the work described herein, would not have been possible.

“Nothing in the world can take the place of persistence. Talent will not; nothing is more common than unsuccessful men with talent. Genius will not; unrewarded genius is almost a proverb. Education will not; the world is full of educated derelicts. Persistence and determination alone are omnipotent.”

Calvin Coolidge
30th President of the United States of America

Acknowledgements

I would like to use these pages to briefly acknowledge and thank the people who have made the completion of the research described in this thesis possible. First, I must thank my advisor, Prof. Sita, for his assistance, guidance, and constant support over the past five years. Not only has Dr. Sita taught me an extraordinary amount regarding the chemistry of organometallics, he has helped me learn how to be a successful scientist, and his passion for chemistry and science generally has been nothing short of invigorating. I also wish to thank Prof. Vedernikov and Prof. Davis for their support in applying for fellowships over the past several years.

There are several staff members of the Department of Chemistry and Biochemistry who have played instrumental roles in the execution of this research. Dr. Peter Zavalij provided all of the crystal structures reported in this thesis, and many others which do not appear. I am very grateful for his great work, fast service, and constant willingness to help. I would like to thank Dr. Yiu-Fai Lam and Dr. Yinde Wang for their assistance with the collection of NMR data, for the wonderful job they do in maintaining our great NMR facilities, and their excitement to teach me new techniques. I thank Mr. Scott Taylor for maintaining the department's FTIR, and Dr. Yue Li for his help with MS. Finally, I wish to acknowledge Mr. Bill Griffin and Mr. Levi Gayatao for maintaining a constant supply of nitrogen and argon for our lab, and for their help obtaining supplies necessary to conduct this research.

I am thankful for all the members of the Sita Group, both past and present, for their friendship and camaraderie, and for making our lab a great place to work. In

particular, I wish to thank Dr. Brendan Yonke for his guidance getting started in the lab during my first year, and for all of his help thereafter. Brendan also made several seminal discoveries which laid the groundwork for the results presented in Chapter 4. I thank Kaitlyn Crawford for her support as we both simultaneously worked on writing our theses and applying for jobs side by side in the materials lab. Lastly, I am very thankful to have had the opportunity to work along side Andrew Keane throughout our graduate school careers. Andrew and I have worked closely together over the past several years, and have had many late nights together either working in lab, or talking chemistry and identifying solutions to current roadblocks or the next problems to tackle. More importantly, however, Andrew has been a great friend, and I wish him the best as he begins the next step in his career.

I would not be in a position to write this thesis if it were not for the support of my family. I thank my parents for supporting my education from a very young age all the way to graduate school. They provided me with every tool I needed along the way to be where I am today, and always encouraged my natural curiosity. I also learned many valuable lessons from them, most importantly that nothing comes easy in life, but that anything is possible with hard work.

I would be remiss if I did not acknowledge the contribution of my two wonderful, yet crazy dogs, Ponce and Yoshi, who can always put a smile on my face at the end of a long day. And lastly, I would not be where I am today without my best friend and wonderful wife, Elise. There truly are no words that can fully describe the support she has given me that has allowed for the completion of this thesis.

Table of Contents

| | |
|--|------|
| Dedication..... | ii |
| Acknowledgements..... | iv |
| Table of Contents..... | vi |
| List of Figures..... | viii |
| List of Schemes..... | x |
| List of Abbreviations..... | xii |
| Chapter 1: The Use of Organometallic Compounds in the ‘Green’ Synthesis of Commodity Chemicals..... | 1 |
| 1.1 Introduction..... | 1 |
| 1.2 Activation and Fixation of Carbon Dioxide..... | 2 |
| 1.2.1 Coordination of CO ₂ | 3 |
| 1.2.2 CO ₂ as a Reagent..... | 7 |
| 1.3 Activation and Fixation of Dinitrogen..... | 10 |
| 1.3.1 Group 4 Metallocenes..... | 11 |
| 1.3.2 Group 6 Dinitrogen Compounds..... | 15 |
| 1.3.3 Molybdenum Catalyzed NH ₃ Synthesis..... | 17 |
| 1.4 CpAm Ligand Framework..... | 19 |
| 1.4.1 Cyclopentadienyl Ligand and Metallocene Environment..... | 20 |
| 1.4.2 Amidinate Ligands and Bisamidinate Environment..... | 21 |
| 1.4.3 Cyclopentadienyl/Amidinate Ligand Framework..... | 22 |
| 1.5 References..... | 26 |
| Chapter 2: Oxygen Atom Transfer Reactions Mediated by Group 6 CpAm Compounds..... | 30 |
| 2.1 Introduction..... | 30 |
| 2.2 CpAm M(VI) Dioxo Compounds for OAT Reactions..... | 32 |
| 2.2.1 Background..... | 32 |
| 2.2.2 Synthesis and Characterization of CpAm M(VI) Group 6 Dioxo Compounds..... | 33 |
| 2.2.3 OAT Reactions of CpAm M(VI) Dioxo Compounds..... | 36 |
| 2.3 Catalytic Sulfoxide Deoxygenation..... | 41 |
| 2.3.1 Background..... | 41 |
| 2.3.2 Reactivity of CpAm Compounds with Sulfoxides..... | 42 |
| 2.4 Conclusion..... | 46 |
| 2.5 References..... | 47 |
| Chapter 3: Catalytic Sulfur Atom Transfer Reactions Employing Elemental Sulfur..... | 49 |
| 3.1 Introduction..... | 49 |
| 3.2 Carbonyl Sulfide..... | 51 |
| 3.2.1 Background..... | 51 |
| 3.2.2 Synthesis and Characterization of New Compounds and SAT Reactions..... | 53 |
| 3.2.3 ‘On-Demand’ COS Production..... | 67 |
| 3.3 Isothiocyanates..... | 70 |
| 3.3.1 Background..... | 70 |

| | |
|---|-----|
| 3.3.2 Synthesis and Characterization of New Compounds and SAT Reactions | 71 |
| 3.3.3 'On-Demand' Isothiocyanate Synthesis | 77 |
| 3.4 C=S Bond Cleavage Reactions | 79 |
| 3.4.1 CS ₂ Activation | 80 |
| 3.4.2 Isothiocyanate Activation | 83 |
| 3.5 Conclusion | 85 |
| 3.6 References | 86 |
| Chapter 4: Complete Synthetic Cycles for the Generation of –ER ₃ Derivatized Isocyanates through Dinitrogen Fixation | 90 |
| 4.1 Introduction | 90 |
| 4.2 Synthesis of CpAm Mono(Carbonyl) Compounds Bearing Labile Ligands | 97 |
| 4.2.1 Background | 97 |
| 4.2.2 L = Sulfide | 101 |
| 4.2.3 L = Olefin – Part 1 | 107 |
| 4.2.4 L = Olefin – Part 2 | 115 |
| 4.3 Tandem Dinitrogen and Carbon Dioxide Fixation | 120 |
| 4.3.1 Background | 120 |
| 4.3.2 Reactivity of Terminal Oxo Compounds | 120 |
| 4.3.3 Synthetic Cycle for N ₂ Fixation | 123 |
| 4.3.4 [2+2] Cycloadditions of CpAm Imido Complexes | 127 |
| 4.4 Conclusion | 132 |
| 4.5 References | 134 |
| Chapter 5: Synthesis, Stability, and Reactivity of Mid Valent Group 6 Alkyl, Alkylidene, and Alkylidyne Complexes | 137 |
| 5.1 Introduction | 137 |
| 5.2 Molybdenum | 139 |
| 5.3 Tungsten | 144 |
| 5.4 Conclusion | 147 |
| 5.5 References | 148 |
| Chapter 6: Summary and Outlook | 151 |
| Appendix: Experimental Procedures | 155 |

List of Figures

| | |
|---|-----|
| Figure 1. Small Molecules and their structures, bond dissociation energies, and abundance in Earth's atmosphere. | 1 |
| Figure 2. (A) Structural and physical properties of CO ₂ . (B) Diagram of CO ₂ LUMO..... | 3 |
| Figure 3. Representation of orbital overlap resulting in decrease of C-O bond order in η^1 -CO ₂ complex 2 | 5 |
| Figure 4. Common bonding motifs for N ₂ coordination..... | 10 |
| Figure 5. Structure of the active site of the nitrogenase enzyme..... | 11 |
| Figure 6. General structure of Nishibayashi's N ₂ reduction catalyst (36) and Schrock's N ₂ reduction catalyst (37) | 17 |
| Figure 7. Structure of early transition metal 'bent' metallocenes with oxidation states and d electron counts | 20 |
| Figure 8. Structure of early transition metal bisamidinate compounds with oxidation states and d electron counts..... | 21 |
| Figure 9. Possible coordination modes of amidinate ligands..... | 22 |
| Figure 10. Structure of early transition metal CpAm compounds with oxidation states and d electron counts | 23 |
| Figure 11. N ₂ activation within early transition metal CpAm complexes | 25 |
| Figure 12. Molecular structure of 55 | 35 |
| Figure 13. Crude ¹ H NMR spectrum of 58 | 37 |
| Figure 14. ¹ H NMR spectra demonstrating the production of compound 48 from reaction of 40 and 54 | 40 |
| Figure 15. NMR spectra demonstrating OAT catalyzed by compound 44 | 45 |
| Figure 16. ¹³ C{ ¹ H} NMR spectra demonstrating catalytic SAT from S ₈ to CO | 55 |
| Figure 17. ¹ H NMR spectra recorded during catalytic SAT from S ₈ to CO | 56 |
| Figure 18. Molecular structure of 70 | 58 |
| Figure 19. Crude ¹ H NMR spectrum of 71 obtained from reaction of 70 with S ₈ | 59 |
| Figure 20. Molecular structure of 71 | 59 |
| Figure 21. ¹ H NMR spectra demonstrating the photolytic conversion of 71 to 75 at timed intervals..... | 61 |
| Figure 22. Molecular structure of 75 | 62 |
| Figure 23. Molecular structure of <i>trans</i> - 77 | 64 |
| Figure 24. ESI-MS of reaction mixture in the synthesis of 77 | 65 |
| Figure 25. Molecular structure of 80 | 72 |
| Figure 26. ¹ H NMR spectra demonstrating the catalytic production of ^t BuNCS from ^t BuNC and S ₈ mediated by 81 | 73 |
| Figure 27. Molecular structure of 84 | 75 |
| Figure 28. Molecular structure of 91 | 82 |
| Figure 29. Molecular structures of 93 and 94 | 84 |
| Figure 30. ¹ H NMR spectra demonstrating the synthesis of 115 | 102 |
| Figure 31. Molecular structure of 115 | 105 |
| Figure 32. Partial ¹³ C{ ¹ H} NMR spectra of 115 and 117 | 106 |
| Figure 33. Molecular structures of 118 and 120 | 110 |

| | |
|--|-----|
| Figure 34. Molecular structures of 119 and 121 | 111 |
| Figure 35. Molecular structure of 123 | 112 |
| Figure 36. NMR spectra of 127 | 116 |
| Figure 37. Molecular structure of 127 | 118 |
| Figure 38. Variable temperature ^1H NMR spectra of 128 | 119 |
| Figure 39. ^1H NMR spectra demonstrating the reactivity of 44 with excess TMSCl , CO_2 , and UV irradiation | 123 |
| Figure 40. Representative ^1H NMR spectra for N_2/CO_2 fixation cycle | 126 |
| Figure 41. Molecular structures of 140 and 141 | 140 |
| Figure 42. Molecular structure of 124 | 146 |

List of Schemes

| | |
|--|----|
| Scheme 1. Synthesis of first η^1 -CO ₂ compounds | 4 |
| Scheme 2. Synthesis of early η^2 -CO ₂ compounds..... | 6 |
| Scheme 3. CO ₂ in the palladium catalyzed synthesis of β,γ -unsaturated carboxylic acids | 7 |
| Scheme 4. Mechanism of CO ₂ /epoxide copolymerization..... | 9 |
| Scheme 5. Nitrogenase catalyzed synthesis of NH ₃ | 11 |
| Scheme 6. N ₂ activation by titanocene | 12 |
| Scheme 7. N ₂ activation by decamethyl/octamethyl zirconocenes | 13 |
| Scheme 8. CO induced N-N bond cleavage within group 4 metallocenes..... | 14 |
| Scheme 9. Thermal N-N bond cleavage by Mo[N(R)Ar] ₃ | 15 |
| Scheme 10. Synthetic N ₂ fixation cycle for synthesis of nitriles | 16 |
| Scheme 11. Schrock cycle for NH ₃ synthesis | 19 |
| Scheme 12. Use of compounds 40 and 41 as M(II) synthons | 30 |
| Scheme 13. Dynamic ‘ring-flipping’ of amidinate ligand..... | 33 |
| Scheme 14. Synthesis of compounds 54 and 55 | 34 |
| Scheme 15. Ring slip of Cp* ligand in dioxo compounds | 36 |
| Scheme 16. Decomposition of compounds 54 and 55 and reaction of compound 59 with O ₂ | 38 |
| Scheme 17. Oxidation of compound 40 by 54 | 39 |
| Scheme 18. OAT from MPSO to compounds 40 and 41 | 42 |
| Scheme 19. Photolytic reaction of compounds 44 and 45 with MPSO..... | 43 |
| Scheme 20. Catalytic cycle for OAT from MPSO to CO | 44 |
| Scheme 21. Catalytic SAT mediated by compound 63 | 50 |
| Scheme 22. Thermal synthesis of COS | 52 |
| Scheme 23. Synthesis of group 5 η^2 -COS compounds..... | 52 |
| Scheme 24. Synthesis of compounds 56 and 68 | 54 |
| Scheme 25. Synthesis of compounds 70 and 71 | 57 |
| Scheme 26. Synthesis of compound 72 | 60 |
| Scheme 27. Photolytic isomerization of compound 71 to 75 | 61 |
| Scheme 28. Synthesis of compound 77 | 63 |
| Scheme 29. Thermal reactivity of compound 77 with ¹³ CO | 66 |
| Scheme 30. Relationship between compounds 71 , 75 , and 77 in photocatalytic synthesis of COS from CO and S ₈ | 67 |
| Scheme 31. ‘On-Demand’ synthesis of COS for the production of ureas..... | 68 |
| Scheme 32. Synthesis of compounds 80 – 82 | 71 |
| Scheme 33. Synthesis of compounds 83 – 85 | 74 |
| Scheme 34. Mechanism for catalytic SAT in the synthesis of isothiocyanates | 77 |
| Scheme 35. ‘On-Demand’ synthesis of COS for the production of aroylthiosemicarbazides..... | 78 |
| Scheme 36. CS ₂ activation by compound 31 | 79 |
| Scheme 37. CS ₂ activation by compound 56 and subsequent reactivity | 81 |
| Scheme 38. <i>tert</i> -Butyl isothiocyanate activation by compound 56 and subsequent reactivity | 83 |

| | |
|---|-----|
| Scheme 39. Photolytic N ₂ cleavage by compound 98 | 92 |
| Scheme 40. Photolytic N ₂ cleavage by compound 102 and subsequent reactivity ... | 93 |
| Scheme 41. Photolytic cleavage of N ₂ by compounds 40 and 41 | 94 |
| Scheme 42. Synthesis of M(IV) imido complexes <i>via</i> photolytic N ₂ fixation | 95 |
| Scheme 43. Incomplete synthetic cycle for N ₂ fixation | 96 |
| Scheme 44. Observed and proposed interconversion of compounds 40 and 41 with 44 and 45 | 98 |
| Scheme 45. Photolytic reactivity of compound 113 | 99 |
| Scheme 46. Proposed regeneration of compounds 40 and 41 from M(CO)(L) precursors..... | 100 |
| Scheme 47. Synthesis of compound 115 | 103 |
| Scheme 48. Synthesis of proposed compound 117 | 105 |
| Scheme 49. Synthesis of M(CO)(olefin) compounds..... | 108 |
| Scheme 50. Synthesis of compound 124 from photolysis of 120 | 114 |
| Scheme 51. Synthesis of compound 41 from photolysis of 121 | 114 |
| Scheme 52. Synthesis of C-H activation compounds 127 and 128 | 117 |
| Scheme 53. Photolytic reactivity of compounds 44 and 45 towards CO ₂ | 120 |
| Scheme 54. Reactivity of metallocene oxo compounds towards TMSCl | 121 |
| Scheme 55. Synthesis of compounds 42 and 108 from 48 and 49 | 122 |
| Scheme 56. Synthesis of compound 42 from 44 | 122 |
| Scheme 57. Synthetic cycle for N ₂ /CO ₂ fixation for the synthesis of –ER ₃ derivatized isocyanates | 124 |
| Scheme 58. [2+2] cycloaddition to produce imido complexes from oxos | 127 |
| Scheme 59. Synthesis of compound 48 <i>via</i> [2+2] cycloaddition of CO ₂ | 129 |
| Scheme 60. ‘One-pot’ reaction to produce compound 42 from 111 and 113 | 130 |
| Scheme 61. Shortened synthetic cycle for N ₂ /CO ₂ fixation for the synthesis of –ER ₃ derivatized isocyanates | 132 |
| Scheme 62. Synthesis of Schrock’s tantalum alkylidene | 137 |
| Scheme 63. Synthesis of compounds 140 and 141 | 139 |
| Scheme 64. Mechanism for the formation of 140 and 141 | 141 |
| Scheme 65. Mechanism of ethene dimerization..... | 143 |
| Scheme 66. Synthesis and mechanism of compound 124 | 144 |
| Scheme 67. Reaction of 124 with nitriles to form compounds 144 – 147 | 147 |

List of Abbreviations

| | |
|-------------------|---|
| ° | degree |
| Å | angstrom |
| atm | atmosphere |
| BDE | bond dissociation energy |
| BHE | beta-hydride elimination |
| cm ⁻¹ | wavenumbers (inverse centimeters) |
| COS | carbonyl sulfide |
| Cp* | pentamethylcyclopentadienyl |
| CpAm | pentamethylcyclopentadienyl, amidinate |
| Cy | cyclohexyl |
| d | days |
| DMF | dimethyl formamide |
| dmpe | 1,2-Bis(dimethylphosphino)ethane |
| e ⁻ | electron |
| ESI-MS | electrospray ionization mass spectrometry |
| Et | ethyl |
| Et ₂ O | diethyl ether |
| eq | equivalent |
| h | hours |
| HMDSO | hexamethyldisiloxane |
| ⁱ Pr | isopropyl |
| IR | infrared (spectroscopy) |
| LUMO | lowest occupied molecular orbital |
| MPSO | methyl phenyl sulfoxide |
| NaHg | 0.5% (w/w) sodium amalgam |
| NMR | nuclear magnetic resonance (spectroscopy) |
| OAT | oxygen atom transfer |
| OTf | trifluoromethanesulfonate |
| Ph | phenyl |
| ppm | parts per million |
| ppt | parts per trillion |
| psi | pounds per square inch |
| SAT | sulfur atom transfer |
| ^t Bu | <i>tert</i> -butyl |
| THF | tetrahydrofuran |
| TMG | trimethylgermyl |
| TMS | trimethylsilyl |
| UV | ultraviolet |
| vs. | versus |
| XRD | X-ray diffraction |

Chapter 1: The Use of Organometallic Compounds in the ‘Green’ Synthesis of Commodity Chemicals

1.1 Introduction

At the heart of modern organometallic chemistry is the pursuit of new compounds which mediate the (catalytic) generation of either i) new molecules which, without the assistance of organometallic complexes, could not be otherwise synthesized, or ii) known molecules through reactions which are considerably more energy efficient and environmentally friendly than those currently employed. Accordingly, research in organometallic chemistry has enjoyed a long and rich history, the impacts of which are innumerable. Today the outcomes of this field continue to be recognized at the highest levels of science, with three Nobel Prizes being awarded to researchers in the field of organometallic chemistry thus far in the 21st century (2001, 2005, and 2010).¹

Of particular current interest is the use of organometallic compounds to activate small molecules which are i) highly abundant in the atmosphere (in the case

| Small Molecule | Dinitrogen | Carbon Dioxide | Dioxygen | Methane |
|-------------------------------------|--------------------------|------------------------------|---------------------|---|
| Structure | $\text{N}\equiv\text{N}$ | $\text{O}=\text{C}=\text{O}$ | $\text{O}=\text{O}$ | $\begin{array}{c} \text{H} \\ \\ \text{H}-\text{C}-\text{H} \\ \\ \text{H} \end{array}$ |
| BDE (kcal/mol) | 226 (N-N) | 127.2 (C-O) | 119.12 (O-O) | 102.7 (C-H) |
| Abundance in Earth's Atmosphere (%) | 78 | 0.04 | 21 | 0.00018 |

Figure 1. Small Molecules and their structures, bond dissociation energies,² and abundance in Earth's atmosphere.

of gasses) or within the Earth herself (in the case of solids or liquids), and/or ii) threats to the long term stability of Earth's climate, and utilize them for the generation of valuable chemicals of biological or commercial importance. Examples of some of the most commonly targeted small molecules are depicted in Figure 1.² Typically, these molecules are inert towards activation without the assistance of organometallic reagents given the presence of strong multiple bonds, which prevent using them in a productive manner. Representative examples regarding the activation and utilization of several important small molecules by organometallic complexes under mild conditions are provided in the following sections, along with appropriate historical contexts, and will be the focus of the original research presented in this thesis.

1.2 Activation and Fixation of Carbon Dioxide

Carbon dioxide (CO₂) is an essential component of Earth's atmosphere, as it plays a key role in the carbon cycle. The impact of human activity on atmospheric CO₂ concentration since the industrial revolution has recently come under intense scrutiny, however, as its role as a greenhouse gas has become more obvious. Human technology which most take for granted, such as transportation, manufacturing, and electricity, account for nearly 85% of current global CO₂ emissions.³ The expansion of industries which provide these and other services has lead to dramatic increases in atmospheric CO₂ concentration (396.0 ± 0.1 ppm in 2013, 142% pre-industrial concentration),⁴ increasing the risk of negative consequences from human caused climate change. The effect is accelerated as natural CO₂ sinks, such as forests, are simultaneously diminished by human activity as well. Although extensive efforts

have been undertaken by nations across the globe to develop technology that reduces emissions of CO₂, as well as all other greenhouse gasses, another, perhaps more attractive approach involves using CO₂ as a C₁ source for the preparation of myriad organic molecules. The primary requirement for successful CO₂ (or any other small molecule) fixation is first the activation, or weakening, of the inert bonds. Accordingly, this has driven many to investigate the ability of transition metals to coordinate CO₂ and study subsequent reactivity, and the topic has been the subject of many reviews over the years.⁵⁻¹⁰

1.2.1 Coordination of CO₂

The CO₂ molecule is rather simple, but its properties must be fully understood in order to properly address its chemistry (Figure 2). It consists of three atoms oriented in a linear geometry. The large difference in electronegativity between oxygen and carbon results in a significant partial positive charge on the central carbon atom, and partial negative charges on the oxygen atoms, however overall the molecule is nonpolar. It consists of two π orbitals which are orthogonal to one

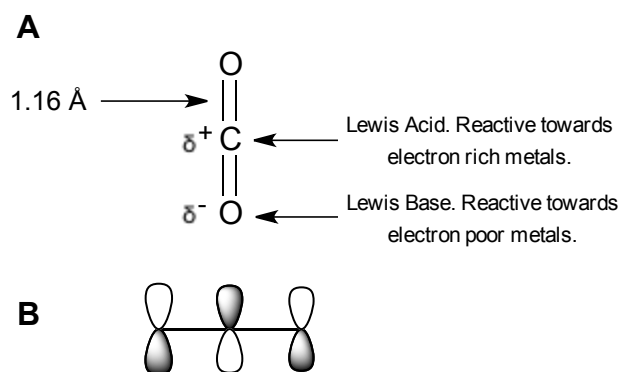
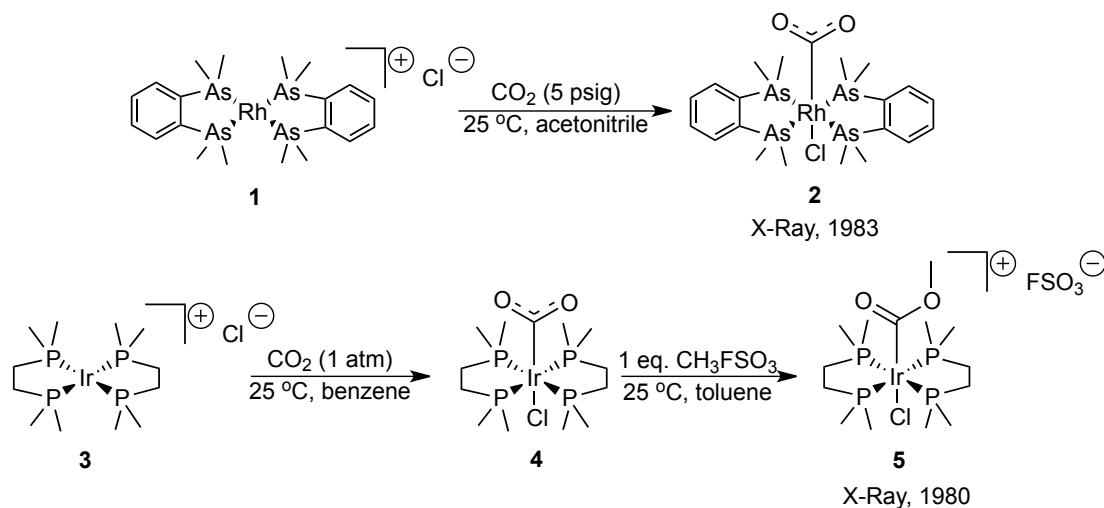


Figure 2. (A) Structural and physical properties of CO₂.
(B) Diagram of CO₂ LUMO.

another, and the lowest unoccupied molecular orbital (LUMO) of CO₂ is the π^* orbital. Orbital overlap and π -backbonding to the π^* orbital is key in coordination of CO₂ (and other small molecules for that matter) to transition metal centers, as will be seen below. Together, these properties allow for several types of coordination of CO₂ to transition metals, however for mononuclear complexes only two are commonly observed.^{8,9}

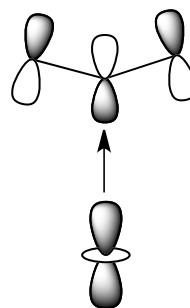
The central carbon atom of CO₂ is very Lewis acidic, however coordination solely through the central carbon atom in a η^1 fashion is possible if the metal center is sufficiently Lewis basic, typically as a result of strongly electron donating ligands. The first structurally characterized η^1 -CO₂ complex was reported by Herskovitz in 1983.¹¹ In this work, a 16 electron rhodium (I) complex bearing two *o*-phenylene-bis(dimethylarsine) (diars) ligands and a chloride counter ion [(diars)₂Rh]Cl (**1**) was exposed to a low pressure of CO₂, which precipitated the new CO₂ compound [(diars)₂ClRh(η^1 -CO₂)] (**2**) within hours (Scheme 1). Compound **2** exhibited pseudo-octahedral geometry about the rhodium center and re-coordination of the chloride

Scheme 1



counter ion. The carbon-oxygen bond lengths were observed to be increased significantly from those of free CO₂ [i.e. $d(\text{CO}) = 1.16 \text{ \AA}$ (CO₂), average $d(\text{CO}) = 1.23 \text{ \AA}$ (**2**)] and the O-C-O bond angle was found to be decreased far from linearity (126°). Both observations result from significant electron density donation to the π^* orbital of CO₂, presumably from the d_z^2 orbital of the rhodium center (Figure 3).

The heavier group 9 analog of compound **1** bearing 1,2-bis(dimethylphosphino)ethane (dmpe) ligands, [(dmpe)₂Ir]Cl (**3**), had previously been reported by the same researchers and was thought to react with CO₂ in the same manner to



yield [(dmpe)₂Ir(η^1 -CO₂)Cl] (**4**), but they were unable to confirm the η^1 coordination of CO₂ through X-ray analysis.¹² Given the similar

Figure 3. Representation of orbital overlap resulting in decrease of C-O bond order in η^1 -CO₂ complex **2**.

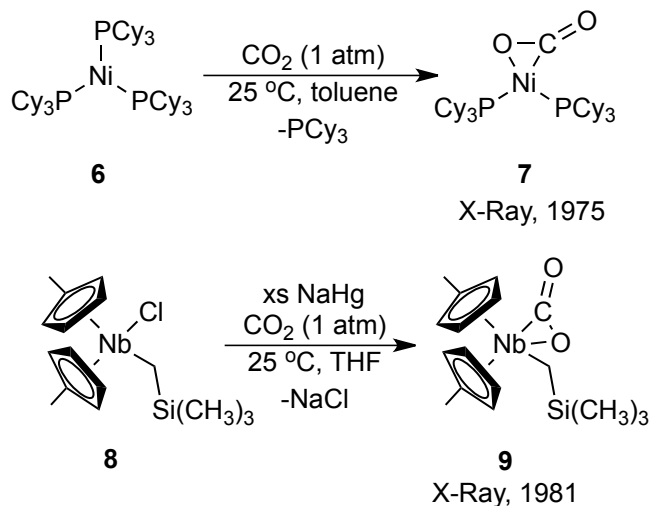
electronics and ligand environment, it was likely that the same coordination mode was in fact employed. Accordingly, the oxygen atoms on **4** were found to be sterically accessible and very nucleophilic, allowing for C-O bond formation on previously inert CO₂ through the addition of methyl fluorosulfate (CH₃FSO₃), a cationic methylating reagent, thus generating the cationic iridium methoxycarbonyl complex [(dmpe)₂Ir(CO₂Me)Cl]FSO₃ (**5**) (Scheme 1).¹³

More common than η^1 coordination through the central carbon atom is the η^2 coordination mode in which the CO₂ molecule bonds to the metal in a κ -C,O fashion. This leads to donation of electron density from a filled π orbital into an empty metal d orbital of appropriate symmetry with simultaneous π -backbonding to the π^* orbital of

CO₂ (similar to Dewar-Chatt-Duncanson model for alkene coordination).^{8,9} The result is a significant decrease in bond order.

The first η^2 -CO₂ complex structurally characterized was synthesized by Aresta and coworkers in 1975 by treatment of (PCy₃)₃Ni (**6**) with CO₂ to yield [(PCy₃)₂Ni(η^2 -CO₂)] (**7**) (Scheme 2).¹⁴ In 1981 the first structurally characterized early transition metal (i.e. group 3 – 7) η^2 -CO₂ complex was reported by Lappert and coworkers.¹⁵ As will become clear in subsequent chapters and sections, early transition metals have played a dominant role in small molecule activation due to their reducing nature, allowing for significant π -backbonding. Typically, these metal compounds require chemical reduction of a high valent metal halide precursor to perform small molecule activation, and may often be supported by two derivatized cyclopentadienyl ligands, referred to as a metallocene. Accordingly, the metallocene

Scheme 2



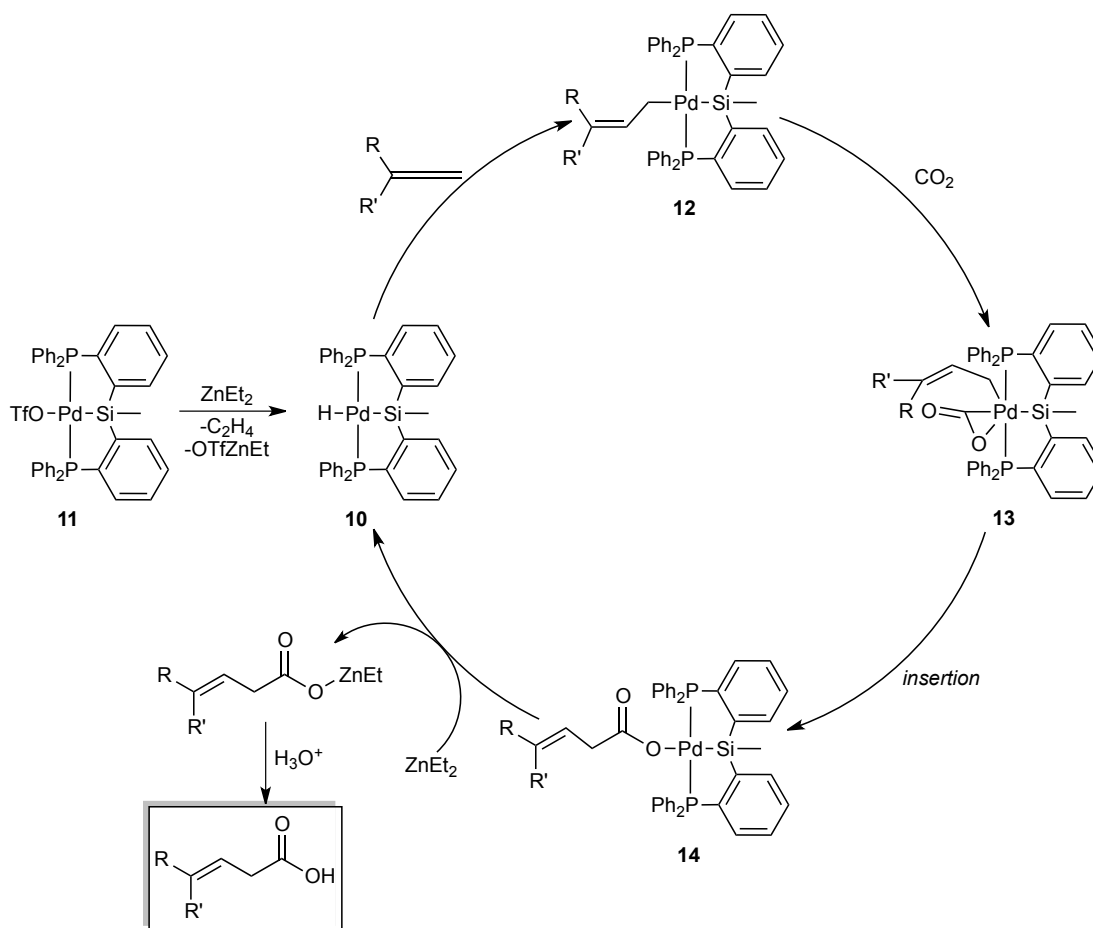
niobium (IV) chloride species $\{[\eta^5\text{-C}_5\text{H}_4(\text{CH}_3)]_2[\text{CH}_2\text{Si}(\text{CH}_3)_3]\text{NbCl}\}$ (**8**) was reduced with excess equivalents of sodium amalgam (NaHg) in the presence of CO₂

to yield $\{[\eta^5\text{-C}_5\text{H}_4(\text{CH}_3)]_2[\text{CH}_2\text{Si}(\text{CH}_3)_3]\text{Nb}(\eta^2\text{-CO}_2)\}$ (**9**) (Scheme 2). As would be expected, the O-C-O bond angle in **9** is significantly smaller than 180° (132°), and both C-O bond lengths are longer than in free CO_2 [$d(\text{CO})_{\text{coord}} = 1.283 \text{ \AA}$, $d(\text{CO})_{\text{noncoord}} = 1.216 \text{ \AA}$], indicative of significant π -backbonding to CO_2 .¹⁵

1.2.2 CO_2 as a Reagent

As a result of the seminal discoveries described in the previous section and the many studies which would soon follow, organometallic compounds for nearly all the transition metals, and even several main group metals, are now known to generate

Scheme 3



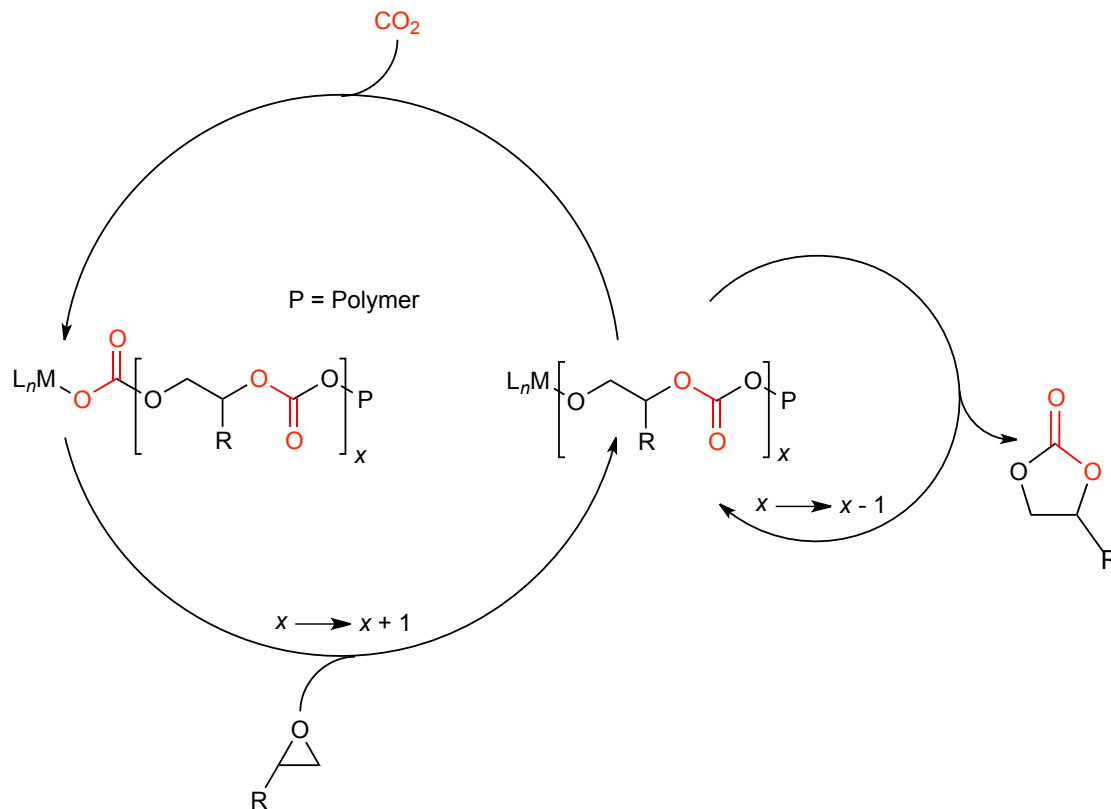
useful organic or macromolecular products through the fixation of CO₂, often catalytically and with high stereoselectivity.¹⁶⁻¹⁹ For example, in 2008 Iwasawa reported the use of a palladium hydride complex supported by a silyl containing pincer ligand (**10**, Scheme 3) to catalyze the synthesis of β,γ -unsaturated carboxylic acids from allenes, CO₂, and diethyl zinc (ZnEt₂) or triethyl aluminum (AlEt₃).²⁰ The use of a silyl group in the pincer ligand was found to be crucial as it causes the palladium center to be sufficiently nucleophilic to form an η^2 -CO₂ species. Remarkably, the catalytic reactions were performed either at room temperature or at only slightly elevated temperatures.

As shown in Scheme 3, compound **10** was generated from the palladium triflate precatalyst **11** through transmetallation with ZnEt₂ (or AlEt₃) followed by β -hydride elimination. Complex **10** reacts readily with the less sterically hindered end of the allene substrate *via* coordination of the allene to palladium, followed by insertion into the palladium hydride bond to generate intermediate **12**. Compound **12** then reacts with CO₂ to form a palladium η^2 -CO₂ species, **13**, in which the CO₂ ligand inserts into the σ -allyl group to generate the carboxylate intermediate **14**. Finally, a second transmetallation and β -hydride elimination regenerates **10**, and treatment with acid protonates the concomitantly formed zinc (or aluminum) carboxylate to provide the desired organic product in high yield. Overall, 13 products were reported with a diverse array of allenes, demonstrating tolerance to various functional groups (ethers, ketones, acetals, esters, etc.).^{20,21}

In addition to the use of CO₂ as a C₁ source in organic synthesis, preparation of polymers from CO₂ is another attractive method for the productive use of the

greenhouse gas, and has been known for over 50 years.²² Today, many organometallic systems have been reported for the copolymerization of CO₂ and epoxides as a green method for the synthesis of polycarbonates.²³⁻²⁵ The mechanism of such catalytic processes is rather simple, as depicted in Scheme 4, and the largest obstacle to overcome has historically been the production of cyclic carbonates as by-products. The benefits of the synthesis of polycarbonates from CO₂ are twofold, in that the production consumes a gas that is hazardous to the environment, and the resulting polymeric materials are biodegradable and not derived from rapidly depleting petrochemical sources. Furthermore, the physical properties of aliphatic polycarbonates may be easily tuned for use in many different applications through variation in the epoxide employed or catalyst/ligand combination used.²⁶

Scheme 4



1.3 Activation and Fixation of Dinitrogen

The activation and fixation of dinitrogen (N_2) has been one of the most popular areas of research for organometallic chemists over the past half century, and the topic has been reviewed extensively over the past decade.²⁷⁻³³ The driving force behind these efforts has ultimately been the development of organometallic species to mediate the direct conversion of N_2 and dihydrogen (H_2) to ammonia (NH_3) under ambient or near ambient conditions. Presently, more than 140 million tons of NH_3 are produced annually through the energy intensive ($T > 600\text{ }^\circ\text{C}$, $p > 500\text{ atm}$) Haber-Bosch process.³⁴ The reason for such high demand for NH_3 is its ubiquitous use as a precursor for other nitrogen containing small molecules, specifically fertilizers. Given that the demand for NH_3 and other N_2 -derived small molecules will only increase as the world population continues to grow, the development of alternative methods to the Haber-Bosch process are more necessary than ever.³⁵

As in the case of CO_2 , there exist many coordination modes for N_2 activation that are relevant to the production of commodity chemicals, which are depicted in Figure 4. Both mononuclear and dinuclear complexes have been reported. In all cases, electron donation from the transition metal center(s) to the LUMO π^* orbital of

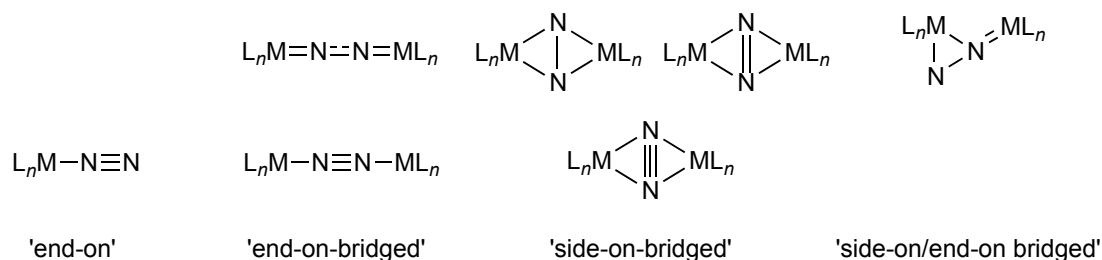
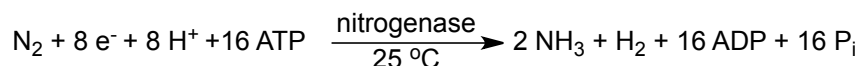


Figure 4. Common bonding motifs for N_2 coordination. Bottom examples show mild extent of N_2 activation, top examples show strong N_2 activation.

N₂ is key to coordination and activation. Traditionally, lengthening of the N-N bond has been used to determine the extent of N₂ activation.

Scheme 5



Catalytic N₂ reduction to NH₃ is known to occur in nature and is mediated by the nitrogenase enzyme, in a process which requires 16 equivalents of ATP (Scheme 5).^{36,37} The mechanism of the reaction is still unknown, however several recent reports have provided evidence that the active site consists of an iron metalloprotein and an iron/molybdenum metalloprotein, between which exists a single carbon ligand (Figure 5).^{38,39} Knowledge of the exact structure and composition of the nitrogenase active site may provide valuable information for the rational design of transition metal N₂ fixation catalysts.

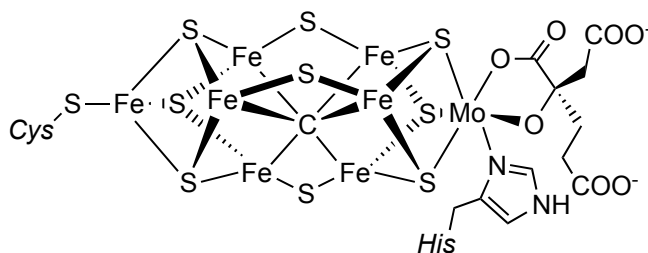


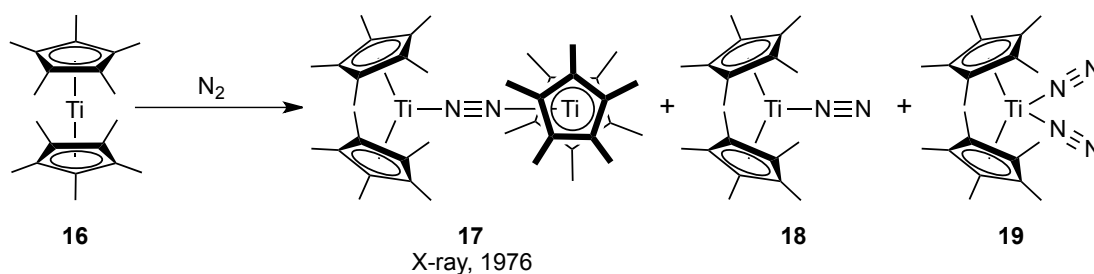
Figure 5. Structure of the active site of the nitrogenase enzyme.

1.3.1 Group 4 Metallocenes

The chemistry of group 4 metallocenes with regard to dinitrogen fixation has been pursued for over 60 years, with the first major achievement reported by Vol'pin

and Shur in 1966, in which it was found that treatment of the titanocene compound $(\eta^5\text{-C}_5\text{H}_5)_2\text{TiCl}_2$ (**15**) with various Grignard reagents under N_2 atmosphere followed by addition of acid yielded NH_3 .⁴⁰ Bercaw and coworkers were the first to report extensively on the organometallic products obtained from reaction of titanocenes with N_2 , and found that many products may be detected depending on solvent, N_2 pressure, and titanocene concentration (Scheme 6).⁴¹ Shortly after this initial report, one of these compounds was isolated as a crystalline solid and the molecular structure was reported.⁴²

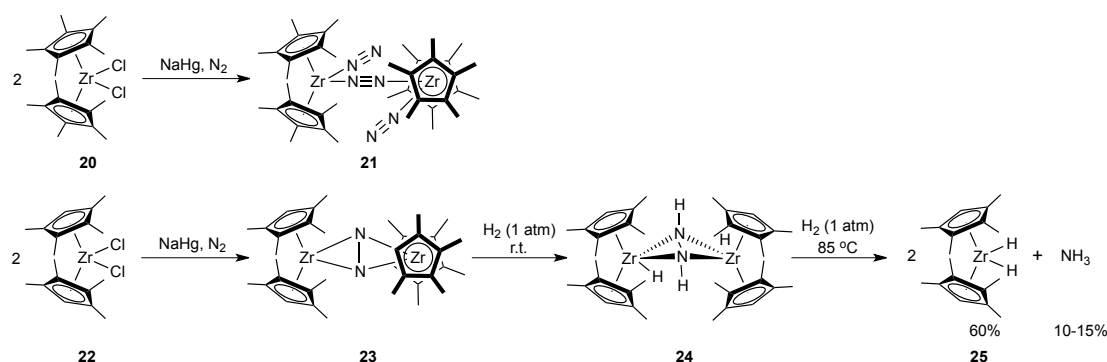
Scheme 6



Work continued on the use of group 4 metallocenes for many years, however recently the area has experienced a revival through the work of Chirik, a former member of the Bercaw group. Chirik had successfully undertaken a systematic study on the effect of substituents on the cyclopentadienyl ligand for N_2 coordination in titanocenes.³⁰ Encouraged by reports from Fryzuk that N_2 can be *partially* hydrogenated with H_2 when bound in a ‘side-on-bridged’ manner between two zirconium centers,⁴³ Chirik sought to investigate the ability of zirconocenes to promote complete N_2 hydrogenation to NH_3 . It had been established by Bercaw that the bulky decamethylzirconocene dichloride $[\eta^5\text{-C}_5(\text{CH}_3)_5]_2\text{ZrCl}_2$ (**20**) forms the ‘end-

on’/’end-on-bridged’ dinitrogen compound $\{[\eta^5\text{-C}_5(\text{CH}_3)_5\text{Zr}(\eta^1\text{-N}_2)]_2(\mu\text{-}\eta^1\text{:}\eta^1\text{-N}_2)\}$ (**21**) upon reduction.⁴⁴ The presence of multiple N₂ ligands is unattractive for N₂ activation, as each acts as a π -acid competing for electron density. Accordingly, reduction of the less sterically bulky zirconocene $[\eta^5\text{-C}_5(\text{CH}_3)_4\text{H}]_2\text{ZrCl}_2$ (**22**) under N₂ led to the coordination of only one N₂ ligand in a more activated ‘side-on-bridged’ mode, to give $\{[\eta^5\text{-C}_5(\text{CH}_3)_4\text{H}]_2\text{Zr}\}_2(\mu\text{-}\eta^2\text{:}\eta^2\text{-N}_2)$ (**23**) (Scheme 7). This compound was found to undergo facile hydrogenation at room temperature to produce the dinuclear zirconium hydride complex $\{[\eta^5\text{-C}_5(\text{CH}_3)_4\text{H}]_2\text{ZrH}\}_2(\mu\text{-}\eta^2\text{:}\eta^2\text{-N}_2\text{H}_2)$ (**24**), in which the bridging nitrogen ligands are partially hydrogenated, which liberates small amounts of NH₃ upon gentle heating under H₂ atmosphere.⁴⁵

Scheme 7

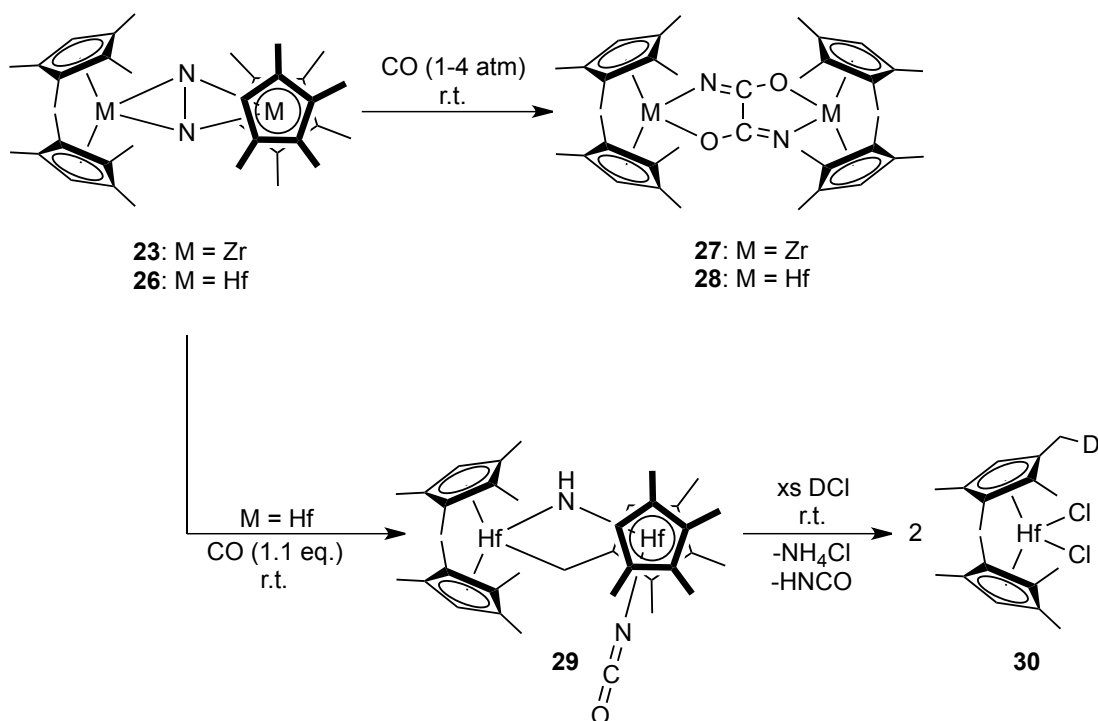


Transition metal mediated formation of nitrogen carbon bonds is also of scientific importance as it may allow for the preparation of nitrogen containing organic molecules through more energy efficient routes. For this reason, the coupling of N₂ and carbon monoxide (CO) is of interest as it may allow for the fixation of two of the most inert molecules known. Group 4 metallocenes have been shown to

mediate such reactions, and it was again found that the substituents on the cyclopentadienyl ligand play a key role in the observed chemistry.

A notable example of nitrogen carbon bond formation within the scope of group 4 metallocenes is the reaction of $\{[\eta^5\text{-C}_5(\text{CH}_3)_4\text{H}]_2\text{M}\}_2(\mu\text{-}\eta^2\text{:}\eta^2\text{-N}_2)$ [M = Zr (**23**), M = Hf (**26**)] with CO. Upon addition of excess CO (1-4 atm) at room temperature, the formation of dinuclear oxamide compounds $\{[\eta^5\text{-C}_5(\text{CH}_3)_4\text{H}]_2\text{M}\}_2(\text{N}_2\text{C}_2\text{O}_2)$ [M = Zr (**27**), M = Hf (**28**)] was observed through CO induced N₂ cleavage with concomitant C-C bond formation. In the case of hafnocene **26**, it was found that slow diffusion of only 1.1 equivalents CO into benzene solution

Scheme 8



lead to the formation of a cyclometallated species bearing a terminal isocyanate and bridging imido ligand (**29**), in which CO induced N₂ bond cleavage had occurred. Treatment of this compound with DCl revealed that C-H bond activation occurred

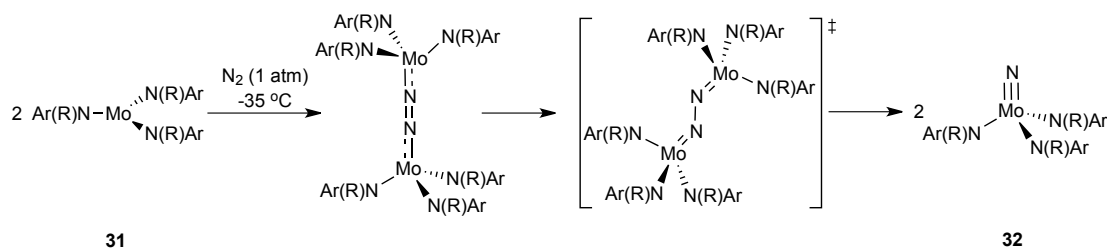
exclusively at a methyl group adjacent to the cyclopentadienyl hydrogen to form the final ‘tuck-over’ compound, and also resulted in the release of NH_4Cl and HNCO (Scheme 8).⁴⁶

1.3.2 Group 6 Dinitrogen Compounds

Although great strides have been made in the use of dinuclear group 4 compounds to mediate N_2 activation and fixation, the ultimate use of such complexes is limited in that they lack the 6 electrons necessary to fully reduce N_2 without the use of additional reagents. For this reason, significant attention has been paid to group 6 compounds to mediate such reactivity. Molybdenum dinitrogen compounds were first reported Hidai and coworkers in 1969, in which molybdenum (0) supported by 1,2-bis(diphenylphosphino)ethane ligands coordinates two N_2 molecules in an ‘end-on’ fashion.^{47,48}

A major breakthrough in this field was reported by Cummins in 1995, in which it was found that a three coordinate molybdenum (III) complex $\text{Mo}[\text{N}(\text{R})\text{Ar}]_3$ [$\text{R} = \text{C}(\text{CD}_3)_2\text{CH}_3$, $\text{Ar} = 3,5\text{-C}_6\text{H}_3(\text{CH}_3)_2$] (**31**) reacts readily with N_2 at sub-ambient temperature (e.g. $-35\text{ }^\circ\text{C}$), yielding the 4 coordinate molybdenum (VI) terminal nitride complex $(\text{N})\text{Mo}[\text{N}(\text{R})\text{Ar}]_3$ (**32**) (Scheme 9).⁴⁹ Mechanistic studies indicated that the

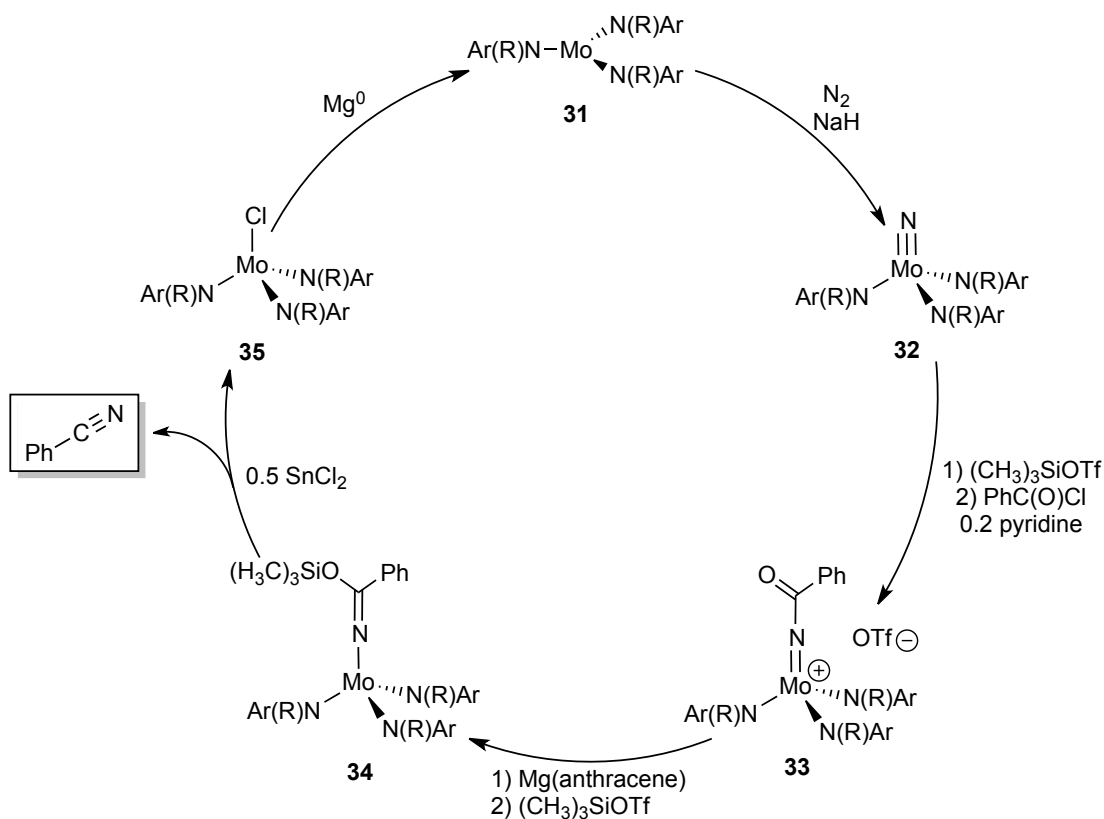
Scheme 9



cleavage of N_2 occurs through the formation of a dinuclear ‘end-on-bridged’ intermediate, which could be detected by NMR, which then goes through a proposed ‘zig-zag’ transition state to form the terminal nitride **32**. ^{15}N labeling was found to be consistent with the hypothesis that NN bond scission is the rate determining step.⁵⁰

The utility of compound **32** for the synthesis of useful organic molecules has been investigated as well. Complex **32** was known to be reactive towards strong electrophiles, specifically $(\text{CH}_3)_3\text{Si}^+$.⁵¹ It was reasoned that the presence of such a Lewis acid could promote the reaction between the nitride ligand of **32** and acid chlorides. Indeed, in the presence of $(\text{CH}_3)_3\text{SiOTf}$ ($\text{OTf} = \text{O}_3\text{SCF}_3$), benzoyl chloride, and a catalytic amount of pyridine, **32** was converted to the benzoylimido salt

Scheme 10



$\{\text{PhC(O)NMo}[\text{N(R)Ar}]\}(\text{OTf})$ (**33**) in good yield. Reduction of **33** with magnesium anthracene followed by treatment with $(\text{CH}_3)_3\text{SiOTf}$ was found to form the $(\text{CH}_3)_3\text{Si}$ -substituted ketimide $\text{Ph}[(\text{CH}_3)_3\text{SiO}]\text{CNMo}[\text{N(R)Ar}]_3$ (**34**), which itself can be converted cleanly to the molybdenum (IV) chloride species $\text{ClMo}[\text{N(R)Ar}]_3$ (**35**), by treatment with SnCl_2 , with concomitant release of phenyl nitrile (PhCN) as confirmed through ^{15}N labeling studies. Lastly, compound **35** could be reduced with magnesium (0) to generate **31**, which cleaves N_2 to regenerate **32** (Scheme 10).⁵² Although the yields associated with each step reported are high ($> 75\%$), the versatility of this system is low. For example, for the synthesis of other nitriles (e.g. acetonitrile), different reagents and methods are required.

1.3.3 Molybdenum Catalyzed NH_3 Synthesis

Several researchers have reported the use of molybdenum compounds to catalyze the direct conversion of N_2 to NH_3 . Nishibayashi has reported that the ‘end-on’/‘end-on-bridged’ dinitrogen compounds $[(\text{PNP})\text{Mo}(\eta^1\text{-N}_2)_2]_2(\mu\text{-}\eta^1\text{:}\eta^1\text{-N}_2)$ [$\text{PNP} =$

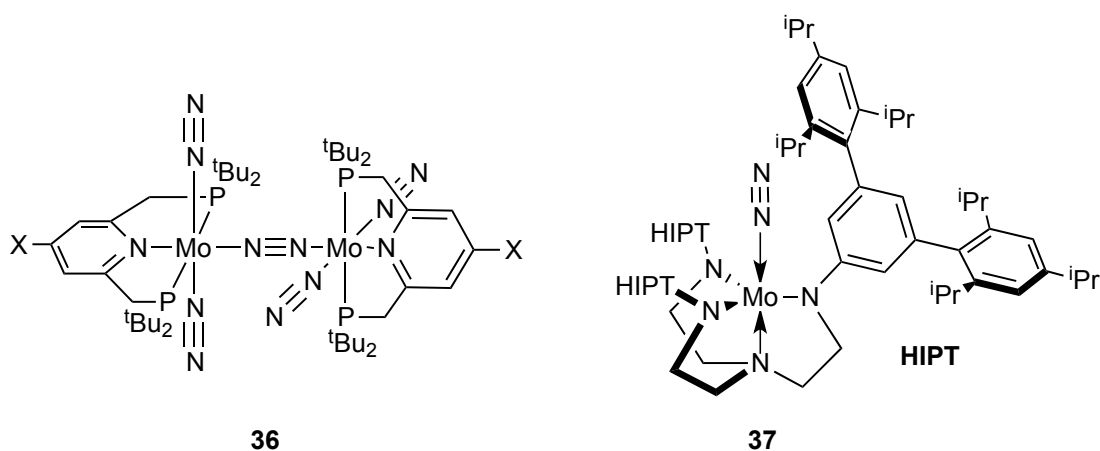


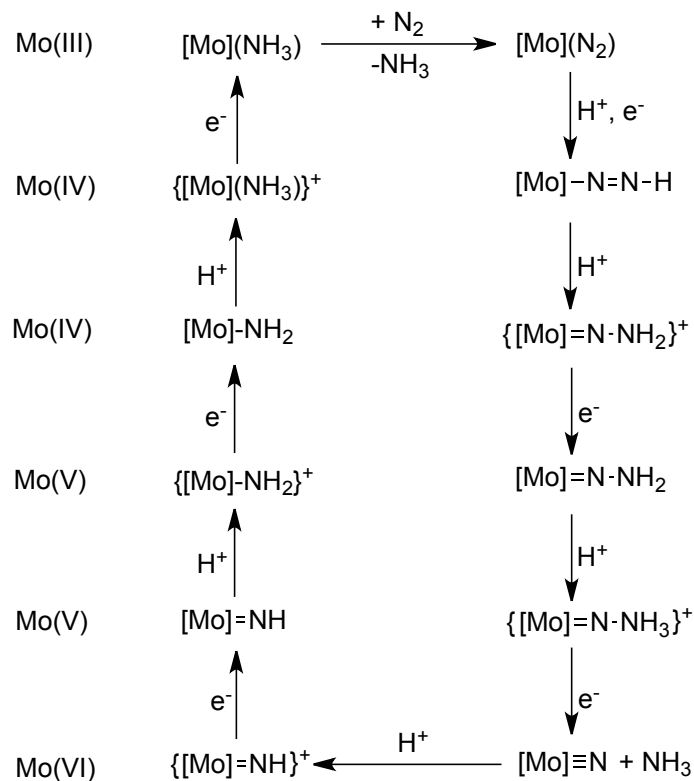
Figure 6. General structure of Nishibayashi's N_2 reduction catalyst (**36**) and Schrock's N_2 reduction catalyst (**37**).

2,6-bis(di-^tBu-phosphinomethyl)pyridine] (**36**) are capable of producing NH₃ in yields up to 26 equivalents on the basis of molybdenum centers present (Figure 6).^{53,54} The mechanism of this process is still unclear, however, as key intermediates proposed have not been isolated or observed. In fact, it is still a matter of some debate whether the mechanism employs a monomeric molybdenum complex as the active catalyst or if the dinuclear structure stays intact.⁵⁵

In 2003, Schrock and Yandulov demonstrated the first example of catalytic NH₃ formation from N₂ within a well defined system.⁵⁶ In this work, the extremely bulky [HIPTN₃N]³⁻ ligand system (Figure 6), was employed to prevent the formation of dinuclear ‘end-on-bridged’ dinitrogen complexes, as it was thought that they would inhibit reaction with protons and electrons. Accordingly, the monomeric [HIPTN₃N] molybdenum (III) ‘end-on’ dinitrogen complex (**37**) was isolated (Figure 6).

It was found that compound **37** could be treated with protons and electrons to yield up to 8 equivalents of NH₃ under N₂ (1 atm). The proton source chosen was 2,6-lutidinium borate [LutH][BAr₄] (Ar = 3,5-(CF₃)₂C₆H₃), which was added in a controlled manner by use of heptane as a solvent. [LutH][BAr₄] is sparingly soluble in hydrocarbon solvent, so it would only slowly react with the highly soluble molybdenum species in solution. The electron source chosen was decamethylchromocene, which was added slowly to the solution *via* syringe pump. Unlike the catalytic systems reported by Nishibayashi, the mechanism for Schrock’s catalyst is relatively well understood. Several key intermediates were independently synthesized and isolated which support the proposed mechanism, which is reminiscent of the Chatt cycle, which involves subsequent addition of protons and

Scheme 11



electrons to coordinated N_2 to produce diazenido, hydrazido, hydrazidium, nitride, imido, and amido complexes (Scheme 11). The main difference between the proposed cycles is the oxidation state of the molybdenum center, which varies between Mo (0) and Mo (III) in the Chatt cycle,³⁶ and between Mo (III) and Mo (VI) in the Schrock cycle.⁵⁶

1.4 CpAm Ligand Framework


One of the most important factors for one to consider when seeking to promote small molecule activation and fixation with organometallic complexes is the selection of a proper supporting ligand framework. The electronic, steric, and redox

properties of supporting ligands are key to tuning the reactivity of a metal compound in virtually every manner imaginable. Accordingly, a brief analysis of ligand properties is appropriate.

1.4.1 Cyclopentadienyl Ligand and Metallocene Environment

As has been seen in the previous sections, metallocenes of the early transition metals have played an enormous role in regard to small molecule activation. Their history is even more rich when one considers the dominant role they have played in the field of olefin polymerization using group 4 metals.^{57,58} With regard to group 6 chemistry,⁵⁹ metallocenes were explored extensively by the groups of Bercaw⁶⁰⁻⁶² and Geoffroy^{63,64} in the late 1980s and early 1990s, and have even appeared in the 21st century in reports from Parkin.⁶⁵

The cyclopentadienyl (Cp) ligand is monoanionic and, in its most common η^5 coordination mode, donates six electrons to the metal center. Accordingly, the oxidation states and electron counts for the commonly observed ‘bent’ metallocene fragments for groups 4 – 6 are shown in Figure 7. Variation in the electronic and

|  | Group | Metals (M) | Oxidation State | d Electron Count |
|---|-------|------------|-----------------|------------------|
| | 4 | Ti, Zr, Hf | IV | 16 |
| | 5 | V, Nb, Ta | IV | 17 |
| | 6 | Cr, Mo, W | IV | 18 |

X, Y = H, Alkyl, Halide, etc.
R = H, Alkyl, etc.

Figure 7. Structure of early transition metal ‘bent’ metallocenes with oxidation states and d electron counts.

steric environments of transition metal centers bearing this ligand can only occur through substitution of one or several of the substituents on the Cp ring. For example, recall that reduction of compound **20** (decamethylzirconocene dichloride) yields the ‘end-on’/‘end-on-bridged’ complex **21**, in which three N₂ ligands exist in the dimeric product.⁴⁴ However, reduction of the sterics in the similar zirconocene **22** (octamethylzirconocene dichloride) allowed for ‘side-on-bridged’ coordination of just one N₂ ligand (**23**). By reducing the sterics about the zirconium centers, the two metals could exist in closer proximity to one another, thus allowing for the ‘side-on-bridged’ activation.⁴⁵ Furthermore, replacement of an electron donating methyl group on each Cp ligand with H made the zirconium less electron rich and, as a result, less likely to bind additional N₂ ligands.

1.4.2 Amidinate Ligands and Bisamidinate Environment

Amidines are another class of ligands that have experienced success in regard to early transition metal chemistry. The amidinate ligand results in a

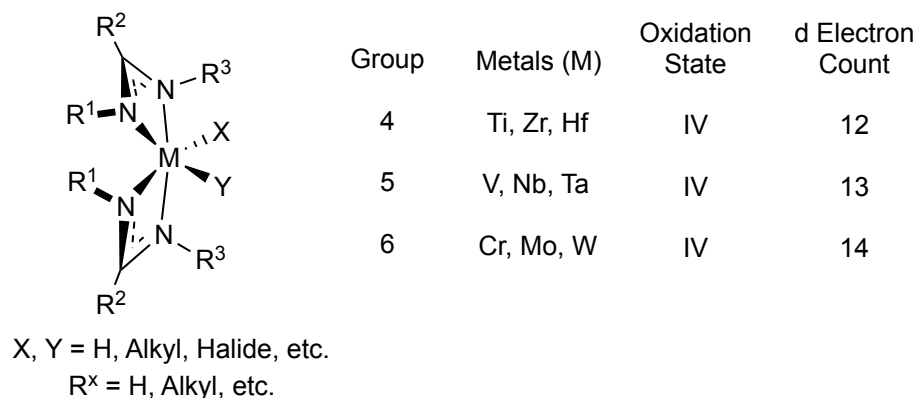


Figure 8. Structure of early transition metal bisamidinate compounds with oxidation states and d electron counts.

significant decrease in electron density placed on the metal in comparison to Cp, as it is a four electron donor (Figure 8). Like Cp, it is also monoanionic. Amidinates may experience a larger variety of coordination modes, either as η^1 , η^2 , or bridging η^2 (A, B, and C, respectively, Figure 9). Furthermore, the electronic and sterics about the metal center may be more easily tuned with amidinate ligands than with Cp ligands through the variation of R^1 , R^2 and/or R^3 (Figure 9), resulting in the ability to vary such factors easily, one of their signature advantages. Bisamidinate compounds are known for a variety of transition metals, which has resulted in noteworthy reactivity.^{66,67} For example, bisamidinates for group 4 compounds became of interest when it was discovered that they may serve as alternatives to metallocenes for olefin polymerization in 1995 by Eisen and a coworker.⁶⁸ Shortly thereafter, titanium⁶⁹ and vanadium⁷⁰ complexes supported by the bisamidinate ligand framework were reported to activate N_2 as well. In the case of vanadium, the activation of N_2 was found to be reversible.⁷⁰

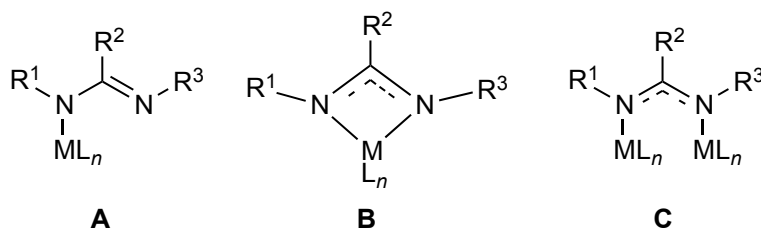


Figure 9. Possible coordination modes of amidinate ligands.

1.4.3 Cyclopentadienyl/Amidinate Ligand Framework

The synthesis of early metal complexes bearing both Cp and amidinate ligands (CpAm ligand framework) became of interest in the early 1990s as many

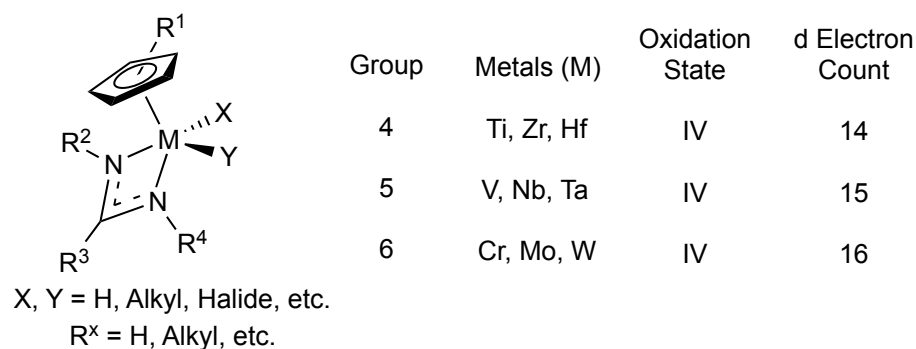


Figure 10. Structure of early transition metal CpAm compounds with oxidation states and d electron counts.

were searching for non-metallocene based initiators for Ziegler-Natta polymerization. One benefit of such a ligand framework is that the electronics lie between the two extremes of the metallocene and bisamidinate ligand environments (Figure 10), and the sterics may be tuned on either ligand. For example, if one wished to increase the sterics generally around the metal center, addition of bulky groups to the Cp ligand may be attractive. However, if one wanted to specifically increase steric bulk on one side of the metal to allow for asymmetric catalysis, changing the substituent R² on the amidinate ligand only would allow one to do so selectively. Green and coworkers reported the synthesis of Cp, benzamidinate compounds (η^5 -C₅H₅)M(Bz)₂{N[Si(Me)₃]₃C(Ph)N[Si(CH₃)₃]} [M = Ti (**38**), Zr (**39**)] and their preliminary reactivity for olefin polymerization in 1993.⁷¹ Sita and coworkers later reported a method for the facile preparation of libraries of such group 4 compounds which are highly active as initiators for the living coordination polymerization of α -olefins,⁷²⁻⁷⁵ and these compounds continue to find use today.^{76,77} This work has been extended to include the synthesis of CpAm compounds of group 5 and 6 metals, which have experienced remarkable success in the activation of small molecules. For

example, N₂ activation by early transition metal CpAm compounds has been explored at great length. What is most noteworthy about such investigations is that the use of a (nearly) identical CpAm ligand environment has allowed for the synthesis of an isostructural series of dinuclear N₂ compounds for groups 4,⁷⁸ 5,^{79,80} and 6.⁸¹ Accordingly, the differences in mode of N₂ coordination, extent of activation, and subsequent reactivity between each metal may be attributed specifically to the metal employed (Figure 11). This has allowed Sita and coworkers to examine the effect of each metal on N₂ activation, allowing for the rational design of N₂ fixation catalysts, a topic which will be explored in the following chapters.

It is proper to note that in the wake of reports from Sita, others have employed the CpAm ligand environment as well for group 4 and 6 metal complexes. For example, Mountford has reported extensively on the synthesis of CpAm titanium imidos and their reactivity.⁸²⁻⁸⁹ On the other hand, Tilley investigated the reactivity of group 6 chloride species with silyl hydrides.⁹⁰

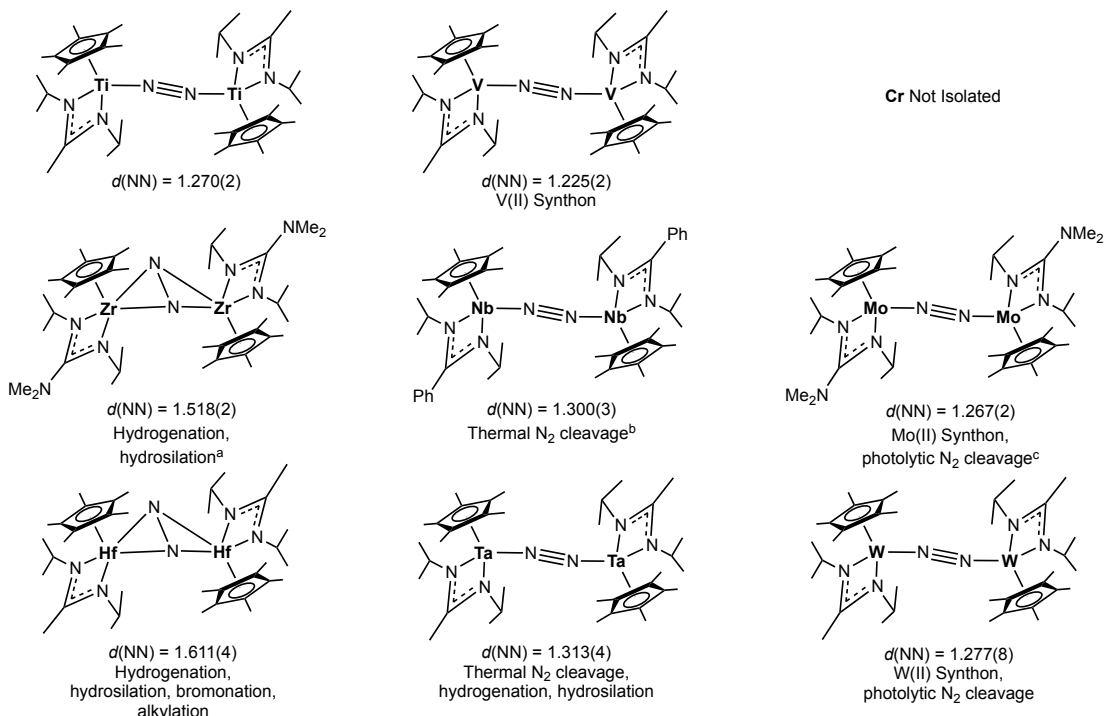


Figure 11. N_2 activation within early transition metal CpAm complexes. ^a The only compound reported utilized the dimethylamino moiety in the distal position of the amidinate ligand. ^b Only the derivative with a phenyl group in the distal position of the amidinate ligand was structurally characterized. Similar reactivity was observed for the acetamidinate (i.e. methyl in distal position) compound. ^c The derivative with a dimethylamino group in the distal position of the amidinate ligand was characterized in the solid state given the high solubility of the acetamidinate complex. Similar reactivity was observed. (Note: Bond lengths reported in Å).

1.5 References

- (1) All Nobel Prizes in Chemistry.
http://www.nobelprize.org/nobel_prizes/chemistry/laureates/ (accessed Jan. 15, 2015).
- (2) Darwent, B. deB. *Bond Dissociation Energies in Simple Molecules*; NSRDS-NBS 31; National Bureau of Standards: Washington, D.C., 1970.
- (3) United States Environmental Protection Agency Overview of Greenhouse Gases.
<http://www.epa.gov/climatechange/ghgemissions/gases/co2.html> (accessed Jan. 15, 2015).
- (4) World Meteorological Organization. *Greenhouse Gas Bulletin*. Geneva, Switzerland, 2014, No. 10.
- (5) Braunstein, P.; Matt, D.; Nobel, D. *Chem. Rev.* **1988**, 88, 747.
- (6) Darensbourg, D. J.; Kudarowski, R. A. *Adv. Organomet. Chem.* **1983**, 22, 129.
- (7) Gibson, D. H. *Chem. Rev.* **1996**, 96, 2063.
- (8) Yin, X.; Moss, J. R. *Coord. Chem. Rev.* **1999**, 181, 27.
- (9) Leitner, W. *Coord. Chem. Rev.* **1996**, 153, 257.
- (10) Palmer, D. R.; van Eldik, R. *Chem. Rev.* **1983**, 83, 651.
- (11) Calabrese, J. C.; Herskovitz, T.; Kinney, J. B. *J. Am. Chem. Soc.* **1983**, 105, 5914.
- (12) Herskovitz, T. *J. Am. Chem. Soc.* **1977**, 99, 2391.
- (13) Harlow, R. L.; Kinney, J. B.; Herskovitz, T. *J. Chem. Soc., Chem. Comm.* **1980**, 813.
- (14) Aresta, M.; Nobile, C. F.; Albano, V. G.; Forni, E.; Manassero, M. *J. Chem. Soc., Chem. Comm.* **1975**, 636.
- (15) Bristow, G. S.; Hitchcock, P. B.; Lappert, M. F. *J. Chem. Soc., Chem. Comm.* **1981**, 1145.
- (16) Kielland, N.; Whiteoak, C. J.; Kleij, A. W. *Adv. Synth. Catal.* **2013**, 355, 2115.
- (17) Blattmann, H.; Fleischer, M.; Baehr, M.; Muelhaupt, R. *Macromol. Rapid Commun.* **2014**, 35, 1238.
- (18) Huang, K.; Sun, C.-L.; Shi, Z.-J. *Chem. Soc. Rev.* **2011**, 40, 2435.
- (19) Sakakura, T.; Choi, J.-C.; Yasuda, H. *Chem. Rev.* **2007**, 107, 2365.
- (20) Takaya, J.; Iwasawa, N. *J. Am. Chem. Soc.* **2008**, 130, 15254.
- (21) North, M. *Angew. Chem. Int. Ed.* **2009**, 48, 4104.
- (22) Inoue, S.; Koinuma, H.; Tsuruta, T. *J. Polym. Sci., Part B: Polym. Phys.* **1969**, 7, 287.
- (23) Luinstra, G. A. *J. Macromol. Sci., Polym. Rev.* **2008**, 48, 192.
- (24) Muelhaupt, R. *J. Macromol. Sci., Macromol. Chem. Phys.* **2013**, 214, 159.
- (25) Coates, G. W.; Moore, D. R. *Angew. Chem. Int. Ed.* **2004**, 43, 6618.
- (26) Thorat, S. D.; Phillips, P. J.; Semenov, V.; Gakh, A. *J. Appl. Polym. Sci.* **2003**, 89, 1163.

- (27) Fryzuk, M. D.; Johnson, S. A. *Coord. Chem. Rev.* **2000**, 200-202, 379.
- (28) MacKay, B. A.; Fryzuk, M. D. *Chem. Rev.* **2004**, 104, 385.
- (29) Fryzuk, M. D. *Acc. Chem. Res.* **2009**, 42, 127.
- (30) Chirik, P. J. *Organometallics* **2010**, 29, 1500.
- (31) Chirik, P. J. *J. Chem. Soc., Dalton Trans.* **2007**, 16.
- (32) Ohki, Y.; Fryzuk, M. D. *Angew. Chem. Int. Ed.* **2007**, 46, 3180.
- (33) Tanabe, Y.; Nishibayashi, Y. *Coord. Chem. Rev.* **2013**, 257, 2551.
- (34) Smil, V. *Enriching the Earth: Fritz Haber, Carl Bosch, and the Transformation of World Food Production*; MIT Press: Cambridge, MA, 2001.
- (35) Gruber, N.; Galloway, N. *Nature* **2008**, 451, 293.
- (36) Burgess, B. K.; Lowe, D. J. *Chem. Rev.* **1996**, 96, 2983.
- (37) Pickett, C. J. *J. Biol. Inorg. Chem.* **1996**, 601.
- (38) Einsle, O.; Tezcan, F. A.; Andrade, S. L. A.; Schmid, D.; Yoshida, M.; Howard, J. B.; Rees, D. C. *Science* **2002**, 297, 1696.
- (39) Lancaster, K. M.; Roemelt, M.; Ettenhuber, P.; Hu, Y.; Ribbe, M. W.; Neese, F.; Bergmann, U.; DeBeer, S. *Science* **2011**, 334, 974.
- (40) Vol'pin, M. E.; Shur, V. B. *Nature* **1966**, 209, 1236.
- (41) Bercaw, J. E. *J. Am. Chem. Soc.* **1974**, 96, 5087.
- (42) Sanner, R. D.; Duggan, D. M.; McKenzie, T. C.; Marsh, R. E.; Bercaw, J. E. *J. Am. Chem. Soc.* **1976**, 98, 8358.
- (43) Fryzuk, M. D.; Love, J. B.; Rettig, S. J.; Young, V. G. *Science* **1997**, 275, 1445.
- (44) Manrique, J. M.; Bercaw, J. E. *J. Am. Chem. Soc.* **1974**, 96, 6229.
- (45) Pool, J. A.; Lobkovsky, E.; Chirik, P. J. *Nature* **2004**, 427, 527.
- (46) Knobloch, D. J.; Lobkovsky, E.; Chirik, P. J. *J. Am. Chem. Soc.* **2010**, 132, 10553.
- (47) Hidai, M.; Tominari, K.; Uchida, Y.; Misono, A. *J. Chem. Soc., Chem. Comm.* **1969**, 814.
- (48) Hidai, M.; Tominari, K.; Uchida, Y. *J. Am. Chem. Soc.* **1972**, 94, 110.
- (49) Laplaza, C. E.; Cummins, C. C. *Science* **1995**, 268, 861.
- (50) Laplaza, C. E.; Johnson, M. J. A.; Peters, J. C.; Odom, A. L.; Kim, E.; Cummins, C. C.; George, G. N.; Pickering, I. J. *J. Am. Chem. Soc.* **1996**, 118, 8623.
- (51) Sceats, E. L.; Figueroa, J. S.; Cummins, C. C.; Loening, N. M.; Van der Wel, P.; Griffin, R. G. *Polyhedron* **2004**, 23, 2751.
- (52) Curley, J. J.; Sceats, E. L.; Cummins, C. C. *J. Am. Chem. Soc.* **2006**, 128, 14036.
- (53) Kuriyama, S.; Arashiba, K.; Nakajima, K.; Tanaka, H.; Kamaru, N.; Yoshizawa, K.; Nishibayashi, Y. *J. Am. Chem. Soc.* **2014**, 136, 9719.
- (54) Arashiba, K.; Miyake, Y.; Nishibayashi, Y. *Nature Chem.* **2011**, 3, 120.
- (55) Tian, Y.-H.; Pierpont, A. W.; Batista, E. R. *Inorg. Chem.* **2014**, 53, 4177.
- (56) Yandulov, D. V.; Schrock, R. R. *Science* **2003**, 301, 76.
- (57) Bochmann, M. *J. Organomet. Chem.* **2004**, 689, 3982.

- (58) Wang, B. *Coord. Chem. Rev.* **2006**, 250, 242.
- (59) Minato, M.; Ito, T. *Coord. Chem. Rev.* **2008**, 252, 1613.
- (60) Parkin, G.; Marsh, R. E.; Schaefer, W. P.; Bercaw, J. E. *Inorg. Chem.* **1988**, 27, 3263.
- (61) Parkin, G.; Bercaw, J. E. *Polyhedron* **1988**, 7, 2053.
- (62) Parkin, G.; Bercaw, J. E. *J. Am. Chem. Soc.* **1989**, 111, 391.
- (63) Pilato, R. S.; Housmekerides, C. E.; Jernakoff, P.; Rubin, D.; Geoffroy, G. L.; Rheingold, A. L. *Organometallics* **1990**, 9, 2333.
- (64) Pilato, R. S.; Rubin, D.; Geoffroy, G. L.; Rheingold, A. L. *Inorg. Chem.* **1990**, 29, 1986.
- (65) Shin, J. H.; Savage, W.; Murphy, V. J.; Bonanno, J. B.; Churchill, D. G.; Parkin, G. *J. Chem. Soc., Dalton Trans.* **2001**, 1732.
- (66) Elkin, T.; Eisen, M. S. *Catal. Sci. Technol.* **2015**, 5, 82.
- (67) Edelmann, F. T. *Chem. Soc. Rev.* **2012**, 41, 7657.
- (68) Herskovics-Korine, D.; Eisen, M. S. *J. Organomet. Chem.* **1995**, 503, 307.
- (69) Hagadorn, J. R.; Arnold, J. *J. Am. Chem. Soc.* **1996**, 118, 893.
- (70) Hao, S.; Berno, P.; Minhas, R. K.; Gambrotta, S. *Inorg. Chim. Acta* **1996**, 244, 37.
- (71) Chernega, A. N.; Gomez, R.; Green, M. L. H. *J. Chem. Soc., Chem. Comm.* **1993**, 2535.
- (72) Jayaratne, K. C.; Keaton, R. J.; Henningson, D. A.; Sita, L. R. *J. Am. Chem. Soc.* **2000**, 122, 10490.
- (73) Sita, L. R.; Babcock, J. R. *Organometallics* **1998**, 17, 5228.
- (74) Jayaratne, K. C.; Sita, L. R. *J. Am. Chem. Soc.* **2000**, 122, 958.
- (75) Koterwas, L. A.; Fettingner, J. C.; Sita, L. R. *Organometallics* **1999**, 18, 4183.
- (76) Crawford, K. E.; Sita, L. R. *ACS Macro Lett.* **2014**, 3, 506.
- (77) Crawford, K. E.; Sita, L. R. *J. Am. Chem. Soc.* **2013**, 135, 8778.
- (78) Hirotsu, M.; Fontaine, P. P.; Zavalij, P. Y.; Sita, L. R. *J. Am. Chem. Soc.* **2007**, 129, 12690.
- (79) Hirotsu, M.; Fontaine, P. P.; Epshteyn, A.; Zavalij, P. Y.; Sita, L. R. *J. Am. Chem. Soc.* **2007**, 129, 9284.
- (80) Keane, A. J.; Yonke, B. L.; Hirotsu, M.; Zavalij, P. Y.; Sita, L. R. *J. Am. Chem. Soc.* **2014**, 136, 9906.
- (81) Fontaine, P. P.; Yonke, B. L.; Zavalij, P. Y.; Sita, L. R. *J. Am. Chem. Soc.* **2010**, 132, 12273.
- (82) Groom, L. R.; Russell, A. F.; Schwarz, A. D.; Mountford, P. *Organometallics* **2014**, 33, 1002.
- (83) Tiong, P.-J.; Nova, A.; Groom, L. R.; Schwarz, A. D.; Selby, J. D.; Schofield, A. D.; Clot, E.; Mountford, P. *Organometallics* **2011**, 30, 1182.
- (84) Guiducci, A. E.; Boyd, C. L.; Clot, E.; Mountford, P. *J. Chem. Soc., Dalton Trans.* **2009**, 2009, 5960.
- (85) Tiong, P.-J.; Nova, A.; Clot, E.; Mountford, P. *J. Chem. Soc., Chem. Comm.* **2011**, 47, 3147.

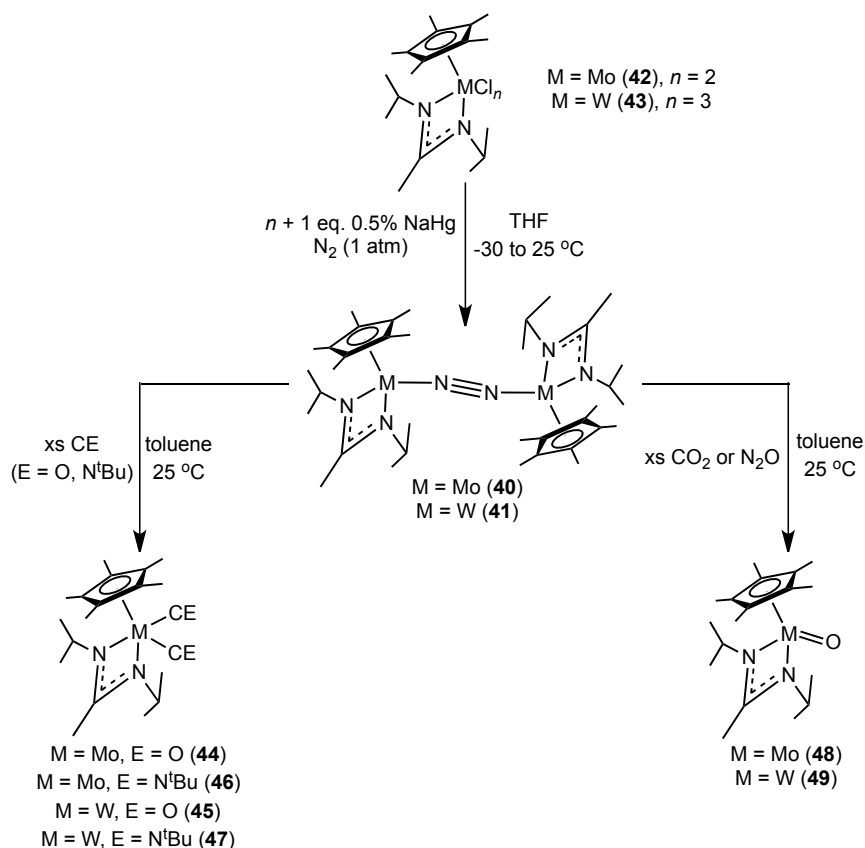
- (86) Tiong, P.-J.; Schofield, A. D.; Selby, J. D.; Nova, A.; Clot, E.; Mountford, P. *J. Chem. Soc., Chem. Comm.* **2010**, 46, 85.
- (87) Tiong, P.-J.; Nova, A.; Schwarz, A. D.; Selby, J. D.; Clot, E.; Mountford, P. *J. Chem. Soc., Dalton Trans.* **2012**, 41, 2277.
- (88) Groom, L. R.; Schwarz, A. D.; Nova, A.; Clot, E.; Mountford, P. *Organometallics* **2013**, 32, 7520.
- (89) Tiong, P.-J.; Groom, L. R.; Clot, E.; Mountford, P. *Chem. Eur. J.* **2013**, 19, 4198.
- (90) Fasulo, M. E.; Tilley, T. D. *J. Organomet. Chem.* **2011**, 696, 1325.

Chapter 2: Oxygen Atom Transfer Reactions Mediated by Group 6 CpAm Compounds

2.1 Introduction

As mentioned in Section 1.4.3, our group has previously synthesized CpAm dinitrogen compounds for molybdenum and tungsten. Specifically, the ‘end-on-bridged’ dinitrogen species $\{\text{Cp}^*\text{M}[\text{N}(\text{iPr})\text{C}(\text{CH}_3)\text{N}(\text{iPr})]\}_2(\mu\text{-}\eta^1:\eta^1\text{-N}_2)$ [$\text{M} = \text{Mo}$ (**40**), $\text{M} = \text{W}$ (**41**)] [$\text{Cp}^* = \eta^5\text{-C}_5(\text{CH}_3)_5$] may be obtained in high yields as crystalline solids through chemical reduction of the chloride precursors $\text{Cp}^*\text{Mo}[\text{N}(\text{iPr})\text{C}(\text{CH}_3)\text{N}(\text{iPr})]\text{Cl}_2$ (**42**) and $\text{Cp}^*\text{W}[\text{N}(\text{iPr})\text{C}(\text{CH}_3)\text{N}(\text{iPr})]\text{Cl}_3$ (**43**),

Scheme 12



respectively, under N₂ atmosphere (Scheme 12).¹ The extent of N₂ activation within these compounds was found to be rather low, with N-N bond lengths elongated only slightly from that of N₂ [e.g. $d(\text{NN}) = 1.277(8) \text{ \AA}$ (**41**), $d(\text{NN}) = 1.097 \text{ \AA}$ (N₂)], and much shorter than their group 4 and 5 analogs.²⁻⁴ Accordingly, it became of interest to utilize compounds **40** and **41** as M(II) synthons, as the N₂ ligand would likely be displaced quite easily as judged by its low degree of activation. Indeed, both **40** and **41** proved reactive towards a variety of reagents. Addition of the π -acids CO and *tert*-butyl isonitrile resulted in the production of M(II) bis(carbonyl) and bis(isonitrile) compounds Cp*M[N(^{*i*}Pr)C(CH₃)N(^{*i*}Pr)](CO)₂ [M = Mo (**44**), M = W (**45**)] and Cp*M[N(^{*i*}Pr)C(CH₃)N(^{*i*}Pr)](CN^{*t*}Bu)₂ [M = Mo (**46**), M = W (**47**)], respectively (Scheme 12).^{1,5} Furthermore, oxidation of the metal center was found to occur through the addition of the greenhouse gasses nitrous oxide (N₂O) and CO₂ to yield the mononuclear terminal oxo compounds Cp*M[N(^{*i*}Pr)C(CH₃)N(^{*i*}Pr)]O [M = Mo (**48**), M = W (**49**)] (Scheme 12). Both **48** and **49** were found to mediate photocatalytic degenerate oxygen atom transfer (OAT) from CO₂ to CO, and **48** was capable of mediating thermal catalytic nondegenerate OAT from N₂O to *tert*-butyl isonitrile.⁵

The ability to use CO₂ and N₂O as oxidants for the oxidation of a wider array of substrates did not appear promising, as **48** and **49** were not reactive towards other small molecules. Therefore, we sought to expand the scope of possible oxygen atom sources in order to provide a more general oxidation catalyst. Specifically, molecular oxygen (O₂) and sulfoxides were targeted, for reasons described below. Furthermore, we were interested in broadening the scope of substrates for such OAT processes. To

this end, sulfides, olefins, and phosphines were investigated as substrates for OAT reactions.

2.2 CpAm M(VI) Dioxo Compounds for OAT Reactions

2.2.1 Background

Every year, millions of tons of oxygen containing small molecules of commercial and medical significance are produced through catalytic oxidation of organic compounds. Given this high demand, methods for such oxidations which are environmentally benign are of considerable interest.⁶ Accordingly, the use of O₂ as an oxidant is an extremely attractive approach for such processes, given its large concentration in the atmosphere and the lack of by products associated with its use. In order for O₂ to be utilized in such a manner, however, metal catalysts must be employed to promote the rate of the reaction and, when appropriate, control stereo- and regioselectivity. The use of transition metals to catalyze such processes have been known for over 80 years,⁷ however the development of new catalysts continues to be of interest.⁸

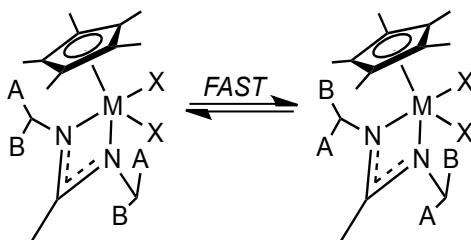
Biological systems are known to catalyze aerobic oxidation employing enzymes with group 6 metals in the active site. In all cases, these metals are in the highest possible oxidation states and operate *via* a M(IV)/M(VI) redox couple.⁹⁻¹¹ Accordingly, many have sought to prepare high valent molybdenum and tungsten dioxo and oxo-sulfido compounds which undergo OAT.^{12,13} Poli and coworkers have demonstrated that the bulky pentabenzylcyclopentadienyl group 6 dioxo species [η^5 -C₅(CH₂Ph)₅]MCl(O)₂ [M = Mo (**50**), M = W (**51**)] serve as competent catalysts for

the epoxidation of cyclooctene, however rather than using O₂ as an oxidant, *tert*-butyl hydroperoxide (^tBuOOH) was employed.¹⁴ Bergman and coworkers have also shown that the less bulky Cp* derivative Cp*MoCl(O)₂ (**52**) may oxidize an even larger array of olefins under similar conditions using ^tBuOOH.¹⁵

2.2.2 Synthesis and Characterization of CpAm M(VI) Group 6 Dioxo Compounds

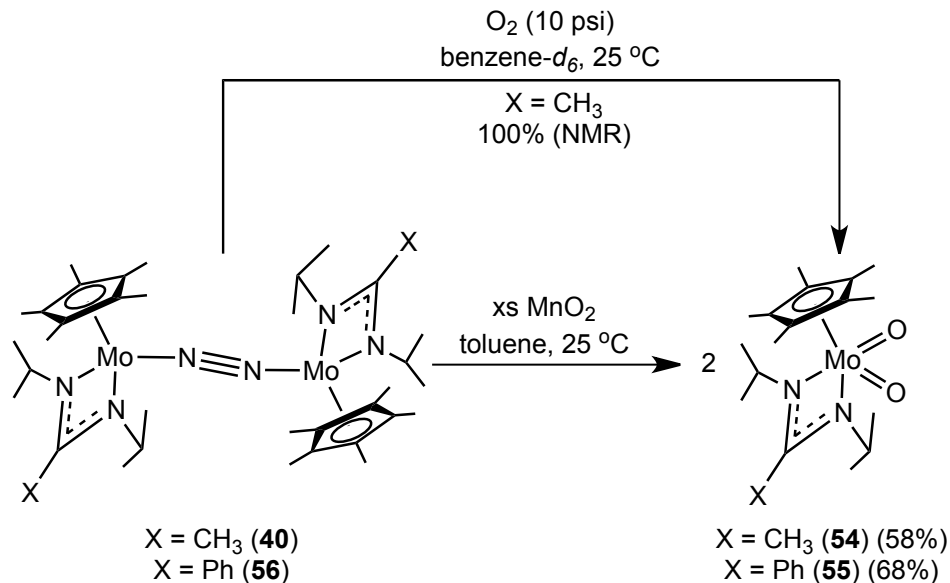
Looking to explore the possibility of utilizing group 6 CpAm compounds for OAT employing O₂ as an oxidant, the reactivity of the molybdenum ‘end-on-bridged’ dinitrogen compound **40** with O₂ was investigated. Upon introduction of O₂ (10 psi) into a benzene-*d*₆ solution of **40**, an immediate color change to pale yellow was observed. ¹H NMR revealed that compound **40** had been completely consumed and cleanly produced a new CpAm compound. Interestingly, this new species displayed 1 doublet in the ¹H NMR spectrum integrating for 12 protons, indicating a C_s symmetric compound which undergoes dynamic ‘ring-flipping’ of the amidinate ligand in solution on the NMR time scale (Scheme 13). Previously, Dr. Brendan Yonke of our group had prepared the tungsten (VI) dioxo complex Cp*W[N(ⁱPr)C(CH₃)N(ⁱPr)](O)₂ (**53**) during an investigation into ‘π-loaded’ CpAm

Scheme 13. Dynamic ‘ring-flipping’ of amidinate ligand where ‘A’ and ‘B’ represent equivalent methyl groups.



compounds. Compound **53** and other high valent, ‘ π -loaded’ species were found to display the same ‘ring-flipping’ behavior in solution.¹⁶ Accordingly, the analogous molybdenum (VI) derivatives $\text{Cp}^*\text{Mo}[\text{N}(\text{iPr})\text{C}(\text{X})\text{N}(\text{iPr})](\text{O})_2$ [$\text{X} = \text{CH}_3$ (**54**), $\text{X} = \text{Ph}$ (**55**)] were prepared through a modified method to that of Yonke. Specifically, the ‘end-on-bridged’ dinitrogen compounds **40** and **56** were reacted with excess manganese (IV) oxide (MnO_2) in toluene at room temperature to provide **54** and **55**, respectively, in moderate yields (Scheme 14). Importantly, the isolation of **54** allowed for the confirmation that this was in fact the product obtained from reaction of **40** and O_2 . The dinitrogen compound **56** was synthesized in an analogous fashion to **40** and isolated in similar yield though reduction of the chloride precursor $\text{Cp}^*\text{Mo}[\text{N}(\text{iPr})\text{C}(\text{Ph})\text{N}(\text{iPr})]\text{Cl}_2$ (**57**).

Scheme 14



Cooling a concentrated Et_2O solution of **55** to -30 °C furnished crystals suitable for X-ray analysis, and the solid state structure is depicted in Figure 12. Compound **55** exhibits Mo-O bond lengths of 1.7166(16) Å and 1.7255(16) Å,

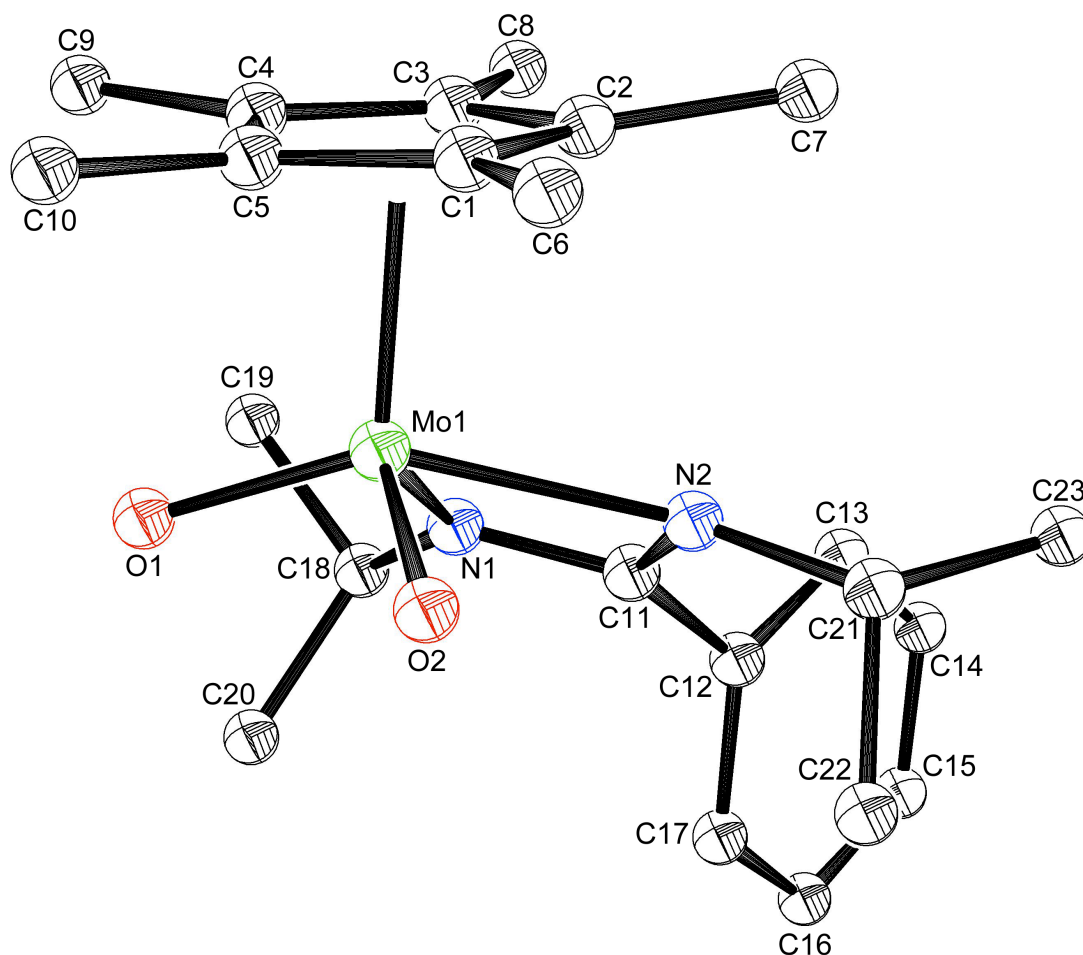
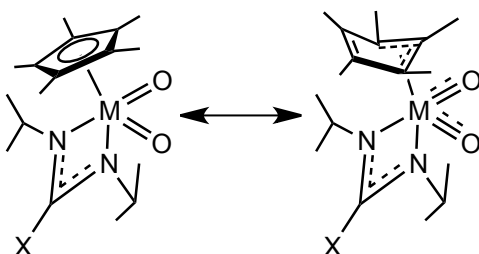


Figure 12. Molecular structure (30% thermal ellipsoids) of **55** (H atoms have been omitted for clarity). Selected bond lengths (Å) and angles (°): Mo1-O1 1.7166(16), Mo1-O2 1.7255(16), Mo1-C1 2.5323(19), Mo1-C2 2.5483(19), Mo1-C3 2.4317(19), Mo1-C4 2.3184(19), Mo1-C5 2.461(2), O1-Mo1-O2 102.19(9).

slightly shorter than its tungsten analog **53** [cf. W-O 1.733(3) Å and 1.749(3) Å],¹⁶ in keeping with the expected periodic trend.¹⁷ Interestingly, the Cp* ligand appears to undergo a ‘ring-slip’ in compound **55** (i.e. Cp* ligand assumes η^3 coordination mode, see Scheme 15), which is evidenced by Mo-C bond lengths ranging between 2.3184(19) Å and 2.5483(19) Å. A similar observation was made for the tungsten derivative **53**.¹⁶ Complexes **53**, **54**, and **55** are heavily ‘ π -loaded’ species, in which the short M-O bond lengths are indicative of bond orders closer to 2.5 than 2. For

comparison, the CpAm M(IV) oxo complexes **48** and **49** have been assigned bond orders of 2.5, and display comparable M-O bond lengths [cf. Mo-O = 1.7033(19) Å and W-O = 1.7234(17) Å].⁵ On the other hand, the previously mentioned Mo(VI) dioxo compound **50** displays much longer Mo-O bond lengths, which are more in line

Scheme 15. Schematic representation of conversion between η^5 and η^3 coordination modes for Cp* ligand.



with a bond order of 2 [cf. Mo-O = 1.891(4) Å and 1.748(5) Å].¹⁴ Given this increased bond order, the d electron counts for molybdenum and tungsten in compounds **53**, **54**, and **55** are greater than 18, as an 18 electron species would be expected if each M-O bond had a bond order of 2. Therefore, the Cp* ligand may relieve this ‘extra’ electron density of the molybdenum center by adopting an η^3 coordination mode.

2.2.3 OAT Reactions of CpAm M(IV) Dioxo Compounds

With the dioxo compounds **53**, **54**, and **55** in hand, and the knowledge that they may be generated from O₂ (for Mo), it next became of interest to test their reactivity towards a variety of substrates. Of primary importance was the reactivity of these species towards olefins in order to assess the possible ability to utilize them as olefin epoxidation catalysts, given the long historical importance of such reactions,¹⁸⁻²⁰ which have often been catalyzed by molybdenum (VI) dioxo compounds.^{14,15,21-24}

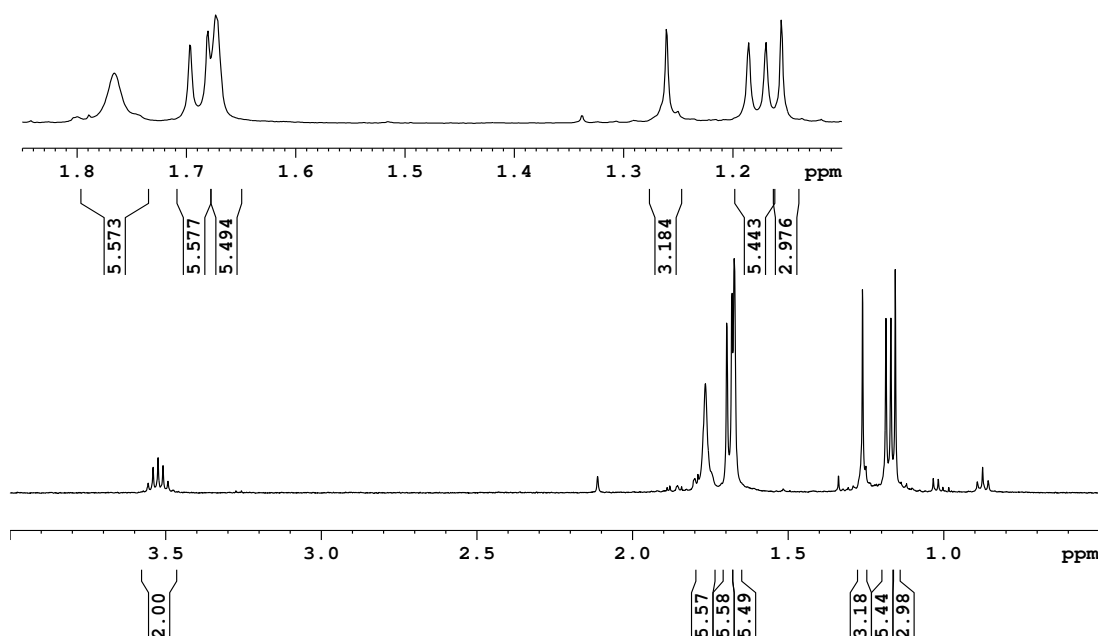
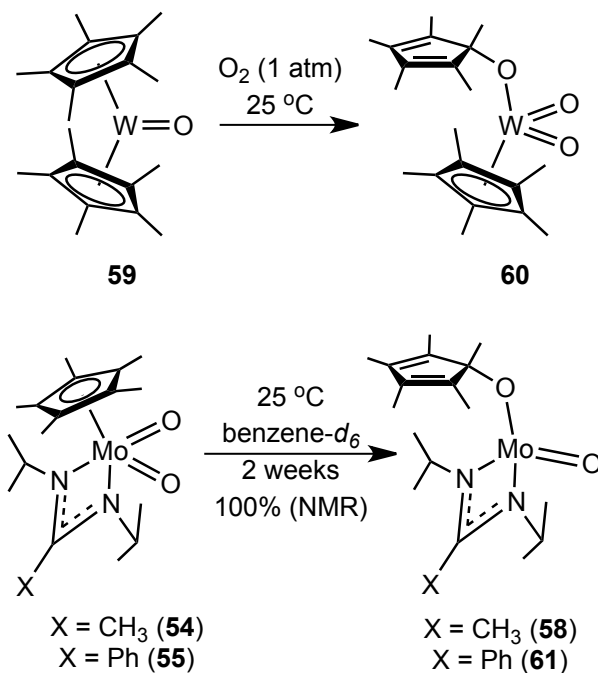


Figure 13. Crude ^1H (400 MHz, benzene- d_6 , 25 °C) NMR spectrum of decomposition product **58**.

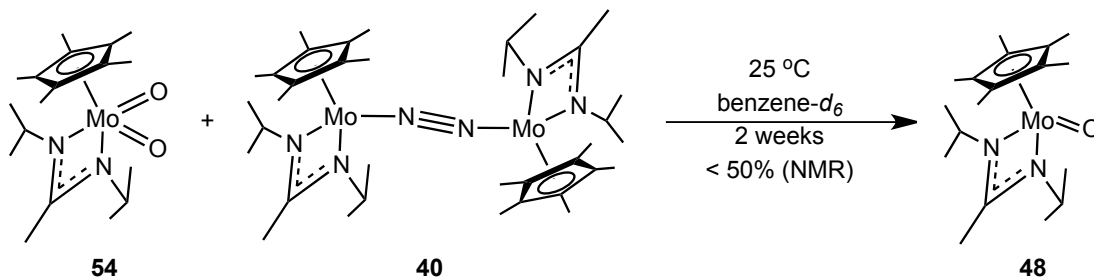
Compounds **53** and **54** were reacted with ethene, 1-hexene, styrene, and *cis*-cyclooctene within sealed NMR tubes to test their reactivity towards olefins. In each case, **53** showed no reaction. The molybdenum analog **54** was found to react slowly over the course of two weeks at 25 °C, however in each case there was no observation of any oxidized organic product. Furthermore, the same CpAm molybdenum species was observed in each case as judged by ^1H NMR, indicating that **54** thermally decomposes to a new CpAm compound (**58**) in solution at 25 °C without any interaction with the olefin substrate. Conclusive evidence for the structure of the **58** could not be obtained through single crystal X-ray diffraction (XRD) given that the new species would not crystallize from common organic solvents, or mixtures thereof. Luckily, the ^1H NMR of **58** provides insight into its structure (Figure 13).

Scheme 16



Compound **58** does not display the characteristic singlet (15 H) for the Cp* ligand observed in nearly all other CpAm compounds, but rather two broadened singlets (6 H each) and one sharp singlet (3 H), indicative of a ‘tuck-in’ complex, in which the Cp* ring has been activated and formed a new bond to an oxo ligand. The fact that two of the singlets for the activated Cp* ligand are broadened is indicative of free rotation about the newly formed C-O bond on the order of the NMR time scale, and coordination of the rest of the Cp* ring through the remaining double bonds is not likely. Bercaw and Parkin have previously demonstrated that the tungstenocene oxo complex Cp*₂WO (**59**) reacts with O₂ to cleanly produce such a ‘tuck-in’ species Cp*W(O)₂[η¹-OC₅(CH₃)₅] (**60**) (Scheme 16).²⁵ Accordingly, it is reasonable to propose that compound **58** exists in solution with structure [η¹-OC₅(CH₃)₅][N(ⁱPr)C(CH₃)N(ⁱPr)]Mo(O) (Scheme 16). Compound **58** likely does not

Scheme 17



bear a second terminal oxo ligand as in the case of **60**, as the insertion into the Cp* ligand is likely driven by reduction in electron density at the metal center. Furthermore, the only source for the additional oxo ligand would be from a second equivalent of **54**, which would result in the formation of the monoxo species **48**, which was not observed by ^1H NMR. Efforts to obtain conclusive evidence of the structure of **58** through decomposition of the analogous phenyl substituted CpAm dioxo species **55** were also unsuccessful, as the resulting Cp* activation product $[\eta^1\text{-OC}_5(\text{CH}_3)_5][\text{N}(\text{iPr})\text{C}(\text{Ph})\text{N}(\text{iPr})]\text{Mo}(\text{O})$ (**61**) also was resistant to crystallization.

Lastly, the oxidation of other reduced substrates was examined, specifically dimethyl sulfide, triphenyl phosphine, and CO. Again, **53** was found to be unreactive towards all reagents, and **54** displayed analogous decomposition as described above. Interestingly, when compound **54** was reacted with the ‘end-on-bridged’ dinitrogen compound **40** (the precursor for its synthesis) in a 1:1 ratio (Scheme 17), slow conversion to the CpAm monoxo compound **48** was observed by ^1H NMR (Figure 14), making compound **40** the only species capable of being oxidized by **54**. After two weeks, conversion slowed to a halt, and unrecognizable decomposition was observed at longer reaction times.

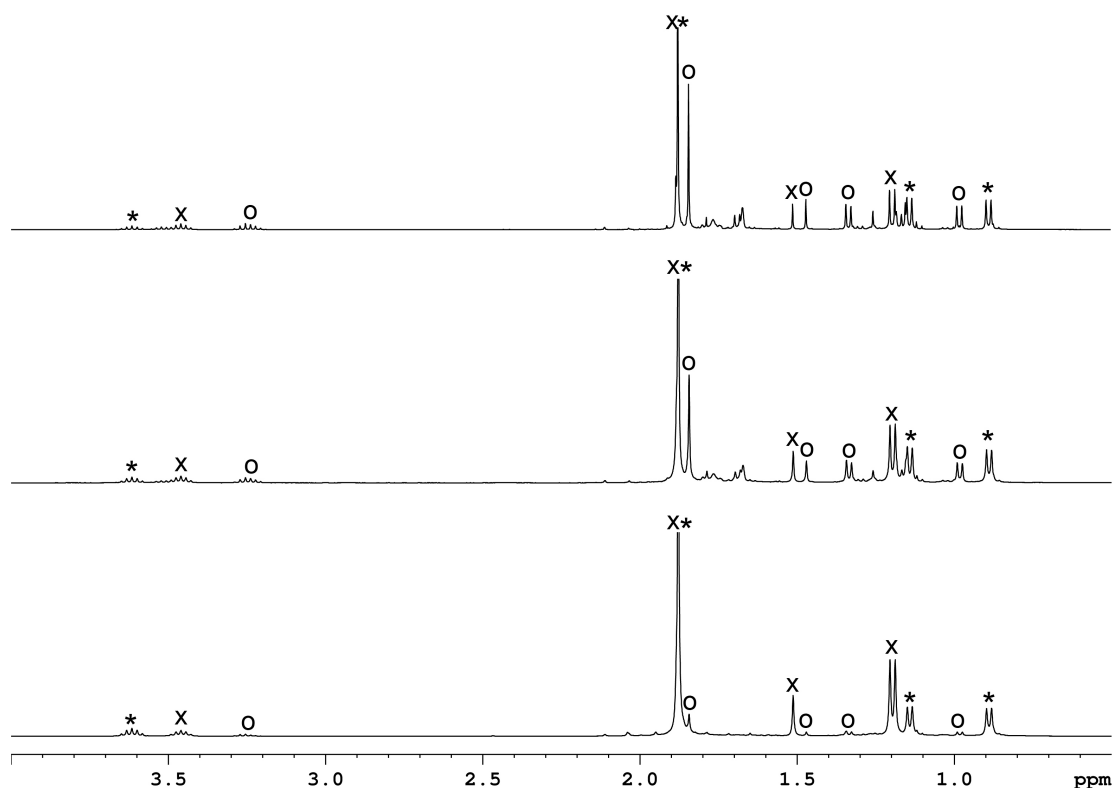


Figure 14. ^1H (400 MHz, benzene- d_6 , 25 °C) NMR spectra demonstrating the production of **48** (o) from reaction of **40** (*) and **54** (x) after 0 d (bottom), 6 d (middle), and 14 d (top). (Note: Cp* resonances for **40** and **54** overlap one another).

At first glance, it may seem odd that the CpAm dioxo compounds **53**, **54**, and **55** do not undergo OAT to common organic substrates, while the very similar Cp dioxo chloride species **50**, **51**, and **52** are catalytically active for such transformations. Likely, the difference in reactivity is a result of both the electronics and sterics of the metal centers. Compounds **50**, **51**, and **52** are 16 electron complexes, making them susceptible to coordination of a substrate to the metal center to undergo OAT. On the other hand, compounds **53**, **54**, and **55** are 18 electron species (perhaps greater, *vide supra*) making them coordinatively saturated and resistant to substrate coordination. Furthermore, the amidinate ligand adds a significant amount of steric bulk compared

to a chloride ligand, making an approach to the metal of a substrate unlikely. In the case of olefin epoxidation, the previously noted catalytic processes are suspected to require the presence of ^tBuOOH to generate the active catalyst, a step which was not desired here. Together, these factors likely contribute to the inability of these species to undergo OAT.

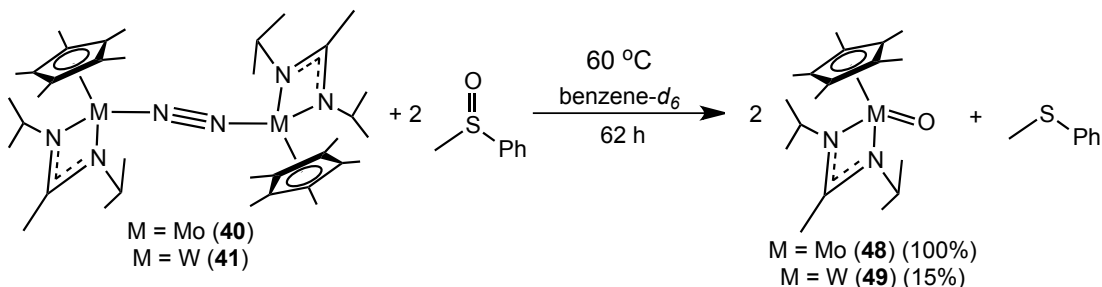
2.3 Catalytic Sulfoxide Deoxygenation

2.3.1 Background

Sulfoxides represent an extremely valuable functional group for asymmetric synthesis of organic and biologically active compounds, mostly due to the large differences in the nature of the substituents on the stereogenic sulfur atom (alkyl groups, oxygen atom, and lone pair).²⁶ Although useful for synthesis, the presence of the sulfoxide functional group in a given product is not always desired. As such, methods for the reduction of sulfoxides have been developed, with the goal of providing processes that show tolerance to a variety of functional groups, proceed under ambient conditions, and do not require the use of harsh reagents. To this end, reports of the catalytic reduction of sulfoxides by copper,²⁷ titanium,²⁸ iron,²⁹ rhenium,^{30,31} and nickel³² catalysts have appeared in the literature, along with reports of stoichiometric sulfoxide reduction employing catecholborane³³ and 2,6-dihydroxypyridine.³⁴

The group 6 oxo complexes **48** and **49** have previously been shown to react with CO to eliminate CO₂ and generate the known bis(carbonyl) compounds **44** and **45**, respectively. Accordingly, we reasoned that OAT from sulfoxides to CO could be

Scheme 18

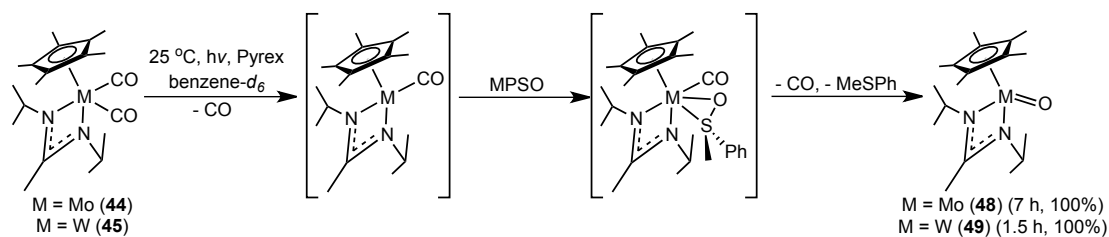


possible using mid valent group 6 CpAm compounds through a similar catalytic cycle (*vide infra*).⁵ Molybdoenzymes (e.g. dimethylsulfoxide reductase) are known to exist in high oxidation states, and function through a Mo(IV)/Mo(VI) redox couple.¹⁰ Accordingly, there have been several reports on the use of high valent group 6 compounds to deoxygenate sulfoxides,^{30,35,36} however none that operate through a more reduced M(II)/M(IV) cycle.

2.3.2 Reactivity of CpAm Compounds with Sulfoxides

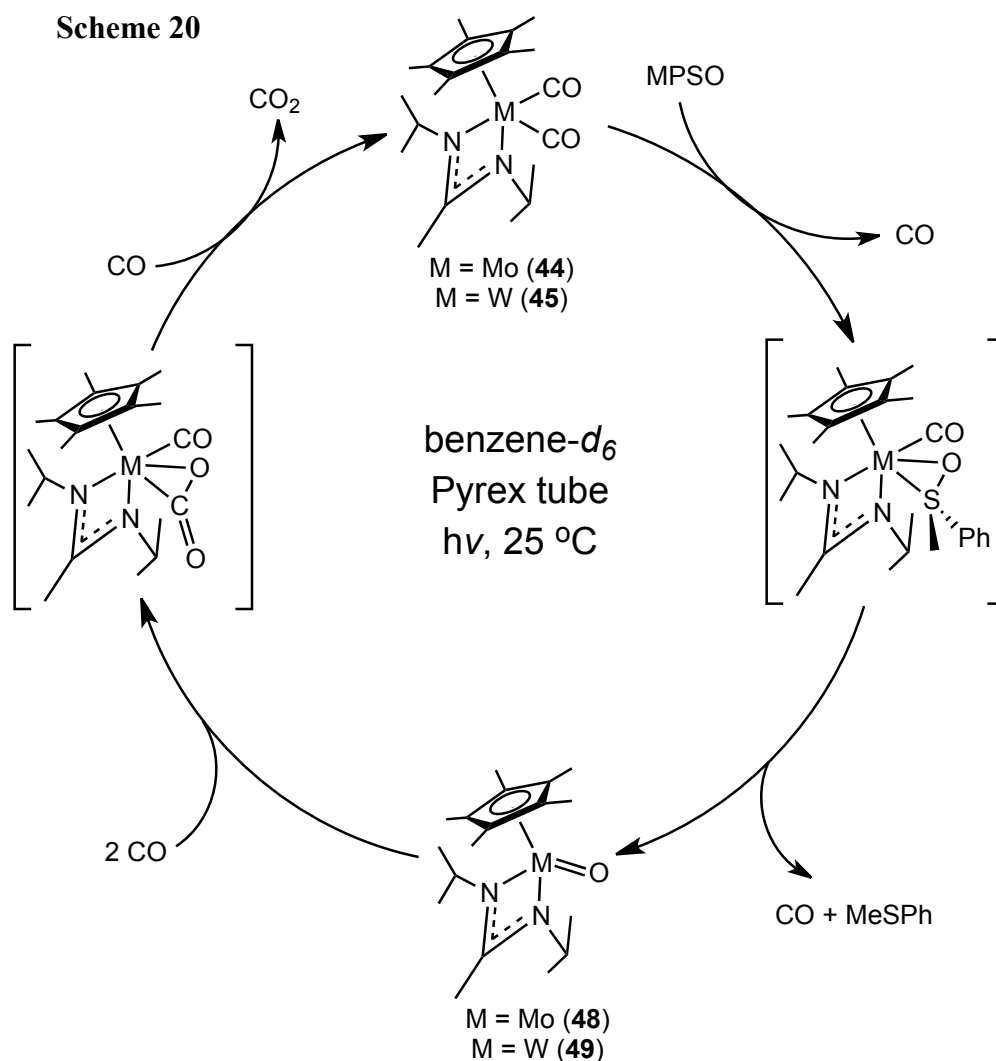
To begin, the ‘end-on-bridged’ dinitrogen compounds **40** and **41** were reacted with methyl phenyl sulfoxide (MPSO). For the molybdenum compound **40**, gentle heating (60 °C) lead to complete conversion to the terminal oxo compound **48** with concomitant formation of thioanisole. The tungsten analog **41** reacted similarly under identical conditions, however the reaction was considerably slower, reaching only 15% completion during the same time period (Scheme 18). Cummins and coworkers have reported similar reactivity of the three coordinate molybdenum amido complex **31**, which reacts with dimethyl sulfoxide (DMSO) to yield a terminal oxo species (O)Mo[N(R)Ar]₃ (**62**) and dimethyl sulfide.³⁷

Scheme 19



Looking next to determine if MPSO could generate the oxo compounds **48** and **49** from more catalytically relevant starting materials, reaction with the bis(carbonyl) species **44** and **45** was explored. In the absence of ultraviolet (UV) light, no reaction between **44** or **45** and MPSO was observed. However, upon irradiation of benzene-*d*₆ solutions of compounds **44** and **45** with excess MPSO within sealed Pyrex NMR tubes with UV light, generation of the corresponding oxo compounds **48** and **49** was observed to occur quickly, as judged by ¹H NMR. Given previously observed photolytic reactivity of compounds **44** and **45**,⁵ it is likely that upon photolysis, one carbonyl ligand dissociates from the metal center, presenting an open coordination site for a substrate. MPSO then coordinates to the metal center in an η² fashion, before cleavage of the S-O bond and dissociation of the remaining carbonyl ligand (Scheme 19).

With the observation that the terminal oxo compounds **48** and **49** could be produced from the bis(carbonyl) species **44** and **45**, along with the knowledge that these bis(carbonyl) species can be regenerated from reaction of **48** and **49** with CO,⁵ a synthetic cycle had been completed. Accordingly, it was of interest to determine if the process could proceed catalytically. To this end, it was found that photolysis of a benzene-*d*₆ solution of either **44** or **45** with one equivalent of MPSO and excess CO



(initial pressure = 10 psi) within a sealed Pyrex NMR tube produced thioanisole and CO_2 catalytically (Scheme 20). The reaction was complete in 5 hours in the case of tungsten, and 16 hours in the case of molybdenum. During the course of the reactions, only the bis(carbonyl) species **44** and **45** are observed by ^1H NMR (Figure 15b). When ^{13}C -labeled CO was employed under identical conditions, production of $^{13}\text{CO}_2$ was confirmed through $^{13}\text{C}\{^1\text{H}\}$ NMR (Figure 15a). Upon addition of excess MPSO (ca. 5 eq.) to identical reaction mixtures, catalysis proceeded as expected but quickly slowed before complete conversion to thioanisole was observed. Eventually,

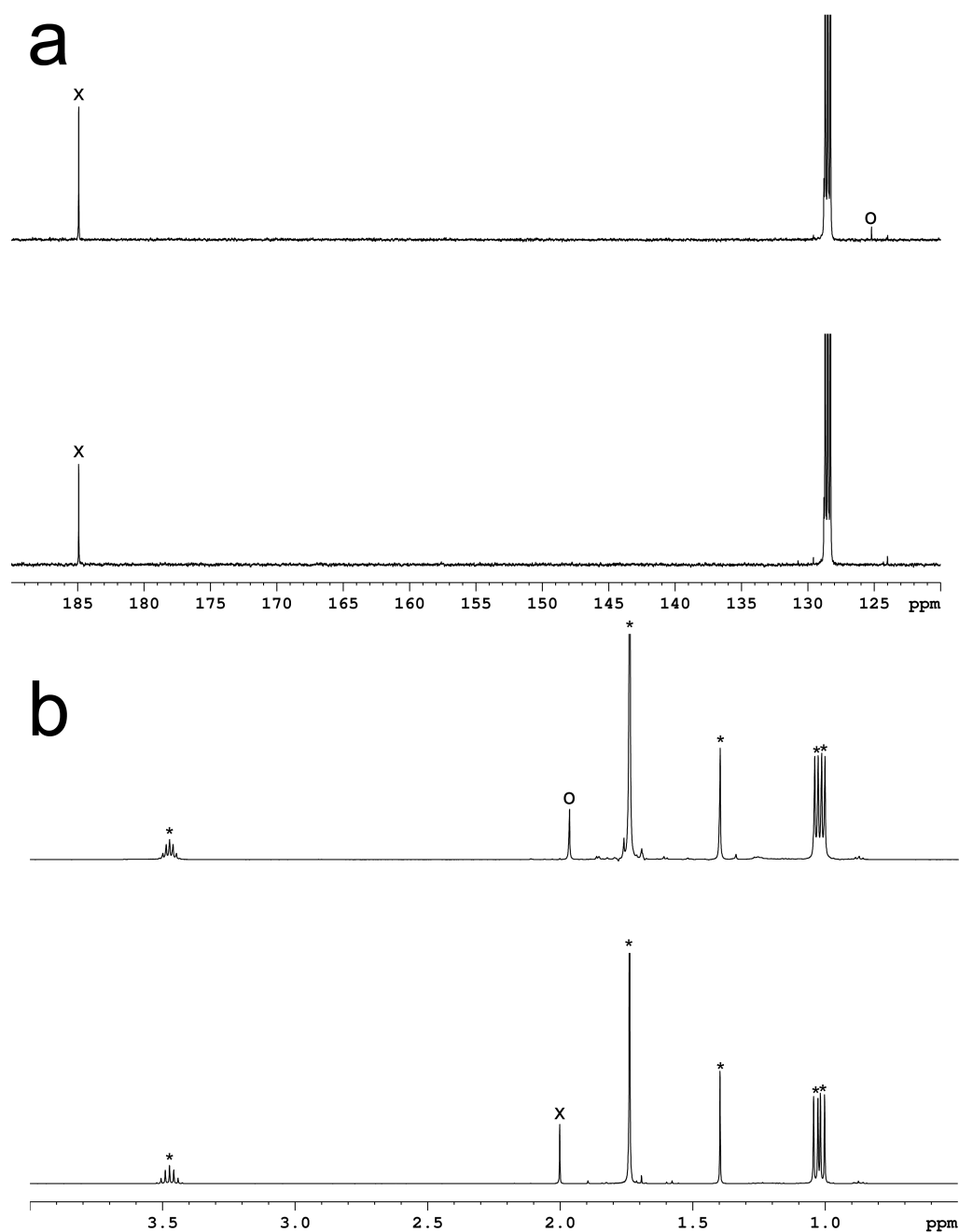


Figure 15. (a) $^{13}\text{C}\{^1\text{H}\}$ (125 MHz, benzene- d_6 , 25 °C) NMR spectra demonstrating the production of $^{13}\text{CO}_2$ (o) from OAT from MPSO to ^{13}CO (x) mediated by **44** after 0 h (bottom) and 3 h (top) UV irradiation. (b) ^1H (400 MHz, benzene- d_6 , 25 °C) NMR spectra demonstrating the production of thioanisole (o) from MPSO (x) catalyzed by **44** (*) after 0 h (bottom) and 24 h (top) UV irradiation.

catalysis halted completely and the catalysts were found to have fully decomposed, as determined by a lack of any identifiable resonances in the ^1H NMR and the presence of brown precipitates in the NMR tubes.

In order to determine the cause of catalyst decomposition, a series of test reactions were performed under controlled conditions. It was found that in the case of tungsten, the oxo complex **49** decomposes in the presence of excess MPSO upon photolysis. Presumably, during catalysis, when an excess amount of substrate is present, it is in sufficient concentration to decompose the short lived intermediate **49**. In the case of molybdenum, no such conclusion could be reached. However, it is possible that during OAT from **48** to CO, the transient intermediate $\text{Cp}^*\text{Mo}[\text{N}(\text{iPr})\text{C}(\text{CH}_3)\text{N}(\text{iPr})](\text{CO})(\eta^2\text{-CO}_2)$ (depicted in Scheme 20) reacts with MPSO, resulting in decomposition. However, given that such a complex cannot be isolated, testing this hypothesis was not possible.

2.4 Conclusions

We have previously shown that the CpAm oxo complexes **48** and **49** may engage in catalytic OAT.^{5,38} Looking to expand upon this chemistry, the ability of the CpAm dioxo species **53**, **54**, and **55** to undergo similar reactions was investigated. Unfortunately, no reaction was observed with a variety of common substrates. In the case of molybdenum compounds **54** and **55**, decomposition to ‘tuck-in’ compounds **58** and **61** was observed by ^1H NMR, however analysis by single crystal XRD proved elusive due to the poor crystallinity of these compounds. Interestingly, compound **54**

could engage in OAT to the ‘end-on’bridged’ dinitrogen compound **40**, but this process was found to be painfully slow and did not reach completion.

The first example of catalytic sulfoxide reduction by mid valent group 6 compounds was achieved and was found to proceed through a mechanism involving the CpAm bis(carbonyl) compounds **44** and **45** and oxo compounds **48** and **49**. This process requires photolysis to proceed, as the photodissociation of a carbonyl ligand is critical to open a coordination site for MPSO to coordinate to the metal center. Unfortunately, in the case of both molybdenum and tungsten, it appears that the substrate reacts in a nonproductive manner with short lived catalytic intermediates. Accordingly, when MPSO is present in sufficiently high concentration, catalysis is inhibited and the intermediates decompose to unidentifiable products.

2.5 References

- (1) Fontaine, P. P.; Yonke, B. L.; Zavalij, P. Y.; Sita, L. R. *J. Am. Chem. Soc.* **2010**, *132*, 12273.
- (2) Hirotsu, M.; Fontaine, P. P.; Epshteyn, A.; Zavalij, P. Y.; Sita, L. R. *J. Am. Chem. Soc.* **2007**, *129*, 9284.
- (3) Hirotsu, M.; Fontaine, P. P.; Zavalij, P. Y.; Sita, L. R. *J. Am. Chem. Soc.* **2007**, *129*, 12690.
- (4) Keane, A. J.; Yonke, B. L.; Hirotsu, M.; Zavalij, P. Y.; Sita, L. R. *J. Am. Chem. Soc.* **2014**, *136*, 9906.
- (5) Yonke, B. L.; Reeds, J. P.; Zavalij, P. Y.; Sita, L. R. *Angew. Chem. Int. Ed.* **2011**, *50*, 12342.
- (6) Hill, C. L. *Nature* **1999**, *401*, 436.
- (7) Lefort, T. E. French Patent 729,952, **1931**.
- (8) Punniyamurthy, T.; Velusamy, S.; Iqbal, J. *Chem. Rev.* **2005**, *105*, 2329.
- (9) Holm, R. H.; Solomon, E. I.; Majumdar, A.; Tenderholt, A. *Coord. Chem. Rev.* **2011**, *255*, 993.
- (10) Schindelin, H.; Kisker, C.; Hilton, J.; Rajagopalan, K. V.; Rees, D. C. *Science* **1996**, *272*, 1615.
- (11) Lorber, C.; Donahue, J. P.; Goddard, C. A.; Nordlander, E.; Holm, R. H. *J. Am. Chem. Soc.* **1998**, *120*, 8102.

- (12) Sugimoto, H.; Tatemoto, S.; Suyama, K.; Miyake, H.; Ito, S.; Dong, C.; Yang, J.; Kirk, M. L. *Inorg. Chem.* **2009**, *48*, 10581.
- (13) Thapper, A.; Donahue, J. P.; Musgrave, K. B.; Willer, M. W.; Nordlander, E.; Hedman, B.; Hodgson, K. O.; Holm, R. H. *Inorg. Chem.* **1999**, *38*, 4104.
- (14) Martins, A. M.; Romao, C. C.; Abrantes, M.; Azevedo, M. C.; Cui, J.; Dias, A. R.; Duarte, M. T.; Lemos, M. A.; Lourenco, T.; Poli, R. *Organometallics* **2005**, *24*, 2582.
- (15) Trost, M. K.; Bergman, R. G. *Organometallics* **1991**, *10*, 1172.
- (16) Yonke, B. L. Ph. D. Dissertation, University of Maryland, **2012**.
- (17) Cordero, B.; Gomez, V.; Platero-Prats, A. E.; Reves, M.; Echeverria, J.; Cremades, E.; Barragan, F.; Alvarez, S. *J. Chem. Soc., Dalton Trans.* **2008**, 2832.
- (18) Katsuki, T.; Sharpless, K. B. *J. Am. Chem. Soc.* **1980**, *102*, 5974.
- (19) Martin, V. S.; Woodard, S. S.; Katsuki, T.; Yamada, Y.; Ikeda, M.; Sharpless, K. B. *J. Am. Chem. Soc.* **1981**, *103*, 6237.
- (20) Chong, A. O.; Sharpless, K. B. *J. Org. Chem.* **1977**, *42*, 1587.
- (21) Figueiredo, S.; Gomes, A. C.; Fernandes, J. A.; Almeida Paz, F. A.; Lopes, A. D.; Lourenco, J. P.; Pillinger, M.; Goncalves, I. S. *J. Organomet. Chem.* **2013**, *723*, 56.
- (22) Coelho, A. C.; Nolasco, M.; Balula, S. S.; Antunes, M. M.; Pereira, C. C. L.; Almeida Paz, F. A.; Valente, A. A.; Pillinger, M.; Ribeiro-Claro, P.; Klinowski, J.; Goncalves, I. S. *Inorg. Chem.* **2011**, *50*, 525.
- (23) Grover, N.; Kuhn, F. E. *Curr. Org. Chem.* **2012**, *16*, 16.
- (24) Jimtaisong, A.; Luck, R. L. *Inorg. Chem.* **2006**, *45*, 10391.
- (25) Parkin, G.; Bercaw, J. E. *J. Am. Chem. Soc.* **1989**, *111*, 391.
- (26) Carreno, M. C. *Chem. Rev.* **1995**, *95*, 1717.
- (27) Enthaler, S.; Weidauer, M. *Catal. Lett.* **2011**, *141*, 833.
- (28) Yoo, B. W.; Min, S. K. *Synth. Commun.* **2011**, *41*, 2993-.
- (29) Cardosa, J. M. S.; Royo, B. *Chem. Comm.* **2012**, *48*, 4944.
- (30) Cabrita, I.; Sousa, S. C. A.; Fernandes, A. C. *Tetrahedron Lett.* **2010**, *51*, 6132.
- (31) Sousa, S. C. A.; Bernardo, J. R.; Romao, C. C.; Fernandes, A. C. *Tetrahedron* **2012**, *68*, 8194.
- (32) Khurana, J. K.; Ray, A.; Singh, S. *Tetrahedron Lett.* **1998**, *39*, 3829.
- (33) Harrison, D. J.; Tam, N. C.; Vogels, C. M.; Langer, R. F.; Baker, R. T.; Decken, A.; Westcott, S. A. *Tetrahedron Lett.* **2004**, *45*, 8493.
- (34) Miller, S. J.; Collier, T. R.; Wu, W. *Tetrahedron Lett.* **2000**, *41*, 3781.
- (35) Whiteoak, C. J.; Britovsek, G. J. P.; Gibson, V. C.; White, A. J. P. *J. Chem. Soc., Dalton Trans.* **2009**, 2337.
- (36) Arumuganathan, T.; Mayilmurugan, R.; Volpe, M.; Mosch-Zanetti, N. C. *J. Chem. Soc., Dalton Trans.* **2011**, 7850.
- (37) Johnson, A. R.; Davis, W. M.; Cummins, C. C.; Serron, S.; Nolan, S. P.; Musaev, D. G.; Morokuma, K. *J. Am. Chem. Soc.* **1998**, *120*, 2071.
- (38) Reeds, J. P.; Yonke, B. L.; Zavalij, P. Y.; Sita, L. R. *J. Am. Chem. Soc.* **2011**, *133*, 18602.

Chapter 3: Catalytic Sulfur Atom Transfer Reactions Employing Elemental Sulfur

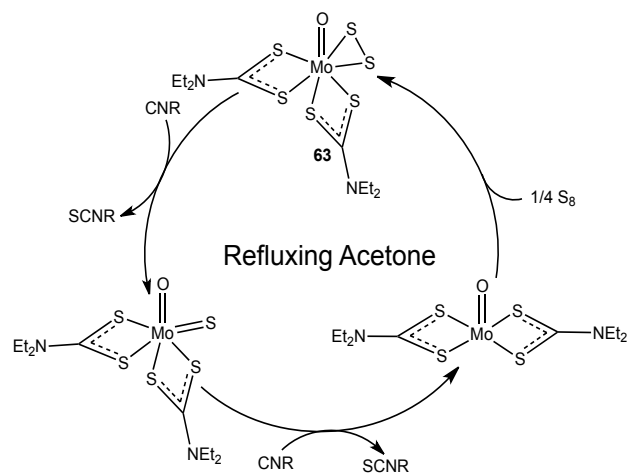
3.1 Introduction

Although catalytic OAT processes mediated by transition metals which employ O₂ as an oxidant are well understood and capable of preparing important small molecules containing nearly all possible oxygen containing functional groups,¹ the analogous sulfur atom transfer (SAT) processes employing elemental sulfur (S₈) are extremely scarce by comparison. S₈ is an attractive source of sulfur for SAT reactions as it is by far the least expensive and most abundant form of the element. As such, it has found use in several other types of applications, including polymer vulcanization, in which crosslinks composed of varying amounts of sulfur atoms lead to increased strength, durability, and elasticity of polymeric materials.²

Exactly 60 years after the first report of metal catalyzed OAT involving O₂,³ Khan and Siddiqui reported the first transition metal mediated catalytic SAT reaction, in which cyclohexene was transformed to cyclohexene sulfide at slightly elevated temperatures in water/ethanol (50/50) using a dinuclear ruthenium catalyst and S₈.⁴ Although this report marked a breakthrough for SAT technology, doubts have been cast on its success, as efforts to duplicate the reaction have failed.⁵

Since this initial report, analogous claims of catalytic SAT still remain scarce. Adam and coworkers have successfully utilized high valent molybdenum species to prepare a variety of sulfur containing small molecules. Specifically, the oxo disulfide molybdenum (VI) compound (S₂CNEt₂)₂Mo(O)(S₂) (**63**) was found to catalyze the

Scheme 21



episulfidation of (E)-cyclooctene and (E)-cyclononene in refluxing acetone to provide moderate yields of the corresponding *trans*-cycloalkene episulfides, in a process involving a Mo(IV)/Mo(VI) cycle.⁶ This process was expanded to include an even wider array of cyclic alkenes and allenes, however it was found that thiiranes serve as better sulfur atom sources for such reactions.⁵ Compound **63** could even be used to generate isothiocyanates from the corresponding isonitriles and S₈, again in a process involving a high valent Mo(IV)/Mo(VI) cycle (Scheme 21) operating at elevated temperatures, however long reaction times were found to be necessary (i.e. several days).⁷

Conversely, catalytic desulfurization of substrates is also of interest, as such processes are key to refining of petroleum feed stocks. Industrial processes for such reactions involve heterogeneous molybdenum or tungsten catalysts operating at high temperatures (> 400 °C).⁸ Accordingly, there has been interest in the development of catalysts which may provide the same reactivity under more reasonable conditions. Espenson and a coworker have reported such a process, in which a rhenium catalyst

desulfurizes a variety of thiiranes in high yield, with triphenyl phosphine present to accept the removed sulfur atom.⁹

Given the large disparity in reports of SAT and OAT in the literature, and our group's previous success in the use of mid valent CpAm group 6 compounds to catalyze OAT reactions, we sought to explore the possibility of catalytic SAT employing S₈. Carbonyl sulfide (COS) and isothiocyanates appeared to be appropriate targets for such reactions, in that they are the sulfur analogues of CO₂ and isocyanates, which we have been successful in preparing catalytically *via* OAT.¹⁰

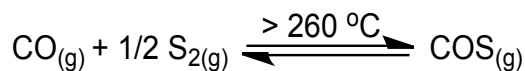
3.2 Carbonyl Sulfide

3.2.1 Background

COS is known to occur naturally on Earth through volcanic events^{11,12} or as a result of biological processes,¹³ and has been detected on a number of other planets as well, where it is considered a biosignature.¹⁴ Presently, COS is also released to the atmosphere from combustion processes, but these constitute only a small fraction of total atmospheric COS concentration (500 ppt).¹⁵ It has been shown that under mild conditions, COS generates oligopeptides from amino acids, indicating that it may have played a critical role in the origin of life.¹⁶⁻¹⁸ It's sources on primordial Earth, however, would have been limited to volcanism, leading some to wonder if alternative sources could have produced COS under prebiotic conditions.

The first laboratory preparation of COS was reported by Than in 1867, in which he found it to exist in equilibrium with CO_(g) and S_{2(g)} at high temperatures (> 260 °C) (Scheme 22).¹⁹ Today, COS is prepared on a preparative scale by reaction of

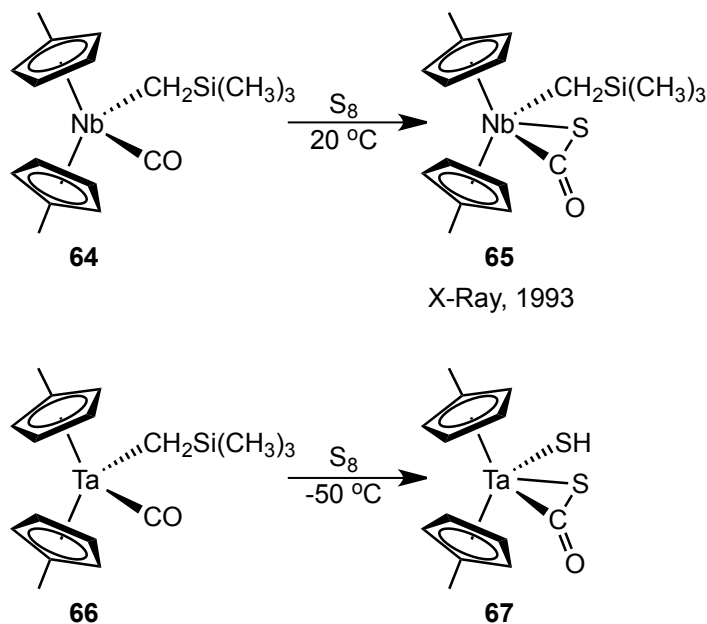
Scheme 22



potassium cyanate with sulfuric acid, a process which requires extensive purification of the product. Specifically, CO_2 , hydrogen sulfide (H_2S), formaldehyde, carbon disulfide (CS_2), and hydrogen cyanide (HCN) are removed by treatment of the crude reaction mixture with cupric sulfate (CuSO_4) and sulfuric acid, passing through aqueous potassium hydroxide, extracting with aniline in ethanol, and treating again with sulfuric acid. Consequently, COS is difficult to prepare in the laboratory and is extremely expensive to purchase. Furthermore, COS is a hazardous substance to handle and transport, as exposure may lead to conjunctivitis, lachrymation, and photophobia.¹⁵

Nicholas and coworkers have demonstrated that η^2 coordinated COS may be

Scheme 23

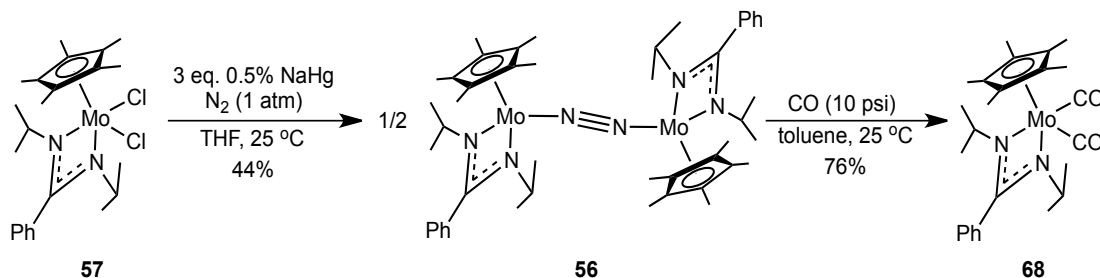


generated directly from CO and S₈ with group 5 metallocene complexes. Specifically, the niobium (III) carbonyl species [η^5 -C₅H₄(CH₃)₂Nb(CO)[CH₂Si(CH₃)₃] (**64**) was treated with 1 equivalent of S₈ at 20 °C to produce the COS species [η^5 -C₅H₄(CH₃)₂Nb[κ -(S,C)COS][CH₂Si(CH₃)₃] (**65**),²⁰ and the similar tantalum (III) carbonyl species [η^5 -C₅H₄(CH₃)₂Ta(CO)(H) (**66**) was found to react with one equivalent of S₈ at lower temperature to produce [η^5 -C₅H₄(CH₃)₂Ta[κ -(S,C)COS](SH) (**67**) (Scheme 23).²¹ In the case of compound **65**, X-ray diffraction provided the solid state structure, thus confirming the η^2 coordination of COS. In both cases, however, release of COS from the metal center was not reported. In fact, no reports for metal mediated production of free COS from its most basic components (i.e. CO and S₈) have appeared in the literature to provide a safe and low energy alternative route for its synthesis. Accordingly, we set out to ascertain whether such a process is possible through the use of mid valent CpAm group 6 compounds.

3.2.2 Synthesis and Characterization of New Compounds and SAT Reactions

As mentioned previously, the CpAm group 6 bis(carbonyl) compounds **44** and **45** are capable of mediating photocatalytic OAT reactions.¹⁰ Accordingly, it appeared reasonable to use a similar compound to catalyze the desired SAT. In this case, however, the use of a phenyl group in the distal position of the amidinate ligand was employed, as it has been shown by Mountford that such a substitution in group 4 CpAm compounds may lead to increased crystallinity.²² As such, the molybdenum (II) bis(carbonyl) compound Cp*Mo[N(ⁱPr)C(Ph)N(ⁱPr)](CO)₂ (**68**) was prepared by

Scheme 24



treatment of the ‘end-on-bridged’ dinitrogen compound **56** with CO, which itself was obtained in moderate yield through chemical reduction (NaHg) of the dichloride precursor (**57**) under N₂ atmosphere, according to well established procedures within our group (Scheme 24).²³ Upon photolysis of a benzene-*d*₆ solution of compound **68** under ¹³CO atmosphere (initial pressure = 10 psi) in the presence of excess S₈ (10 equivalents as a suspension) within a sealed Pyrex NMR tube at 25 °C, generation of ¹³COS was observed to occur by ¹³C{¹H} NMR at the expense of ¹³CO.²⁴ After 105 hours of photolysis, nearly complete consumption of ¹³CO was observed to have occurred, and ¹³COS was the only species seen in the ¹³C{¹H} NMR spectrum (Figure 16), marking the first case for metal mediated synthesis of COS from CO and S₈, and the first preparation under mild conditions which eliminates the generation of myriad by products.

We next set out to determine the mechanism for the observed reaction. NMR spectra recorded at intermediate time points provided useful insight. The most obvious feature we noticed from the ¹³C{¹H} NMR spectra was the lack of the resonance for ¹³C-labeled **68** (δ_{CO} = 269 ppm) at all time points, indicating that **68** serves as a *pre-catalyst*, and does not reenter the catalytic cycle at all. Secondly, two new resonances appeared between 2 and 18 hours indicating that two new ¹³C-labeled

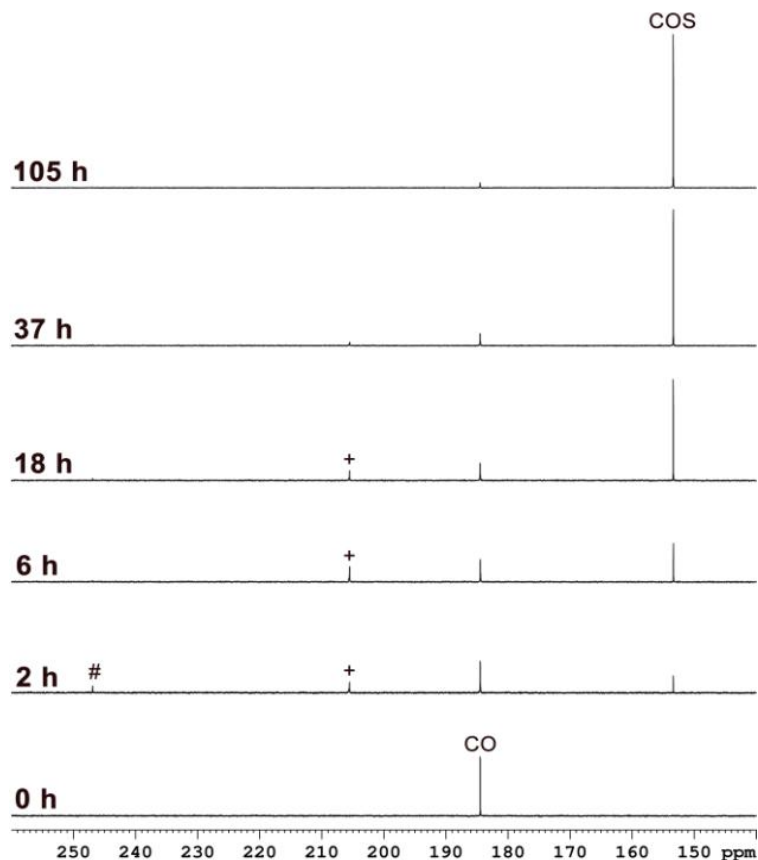


Figure 16. Partial $^{13}\text{C}\{^1\text{H}\}$ (125 MHz, benzene- d_6 , 25 °C) NMR spectra for the photolysis of **68** in the presence of ^{13}CO and excess S_8 at different timed intervals. Labeled resonances are ^{13}C -labeled **71** (#) and ^{13}C -labeled **75** (+).

intermediate species had been generated and slowly consumed (Figure 16, labels # and +). ^1H NMR also revealed the production and disappearance of three new CpAm compounds, two of C_s symmetry and one of C_1 symmetry (Figure 17). Accordingly, it seemed reasonable to assume three new CpAm species had been generated; one of C_s symmetry bearing a carbonyl ligand, one of either C_s or C_1 symmetry bearing a carbonyl ligand, and one without a carbonyl ligand and of either C_s or C_1 symmetry.

A series of NMR experiments were conducted to learn more about the role of these intermediate species in catalysis, and determine their identities. To begin,

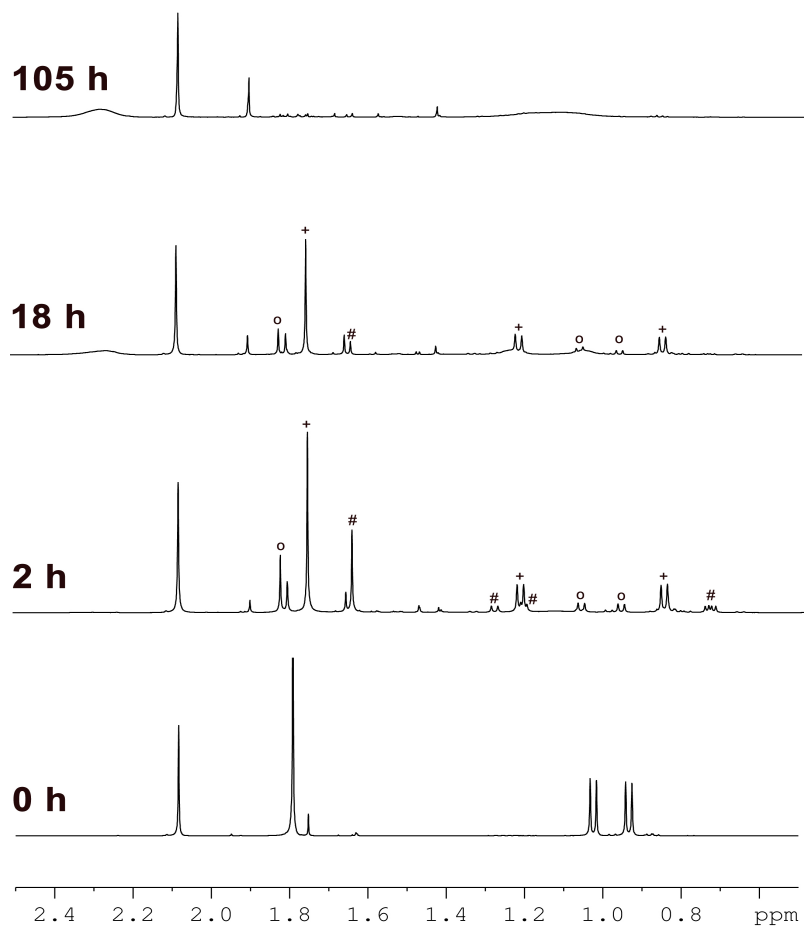
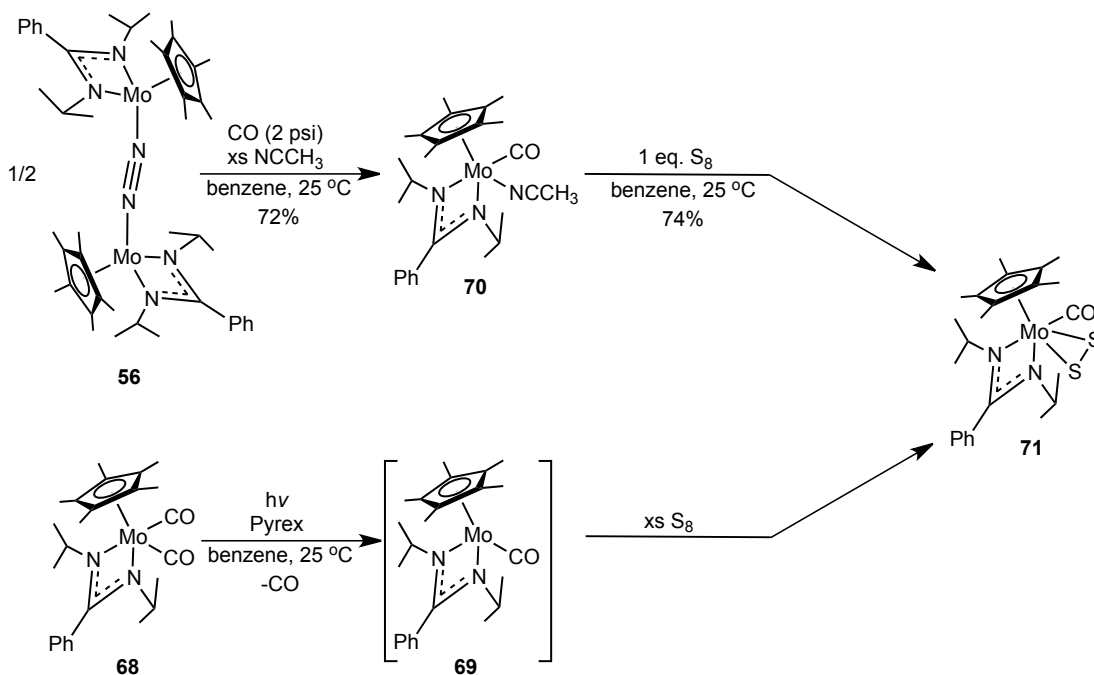


Figure 17. Partial ^1H (400 MHz, benzene- d_6 , 25 $^\circ\text{C}$) NMR spectra for the photolysis of **68** in the presence of ^{13}CO and excess S_8 at different timed intervals. Labeled resonances are **71** (#), **75** (+), and **77** (o). (Note: Unlabeled singlet at 2.08 ppm is durene internal standard).

compound **68** was found to be inert toward reaction with S_8 in the absence of photolysis under Ar atmosphere. However, when photolyzed, the unidentified C_1 symmetric species was observed by ^1H NMR (Figure 17, labeled with #). When ^{13}C -labeled **68** was used instead, $^{13}\text{C}\{^1\text{H}\}$ NMR revealed this new species to be the same as one observed during catalysis (Figure 16, labeled with #). Based on this

Scheme 25



observation and knowledge of the photoreactivity of group 6 CpAm bis(carbonyl) compounds,¹⁰ it seemed reasonable to assume that **68** undergoes photodissociation of one carbonyl ligand upon photolysis to produce the coordinatively unsaturated intermediate Cp*Mo[N(ⁱPr)C(Ph)N(ⁱPr)](CO) (**69**), which then reacts rapidly with S₈ to produce the new C₁ symmetric product. Seeing as **69** cannot be synthesized and isolated, we decided to prepare a model compound bearing a weakly coordinating ligand, which would be easily displaced in order to prepare large quantities of the new intermediate species in a *non-photolytic* manner. Accordingly, the mono(acetonitrile), mono(carbonyl) complex Cp*Mo[N(ⁱPr)C(Ph)N(ⁱPr)](CO)(NCCH₃) (**70**) was prepared by treatment of **56** with excess acetonitrile (ca. 20 equiv.) and CO (2 psi), as depicted in Scheme 25.^{10,25,26} In the solid state, compound **70** was found to display a long C-O bond length [1.183(2)

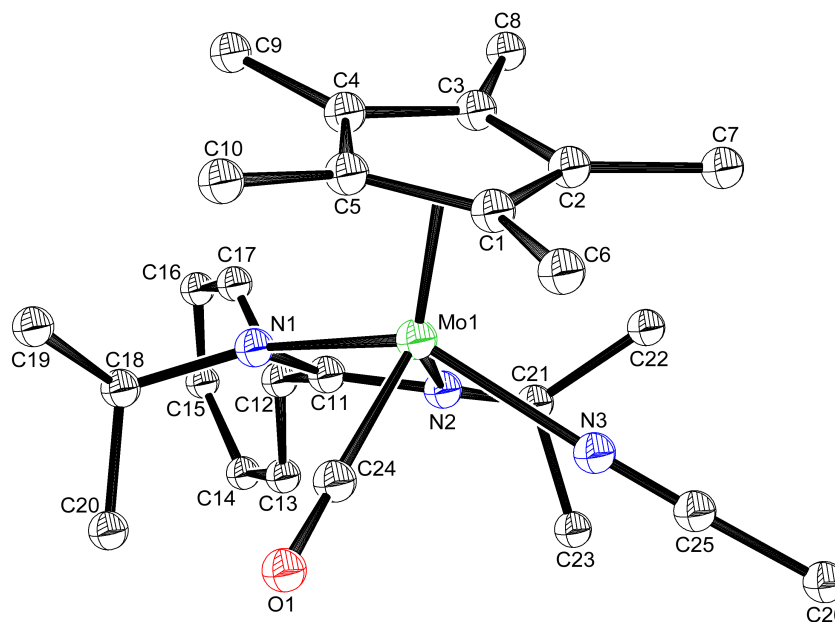


Figure 18. Molecular structure of compound **70** (30% thermal ellipsoids). Hydrogen atoms have been omitted for clarity. Selected bond lengths (Å): Mo1-N3 2.1228(15), N3-C25 1.145(2), Mo1-C24 1.9000(18), C24-O1 1.183(2).

Å] (Figure 18) and a C-O bond stretching frequency of $\nu_{\text{CO}} = 1767 \text{ cm}^{-1}$, indicative of substantial π -backbonding from the molybdenum (II) center to the carbonyl ligand's π^* orbital. This observation is a result of CO being a much stronger π -acid than acetonitrile, and indicated that acetonitrile should be easily displaced as planned. Indeed, upon treatment of **70** with 1 equivalent of S_8 , immediate formation of the new C_1 symmetric species was observed by ^1H NMR, along with free acetonitrile (Figure 19). As Scheme 25 reveals, this method provided for the isolation of the desired intermediate compound as an orange crystalline solid in larger quantities and in high yield, which lead to complete characterization as the molybdenum (IV) mono(carbonyl), disulfide species $\text{Cp}^*\text{Mo}[\text{N}(\text{iPr})\text{C}(\text{Ph})\text{N}(\text{iPr})](\text{CO})(\eta^2\text{-S}_2)$ (**71**) by spectroscopic and elemental (C, H, N) analyses.

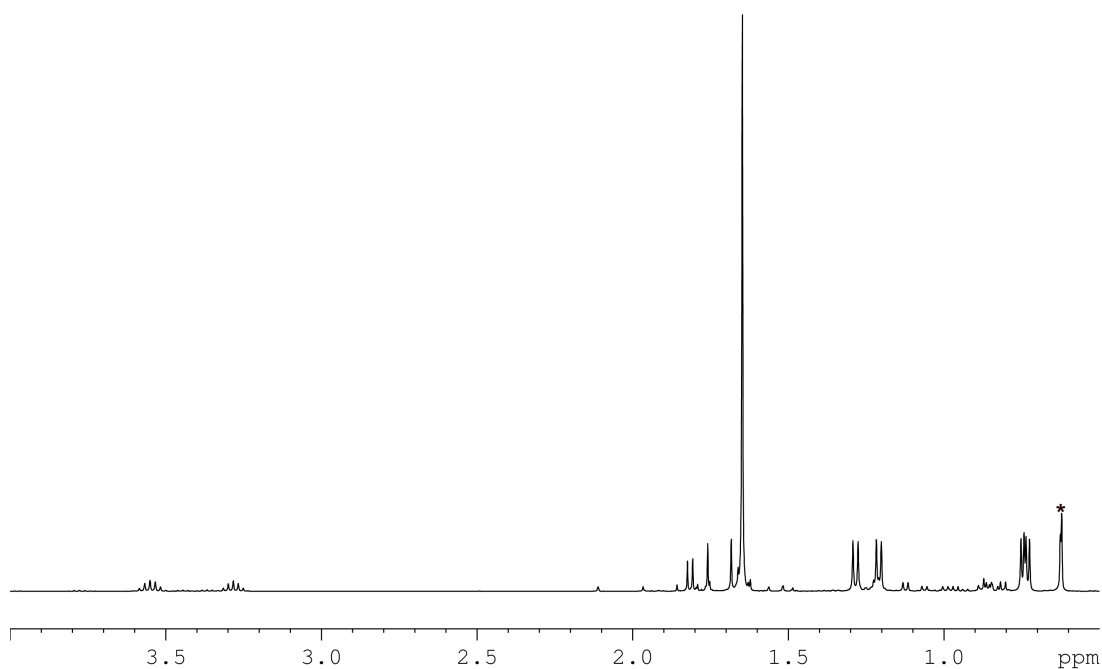


Figure 19. Partial ^1H (400 MHz, benzene- d_6 , 25 °C) NMR spectrum demonstrating the displacement of acetonitrile (labeled with *) from compound **70** by S_8 to generate compound **71**.

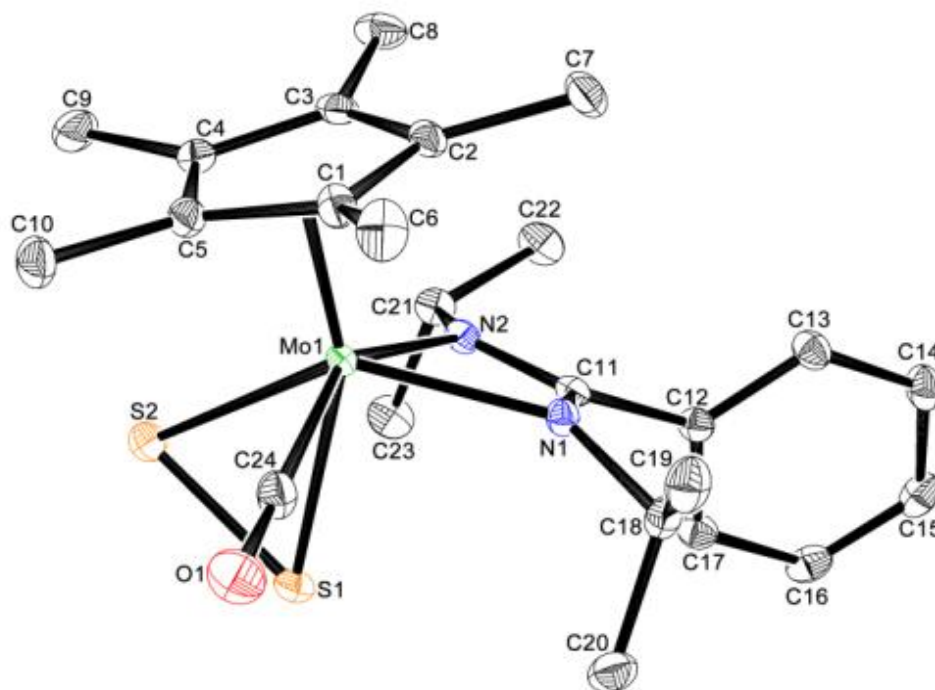
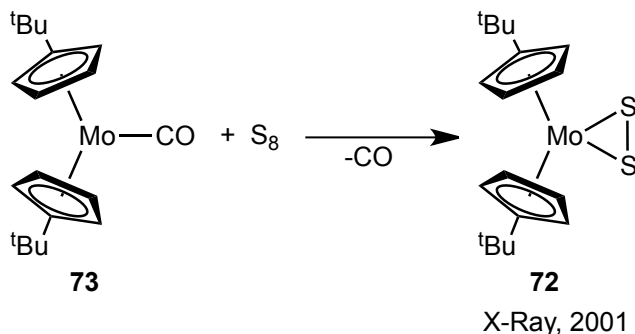


Figure 20. Molecular structure (30% thermal ellipsoids) of compound **71**. H atoms have been omitted for clarity. Selected bond lengths (Å): Mo1-S1 2.4659(4), Mo1-S2 2.4665(4), Mo1-C24 1.9901(17), C24-O1 1.149(2), S1-S2 2.0555(6).

In the solid state (Figure 20), compound **71** exhibits a short C-O bond length of 1.149(2) Å and an IR absorption at $\nu_{\text{CO}} = 1921 \text{ cm}^{-1}$, indicative of only moderate π -backbonding to the CO ligand. On the other hand, the S-S bond of 2.0555(6) Å is considerably longer than that in free S_2 (1.887 Å).²⁷ This phenomenon is likely the result of S_2 acting as a better π -acceptor than CO (*vide infra*), resulting in the S-S bond order being closer to one than two, and leading to the assignment of **71** as a molybdenum (IV) complex.

Scheme 26



Although η^2 disulfide complexes have been reported for molybdenum, they typically are high valent and/or ionic inorganic clusters.^{5-7,28,29} However, Parkin and coworkers have reported the synthesis of the molybdenum (IV) disulfide metallocene compound $[\eta^5\text{-C}_5\text{H}_4(\text{tBu})]_2\text{Mo}(\eta^2\text{-S}_2)$ (**72**) by treatment of the carbonyl precursor $[\eta^5\text{-C}_5\text{H}_4(\text{tBu})]_2\text{Mo}(\text{CO})$ (**73**) with S_8 (Scheme 26).³⁰ Compound **72** exhibited a slightly longer S-S bond length than **71** [$d(\text{SS}) = 2.091(2) \text{ Å}$], indicative of more substantial π -backbonding to the π^* orbital of S_2 . This observation is not surprising, given that **72** does not possess a carbonyl ligand, as does **71**, which likely competes with S_2 for electron density from the d^2 metal center. It is interesting to note that in order for compound **72** to form, the carbonyl ligand of its precursor **73** must be lost. On the

Scheme 27

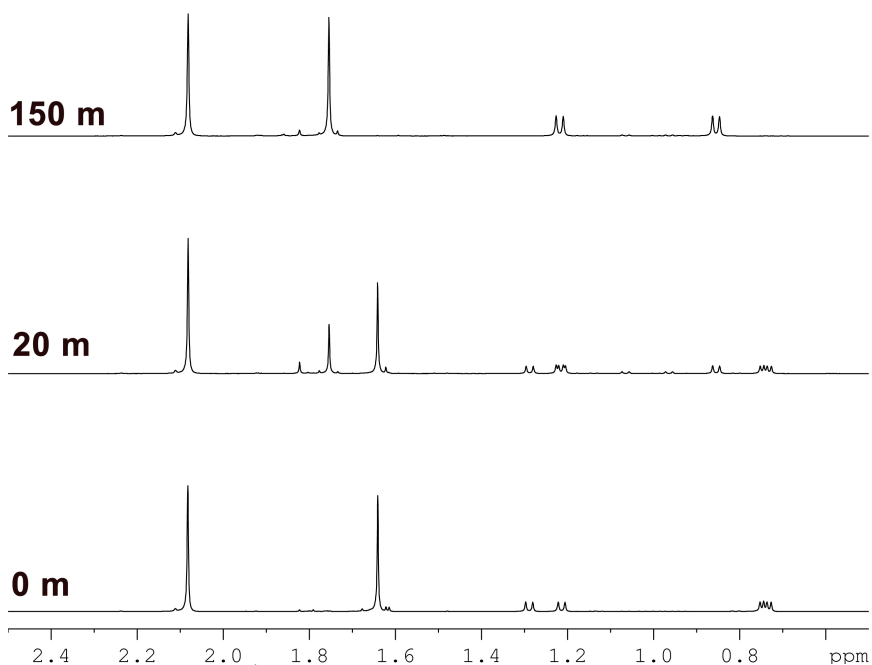
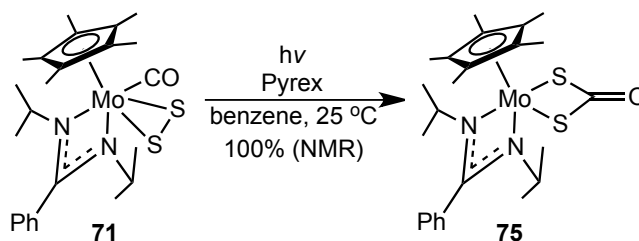


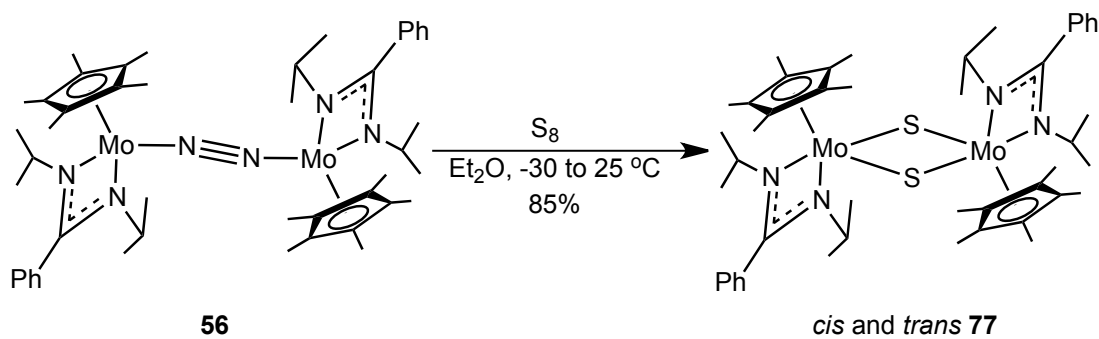
Figure 21. Partial ^1H (400 MHz, benzene- d_6 , 25 $^\circ\text{C}$) NMR spectra demonstrating the photolytic conversion of **71** to **75** at timed intervals. (Note: The singlet at 2.08 ppm is durene internal standard.)

other hand, compound **71** is capable of maintaining a carbonyl ligand. This is due to the fact that the metallocene ligand framework provides two electrons more than the CpAm environment. Accordingly, compound **72** is an 18 electron species, which is not capable of bearing an additional ligand. Importantly, the observation that the carbonyl ligand in **73** is displaced easily by treatment with S_8 further demonstrates the greater π -acidity of the S_2 ligand compared to CO, providing an explanation for the significant S-S bond elongation in **71** relative to the minor C-O bond elongation.

$^{13}\text{C}\{^1\text{H}\}$ NMR revealed **75** to be the second transient species observed during catalysis (Figures 16 and 17, labeled with +). Interestingly, when the identical reaction depicted in Scheme 27 was performed beginning with unlabeled **71** under a ^{13}CO atmosphere, ^{13}C -labeled **75** was observed by $^{13}\text{C}\{^1\text{H}\}$ NMR. Likely, this reaction proceeds through an associative mechanism in which CO is exchanged for ^{13}CO , followed by intramolecular insertion of ^{13}CO into the S-S bond. Lastly, photolysis of compound **75** lead solely to slow photodegradation after extended periods of time.

In contrast to the photochemical isomerization of **71** to the dithiocarbonate species **75** in the *absence* of other chemical reagents for short periods of time, photolysis of ^{13}C -labeled **71** in the presence of excess S_8 under Ar atmosphere produced a mixture of ^{13}C -labeled compound **75**, ^{13}COS , and the remaining C_s symmetric species observed during catalysis by NMR (Figure 17, labeled with o). Given the C_s symmetry of this species and the lack of a carbonyl ligand, it seemed reasonable to tentatively assign it as a terminal sulfide complex, analogous to the terminal oxo complex **48**. In order to isolate such a species, an alternative method for

Scheme 28



its preparation was sought out. Cummins and coworkers have shown that treatment of the three coordinate molybdenum species **31** with S₈ produces the four coordinate terminal sulfide complex (S)Mo[N(R)Ar]₃ (**76**) under mild conditions.³⁹ Accordingly, as Scheme 28 reveals, treatment of the ‘end-on-bridged’ dinitrogen species **56** with S₈ lead to the isolation of a red, crystalline product in good yield which proved to be the as of yet unidentified intermediate (by ¹H NMR, Figure 17, labeled with o). X-ray analysis revealed the new species to be the dimer of the proposed molybdenum (IV) sulfide compound, specifically {Cp*Mo[N(ⁱPr)C(Ph)N(ⁱPr)]₂(μ-S)₂ (**77**). Both the *cis* and *trans* isomers of **77** were structurally characterized, however only the structure for *trans*-**77** is depicted in Figure 23. Bridging sulfide species for molybdenum compounds have been reported previously,⁴⁰ as well as for CpAm titanium complexes.⁴¹

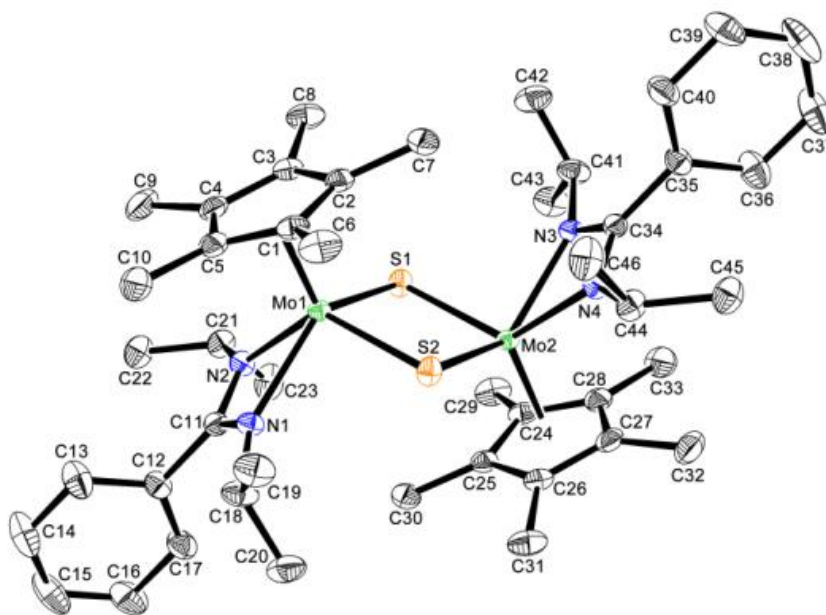


Figure 23. Molecular structure (30% thermal ellipsoids) for *trans*-**77**. H atoms have been omitted for clarity. Selected bond lengths (Å) and angles (°): Mo1-S1 2.3408(7), S1-Mo1-S2 91.40(2), Mo1-S1-Mo2 88.60(2).

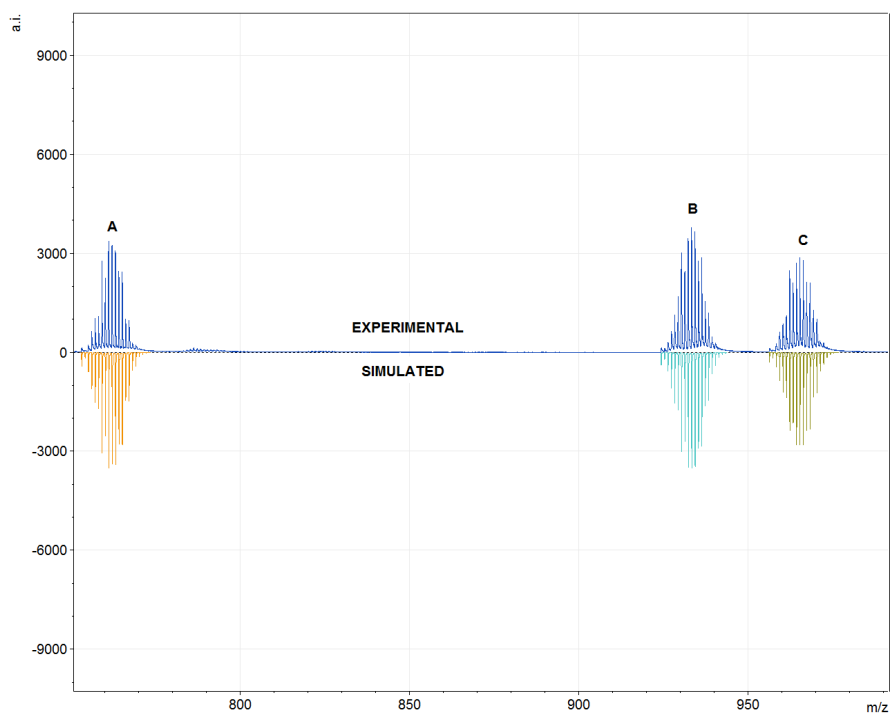
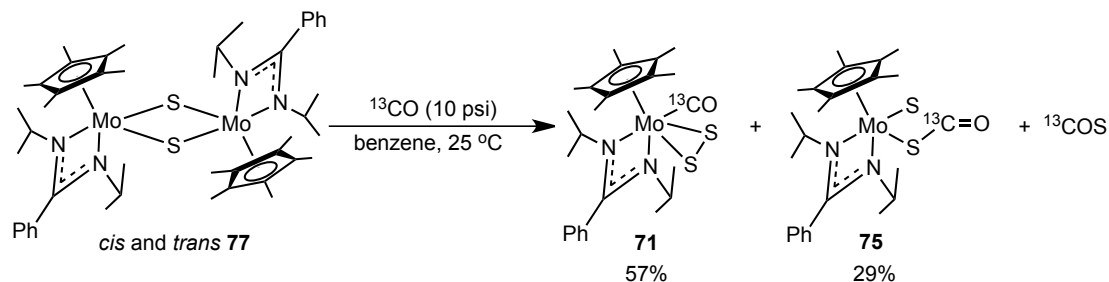


Figure 24. Partial experimentally found (ESI+, Et₂O) and simulated mass spectrum of the mixture of products obtained in the synthesis of **77**. Labeled resonances correspond to **79** (A), **77** (B), and **78** (C).

Although in the solid state compound **77** exists as a dimer (both *cis* and *trans*), its solution structure is less clear. Specifically, only one set of CpAm resonances are ever observed in the ¹H NMR spectrum, even down to the limiting temperature of -90 °C in toluene-*d*₈ solution. This indicates that compound **77** is involved in a rapid dynamic monomer – dimer equilibrium at all temperatures. Further complicating matters is the fact that satisfactory elemental (C, H, N) analysis for **77** could not be obtained, despite repeated efforts, and close examination of ¹H NMR spectra for crystalline samples of **77** reveal the presence of paramagnetic impurities which could not be removed. In one experiment, this impurity was judged to account for 20% by weight of the entire sample (by integration vs. durene internal standard). Furthermore, during catalytic production of COS, similar paramagnetic resonances

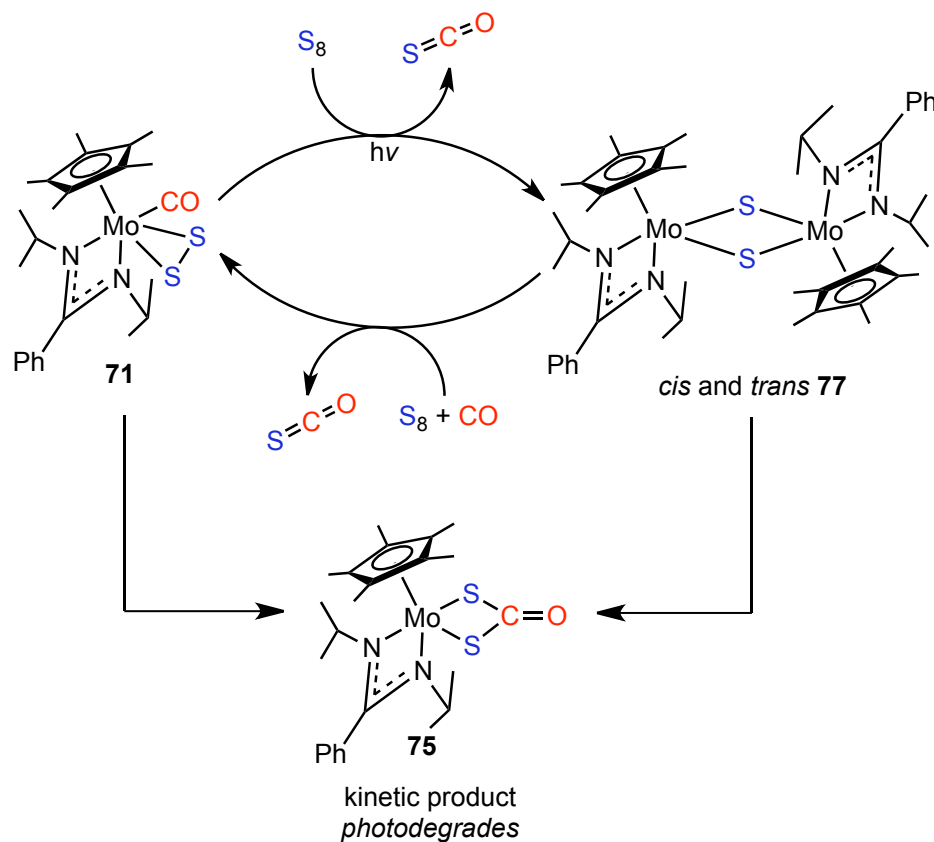
Scheme 29



appear at longer reaction times in the ^1H NMR (Figure 17). In order to determine the nature of these unknown compounds, which could not be characterized by X-ray diffraction, electrospray ionization mass spectrometry (ESI-MS) was employed, which revealed the presence of two additional (M+H) clusters. Simulations were carried out, and these (M+H) clusters were found to correspond to a dinuclear [Mo(V), Mo(V)] tris(sulfide) species $\{\text{Cp}^*\text{Mo}[\text{N}(\text{iPr})\text{C}(\text{Ph})\text{N}(\text{iPr})]\}_2(\text{S})_3$ (**78**) and a dinuclear [Mo(IV), Mo(V)] tris(sulfide) species $\text{Cp}^*\text{Mo}[\text{N}(\text{iPr})\text{C}(\text{Ph})\text{N}(\text{iPr})](\text{S})_3\text{Cp}^*\text{Mo}$ (**79**), in which one amidinate ligand had been lost (Figure 24).

Although **77** could not be isolated without contamination of these proposed species, investigations into its role in the catalytic production of COS were conducted. Importantly, treatment of compound **77** with ^{13}CO lead to the *non-photolytic* production of ^{13}C -labeled **71** (57%), ^{13}C -labeled **75** (29%) and free ^{13}COS (unquantified) at room temperature (Scheme 29). Importantly, the quantities of compounds **71** and **75** observed to have been formed suggest that the paramagnetic tris(sulfide) species **78** and **79** must be involved in the SAT process, as they are required to provide sufficient amounts of sulfur to maintain proper stoichiometry. Together, the observation that compounds **71** and **75** and COS may be obtained from

Scheme 30

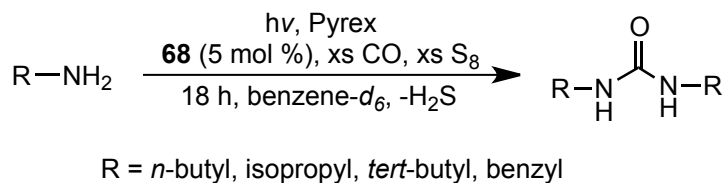


77 by treatment with CO, that **77** and COS are generated from photolysis of **71** in the presence of S_8 , and that **75** appears to slowly photodegrade, lead to the determination that compounds **71** and **77** are intermediates in the catalytic cycle for COS production, but that **75** is likely a kinetic product not involved (Scheme 30). Compound **75** does not build up in solution, however, as it slowly degrades under reaction conditions.

3.2.3 'On-Demand' COS Production

Compound **68** serves well to generate COS from CO and S_8 , which are themselves inexpensive and easily accessible reagents, however there remain considerable safety concerns associated with the use of COS (*vide supra*).

Scheme 31



Accordingly, we set out to determine if compound **68** could mediate ‘on-demand’ production of COS, wherein the valuable reagent would be generated from its simplest components in the presence of other reactants to produce more complex organic molecules. Such a process would obviate the need to store and handle the hazardous material, yet still allow for its use. To this end, symmetric ureas were targeted to prove such a concept, as they are well known to form from the reaction of amines and COS, in a process which generates H₂S as the only by product.¹⁹

As depicted in Scheme 31, benzene-*d*₆ solutions containing a primary amine, excess equivalents of S₈, CO (initial pressure = 10 psi), and a catalytic amount of compound **68** (5 mol %), were photolyzed for 18 hours, at which point complete conversion to the corresponding 1,3-disubstituted ureas was observed. The identity of each urea was confirmed by redissolving in either DMSO-*d*₆ or chloroform-*d* and comparing against literature values.^{42,43} This procedure was found to function on a preparative scale with a catalyst loading as low as 0.5 mol % (for R = ^tBu, Scheme 31). The success of this process demonstrates the tolerance of all catalytically active species in the generation of COS to protic reagents. Furthermore, it is important to note that the amines and solvent employed in this process were degassed, but not dried, indicating that the active species are immune to the presence of trace moisture as well.

It is worth noting that ureas are known to form from the reaction of CO, amines, and S₈ without the use of a metal catalyst, however these processes require high temperatures and pressures,⁴⁴ and control reactions confirmed that no such transformation occurred under the conditions we sought to employ. Specifically, each primary amine employed above was photolyzed in the presence of excess S₈ under CO atmosphere (10 psi) and no reaction was observed. On the other hand, McElwee-White and coworkers have established that group 6 carbonyl complexes [e.g. inexpensive and commercially available W(CO)₆] serve as precatalysts for the synthesis of substituted ureas, however these reactions occur only at high temperatures and pressures, and require the use of sacrificial oxidants (e.g. I₂).⁴⁵⁻⁵⁰ This type of reaction is distinct from the ‘on-demand’ processes described here, in that they involve coordination of both the amine and CO substrates to the metal center in the product forming step, whereas the reaction presented in Scheme 31 involves a much simpler mechanism, in which the metal is solely responsible for the *in situ* generation of COS. This was proven by conducting control reactions in the absence of excess S₈, which produced no urea product, thus proving the ineffectiveness of compound **68** to be involved in such a complex mechanism. Furthermore, when ‘on-demand’ reactions were carried out using ¹³CO, ¹³C{¹H} NMR spectra revealed the coproduction of both ¹³C-labeled urea and ¹³COS.

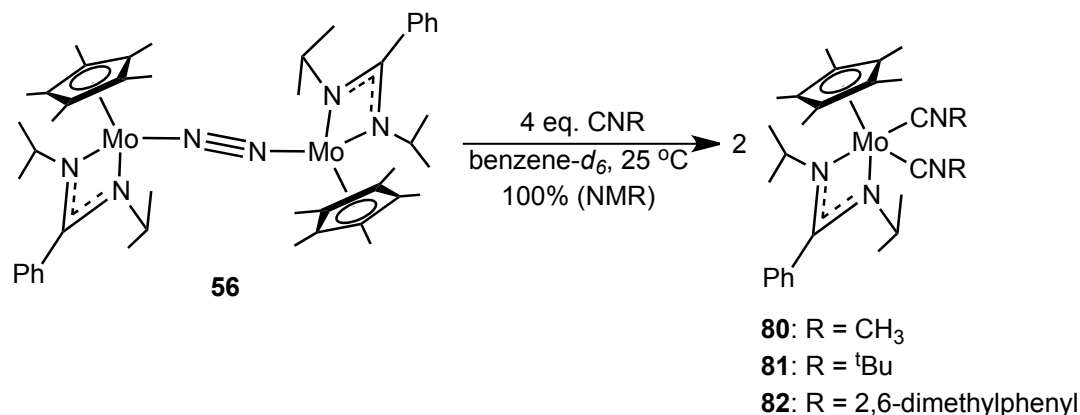
3.3 Isothiocyanates

3.3.1 Background

Isothiocyanates ($\text{S}=\text{C}=\text{NR}$) are a class of small molecules, known to occur naturally on Earth in plants and marine sponges,⁵¹⁻⁵⁵ which have gained considerable attention from the medical community over the past several decades as their role in the prevention of various forms of cancer and in the treatment of HIV, among other ailments, has become better understood.^{56,57} In terms of synthetic chemistry, isothiocyanates are attractive building blocks for the preparation of more complex molecules bearing both nitrogen and sulfur atoms, such as thioureas, which are themselves useful precursors for the synthesis of heterocycles and carbodiimides.⁵⁸⁻⁶³ Methods for the preparation of isothiocyanates are unappealing, however, as they have historically required the use of hazardous or unpleasant reagents, such as CS_2 or thiophosgene (Cl_2CS),^{62,64-68} or offer only a narrow scope of functional group tolerance.^{69,70} Accordingly, methods to avoid the use of isothiocyanates have been developed over the years.^{71,72}

One can imagine that a simple method for the preparation of an isothiocyanate that exhibits high functional group tolerance would involve the direct sulfidation of the corresponding isonitrile ($\text{C}\equiv\text{NR}$). Ideally, such a process would involve S_8 as the source of sulfur, as it is the most abundant and inexpensive form of the element known. Accordingly, such methods were reported in the early 1990's, however these processes suffered from their own drawbacks. Specifically, they employed the toxic main group metals tellurium and selenium as catalysts.^{73,74} Only recently has the transition metal mediated sulfidation of isonitriles been reported, however such

Scheme 32



reactions employ the use of expensive rhenium catalysts, or require long reaction times in the case of more Earth abundant molybdenum (*vide supra*).^{7,75} Given the success of the mid valent molybdenum (II) bis(carbonyl) complex **68** to catalyze SAT to CO from S₈, we wondered if the analogous chemistry could be applied to isoelectronic isonitriles.

3.3.2 Synthesis and Characterization of New Compounds and SAT Reactions

As demonstrated above, the N₂ ligand of the group 6 CpAm ‘end-on-bridged’ dinitrogen complexes may be displaced easily through the addition of a strong π -acid. Accordingly, treatment of compound **56** with 4 equivalents of methyl, *tert*-butyl, and 2,6-dimethylphenyl isonitrile in benzene-*d*₆ solution lead to quantitative conversion to the bis(isonitrile) compounds Cp*Mo[N(ⁱPr)C(Ph)N(ⁱPr)](CNR)₂ [R = CH₃ (**80**), C(CH₃)₃ (**81**), and 2,6 dimethylphenyl (**82**)], respectfully, as depicted in Scheme 32. CpAm group 6 M(II) bis(isonitrile) complexes have been described previously by our group for 2,6-dimethylphenyl and *tert*-butyl isonitrile (although these complexes utilized a methyl group in the distal position of the amidinate ligand).^{10,23}

Accordingly, we chose compound **80** (methyl isonitrile) to fully characterize, as it was the most unique compound synthesized in this study. Single crystals of **80** were easily obtained from cooling of a concentrated pentane solution, and the molecular structure is depicted in Figure 25. As has been observed for other bis(isonitrile)

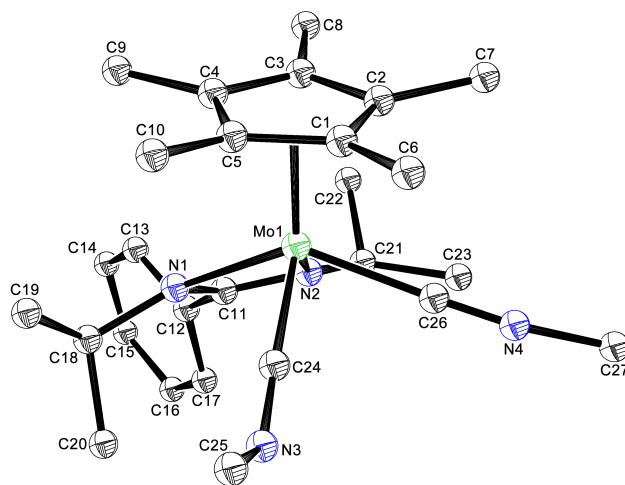


Figure 25. Molecular structure (30% thermal ellipsoids) of **80**. H atoms have been removed for clarity. Selected bond lengths (Å) and angles (°): Mo1–C24 1.9342(19), Mo1–C26 2.038(2), C24–N3 1.221(2), C26–N4 1.163(2), C24–N3–C25 129.6(2), C26–N4–C27 166.9(2).

species reported by our group,²³ one isonitrile ligand in the solid state structure of complex **80** is coordinated to the molybdenum center in a near linear fashion, while the other is distinctly non linear and features a C-N-C bond angle reminiscent of an sp^2 hybridized nitrogen atom [cf. bond angles of C26–N4–C27 = 166.9(2)° and C24–N3–C25 = 129.6(2)°, respectfully, Figure 25]. This observation is consistent with a large degree of π -backbonding from the molybdenum (II) center to the π^* orbital of the isonitriles, and is supported by the observed IR stretching frequencies ν_{CN} = 2086, 1767 cm^{-1} . In solution, however, compounds **80** – **82** display apparent C_s symmetry,

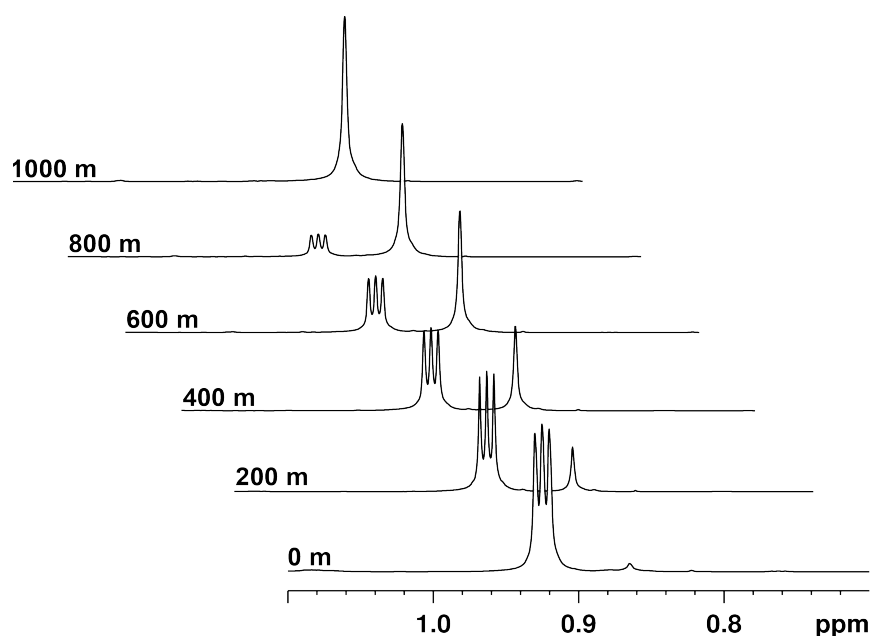
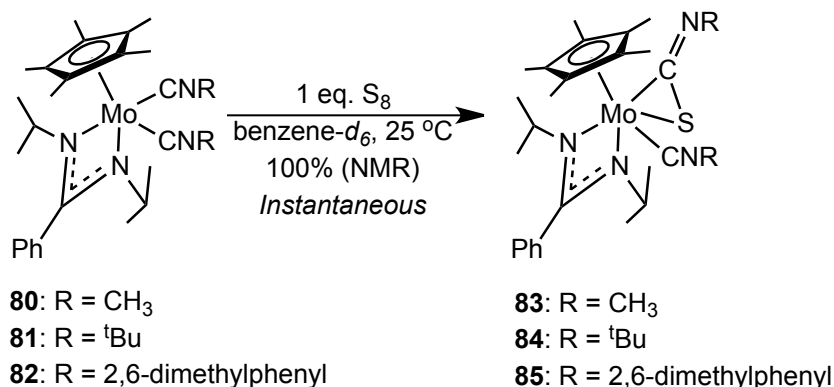


Figure 26. Partial ^1H (400 MHz, benzene- d_6 , 50 $^\circ\text{C}$) NMR spectra demonstrating the production of $^t\text{BuNCS}$ (singlet) from $^t\text{BuNC}$ (triplet) in the presence of 5 mol % **81**. Spectra were recorded every 200 min and are vertically displayed with a horizontal offset of 0.02 ppm.

indicating that the isonitrile groups are magnetically and, presumably, chemically equivalent.

Looking to determine if compounds **80** – **82** were capable of *thermally* catalyzing the direct sulfidation of the corresponding isonitriles, each was treated with excess equivalents of the proper isonitrile and S_8 . In the case of methyl and *tert*-butyl isonitrile, catalytic production of methyl and *tert*-butyl isothiocyanate was observed by ^1H NMR to occur at 25 $^\circ\text{C}$ in benzene- d_6 solution, and faster turnover was observed upon gentle heating (Figure 26). In the case of 2,6-dimethylphenyl isonitrile, heating was essential to observe catalytic turnover to the product 2,6-dimethylphenyl isothiocyanate. Importantly, as in the case of catalytic COS production, catalysis was not inhibited when the solvent and liquid reagents were not

Scheme 33



dried prior to use, indicating that this catalytic process too is immune to trace moisture.

Looking to probe the mechanism of the present catalytic cycle, it was observed by ¹H NMR that for the sulfidation of all three isocyanides, only one CpAm species of apparent C_s symmetry appeared to be in solution, which were determined to be the catalyst resting states. For the bulky *tert*-butyl derivative, however, these peaks were broadened, leading to the assumption that the resting state may actually be of C₁ symmetry, but involved in dynamic ‘ring-flipping’ of the amidinate ligand on the NMR time scale. In the course of efforts to determine the nature of these catalyst resting states, compounds **80** – **82** were treated with 1 equivalent S₈ in benzene-*d*₆ solution in the absence of excess isocyanide (Scheme 33), which lead to immediate quantitative generation of the catalyst resting state species (referred to as **83** – **85**, respectfully) as judged by ¹H NMR. Efforts to isolate these species initially proved futile, as they decomposed quickly during standard work up procedures. However, single crystals of **84** were obtained by treatment of compound **81** (generated *in situ*) with one equivalent of S₈ in toluene solution for 10 minutes, followed by immediate

removal of solids by filtration, layering with pentane, and cooling to -30 °C. The solid state molecular structure of **84** is depicted in Figure 27. On the basis of the knowledge of the structure of **84** and the similar NMR spectra for all three observed catalyst resting states, it seemed reasonable to identify the resting state compounds as the ‘side-bound’ isothiocyanate species $\text{Cp}^*\text{Mo}[\text{N}(\text{iPr})\text{C}(\text{Ph})\text{N}(\text{iPr})](\text{CNR})[\kappa\text{-(S,C)SCNR}]$ [$\text{R} = \text{CH}_3$ (**83**), $\text{C}(\text{CH}_3)_3$ (**84**), and 2,6 dimethylphenyl (**85**)], respectfully.

Compound **84** represents a rare example of a structurally characterized ‘side-bound’ isothiocyanate complex for molybdenum and, to the best of our knowledge, is the only such example generated through the insertion of a sulfur atom into a metal – carbon bond. It should be noted, however, that insertion of sulfur into other metal carbon bonds, such as $\text{Ni-C}_{\text{aryl}}$, have been observed.⁷⁶ Examples of ‘side-bond’

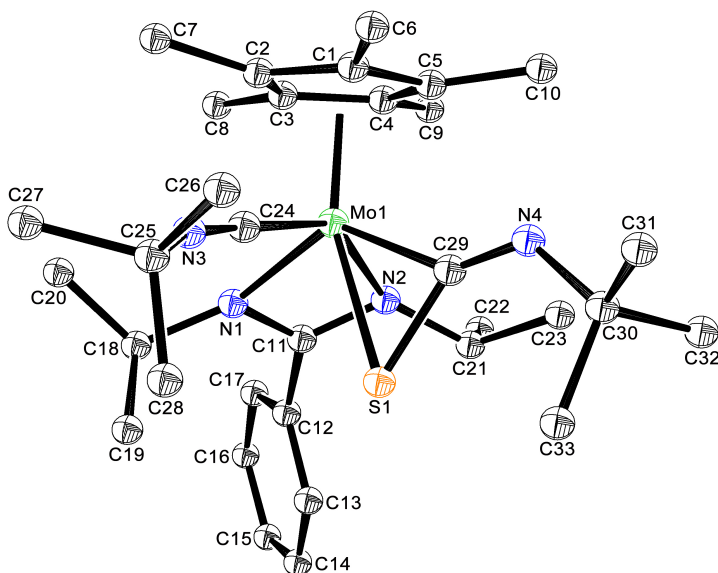
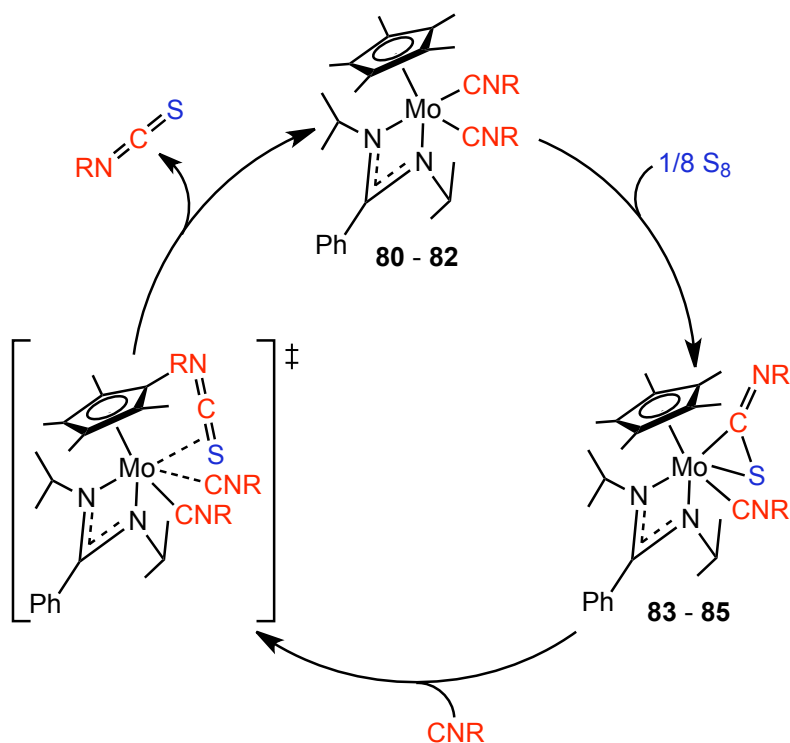


Figure 27. Molecular structure (30% thermal ellipsoids) of **84**. H atoms have been removed for clarity. Selected bond lengths (Å) and angles (°): Mo1–C24 2.050(2), Mo1–S1 2.4978(6), Mo1–C29 2.117(2), C29–N4 1.255(3), S1–C29 1.776(2), C24–N3 1.168(2), N3–C25 1.455(3), S1–C29–N4 136.91(18), C24–N3–C25 159.5(2).

isothiocyanates have been reported for nickel,⁷⁷ vanadium,⁷⁸ iridium,⁷⁹ and molybdenum (0) species,⁸⁰ however in all cases these were generated through the addition of an isothiocyanate to the proper metal precursor. The C-S bond length of 1.776(2) Å for compound **84** is longer than other ‘side-bound’ isothiocyanate complexes reported, which leads to the formal oxidation state assignment of +4 for the molybdenum center.

Having firmly established the identity of the catalyst resting states, we were interested in elucidating the mechanism for the catalytic sulfidation of isonitriles. To this end, variable temperature ¹H NMR experiments were conducted, which allowed for an Eyring analysis. Specifically, compound **81** (5 mol %) was employed to catalyze the sulfidation of *tert*-butyl isonitrile at several temperatures under pseudo-first order conditions with respect to S₈. Most informative was the value obtained for the entropy of activation, $\Delta S^\ddagger = -13(7) \text{ cal mol}^{-1} \text{ K}^{-1}$, the large negative value of which indicated a highly ordered transition state. This data, along with the observation that the bis(isonitrile) compounds rapidly convert to the catalyst resting states upon addition of S₈, indicate that the reaction proceeds through the mechanism depicted in Scheme 34. First, one sulfur atom inserts into the Mo-C bond of compounds **80** – **82** to generate the catalyst resting states **83** – **85**, followed by reductive elimination of the isothiocyanate that occurs with concomitant coordination of another isonitrile through an associative mechanism, forming an unobserved transition state, which then go on to regenerate the original catalysts.

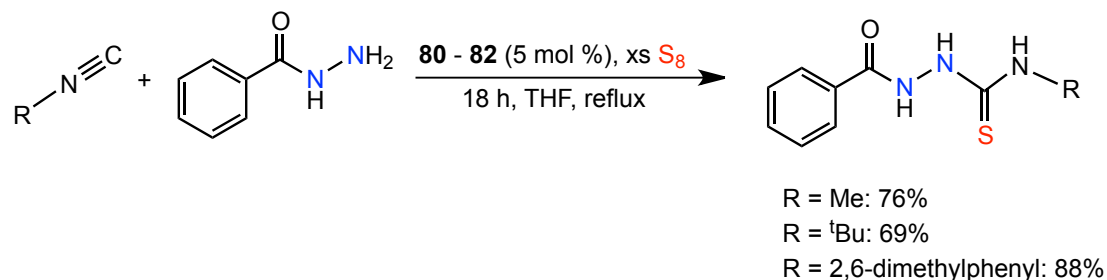
Scheme 34



3.3.3 ‘On-Demand’ Isothiocyanate Synthesis

With the catalytic production of isothiocyanates *via* molybdenum catalyzed SAT well established, we next became interested in determining if these reagents too could be produced in an ‘on-demand’ fashion, as in the case of COS production. Isothiocyanates are known to be flammable, toxic compounds.⁸¹ As such, a process for their synthesis and use that eliminates the need to isolate, purify, store, and handle them seemed highly appealing. Accordingly, the catalytic SAT reactions described above were repeated on a preparative scale in the presence of benzhydrazide according to the conditions of Scheme 35 in order to synthesize 1-aryylthiosemicarbazides. Such products were targeted as they are known to form

Scheme 35



under mild conditions from the reaction of benzhydrazide and isothiocyanates, and they are useful precursors for triazoles, which find use in the treatment of spasticity.⁶¹

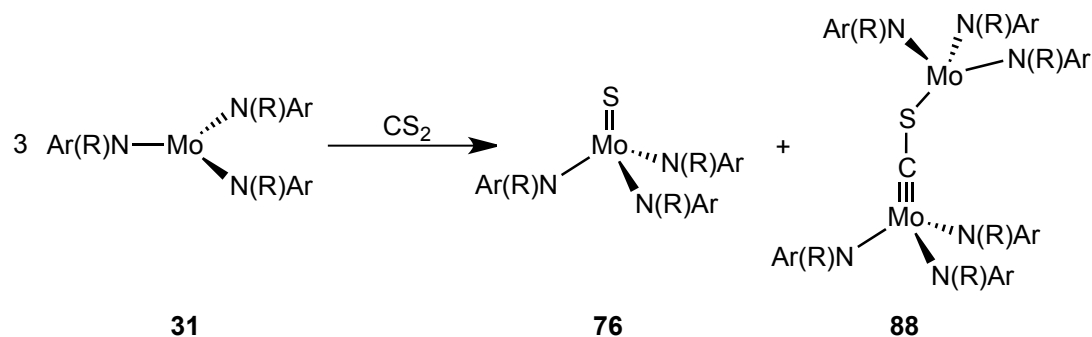
As revealed in Scheme 35, isonitriles, sulfur, and benzhydrazide are converted to the corresponding 1-arylthiosemicarbazides in the presence of catalytic amounts of compounds **80 – 82** (5 mol %). Compounds **80 – 82** serve to first generate the isothiocyanate from sulfur and the isonitrile, and this newly formed product then reacts with benzhydrazide to form the final 1-arylthiosemicarbazide product. The organic products were easily isolated in good yields simply by removal of solids by filtration through a plug of silica with ethyl acetate and washing with brine, and were characterized by 1H and $^{13}C\{^1H\}$ NMR, as well as ESI-MS. The fact that high yields of these products are obtained provides evidence that compounds **80 – 82**, along with all other intermediates involved in the catalytic synthesis of isothiocyanates, are immune to the presence of protic and Lewis basic reagents, as in the case of ‘on-demand’ COS production. Extension of this work to include benzhydrazides bearing various substituents in the *para* position are currently in progress. The use of primary amines in order to synthesize thioureas through ‘on-demand’ isothiocyanate synthesis could not be performed, however, given that it has been reported recently that the reaction of sulfur, primary amines, and isonitriles occurs spontaneously to produce

these products (i.e. it is a self-catalyzed reaction).⁸² Control reactions were performed to confirm that this self-catalyzed methodology could *not* be applied to reaction with benzhydrazide(s), the reason for which may be a result of the difference in basicity of primary amines and benzhydrazide(s).

3.4 C=S Bond Cleavage Reactions

During the course of the studies described thus far, it became of interest to investigate the activation of sulfur containing heteroallenes, as they may provide alternative routes to metal – sulfide compounds.³⁹ Furthermore, it was of interest to explore the chemistry of such compounds with regard to mid valent CpAm species specifically, as they appeared unreactive towards the heteroallene products described above. On the other hand, some groups have explored the activation of these sulfur containing small molecules as models for the activation of their less reactive analog CO₂,⁸³ which we have previously shown can be activated by the ‘end-on-bridged’ dinitrogen species **40** and **41**.¹⁰ Accordingly, the activation of CS₂ and *tert*-butyl isothiocyanate was investigated, and the results are described below.⁸⁴ Activation of COS was also explored, however no identifiable products were obtained.

Scheme 36



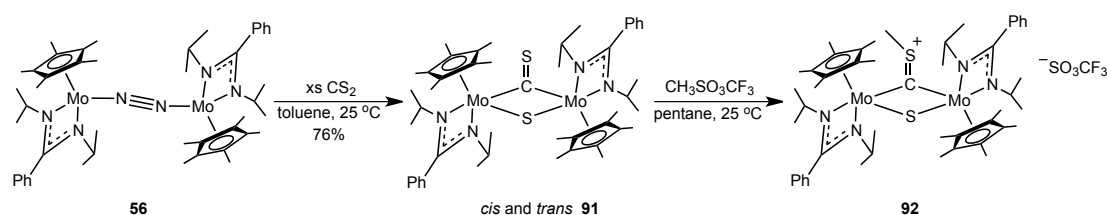
3.4.1 CS₂ Activation

The first major report regarding the transition metal mediated activation of CS₂ came in 1966, when Wilkinson and Baird reported that treatment of the rhodium (I) complex (PPh₃)RhCl (**86**) with CS₂ lead to C-S bond cleavage to produce the thiocarbonyl species *trans*-(PPh₃)₂RhCl(CS) (**87**).⁸⁵ Cummins and coworkers discovered that CS₂ may be activated by the molybdenum (III) species **31** to generate the terminal sulfide compound **76**, and the dinuclear thiocarbonyl complex {Mo[N(R)Ar]₃}₂(μ-CS) (**88**), in which the two metal centers have formal oxidation states of +6 and +4 (Scheme 36).³⁹ This report was particularly noteworthy, as one C-S bond of CS₂ had been completely cleaved, and the resulting thiocarbonyl was then significantly activated.⁸⁶ Fryzuk later reported the ‘complete disassembly’ of CS₂ in 2010, by reaction with the ‘side-on/end-on’ dinitrogen complex [(NPN)Ta]₂(μ-H)₂(μ-η²:η¹-N₂) {where (NPN) = PhP[CH₂Si(CH₃)₂NPh]₂} (**89**), to yield [(NPN)Ta]₂(μ-S)₂(μ-CH₂) (**90**), in which both C-S bonds were fully cleaved, the first time such a reaction had been reported.⁸⁷

Here, we found that the ‘end-on-bridged’ dinitrogen compound **56** again served as an easily accessible Mo(II) synthon for the activation of CS₂. Specifically, as revealed in Scheme 37, N₂ was displaced upon addition of CS₂ to a toluene solution of **56**, as judged by the immediate effervescence and color change to forest green, which allowed for isolation of dark green crystals of the bridging thiocarbonyl, bridging sulfide species {Cp*Mo[N(ⁱPr)C(Ph)N(ⁱPr)]}₂(μ-S)(μ-CS) (**91**) in high yield. Single crystals were easily obtained by cooling a concentrated pentane solution of **91** to -30 °C, and the molecular structure is depicted in Figure 28. Bridging thiocarbonyl

compounds are well known for the entire transition metal series.⁸⁸ However, to the best of our knowledge, compound **91** is unique in that it is the first to be reported in which one bond of CS₂ is fully cleaved in a homo-bimetallic system without loss of the sulfide ligand. For instance, similar compounds have been synthesized, however require multiple steps and more than one metal (e.g Fe and Co) to form a hetero-trimetallic cluster.⁸⁹

Scheme 37



In the solid state, compound **91** displays a very long C-S bond length of 1.697 Å, a result of the thiocarbonyl ligand being the only π -acceptor present between two d³ metal centers. ¹H NMR revealed that in benzene-*d*₆ solution, compound **91** exists as a 1:1 mixture of *cis* and *trans* isomers. However, unlike in the case of the bridging disulfide compound **77**, there exists no evidence for interconversion between these isomers. Based on the molecular structure of compound **91**, the formal oxidation state of +3 was assigned to each molybdenum center. The diamagnetic nature of compound **91** as judged by ¹H NMR therefore likely results from the existence of a Mo-Mo bond [$d(\text{Mo1-Mo2}) = 2.8602(8)$ Å].

Bridging thiocarbonyl compounds are typically nucleophilic at the thiocarbonyl sulfur atom.⁸⁸ Given this trend, and the high degree of π -backdonation to the π^* orbital in compound **91**, we sought to probe its reactivity towards electrophiles. As Scheme 37 also depicts, compound **91** was easily methylated using

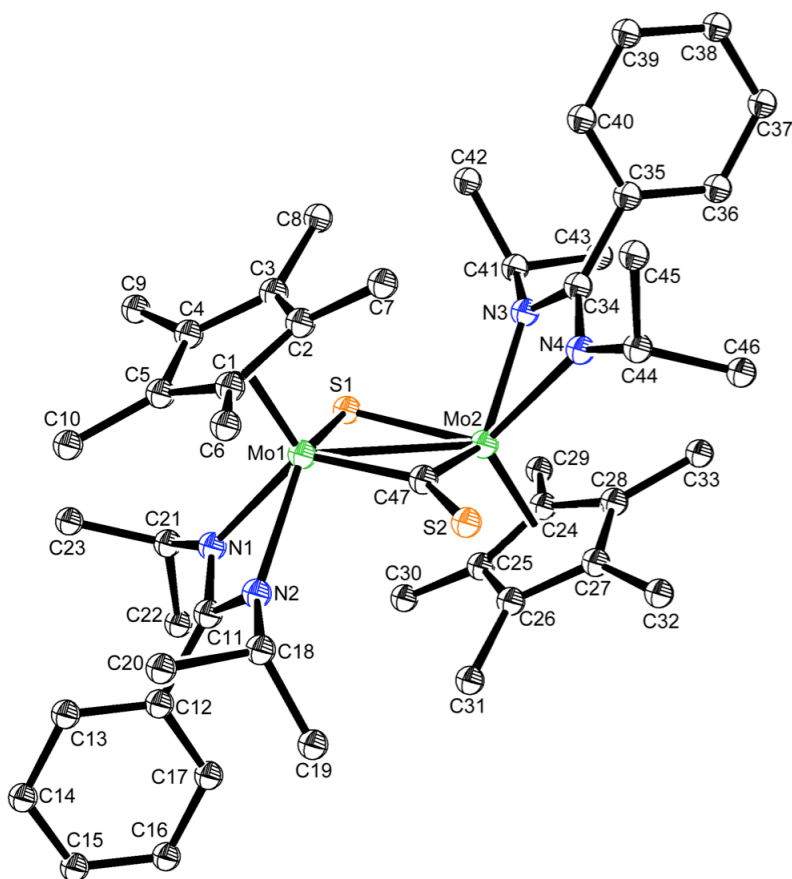


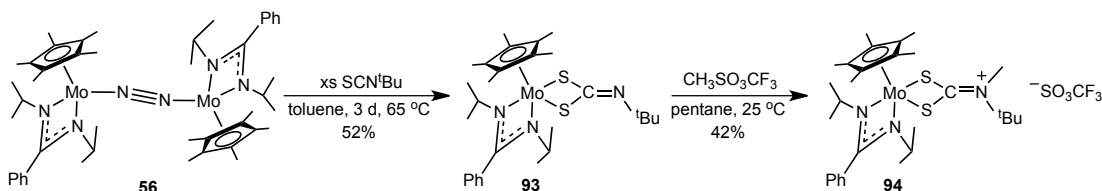
Figure 28. Molecular structure (30% thermal ellipsoids) of compound **91**. H atoms have been omitted for clarity. Selected bond lengths (Å) and angles (°): Mo1-S1 2.417(3), Mo2-S1 2.437(3), Mo1-C47 1.949(10), Mo2-C47 1.894(11), C47-S2 1.698(10), Mo1-S1-Mo2 72.20(8), Mo1-C47-Mo2 96.2(5).

methyl triflate ($\text{CH}_3\text{SO}_3\text{CF}_3$) in pentane at room temperature, resulting in the immediate formation of a light green precipitate, which we believe to be $\{\text{Cp}^*\text{Mo}[\text{N}(\text{iPr})\text{C}(\text{Ph})\text{N}(\text{iPr})]\}_2(\mu\text{-S})[\mu\text{-CS}(\text{CH}_3)](\text{SO}_3\text{CF}_3)$ (**92**). Efforts to characterize this compound were not successful, however, given that it was found to be only sparingly soluble in all common organic solvents, including those which are polar and/or halogenated.

3.4.2 Isothiocyanate Activation

The reactivity of isothiocyanates towards mid valent CpAm molybdenum complexes was of great interest to us in order to determine if these heteroallenes interact at all with the molybdenum species present in catalysis, as discussed in Section 3.3. In order to test such reactivity, compound **56** was again employed, and was found to react slowly with *tert*-butyl isothiocyanate at elevated temperatures to generate the molybdenum (IV) dithiocarbonimidate complex Cp*Mo[N(ⁱPr)C(Ph)N(ⁱPr)][κ-(*S,S*)S₂CN^tBu] (**93**), as shown in Scheme 38. The generation of dithiocarbonimidate complexes is known to occur upon reaction with isothiocyanates for a variety of transition metals, however these typically result in the

Scheme 38



generation of an isonitrile ligand as well, as the result of the initial S-C bond cleavage step.^{90,91} Compound **93** does not exhibit such a structure, and attempts to isolate an intermediate complex (i.e. an η^2 isothiocyanate complex) through the addition of just two equivalents of *tert*-butyl isothiocyanate to **56**, in order to gain mechanistic insight into the transformation, proved unsuccessful.

Compound **93** displays *C*₁ symmetry in benzene-*d*₆ solution as judged by ¹H NMR, which is consistent with the structural parameters provided through the X-ray structure in Figure 29. Specifically, the C-N bond length observed for the dithiocarbonimidate ligand (C24-N3) of 1.2631(15) Å is within the range of a C-N

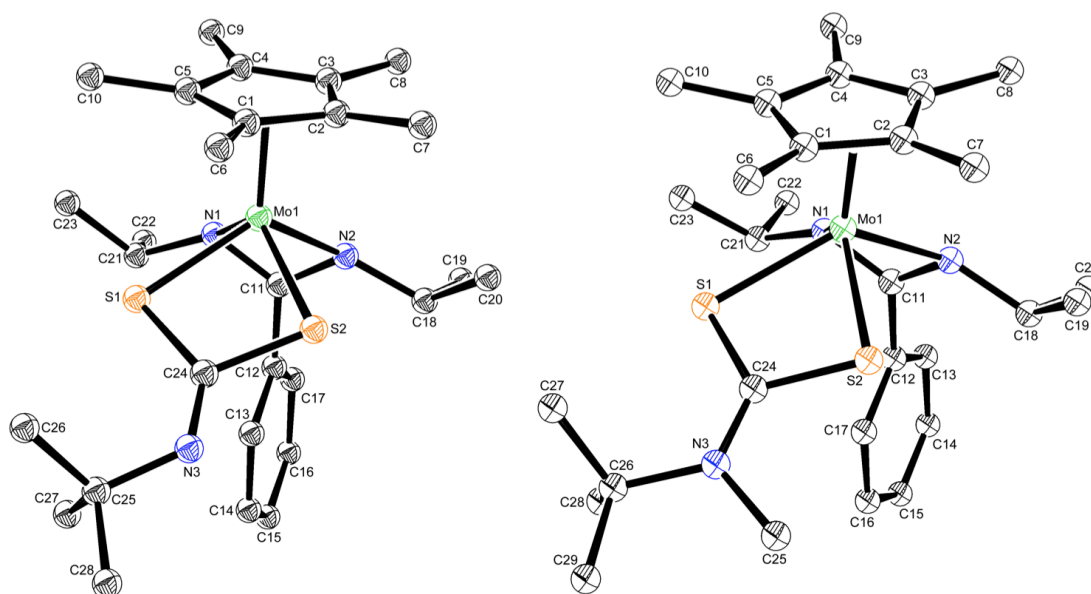


Figure 29. Molecular structures (30% thermal ellipsoids) of compounds **93** (left) and **94** (right). H atoms and counter ion have been omitted for clarity. Selected bond lengths (Å) and angles (°) for **93**: Mo1-S1 2.3694(4), Mo1-S2 2.3763(3), S1-C24 1.7832(12), S2-C24 1.7963(12), C24-N3 1.2631(15), C24-N3-C25 123.26(10); for **94**: Mo1-S1 2.4155(10), Mo1-S2 2.4038(11), S1-C24 1.744(4), S2-C24 1.750(4), C24-N3 1.309(5), C24-N3-C26 124.3(3), C24-N3-C25 118.0(3), C26-N3-C25 117.7(3).

double bond, preventing any free rotation about this bond in solution, resulting in overall C_1 symmetry. Such ligands are known to be quite nucleophilic at the nitrogen atom, and prone to methylation and protonation.^{90,92} Accordingly, as Scheme 38 further reveals, treatment of **93** with methyl triflate in pentane lead to the immediate precipitation of an orange powder. Redissolving in benzene followed by slow diffusion of pentane at room temperature lead to the isolation of the methylated product, $\text{Cp}^*\text{Mo}[\text{N}(\text{iPr})\text{C}(\text{Ph})\text{N}(\text{iPr})][\kappa\text{-(}S,S\text{)S}_2\text{CN}(\text{CH}_3)^t\text{Bu}](\text{SO}_3\text{CF}_3)$ (**94**) in moderate yield. The molecular structure of compound **94** was confirmed through single crystal X-ray diffraction, revealing the C-N bond length of the dithiocarbonimide ligand to be elongated only slightly, implying that the positive

charge of compound **94** is localized to the methylated sp^2 hybridized nitrogen atom (N3, Figure 29).

Characterization of compound **93** was key in regard to the catalytic production of isothiocyanates. Specifically, the fact that **93** is not observed at all during catalysis (for catalyst **81**) lead to the determination that such a species is not formed, therefore eliminating the possibility that such compounds are involved in the catalytic cycle.

3.5 Conclusion

We have found that two catalytic SAT transfer reactions may be mediated by mid valent CpAm molybdenum species. Specifically, the first case for the sulfidation of CO to generate COS under ambient conditions has been developed. This process is remarkably tolerant to protic reagents and trace amounts of moisture, allowing for the ‘on-demand’ generation of COS for the preparation of more complex organic molecules in a facile, inexpensive manner. Furthermore, given the reducing atmosphere of primordial Earth, the process described, involving mid valent molybdenum species, provides insight into the possible metal catalyzed generation of COS for the generation of the first oligopeptides billions of years ago.¹⁸

On the other hand, only the third method for the direct sulfidation of isonitriles mediated by a transition metal has been developed. This process stands out among others that have been reported, however, as it i) involves the use of inexpensive molybdenum catalysts, ii) requires short reaction times under reasonable conditions, and iii) is tolerant to the presence of trace moisture. Importantly, this

process allows for the ‘on-demand’ synthesis of isothiocyanates for the preparation of more complex compounds of pharmaceutical relevance in good yields.

Lastly, activation of sulfur containing heteroallenes was observed to occur cleanly in the case of CS₂ and *tert*-butyl isothiocyanate. In the former case, a unique activation mode was discovered, resulting in the formation of a nucleophilic thiocarbonyl complex. On the other hand, the activation of *tert*-butyl isothiocyanate gave a more well known type of product. The characterization of this species was critical in excluding such a complex from the mechanism involved in the catalytic generation of isothiocyanates.

3.6 References

- (1) Punniyamurthy, T.; Velusamy, S.; Iqbal, J. *Chem. Rev.* **2005**, *105*, 2329.
- (2) Donahue, J. P. *Chem. Rev.* **2006**, *106*, 4747.
- (3) Lefort, T. E. French Patent 729,925, **1931**.
- (4) Khan, M. M. T.; Siddiqui, M. R. F. *Inorg. Chem.* **1991**, *30*, 1157.
- (5) Adam, W.; Bargon, R. M.; Schenk, W. A. *J. Am. Chem. Soc.* **2003**, *125*, 3871.
- (6) Adam, W.; Bargon, R. M. *Chem. Comm.* **2001**, 1910.
- (7) Adam, W.; Bargon, R. M.; Bosio, S. G.; Schenk, W. A.; Stalke, D. J. *Org. Chem.* **2002**, *67*, 7037.
- (8) Angelici, R. J. *Acc. Chem. Res.* **1988**, *21*, 387.
- (9) Jacob, J.; Espenson, J. H. *Chem. Comm.* **1999**, 1003.
- (10) Yonke, B. L.; Reeds, J. P.; Zavalij, P. Y.; Sita, L. R. *Angew. Chem. Int. Ed.* **2011**, *50*, 12342.
- (11) Rassmussen, R. A.; Khalil, A. K.; Dalluge, R. W.; Penkett, S. A.; Jones, B. *Science* **1982**, *215*, 665.
- (12) Halmer, M. M.; Schmincke, H. U. *J. Volcanol. Geotherm. Res.* **2002**, *115*, 511.
- (13) Ferek, R. J.; Andreae, M. O. *Nature* **1984**, *307*, 148.
- (14) Domagal-Goldman, S. D.; Meadows, V. S.; Claire, M. W.; Kasting, J. F. *Astrobiology* **2011**, *11*, 419.
- (15) Svoronos, P. D. N.; Bruno, T. J. *Ind. Eng. Chem. Res.* **2002**, *41*, 5321.
- (16) Huber, C.; Wachtershauser, G. *Science* **1998**, *281*, 670.

- (17) Huber, C.; Eisenreich, W.; Hecht, S.; Wachtershauser, G. *Science* **2003**, *301*, 938.
- (18) Leman, L.; Orgel, L.; Ghadiri, M. R. *Science* **2004**, *304*, 283.
- (19) Ferm, R. J. *Chem. Rev.* **1957**, *57*, 621.
- (20) Fu, P.-F.; Khan, M. A.; Nicholas, K. M. *Organometallics* **1993**, *12*, 3790.
- (21) Winkler, U.; Khan, M. A.; Nicholas, K. M. *Inorg. Chem. Commun.* **1998**, *1*, 317.
- (22) Groom, L. R.; Schwarz, A. D.; Nova, A.; Clot, E.; Mountford, P. *Organometallics* **2013**, *32*, 7520.
- (23) Fontaine, P. P.; Yonke, B. L.; Zavalij, P. Y.; Sita, L. R. *J. Am. Chem. Soc.* **2010**, *132*, 12273.
- (24) Gombler, W. Z. *Naturforsch* **1981**, *36b*, 1561.
- (25) Reeds, J. P.; Yonke, B. L.; Zavalij, P. Y.; Sita, L. R. *J. Am. Chem. Soc.* **2011**, *133*, 18602.
- (26) Yonke, B. L.; Reeds, J. P.; Fontaine, P. P.; Zavalij, P. Y.; Sita, L. R. *Organometallics* **2014**, *33*, 3239.
- (27) Meyer, B. *Chem. Rev.* **1976**, *76*, 367.
- (28) Muller, A.; Jaegermann, W.; Enemark, J. H. *Coord. Chem. Rev.* **1982**, *46*, 245.
- (29) Coucouvanis, D.; Hadjikyriacou, A.; Draganjac, M.; Kanatzidis, M. G.; Ileperuma, O. *Polyhedron* **1986**, *5*, 349.
- (30) Shin, J. H.; Savage, W.; Murphy, V. J.; Bonanno, J. B.; Churchill, D. G.; Parkin, G. *J. Chem. Soc., Dalton Trans.* **2001**, 1732.
- (31) Howard, W. A.; Parkin, G.; Rheingold, A. L. *Polyhedron* **1995**, *14*, 25.
- (32) Gaffney, T. R.; Ibers, J. A. *Inorg. Chem.* **1982**, *21*, 2851.
- (33) Gaffney, T. R.; Ibers, J. A. *Inorg. Chem.* **1982**, *21*, 2860.
- (34) Perpignan, M. F.; Ballester, L.; Gonzalez-Casso, M. E.; Santos, A. *J. Chem. Soc., Dalton Trans.* **1987**, 281.
- (35) Tenorio, M. J.; Puerta, M. C.; Valerga, P. *J. Chem. Soc., Dalton Trans.* **1996**, 1935.
- (36) Travnický, Z.; Pastorek, R.; Sindelar, Z.; Klicka, R.; Marek, J. *Trans. Metal Chem.* **1996**, *21*, 81.
- (37) Contreras, R.; Valderrama, M.; Riveros, O.; Moscoso, R.; Boys, D. *Polyhedron* **1996**, *15*, 183.
- (38) Tay, E. P. L.; Kuan, S. L.; Leong, W. L.; Goh, L. Y. *Inorg. Chem.* **2007**, *46*, 1440.
- (39) Johnson, A. R.; Davis, W. M.; Cummins, C. C.; Serron, S.; Nolan, S. P.; Musaev, D. G.; Morokuma, K. *J. Am. Chem. Soc.* **1998**, *120*, 2071.
- (40) Rakowski DuBois, M.; DuBois, D. L.; VanDerveer, M. C.; Haltiwanger, R. C. *Inorg. Chem.* **1981**, *20*, 3064.
- (41) Guiducci, A. E.; Boyd, C. L.; Mountford, P. *Organometallics* **2006**, *25*, 1167.
- (42) Liu, P.; Wang, Z.; Hu, X. *J. Org. Chem.* **2012**, 1994.
- (43) Gabriele, B.; Salerno, G.; Mancuso, R.; Costa, M. *J. Org. Chem.* **2004**, *69*, 4741.

- (44) Franz, R. A.; Applegath, F.; Morriss, F. V.; Baiocchi, F. *J. Org. Chem.* **1961**, *26*, 3306.
- (45) McCusker, J. E.; Abboud, K. A.; McElwee-White, L. *Organometallics* **1997**, *16*, 3863.
- (46) McCusker, J. E.; Main, A. D.; Johnson, K. S.; Grasso, C. A.; McElwee-White, L. *J. Org. Chem.* **2000**, *65*, 5216.
- (47) McCusker, J. E.; Qian, F.; McElwee-White, L. *J. Mol. Catal. A: Chem.* **2000**, *159*, 11.
- (48) Qian, F.; McCusker, J. E.; Zhang, Y.; Main, A. D.; Chlebowski, M.; Kokka, M.; McElwee-White, L. *J. Org. Chem.* **2002**, *67*, 4086.
- (49) Diaz, D. J.; Darko, A. K.; McElwee-White, L. *Eur. J. Org. Chem.* **2007**, 4453.
- (50) Zhang, L.; Darko, A. K.; Johns, J. I.; McElwee-White, L. *Eur. J. Org. Chem.* **2011**, 6261.
- (51) Fahay, J. W.; Zalcman, A. T.; Talalay, P. *Phytochem.* **2001**, *56*, 5.
- (52) Simpson, J. S.; Garson, M. J. *Tetrahedron Lett.* **1998**, *39*, 5819.
- (53) He, H. Y.; Salva, J.; Catalos, R. F.; Faulkner, J. *J. Org. Chem.* **1992**, *57*, 3191.
- (54) He, H. Y.; Faulkner, D. J.; Shumsky, J. S.; Hong, K.; Clardy, J. *J. Org. Chem.* **1989**, *54*, 2511.
- (55) Fahey, J. W.; Talalay, P. *Food and Chem. Toxicology* **1999**, *37*, 973.
- (56) Bianchini, F.; Vainio, H. *Drug. Met. Rev.* **2004**, *36*, 655.
- (57) Zhang, X. C.; Neamati, N.; Lee, Y. K.; Orr, A.; Brown, R. D.; Whitaker, N.; Pommier, Y.; Burke, T. R. *Bioorg. Med. Chem.* **2001**, *9*, 1649.
- (58) Mukerjee, A. K.; Ashare, R. *Chem. Rev.* **1991**, *91*, 1.
- (59) Liu, Z.; Yi, Y.; Zhao, J.; Tang, M. *Synthetic Commun.* **2012**, *42*, 55.
- (60) Iwakura, Y.; Noguchi, K. *Bull. Chem. Soc. Jpn.* **1967**, *40*, 2383.
- (61) Kane, J. M.; Staeger, M. A.; Dalton, C. R.; Miller, F. P.; Dudley, M. W.; Ogden, A. M. L.; Kehne, J. H.; Ketteler, H. J.; McCloskey, T. C.; Senyah, Y.; Chmielewski, P. A.; Miller, J. A. *J. Med. Chem.* **1994**, *37*, 125.
- (62) Dyer, E.; Johnson, T. B. *J. Am. Chem. Soc.* **1932**, *54*, 777.
- (63) Tale, P. V.; Deshmukh, S. P. *Heteroat. Chem.* **2006**, *17*, 306.
- (64) Hodgkins, J. E.; Reeve, W. P. *J. Org. Chem.* **1964**, *29*, 3098.
- (65) Hodgkins, J. E.; Ettlinger, M. G. *J. Org. Chem.* **1956**, *21*, 404.
- (66) Wong, R.; Dolman, S. J. *J. Org. Chem.* **2007**, *72*, 3969.
- (67) Azizi, N.; Khajeh-Amiri, A.; Ghafari, H.; Bolourtchian, M. *Mol. Divers.* **2011**, *15*, 157.
- (68) Sureshbabu, V. V.; Naik, S. A.; Hemantha, H. P.; Narendra, N.; Das, U.; Row, T. N. G. *J. Org. Chem.* **2009**, *74*, 5260.
- (69) Li, Z.-Y.; Ma, H.-Z.; Han, C.; Xi, H.-T.; Meng, Q.; Chen, X.; Sun, X.-Q. *Synthesis* **2013**, *45*, 1667.
- (70) Zhang, X.; Lee, Y. K.; Kelley, J. A.; Burke Jr., T. R. *J. Org. Chem.* **2000**, *65*, 6237.
- (71) Varun, B. V.; Prabhu, K. R. *RSC Adv.* **2013**, *3*, 3079.

- (72) Katritzky, A. R.; Ledoux, S.; Witek, R. M.; Nair, S. K. *J. Org. Chem.* **2004**, *69*, 2976.
- (73) Fujiwara, S.; Shin-Ike, T.; Aoki, M.; Okada, K.; Miyoshi, N.; Kambe, N. *Tetrahedron Lett.* **1991**, *32*, 3503.
- (74) Fujiwara, S.; Shin-Ike, T.; Okada, N.; Aoki, M.; Kambe, N.; Sonoda, N. *Tetrahedron Lett.* **1992**, *33*, 7021.
- (75) Arisawa, M.; Ashikawa, M.; Suwa, A.; Yamaguchi, M. *Tetrahedron Lett.* **2005**, *46*, 1727.
- (76) Han, R.; Hillhouse, G. L. *J. Am. Chem. Soc.* **1998**, *120*, 7657.
- (77) Huang, N.; Li, X.; Xu, W.; Sun, H. *Inorg. Chim. Acta* **2013**, *394*, 446.
- (78) Gambarotta, S.; Fiallo, M. L.; Floriani, C.; Chiesi-Villa, A.; Guastini, C. *Inorg. Chem.* **1984**, *23*, 3532.
- (79) Merola, J. S.; Grieb, A. W. *Acta. Cryst.* **2014**, *E70*, 352.
- (80) Ohnishi, T.; Seino, H.; Hidai, M.; Mizobe, Y. *J. Organomet. Chem.* **2005**, *690*, 1140.
- (81) For a representative MSDS, see: *tert-Butyl isothiocyanate*; MSDS No. sc-236985; Santa Cruz Biotechnology, Inc.: Santa Cruz, CA, July 30, 2011.
- (82) Nguyen, T. B.; Ermolenko, L.; Al-MourBIT, A. *Synthesis* **2014**, *46*, 3172.
- (83) Gibson, J. A. E.; Cowie, M. *Organometallics* **1984**, *3*, 984.
- (84) Pandey, K. K. *Coord. Chem. Rev.* **1995**, *140*, 37.
- (85) Baird, M. C.; Wilkinson, G. *Chem. Comm.* **1966** 267.
- (86) Ariafield, A.; Brookes, N. J.; Stranger, R.; Yates, B. F. *J. Am. Chem. Soc.* **2008**, *130*, 11928.
- (87) Ballmann, J.; Yeo, A.; MacKay, B. A.; van Rij, S.; Partick, B. O.; Fryzuk, M. D. *Chem. Comm.* **2010**, *46*, 8794.
- (88) Petz, W. *Coord. Chem. Rev.* **2008**, *252*, 1689.
- (89) Manning, A. R.; O'Dwyer, L.; McArdle, P. A.; Cunningham, D. *J. Organomet. Chem.* **1998**, *551*, 139.
- (90) Dai, Q. X.; Seino, H.; Mizobe, Y. *J. Chem. Soc., Dalton Trans.* **2011**, *40*, 11822.
- (91) Bowden, F. L.; Giles, R.; Haszeldine, R. N. *Chem. Comm.* **1974**, 578.
- (92) Miller, D. J.; Rakowski DuBois, M. *J. Am. Chem. Soc.* **1980**, *102*, 4925.

Chapter 4: Complete Synthetic Cycles for the Generation of –ER₃ Derivatized Isocyanates through Dinitrogen Fixation

4.1 Introduction

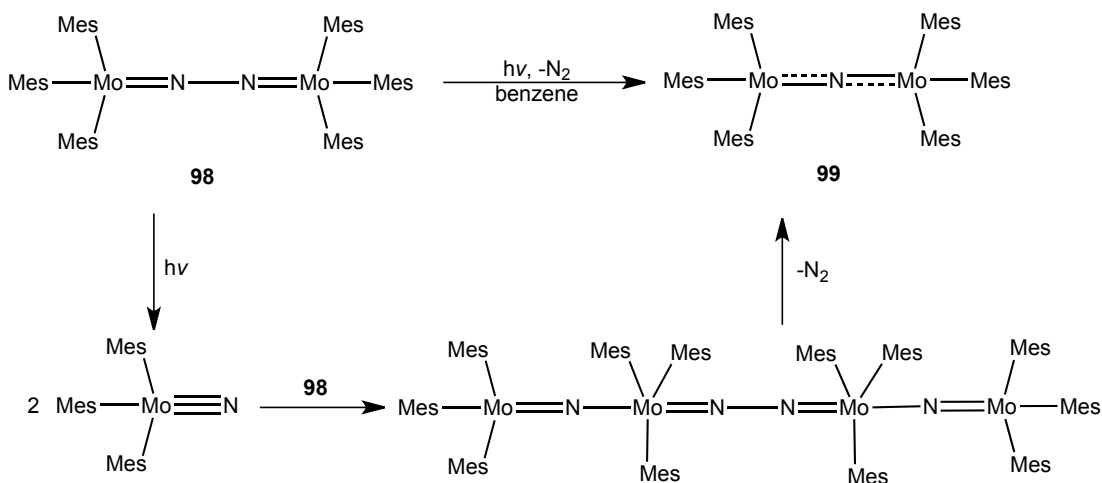
As discussed in Section 1.3, the synthesis of nitrogen containing organic products directly from N₂ is a longstanding scientific challenge. The first step to overcoming this hurdle is the activation and/or cleavage of the inert N₂ molecule, a notoriously difficult task given the molecule's extremely strong triple bond (BDE = 226 kcal/mol).¹ To this end, following the foundational work by Cummins and coworkers on the thermal cleavage of N₂ using the three coordinate molybdenum species **31**,^{2,3} several reports regarding the formation of mononuclear and dinuclear metal nitride complexes derived directly from N₂ quickly appeared in the literature,⁴⁻⁶ and continue to be of interest today.^{7,8} Sita has previously described the activation and cleavage of dinitrogen using early transition metals supported by the CpAm ligand environment for all group 4 – 6 metals, save chromium (see Figure 11, Chapter 1).⁹⁻¹² Within these reports, several noteworthy discoveries stand out. In the case of the 'side-on-bridged' hafnium compound {Cp*[N(Et)C(CH₃)N(Et)]Hf}₂(μ-η²:η²-N₂) (**95**), the longest reported N-N bond length within an organometallic N₂ compound was observed.¹¹ In regard to group 5 metals, it was found that the 'end-on-bridged' tantalum (IV) compound {Cp*[N(ⁱPr)C(CH₃)N(ⁱPr)]Ta}₂(μ-η¹:η¹-N₂) (**96**) readily cleaves N₂ when warmed above 0 °C in hydrocarbon solvent to cleanly yield the tantalum (V) bridging nitride species {Cp*[N(ⁱPr)C(CH₃)N(ⁱPr)]Ta(μ-N)}₂ (**97**), marking the first example for the well defined thermal cleavage of N₂ to produce such

a compound.⁹ Remarkably, in the course of mechanistic investigations into whether the observed N₂ cleavage proceeds through an intermolecular or intramolecular pathway, it was discovered by Andrew Keane that the barrier for N₂ cleavage within such group 5 (Ta and Nb) complexes may be finely tuned simply through varying the steric nature of the amidinate ligand through the facile substitution of different groups in the distal position. Accordingly, a series of kinetic studies revealed that as the steric bulk of the amidinate ligand increased, the observed rate of N₂ cleavage slowed. Ultimately, it was proven that the observed N₂ cleavage occurs through an intramolecular mechanism.¹²

Although N₂ cleavage under mild conditions has been a topic of considerable interest and has been employed successfully for the generation of useful organic compounds derived directly from N₂,¹³ many bimetallic N₂ complexes do not give rise to thermal N-N bond scission; rather, significant reduction of the N-N bond order is observed without the final cleavage step.^{14,15} This inactivity towards complete N-N bond scission greatly limits the ability of many organometallic systems to allow for the functionalization of N₂ and, ultimately, the generation of useful nitrogen containing organic compounds. Such limitations remain a key hurdle to overcome in the quest for catalytic N₂ fixation processes.

In 2001, Floriani reported a possible solution to this problem. The molybdenum ‘end-on-bridged’ dinitrogen complex [(Mes)₃Mo]₂(μ-η¹:η¹-N₂) [Mes = 2,4,6-(CH₃)₃C₆H₂] (**98**) was prepared and isolated, however it was found that although the bond order of the N₂ ligand was greatly reduced, the final cleavage step had not occurred, and could not be induced through heating. However, photolysis of

Scheme 39



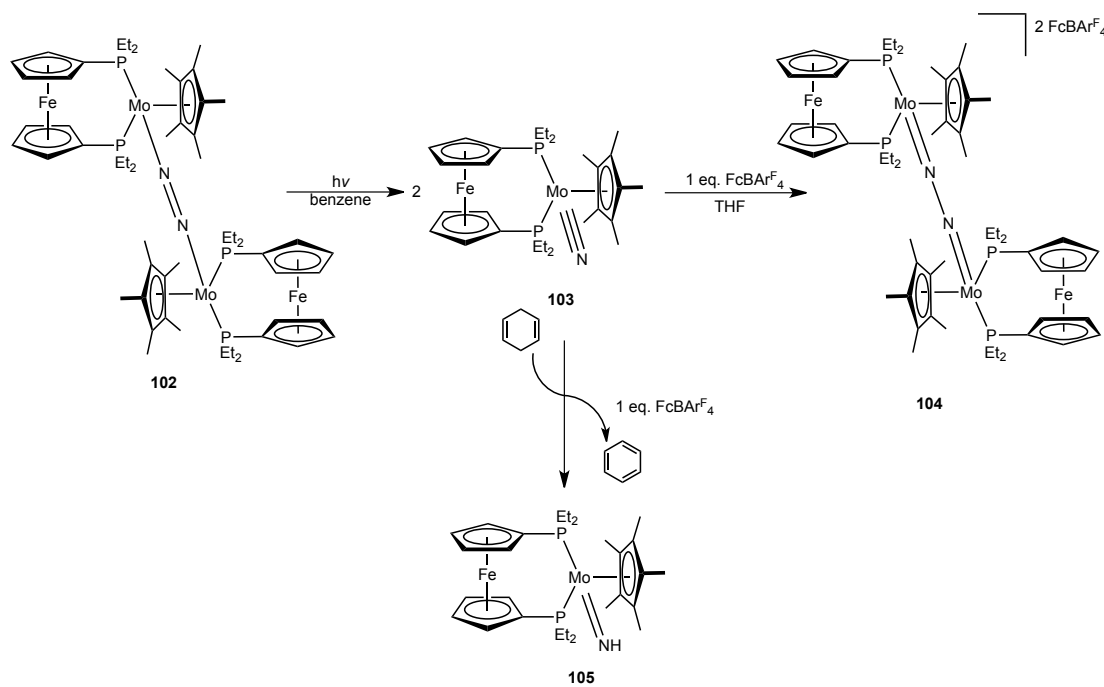
a benzene solution of **98** at room temperature yielded the bridging nitride compound [(Mes)₃Mo]₂(μ-N) (**99**). Likely, the existence of only one nitrogen atom bridging the two molybdenum centers is a result of the generation of mononuclear nitride species in solution which then act as Lewis bases on as of yet unreacted **98**, generating an intermediate species which then releases N₂, a hypothesis which was supported by the observation that 0.5 equivalents of N₂ were measured to have been released during photolysis (Scheme 39).¹⁶

Since this seminal work, Cummins has shown that similar photoreactivity is observed employing the same three coordinate species which thermally cleaves N₂, but such chemistry must be done at low temperatures to prevent the known thermal cleavage from occurring.¹⁷ Also, Vogler demonstrated that in aqueous solution, the cationic, ‘end-on-bridged’ dinuclear osmium species [(NH₃)₅Os]₂(μ-η¹:η¹-N₂) (**100**), which possesses a very short N-N bond length for the N₂ ligand, undergoes N₂ bond cleavage to produce two equivalents of an osmium (VI) nitride complex [(NH₃)₄Os(N)] (**101**).¹⁸

More recently, Nishibayashi reported that the ‘end-on-bridged’ molybdenum compound **102** supported by ferrocenyldiphosphine ligands may photolytically cleave N_2 to produce the corresponding molybdenum nitride species **103** (Scheme 40). Oxidation of the newly formed nitride was found to reform the N-N bond to produce a cationic species (**104**), which has not been previously observed in molybdenum dinitrogen chemistry.¹⁹ Most importantly, addition of 1,4 cyclohexadiene at room temperature to **103** in the presence of an oxidizing agent lead to hydrogen atom transfer (HAT) to the nitride ligand, yielding the parent imido **105** and benzene. Furthermore, addition of a proton source and reductant to **103** lead to the formation of small amounts of ammonia (Scheme 40).²⁰

Within the scope of the CpAm ligand environment, it was previously found by Dr. Brendan Yonke that the group 6 ‘end-on-bridged’ N_2 complexes **40** and **41** are

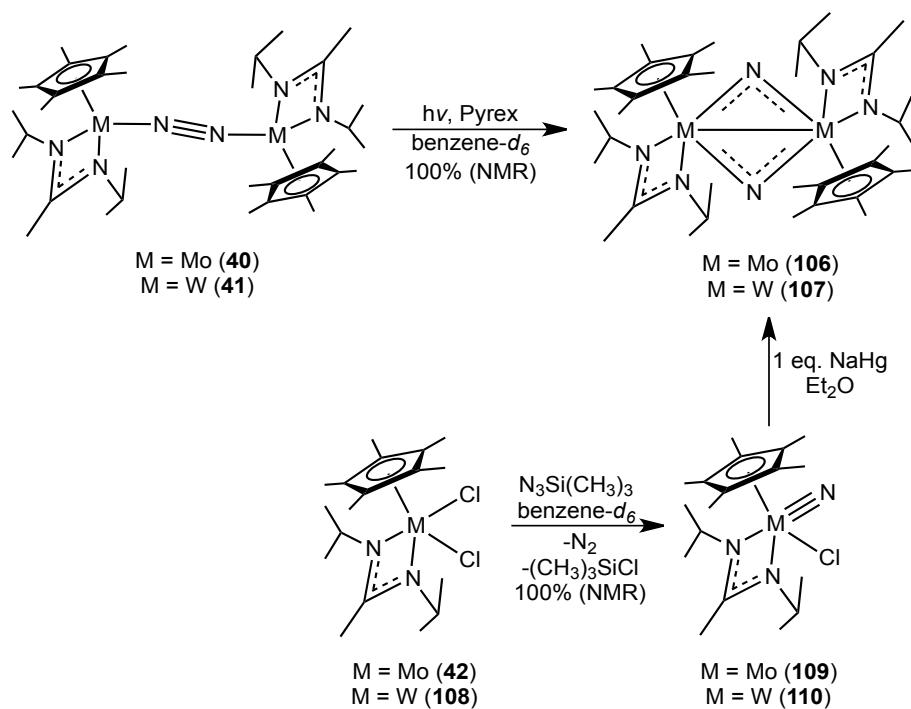
Scheme 40



thermally inert, even at elevated temperatures.¹⁰ However, upon photolysis of these compounds in benzene-*d*₆ solution within a sealed Pyrex tube, slow disappearance of the diamagnetic resonances for **40** and **41** was observed by ¹H NMR, while giving rise to new species (paramagnetic for **40**, diamagnetic for **41**). Believing these to possibly be the corresponding M(V) nitride species as a result of photolytic N₂ cleavage, an alternative route was developed for their synthesis as summarized in Scheme 41, which lead to the generation of large amounts of what were determined to be the bridging nitride species {Cp*[N(^{*i*}Pr)C(CH₃)N(^{*i*}Pr)]M(μ-N)}₂ [M = Mo (**106**), M = W (**107**)] by X-ray crystallography (although a photolytic N₂ extrusion product has also been crystallographically identified in the case of compound **40**).²¹

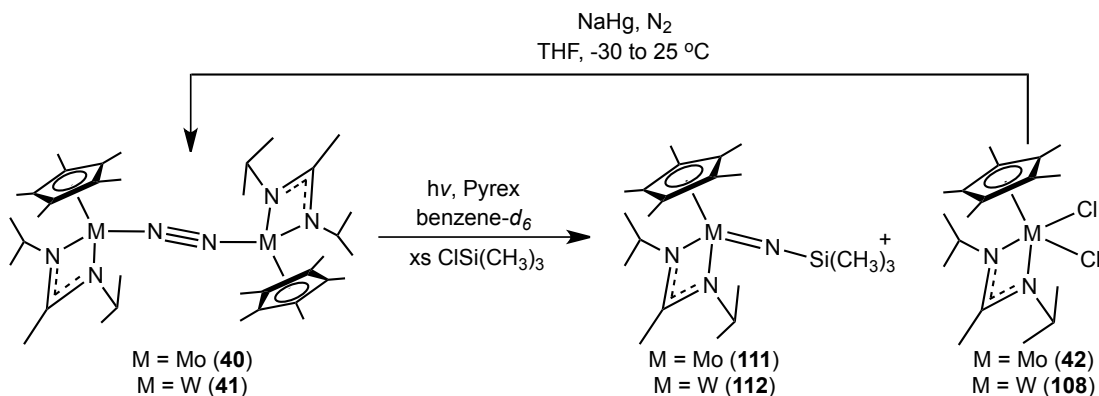
With the structure of these N₂ cleavage species firmly established, Keane began investigating the possible role they may play in N₂ fixation. Interestingly, it

Scheme 41



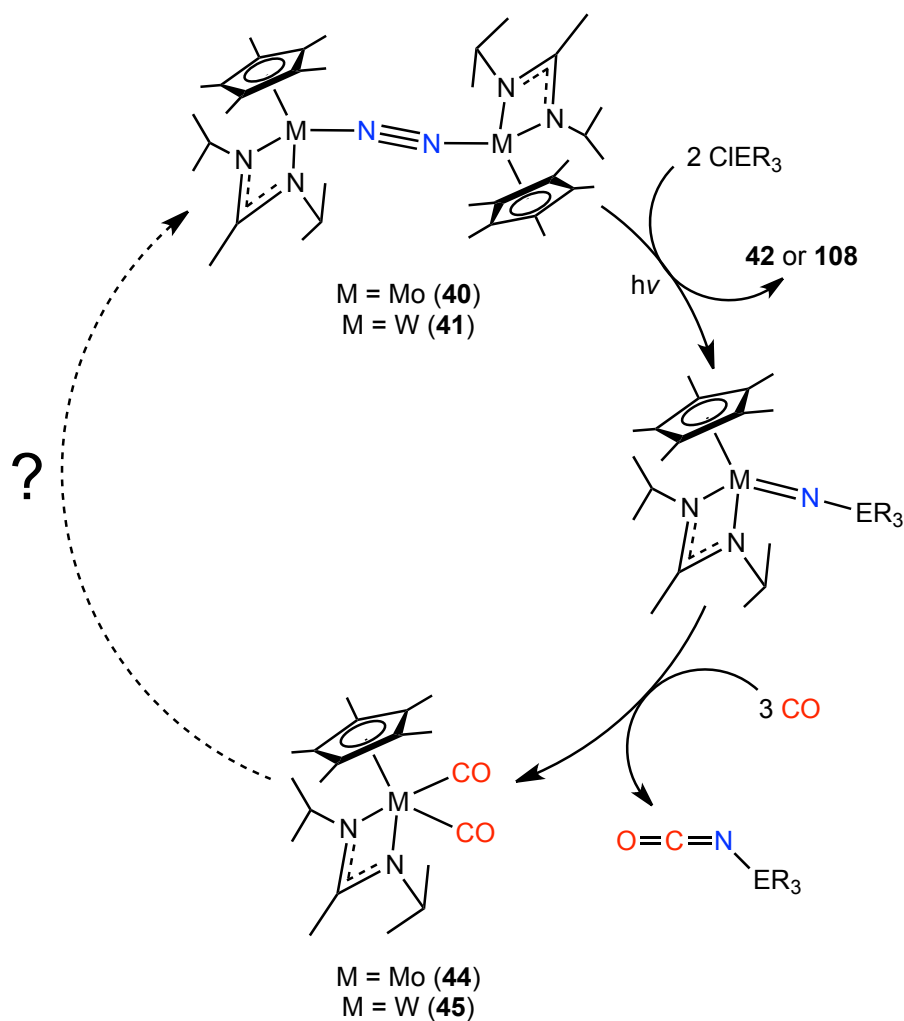
was found that when the photolysis of the ‘end-on-bridged’ compounds **40** and **41** was repeated in the presence of excess equivalents of trimethylsilyl chloride (TMS-Cl), drastically different reactivity was observed as judged by ^1H NMR. Specifically, generation of the previously reported M(IV) TMS imido complexes $\text{Cp}^*[\text{N}(\text{iPr})\text{C}(\text{CH}_3)\text{N}(\text{iPr})]\text{M}(\text{N-TMS})$ [$\text{M} = \text{Mo}$ (**111**), $\text{M} = \text{W}$ (**112**)]²² was observed, along with the M(IV) dichloride species **42** and **108**, which are themselves precursors for the generation of **40** and **41** (Scheme 42). The preparation of these group 6 imido complexes directly from N_2 was an exceptional discovery, as it has been well established that they react with CO quantitatively to generate the bis(carbonyl) compounds **44** and **45**, with concomitant release of TMS isocyanate ($\text{O}=\text{C}=\text{N-TMS}$) under ambient conditions.²² Keane then further generalized this chemistry to allow for the direct formation of five different $-\text{ER}_3$ derivatized isocyanates directly from N_2 , which was proven through the use of ^{15}N -labeled precursors and both one and two dimensional NMR ($\text{E} = \text{group 14 element}$). Furthermore, isoelectronic isonitriles were found to react similarly with these imido compounds, and produced the corresponding carbodiimides and M(II) bis(isonitrile) species.²³

Scheme 42



Together, the combined findings of Yonke and Keane presented a firm foundation for our group's N_2 fixation project in that they provided for a simple route to a wide array of $-ER_3$ derivatized isocyanates and carbodiimides derived directly from N_2 . Accordingly, such a process would be extremely valuable for the generation of small amounts of doubly-labeled (i.e. $^{13}C/^{15}N$) isocyanate and carbodiimide reagents, which may not be easily obtained otherwise. However, given our desire to develop a complete synthetic cycle for N_2 fixation, ideally one which presents a promising future for catalysis, we next turned towards the chemistry of the

Scheme 43



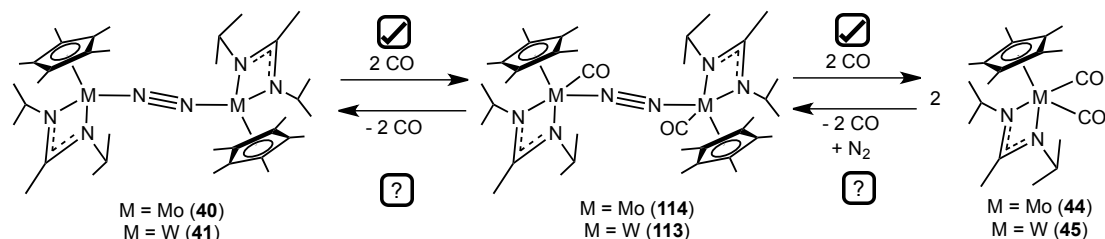
bis(carbonyl) compounds **44** and **45** for investigation. Specifically, the regeneration of the ‘end-on-bridged’ N₂ compounds **40** and **41** from these thermally inert carbonyl species was targeted, as this remained the final roadblock to completion of the desired N₂ fixation cycle (Scheme 43).

4.2 Synthesis of CpAm Mono(Carbonyl) Complexes Bearing Labile Ligands

4.2.1 Background

It has been well established in the literature that the bis(carbonyl) compounds **44** and **45** are easily generated by treatment of a toluene solution of the ‘end-on-bridged’ dinitrogen species **40** and **41**, respectively, with CO (10 psi).¹⁰ Less clear, however, was the mechanism through which this transformation occurs. Specifically, do the first two equivalents of CO displace the bridging N₂ ligand to produce two equivalents of a CpAm mono(carbonyl) species, which then quickly bonds an additional two equivalents, or do they add to the metal centers to create a dinuclear intermediate, in which the CO ligands add in a 1,4 manner across the M-N-N-M core, from which N₂ is then displaced by the second equivalents of CO? In the case of molybdenum, charging a benzene-*d*₆ solution of **40** with CO leads to an immediate color change to deep, forest green, which persists for only several seconds before becoming red. Analysis of this mixture by ¹H NMR before the reaction is allowed to reach completion reveals only the presence of **40** and the expected bis(carbonyl) product **44**. However, in the case of tungsten, the benzene-*d*₆ solution remains green (which, coincidentally, is the color of compound **41** as well) over the course of long time periods (i.e. > 24 h) before the characteristic orange color of **45** is observed, and

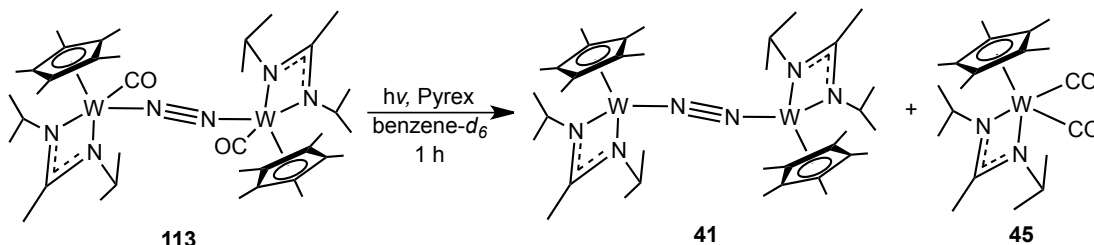
Scheme 44



three days are needed for the reaction to reach completion. During the period when the solution is still green, ^1H NMR confirms the existence of a new C_1 symmetric product, which supports the hypothesis that an intermediate 1,4-bis(carbonyl) compound likely exists before complete conversion to **45**. Fortunately, it was found that this intermediate species (**113**) could be isolated in analytically pure form as a green, crystalline solid, for which single crystals suitable for X-ray diffraction were obtained, confirming it to be the dinuclear carbonyl, ‘end-on-bridged’ compound $\{\text{Cp}^*[\text{N}(\text{iPr})\text{C}(\text{CH}_3)\text{N}(\text{iPr})]\text{W}(\text{CO})\}_2(\mu\text{-}\eta^1\text{:}\eta^1\text{-N}_2)$ (**113**).²¹ Presumably, the analogous molybdenum species $\{\text{Cp}^*[\text{N}(\text{iPr})\text{C}(\text{CH}_3)\text{N}(\text{iPr})]\text{Mo}(\text{CO})\}_2(\mu\text{-}\eta^1\text{:}\eta^1\text{-N}_2)$ (**114**) exists as well, however in this case it is extremely short lived and unable to be observed by ^1H NMR.

The knowledge that such carbonyl/‘end-on-bridged’ dinitrogen species exist was very encouraging. We reasoned that if these compounds are intermediates in the generation of **44** and **45** from **40** and **41**, respectively, that they may also be intermediates for the reverse reaction under the proper conditions (Scheme 44). Seeking to probe the possibility of such a transformation, we first decided to investigate the photoreactivity of **113**, as it can be isolated and handled at room temperature without significant decomposition. Interestingly, photolysis of a

Scheme 45

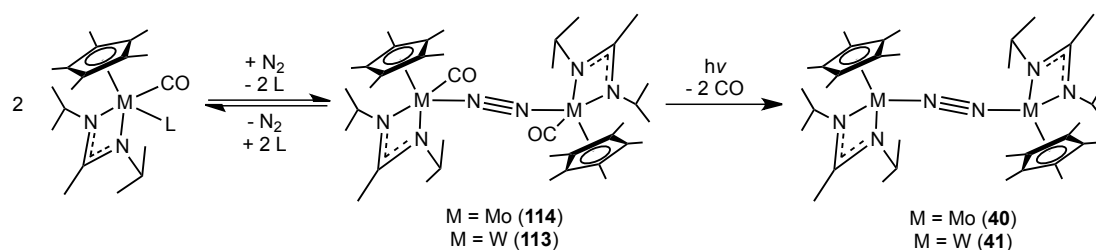


benzene- d_6 solution of **113** within a Pyrex tube generated **41** and **45** in a 1:1 ratio, as judged by ^1H NMR, after only one hour (Scheme 45). We reasoned that if the molybdenum analog could be isolated, it would likely behave in the same fashion. Accordingly, the only challenge remaining was the formation of these intermediate compounds **114** and **113** directly from the bis(carbonyl) species **44** and **45**, respectively. Given the observed reactivity of **113**, we assumed we would more likely observe direct formation of either the ‘end-on-bridged’ N_2 compounds **40** and **41**, or their cleavage products **106** and **107**. Unfortunately, even though **44** and **45** have been shown to be photoreactive compounds, the direct transformation to **114** and **113** was found to be impossible under N_2 atmosphere upon photolysis. Specifically, even when quartz tubes were employed rather than Pyrex, and the solvent used was UV-transparent THF- d_8 , none of the desired products (**40**, **41**, **113**, nor **114**) were able to be detected. Specifically, in the case of molybdenum, the formation of unidentifiable paramagnetic species was observed, and in the case of tungsten no reaction was observed.

We reasoned that the presence of CO in the reaction mixtures described above may prohibit the coordination of N_2 , even upon photolysis, given the fact that CO is such a strong π -acceptor. For instance, once CO is lost as a result of UV irradiation, allowing for coordination of N_2 , it could easily displace the more labile N_2 ligand

before dimerization occurs, even if N_2 is present in large excess. The barrier to overcome this issue is worsened by the fact that a significant entropic penalty must be paid in order to push the reaction depicted in Scheme 44 to the left. To circumvent this problem, we sought to prepare a library of compounds of general formula $\text{Cp}^*[\text{N}(\text{iPr})\text{C}(\text{CH}_3)\text{N}(\text{iPr})]\text{M}(\text{CO})(\text{L})$ ($\text{M} = \text{Mo}, \text{W}$), where L is a more labile, less π -acidic ligand capable of being displaced by N_2 . Ideally, once L is displaced by N_2 , it will not inhibit dimerization, allowing for the reaction to proceed as desired. Even if an equilibrium is established in which only a small amount of the desired intermediate compounds **114** and **113** are formed, under photolytic conditions the remaining carbonyl ligands should dissociate rapidly and irreversibly. Thus, according to Le Chatelier's Principle, the reaction will continue to proceed to the right (Scheme 46) regardless of the equilibrium given the fact that **114** and **113** would be immediately consumed. In order to test this hypothesis, compounds where $\text{L} =$ sulfides and olefins were targeted.

Scheme 46



4.2.2 L = Sulfide

An attractive class of ligand for the synthesis of the type of complex described above was sulfides, as they are known to coordinate to organometallic compounds easily, and are not overly competitive for π -backbonding, as is CO. However, given the presence of two lone pairs on the central sulfur atom, it was recognized from the start of this study that a combination of both σ - and π -donation to the metal center could result in resistance to displacement by N_2 . On the other hand, however, it has been shown that once coordinated, sulfide ligands may be alkylated to yield complexes bearing sulfonium ions as cationic ligands.^{24,25} Despite the positive charge, these ligands still possess one lone pair of electrons on the sulfur. Accordingly, they are still capable of σ -donation to the metal center.²⁶ At first glance, it would appear that such a ligand would be displaced readily, simply due to the electrostatic repulsion between the cationic sulfur and metal center, however it must be realized that upon alkylation, the sulfonium ligand becomes a viable π -acceptor. With this all in mind, we set out to prepare mono(carbonyl), mono(sulfide) complexes and, if need be, their sulfonium counterparts, and determine if such ligands may be displaced by N_2 .

Initially, we aimed to prepare compounds with sulfide ligands in which the substituents on the sulfur were large and electron withdrawing. The reason for this was that the larger the substituents were on the sulfide, the more steric repulsion would be experienced around the metal center, making displacement by the small N_2 ligand favorable. On the other hand, an electron withdrawing substituent would likely make the sulfur atom more electron poor, thus limiting the extent to which it

may engage in undesirable π -donation, again making the sulfide overall more easily displaced. Given these two criteria, we reasoned phenyl substituted sulfides would best suit our needs. Accordingly, the reactivity of the bis(carbonyl) tungsten compound **45** was first investigated. Upon photolysis in benzene- d_6 solution of **45** within a Pyrex tube, only slow decomposition was observed by ^1H NMR in the presence of thioanisole and *p*-fluorothioanisole. Small amounts of what were believed to be the desired CpAm species were able to be detected, but only in extremely low concentration, and efforts to isolate these species were unsuccessful.

Believing that perhaps phenyl substituted sulfides were in fact too sterically encumbering to coordinate to the tungsten center, the reactivity of dimethyl sulfide was investigated instead. In this case, it was found that photolysis of **45** under

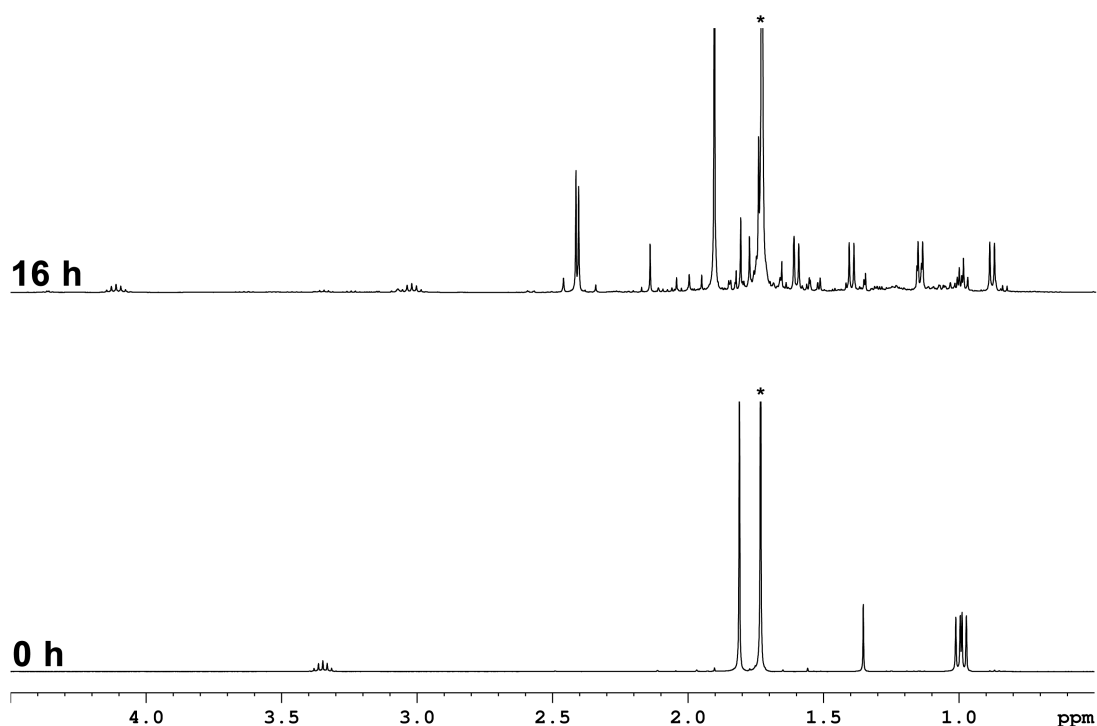
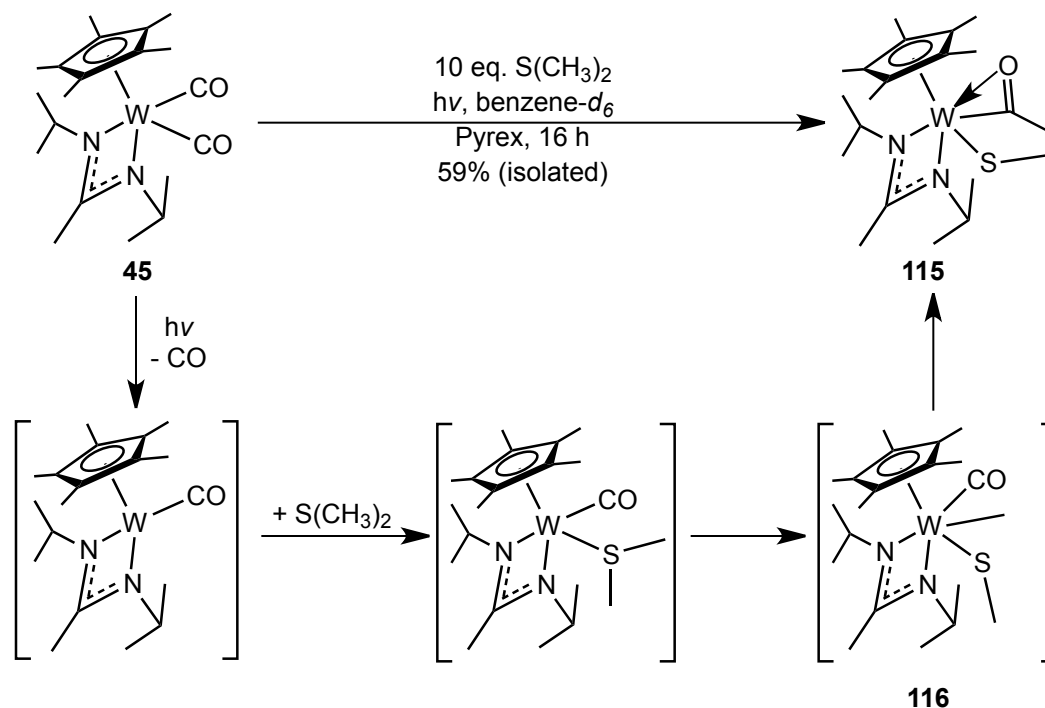


Figure 30. ^1H (400 MHz, benzene- d_6 , 25 °C) NMR spectra demonstrating the photolytic conversion of **45** to **115** in the presence of excess dimethyl sulfide (labeled with *) at two time points.

Scheme 47



identical conditions in the presence of excess (ca. 10 equivalents) dimethyl sulfide lead to quantitative conversion to a new C_1 symmetric species (**115**) over the course of 16 hours, as judged by ^1H NMR (Figure 30). When the reaction was performed under N_2 atmosphere (10 psi), no generation of the ‘end-on-bridged’ N_2 compounds **41** nor **113** was observed, however.

On the basis of ^1H NMR, it was initially believed that compound **115** was the desired mono(carbonyl), mono(sulfide) species $\text{Cp}^*[\text{N}(\text{iPr})\text{C}(\text{CH}_3)\text{N}(\text{iPr})]\text{W}(\text{CO})[(\text{CH}_3)_2\text{S}]$, and attempts to confirm this proposed structure were made. Fortunately, **115** was found to be extremely crystalline, allowing for isolation in moderate yield (59%) (Scheme 47). Preparation of ^{13}C -labeled **115** was accomplished beginning with ^{13}C -labeled **45**, and the $^{13}\text{C}\{^1\text{H}\}$ NMR spectrum revealed a single resonance at 276 ppm ($^1J_{\text{WC}} = 72$ Hz). This chemical shift was the first indication we had that compound **115** may in fact not be the species we

had envisioned preparing. Legzdins and coworkers have shown that tungsten η^2 -acyl complexes typically display chemical shifts between 280 and 296 ppm, with similar W-C coupling.²⁷ Indeed, upon isolation of single crystals of **115** by cooling a concentrated Et₂O solution to -30 °C, XRD revealed this compound to in fact be the tungsten (IV) structural isomer of the desired product, namely Cp*[N(ⁱPr)C(CH₃)N(ⁱPr)]W[η^2 -C(O)CH₃](SCH₃), and the molecular structure is depicted in Figure 31. The assignment of the carbonyl group as an η^2 -acyl ligand is supported by the short W-O bond length of 2.209(2) Å, which is nearly identical to that reported by Legzdins [cf. 2.202(3) Å],²⁷ and a C-O bond length within the range of a C-O double bond of 1.282(4) Å. Presumably, as Scheme 47 also reveals, the envisioned mono(carbonyl), mono(sulfide) compound does in fact form upon photolysis and loss of a carbonyl ligand from **45**, however the resulting sulfide is then activated, producing an intermediate tungsten (IV) methyl compound (**116**), followed by insertion of the carbonyl group into the newly formed W-C bond.

Hoping that this new species could serve as a viable precursor for the regeneration of the ‘end-on-bridged’ N₂ complex **41**, compound **115** was treated with excess N₂ under higher pressures (ca. 90 psi). Still, no reaction was observed, and upon photolysis of this same reaction mixture only decomposition was observed by ¹H NMR, thereby confirming that compound **115** cannot serve as a precursor for **41**.

Before the molecular structure of **115** was confirmed by X-ray analysis, we had become interested in observing its reactivity with N₂ in the presence of methylating agents. Addition of a slight excess of methyl triflate to a benzene-*d*₆ solution of **115** in the presence of N₂ (Scheme 48) lead to the immediate observation

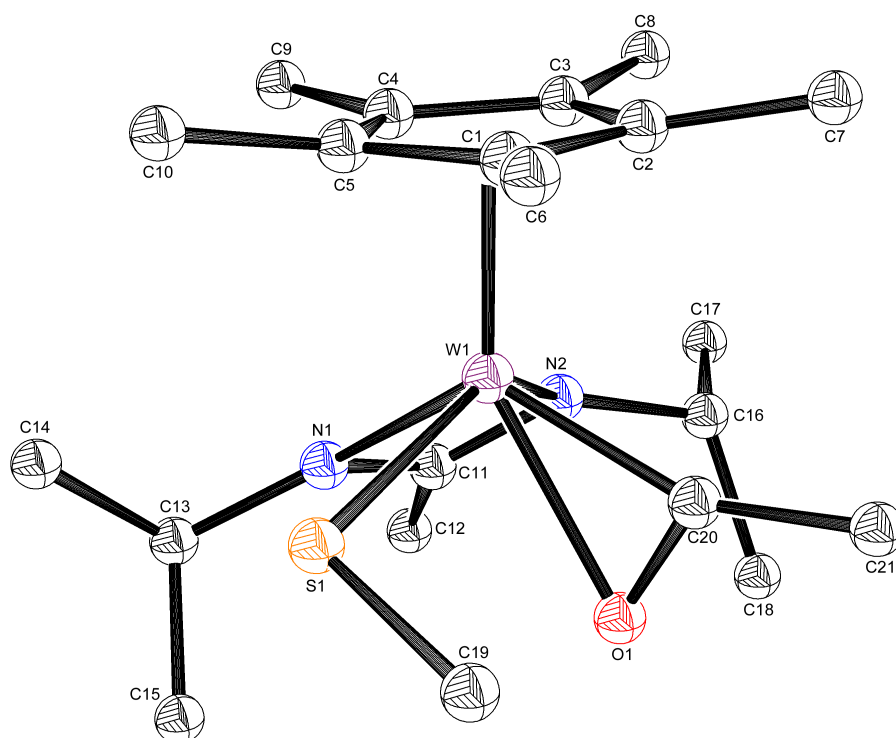
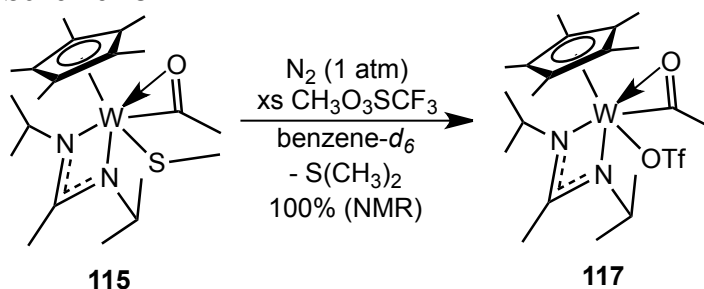


Figure 31. Molecular structure (30% thermal ellipsoids) of compound **115**. H atoms have been omitted for clarity. Selected bond lengths (Å) and angles (°): W1-S1 2.4708(8), S1-C19 1.818(4), W1-C20 1.973(3), W1-O1 2.209(2), C20-O1 1.282(4), C20-C21 1.484(5), W1-S1-C19 109.98(12), W1-C20-C21 156.4(3), W1-C20-O1 82.54(19).

of a new C_1 symmetric product (**117**) by ^1H NMR, along with free dimethyl sulfide. This new species exhibited a nearly identical resonance in the $^{13}\text{C}\{^1\text{H}\}$ NMR spectrum as **115** when the reaction was performed beginning with ^{13}C -labeled **115** ($\delta_{117} = 275$ ppm, $^1J_{\text{WC}} = 73$ Hz) (Figure 32), and a resonance in the ^{19}F NMR spectrum

Scheme 48



at -78.3 ppm. Given these observations and the now known molecular structure of the starting compound **115**, the most logical structure for **117** was assigned as the tungsten (IV) η^2 -acyl, triflate species $\text{Cp}^*[\text{N}(\text{iPr})\text{C}(\text{CH}_3)\text{N}(\text{iPr})]\text{W}[\eta^2\text{-C}(\text{O})\text{CH}_3](\text{O}_3\text{SCF}_3)$. Unfortunately, single crystals suitable for X-ray diffraction of **117** could not be obtained.

Given the observed reactivity of the tungsten bis(carbonyl) compound **45** towards sulfides upon photolysis, the analogous chemistry of the molybdenum derivative was not explored in depth. Upon photolysis of **44** in the presence of excess dimethyl sulfide, new paramagnetic resonances were observed by ^1H NMR. Initial efforts to characterize the product(s) of this reaction were unsuccessful, as only the starting material **44** could be recovered from the reaction mixture, despite being completely consumed as judged by ^1H NMR during photolysis.

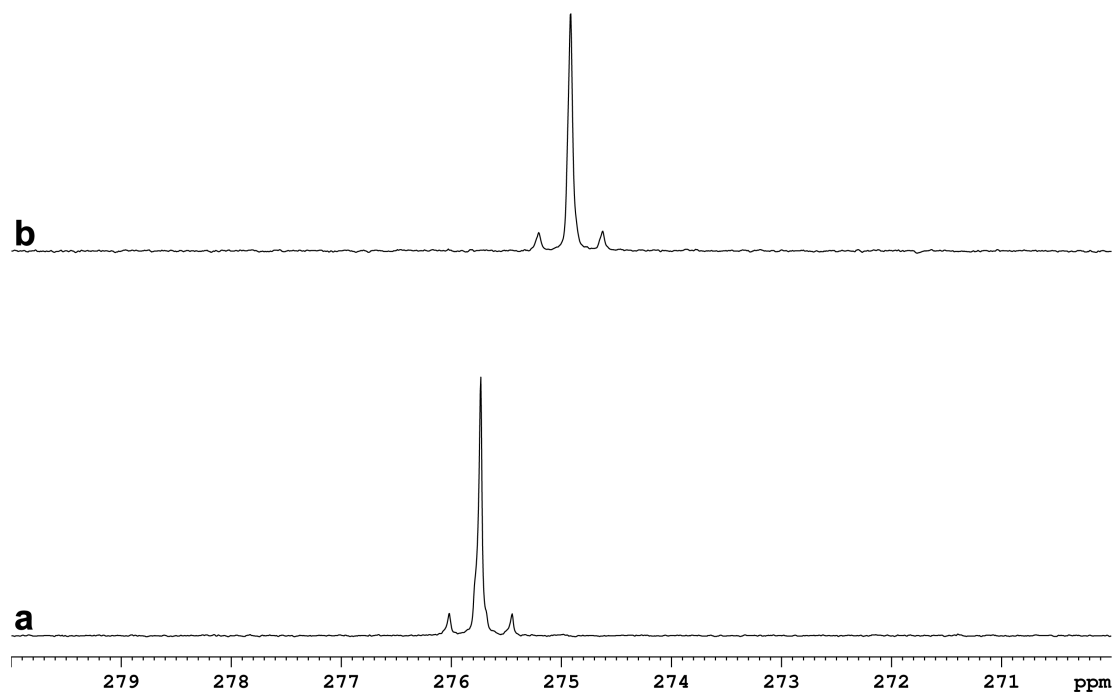


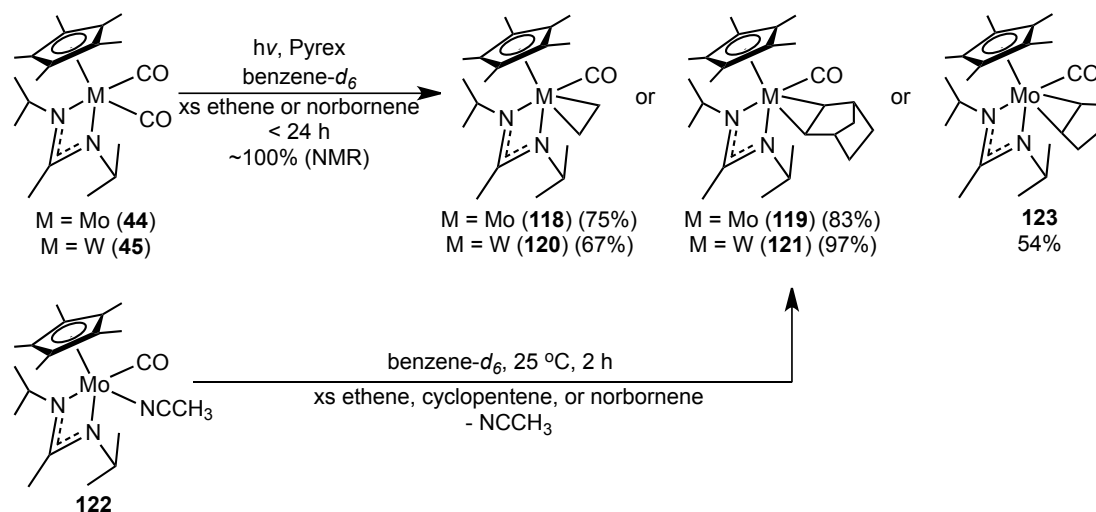
Figure 32. Partial $^{13}\text{C}\{^1\text{H}\}$ (125 MHz, benzene- d_6 , 25 °C) NMR spectra demonstrating the conversion of ^{13}C -labeled **115** (a) to ^{13}C -labeled **117** (b) upon addition of methyl triflate.

4.2.3 L = Olefin – Part 1

We next targeted the synthesis of compounds in which the labile ligand present on the metal center is a coordinated olefin. Although olefins are known to be π -acceptors,²⁸ it was reasoned that the degree to which they compete for electron density with N₂ could be tuned easily through the addition of various substituents which are electron donating (e.g. alkyl groups), making them less π -acidic. Also, the sterics about the olefin can easily be tuned, allowing for the placement of large olefins which would be sterically demanding at the metal center, and more likely to be displaced by smaller N₂. Although such transformations are not common, it has been shown that olefins may be displaced by N₂ in the preparation of ‘end-on-(bridged)’ N₂ compounds.^{10,29} Accordingly, we set out to synthesize a library of mono(carbonyl), mono(olefin) compounds, and to determine their ability to serve as precursors for the regeneration of the ‘end-on-bridged’ N₂ compounds **40** and **41**.

The photolytic reactivity of the bis(carbonyl) compounds **44** and **45** with ethene and norbornene will be presented first. Photolysis of **44** and **45** in benzene-*d*₆ solution within a Pyrex tube with excess ethene or norbornene for time periods of less than 24 hours generated the desired mono(carbonyl), mono(olefin) species Cp*[N(^{*i*}Pr)C(CH₃)N(^{*i*}Pr)]M(CO)(olefin) [M = Mo, olefin = ethene (**118**); M = Mo, olefin = norbornene (**119**), M = W, olefin = ethene (**120**); M = W, olefin = norbornene (**121**)] in near quantitative yield as judged by ¹H NMR (Scheme 49). These products could be isolated easily in analytically pure form in yields ranging from 67 – 97%. In the case of molybdenum, it was found that the same mono(carbonyl), mono(olefin) compounds could be generated thermally by addition

Scheme 49



of the desired olefin to the mono(carbonyl), mono(acetonitrile) compound **122** (Scheme 49), the synthesis of which has been described previously by our group.²²

Compound **122** allowed for the generation of another mono(carbonyl), mono(olefin) species, which was not accessible from the bis(carbonyl) compound **44**. Specifically, photolysis of **44** in the presence of cyclopentene gave no evidence for the generation of the desired product. However, the mono(carbonyl), mono(cyclopentene) compound $\text{Cp}^*[\text{N}(\text{iPr})\text{C}(\text{CH}_3)\text{N}(\text{iPr})]\text{Mo}(\text{CO})(\text{C}_5\text{H}_8)$ (**123**) could be isolated in fair yield by treatment of **122** with cyclopentene at room temperature (Scheme 49). Unfortunately, although the analogous tungsten compound was observed to form by ^1H NMR through photolysis of **45** in the presence of excess cyclopentene, it could not be characterized as it existed exclusively as an oil.

It is worth noting here that many other olefins (e.g. 1-butene, *cis*-2-butene, *trans*-2-butene, propene, cyclohexene, tetramethylethene) were employed in efforts to broaden the scope of mono(carbonyl), mono(olefin) compounds in our library.

However, for a variety of reasons, the desired products were not observed or could not be isolated. Accordingly, they will not be discussed here. On the other hand, several other olefins (e.g. *neo*-hexene, *iso*-butene) lead to the clean formation and isolation of rather surprising products. A discussion of these compounds is provided in the following section (4.2.4).

The main features we wished to study for each of these new compounds were the relative C-O bond lengths observed, the C-O bond stretching frequencies, and the C-C bond lengths of the coordinated olefins relative to the free C-C bond length.³⁰⁻³² In order to accomplish this, single crystals for each compound described above were analyzed by XRD to provide the molecular structures, which are shown in Figures 33 – 35, and IR spectroscopy was employed to determine the C-O bond stretching frequencies. These data are summarized in Table 1. In general, the CO bond order is more significantly reduced in the tungsten complexes than it is in molybdenum as determined by the C-O bond lengths and IR stretching frequencies, a trend which is in keeping with the observed physical data for compounds **44** and **45**.¹⁰ Similarly, more C-C bond lengthening is observed within the tungsten compounds than their molybdenum counterparts. In all cases, however, the olefin ligands display a significant amount of π -backbonding from the metal centers as evidenced by rather extensive bond lengthening, which we feared may inhibit their ability to be displaced by N₂ (*vide infra*). It is worth noting that many group 6 compounds bearing ethene (and other olefin) ligands have appeared in the literature, however these compounds are generally in higher oxidation states and, not surprisingly, typically possess C-C bond lengths of the coordinated ethene molecule shorter than those exhibited by

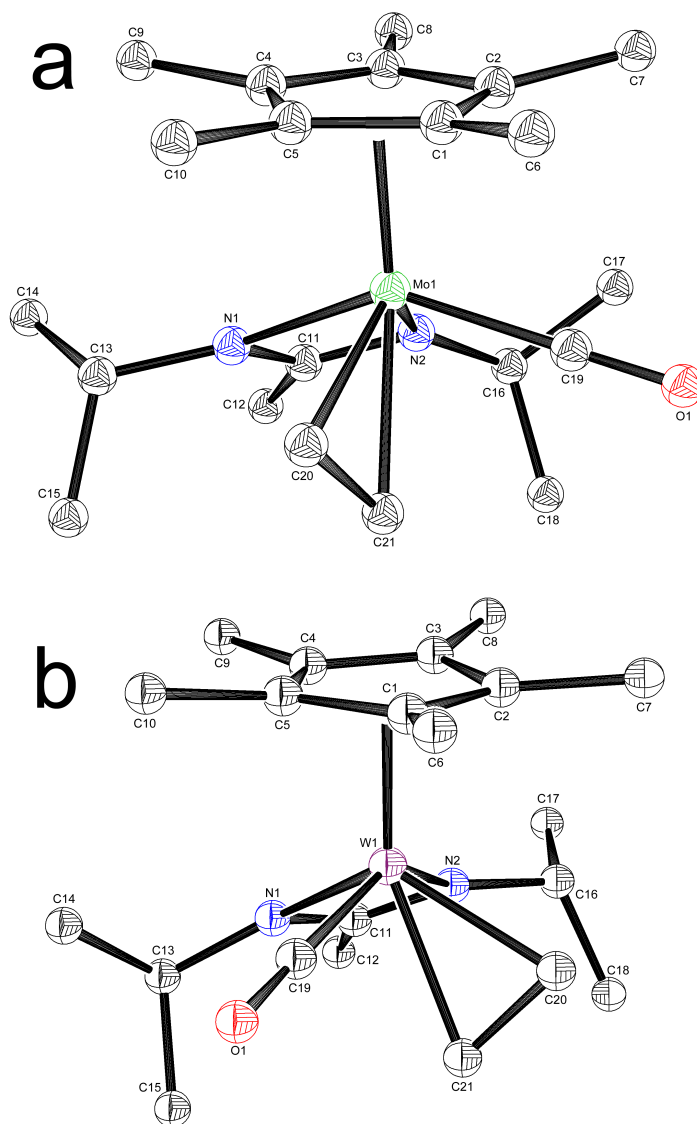


Figure 33. Molecular structures (30% thermal ellipsoids) of compounds **118** (a) and **120** (b).

compounds **118** and **120**, as a result of the fact that they contain less electron density at the metal center to donate to the olefin π^* orbitals.³³⁻³⁵ On the other hand, the C-C bond lengths observed in the mono(carbonyl), mono(ethene) compounds **118** and **120** are in keeping with reported values for other mid and low valent group 6 ethene compounds.³⁶⁻³⁸

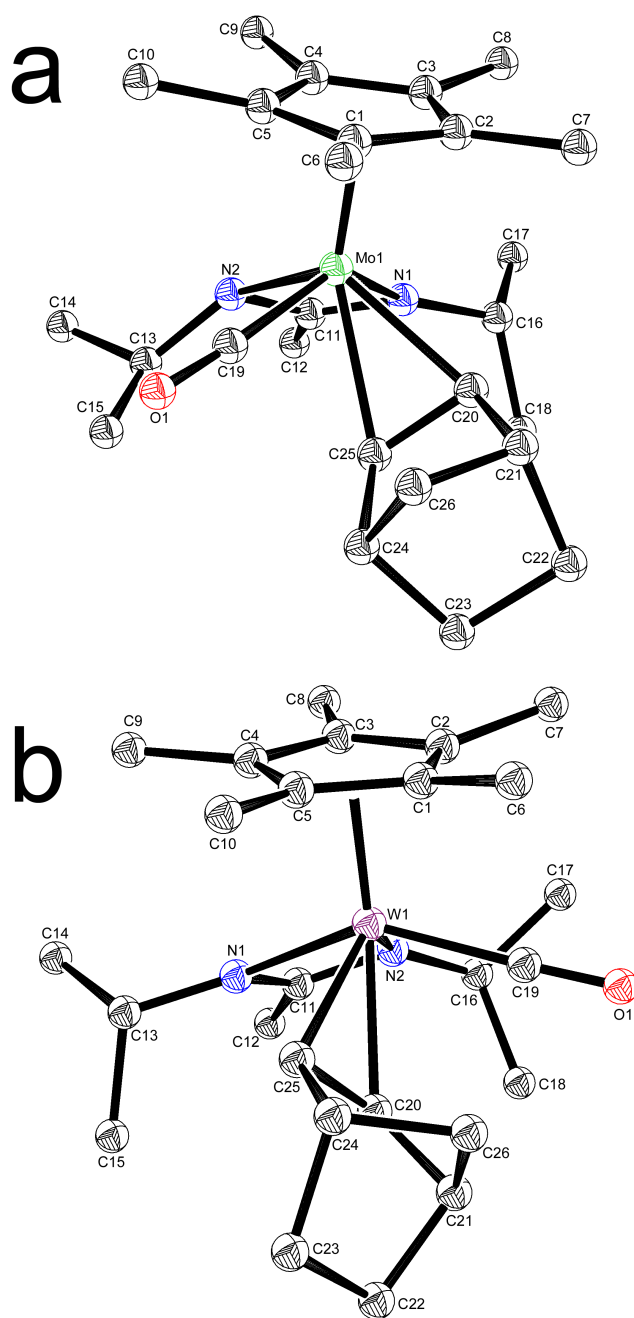


Figure 34. Molecular structures (30% thermal ellipsoids) of compounds **119** (a) and **121** (b).

It is interesting to note that for the molybdenum compounds **118** and **119**, a rather unintuitive trend was observed. Specifically, given the fact that norbornene is a highly strained cyclic olefin, we imagined that **119** would display a shorter C-O bond length than in **118**. The reason for the expected observation would be that

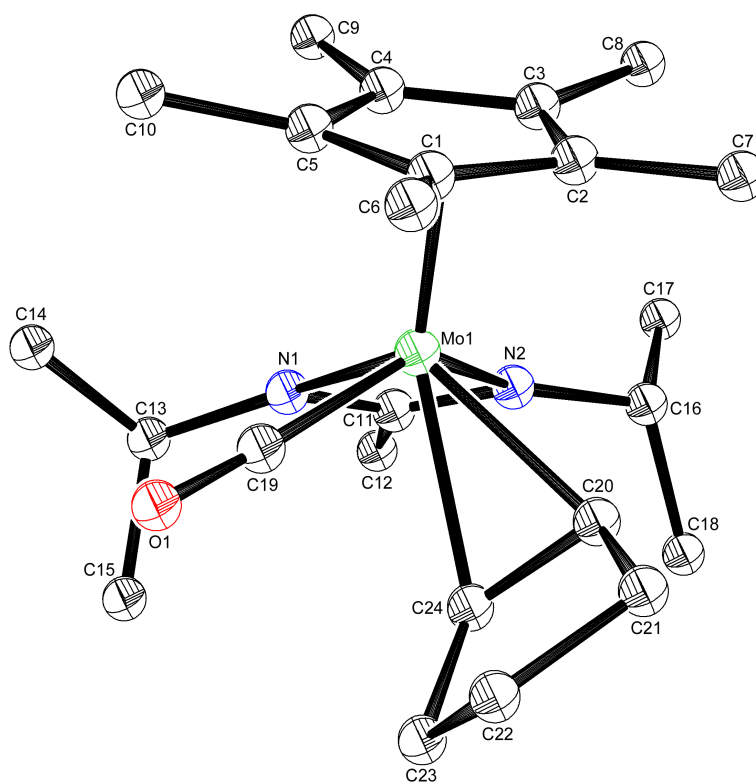


Figure 35. Molecular structure (30% thermal ellipsoids) of compound **123**.

norbornene would act as a stronger π -acid than ethene, and therefore the carbonyl ligand in **119** would experience less π -backbonding than in **118**. However, the opposite trend was observed, with **118** displaying the shorter C-O bond length of 1.1595(15) Å compared to 1.172(4) Å in **119**. Furthermore, the C-C bond for the norbornene ligand in **119** was found to be elongated by only 0.097 Å from that in the free molecule, while the C-C bond length in **118** was 0.1025 Å longer than in free ethene. Together, these data indicate that ethene acts as a better π -acceptor than norbornene. Presently, the most obvious rationale for this counterintuitive observation is that the norbornene ligand in **119** is much more sterically demanding than the small ethene ligand in **118**. Accordingly, ethene may exist closer to the

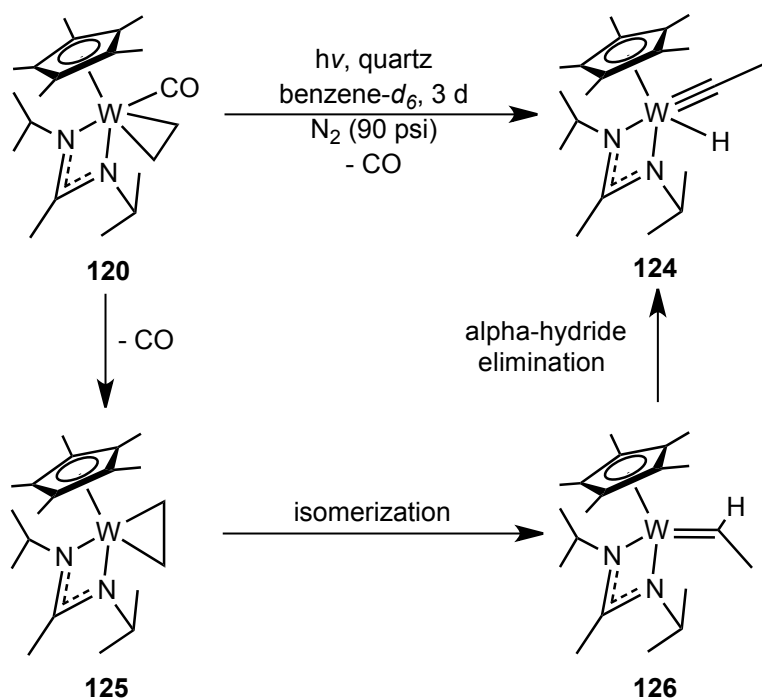
| Compound | $d(\text{CO})$ (Å) | ν_{CO} (cm ⁻¹) | $d(\text{C-C})$ (Å) | $\Delta d(\text{C-C})$ (Å) ^a |
|------------|--------------------|---------------------------------------|---------------------|---|
| 118 | 1.1595(15) | 1867.0 | 1.433(2) | 0.1025 |
| 119 | 1.172(4) | 1859.2 | 1.433(5) | 0.097 |
| 123 | 1.165(3) | 1861.0 | 1.449(3) | 0.126 |
| 120 | 1.161(5) | 1858.1 | 1.452(8) | 0.122 |
| 121 | 1.171(3) | 1844.2 | 1.478(3) | 0.142 |

Table 1. Selected structural and spectral data for compounds **118** – **121** and **123**. ^aSee references 30 – 32 for bond lengths of free olefins.

molybdenum center than norbornene, allowing for greater overlap of the necessary orbitals to allow for π -backbonding. This hypothesis is supported by the fact that the average Mo-C bond length in **118** is 2.226 Å, while in **119** it is slightly longer (2.254 Å).

With compounds **118** – **121** in hand, each of which could be prepared directly from the bis(carbonyl) species **44** and **45**, we next sought to investigate their reactivity towards N₂. In the case of the molybdenum compounds **118** and **119**, pressurizing benzene-*d*₆ solutions with N₂ up to 90 psi lead to no observable reaction by ¹H NMR. Upon photolysis within a quartz tube, only slow decomposition was observed, and no generation of either the ‘end-on-bridged’ or cleaved N₂ species **40** or **106** could be detected. Repeating the reactions with the tungsten analogs **120** and **121**, again it was found that no thermal reaction was observed by ¹H NMR. Upon photolysis, however, more interesting reactivity was discovered. Specifically, in the case of the mono(carbonyl), mono(ethene) compound **120**, photolysis lead to the observation of small amounts of the tungsten (VI) ethylidyne hydride complex **124** (Scheme 50). The preparation and characterization of compound **124** will be presented in the following chapter. However, in the present case, this species likely forms as the result of photodissociation of the carbonyl ligand in **120** to provide a

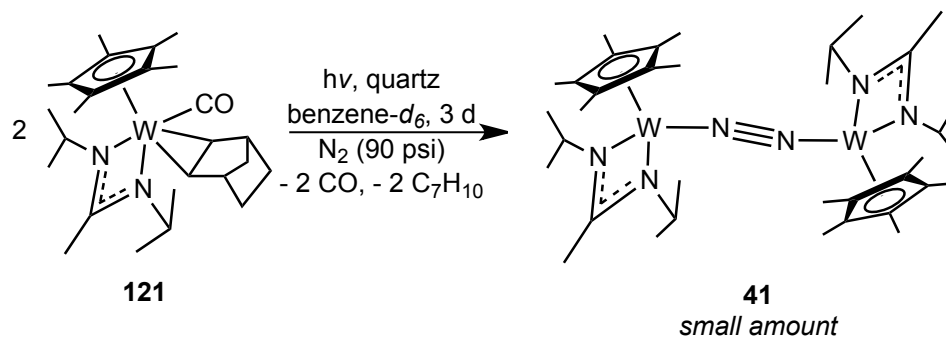
Scheme 50



mono(ethene) intermediate **125**, which then isomerizes to the ethylidene compound **126**, followed by the final step of α -hydride elimination to yield the final product **124** (Scheme 50).³⁹

More interesting was the reaction of the mono(carbonyl), mono(norbornene) compound **121** which, upon photolysis under a high pressure of N_2 (90 psi) within a

Scheme 51



quartz tube lead to the formation of small amounts of the ‘end-on-bridged’ N₂ compound **41** as judged by ¹H NMR (Scheme 51). Possibly, the second isomerization step that is proposed to occur upon loss of a carbonyl ligand from **120** is not able to occur in compound **121**, preventing such a decomposition path from being followed. Rather, then, N₂ is able to compete with norbornene for electron density from the tungsten center. This then allows for the formation of a very small amount of the ‘end-on-bridged’ N₂, mono(carbonyl) compound **113** to form which, when photolyzed, undergoes rapid dissociation of the remaining carbonyl ligands (*vide supra*). Unfortunately, the observed reaction is sluggish, and decomposition of **121** was also observed by ¹H NMR to occur at a much faster rate than the generation of **41**. Accordingly, even though the observation of small amounts of **41** marked the completion of a synthetic cycle for N₂ fixation, the ability to utilize such a process for the generation of N₂-derived organic products did not seem plausible.

4.2.4 L = Olefin – Part 2

In the course of studies into the synthesis of group 6 CpAm mono(carbonyl), mono(olefin) complexes, several surprising discoveries were made in regard to tungsten, which are presented here. First, we were interested in preparing such a complex in which the coordinated olefin bore alkyl groups, with the hope that it would make the olefin less π -acidic. Cyclic olefins had been unsuccessful with the exception of norbornene, and no clean reaction was observed with propene, 1-butene, *cis*-2-butene, *trans*-2-butene, or tetramethylethene. However, photolysis of the bis(carbonyl) compound **45** in the presence of *iso*-butene (10 psi) in benzene-*d*₆

solution within a sealed Pyrex tube lead to the formation of a new C_1 symmetric species. The most striking feature of this new compound was the presence of a new upfield triplet of triplets in the ^1H NMR at -0.88 ppm ($^1J_{\text{WH}} = 55$ Hz, $^2J_{\text{HH}} = 3$ Hz), indicating the presence of a hydride ligand which experiences coupling to both the ^{183}W center and another proton. $^{13}\text{C}\{^1\text{H}\}$ NMR revealed no resonance which could be assigned to a carbonyl ligand, but did display two resonances at 45.7 and 53.2 ppm

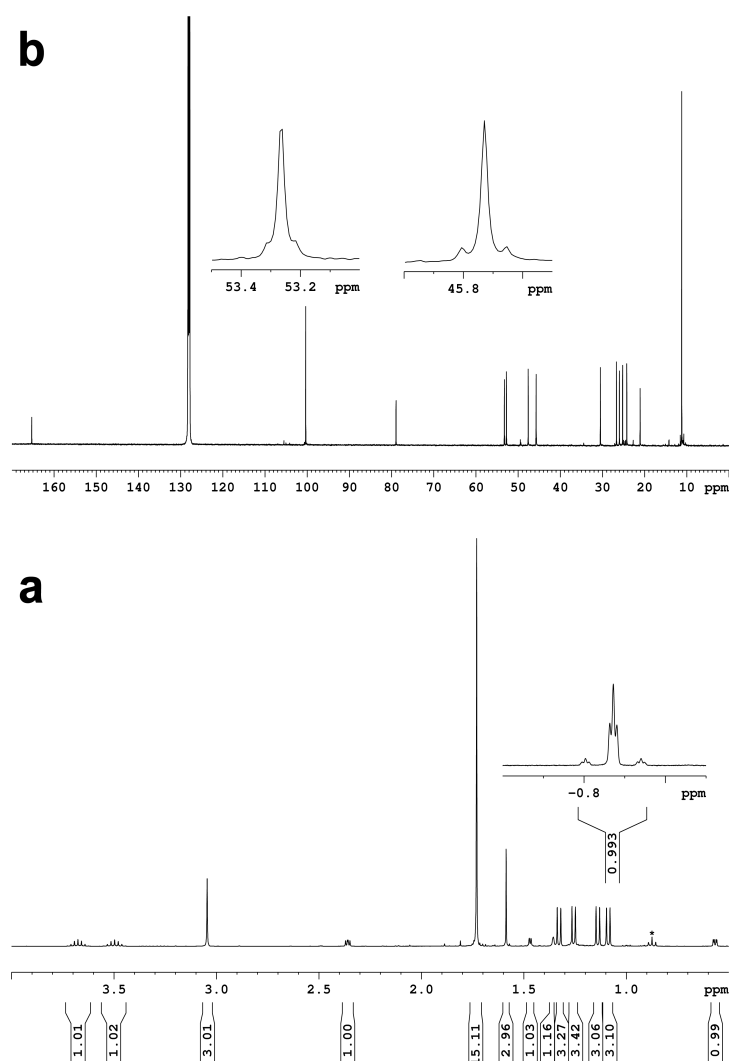
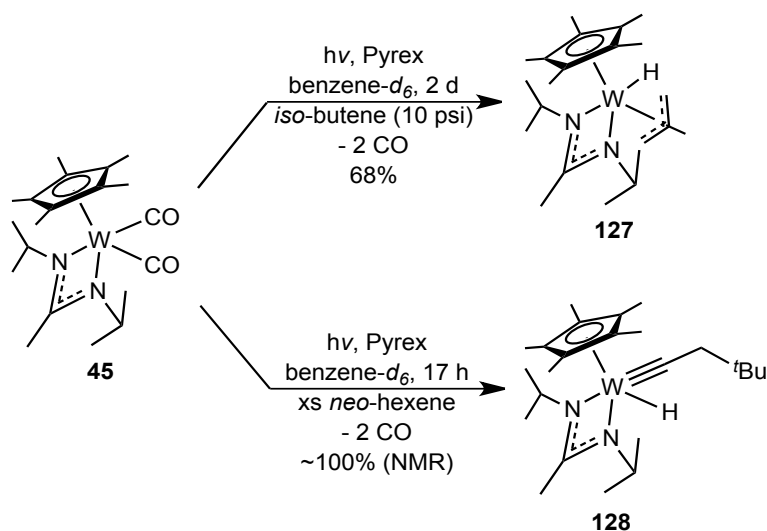


Figure 36. a) ^1H (400 MHz) and b) $^{13}\text{C}\{^1\text{H}\}$ (125 MHz) (benzene- d_6 , 25 $^\circ\text{C}$) NMR spectra of compound **127** (* marks pentane solvent impurity).

with coupling to the ^{183}W center ($^1J_{\text{WC}} = 19 \text{ Hz}$ and 12 Hz , respectively) (Figure 36). Together, these observations suggested that both carbonyl ligands had been lost from compound **45** during photolysis, and C-H bond activation at one of the *iso*-butene methyl groups had occurred to produce the tungsten (IV) allyl hydride complex $\text{Cp}^*[\text{N}(\text{iPr})\text{C}(\text{CH}_3)\text{N}(\text{iPr})]\text{W}(\text{H})(\eta^3\text{-C}_4\text{H}_7)$ (**127**) (Scheme 52). This prediction was confirmed by single crystal X-ray diffraction, which provided the molecular structure of compound **127** depicted in Figure 37. Specifically, the designation of **127** as an η^3 -allyl complex is supported by the fact that the C19-C20 and C20-C21 bond lengths (Figure 37) are nearly identical [$1.411(7) \text{ \AA}$ and $1.409(7) \text{ \AA}$, respectfully], and these values are in keeping with other tungsten (IV) allyl hydride compounds.^{40,41} Compound **127** was found to be stable in solution over the course of several days, even at elevated temperatures. Given this observation, further reactivity of this species was not explored as it did not appear to be a viable precursor for the synthesis of **41**.

Scheme 52



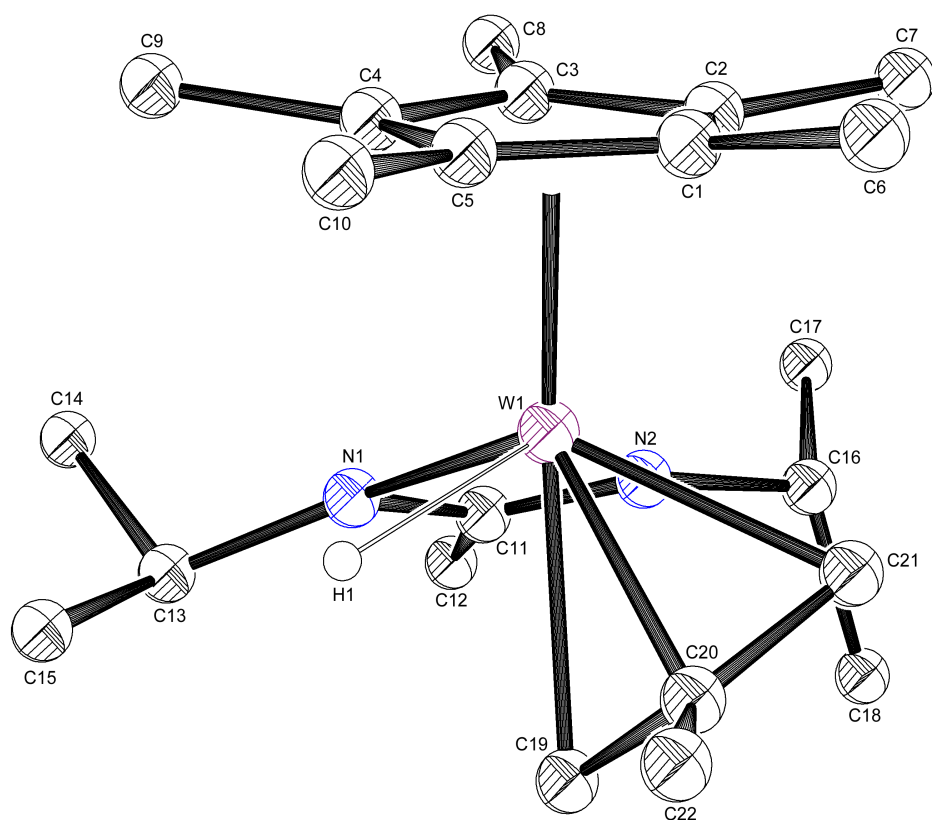


Figure 37. Molecular structure (30% thermal ellipsoids) of compound **127**. Selected bond lengths (Å) and angles (°): W1-H1 1.94(5), W1-C19 2.250(5), W1-C20 2.187(4), W1-C21 2.235(4), C19-C20 1.411(7), C20-C21 1.409(7), C20-C22 1.520(6), C19-C20-C21 111.5(4).

The reactivity of *neo*-hexene was explored next, as it was believed that an olefin lacking β -hydrogens would be immune to the decomposition observed in the formation of **127**. Furthermore, this olefin should be electron rich and sterically bulky due to the presence of the *tert*-butyl group, which in theory should make it easy to displace from the tungsten center. Accordingly, as Scheme 52 further reveals, **45** was photolyzed in the presence of excess equivalents of *neo*-hexene, which lead to the formation of the new species **128**, which also displayed a hydride resonance in the ^1H NMR (6.69 ppm, $^1J_{\text{WH}} = 95$ Hz). Compound **128** was noticeably different in

nature from **127**, as it appeared to undergo dynamic ring flipping of the amidinate ligand on the NMR time scale, as evidenced by broadening of the resonances for the isopropyl group protons. Variable temperature ^1H NMR allowed for the sharpening of these peaks upon heating (Figure 38), at which point apparent C_s symmetry was observed for **128**, which in actuality is of C_1 symmetry. Given the lack of β -hydrogens in *neo*-hexene, we inferred that compound **128** could not be an allyl hydride such as **127**. The fact that the amidinate ligand is involved in dynamic ring flipping instead lead us to believe that **128** is a heavily ' π -loaded' complex. Accordingly, compound **128** is likely the alkylidyne hydride species depicted in Scheme 52, however single crystals could not be obtained to confirm this assignment. The mechanism for the formation of compound **128** is believed to be analogous to that for **124**, as depicted in Scheme 50.

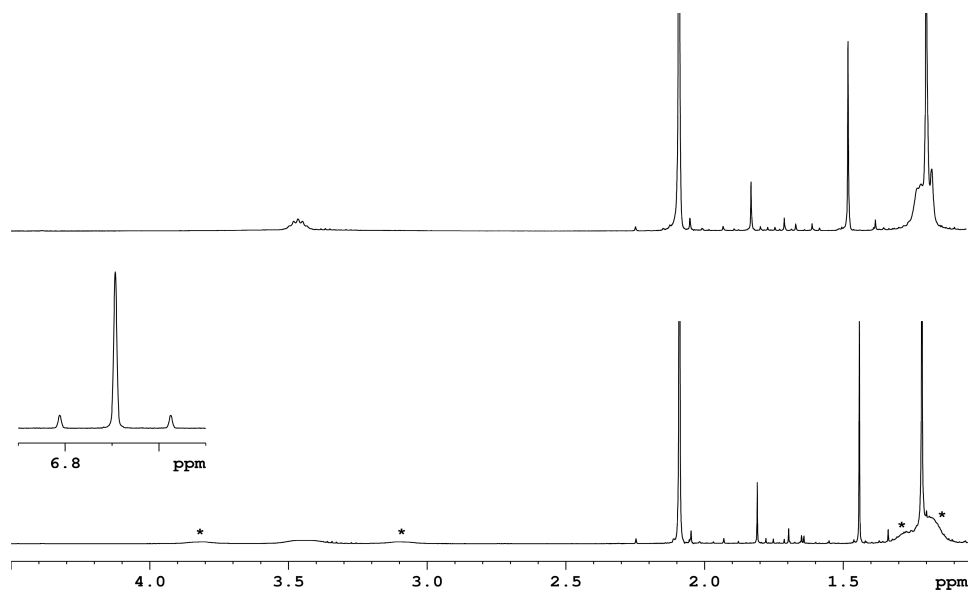


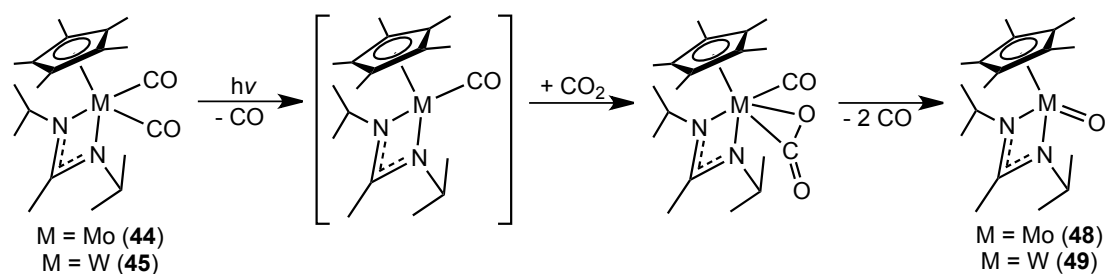
Figure 38. ^1H (400 MHz, benzene- d_6) NMR spectra of compound **128** at 25 °C (bottom) and 70 °C (top) with inset showing tungsten hydride resonance.

4.3 Tandem Dinitrogen and Carbon Dioxide Fixation

4.3.1 Background

Looking for alternative methods to complete the synthetic cycle depicted in Scheme 43, we decided to revisit known chemistry with regard to the bis(carbonyl) compounds **44** and **45**. Most notably, these complexes have been shown previously to react photolytically with CO₂ to generate the M(IV) terminal oxo species **48** and **49** quantitatively through the mechanism in Scheme 53.⁴² Given this well established transformation, we next turned to investigate the chemistry of these oxo compounds to determine if they may serve as viable precursors for the ‘end-on-bridged’ dinitrogen compounds **40** and **41**, respectfully. If successful, such a transformation would be noteworthy in that it would couple two of the most important challenges that face synthetic chemists today, namely the fixation of N₂ and CO₂, the reasons for which have been described in Chapter 1.

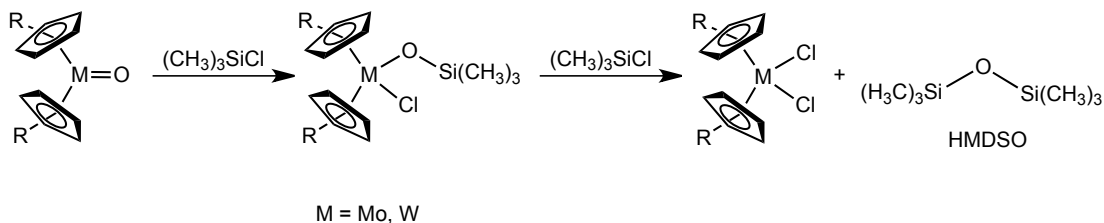
Scheme 53



4.3.2 Reactivity of Terminal Oxo Compounds

It has been shown by Marks,⁴³ Parkin,⁴⁴ and Geoffroy⁴⁵ that group 6 terminal oxo complexes supported by the metallocene ligand framework react with TMSCl to provide the corresponding dichloride complexes in high yields, along with concomitant formation of hexamethyldisiloxane {[(CH₃)₃Si]₂O, HMDSO}, as shown

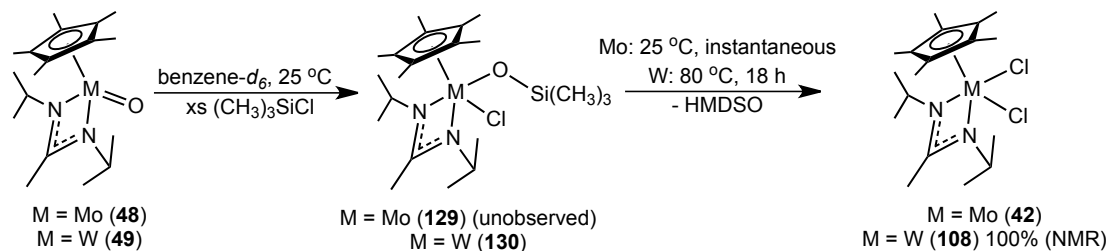
Scheme 54



in Scheme 54. On the other hand, the CpAm group 6 dichloride compounds **42** and **108** may be reduced with NaHg under N₂ atmosphere to provide the ‘end-on-bridged’ N₂ complexes **40** and **41** in high yield as well.¹⁰ Accordingly, we sought to determine if the CpAm oxo compounds **48** and **49** followed similar reactivity to their metallocene counterparts to produce the dichloride compounds **42** and **108**, as such a transformation would allow for the completion of the desired synthetic cycle. Indeed, as shown in Scheme 55, treatment of the molybdenum oxo compound **48** with excess equivalents of TMSCl in benzene-*d*₆ solution at room temperature lead to immediate formation of the paramagnetic dichloride complex **42**, as evidenced by the observation of HMDSO and diagnostic broad resonances in the ¹H NMR spectrum. In the case of tungsten, immediate generation of the W(IV) siloxy chloride intermediate complex Cp*[N(ⁱPr)C(CH₃)N(ⁱPr)]W[OSi(CH₃)₃]Cl **130** was observed by ¹H NMR, and heating to 80 °C for 16 hours lead to quantitative conversion to the dichloride compound **108** (Scheme 55).

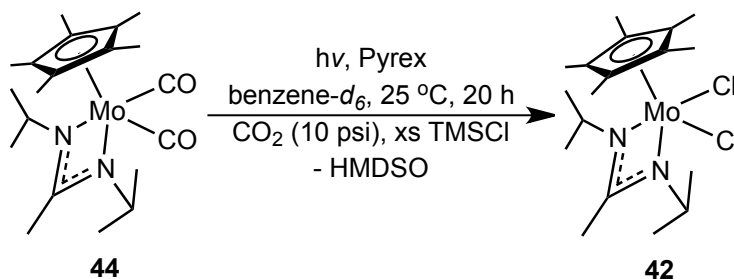
Having successfully demonstrated that the dichloride compounds **42** and **108** may be generated from the oxo complexes **48** and **49**, we were next interested in determining if such a process could be repeated successfully beginning with the bis(carbonyl) compounds **44** and **45**. In doing so, we hoped that we could reduce the

Scheme 55



overall process for the complete synthetic cycle by one step, and remove the need to isolate the oxo species. In the case of molybdenum, this process worked as planned. Specifically, as revealed in Scheme 56, photolysis of compound **44** in benzene- d_6 solution in the presence of excess equivalents of TMSCl and CO_2 for 20 hours lead to complete conversion to the paramagnetic dichloride complex **42** and HMDSO as judged by 1H NMR (Figure 39). In the case of the analogous tungsten complex **45**, this one pot process was not successful, likely due to the fact that the siloxy chloride intermediate **130** does not go on to form the dichloride compound without heating. Accordingly, it may decompose upon long exposure to UV irradiation in the presence of TMSCl at ambient temperature.

Scheme 56



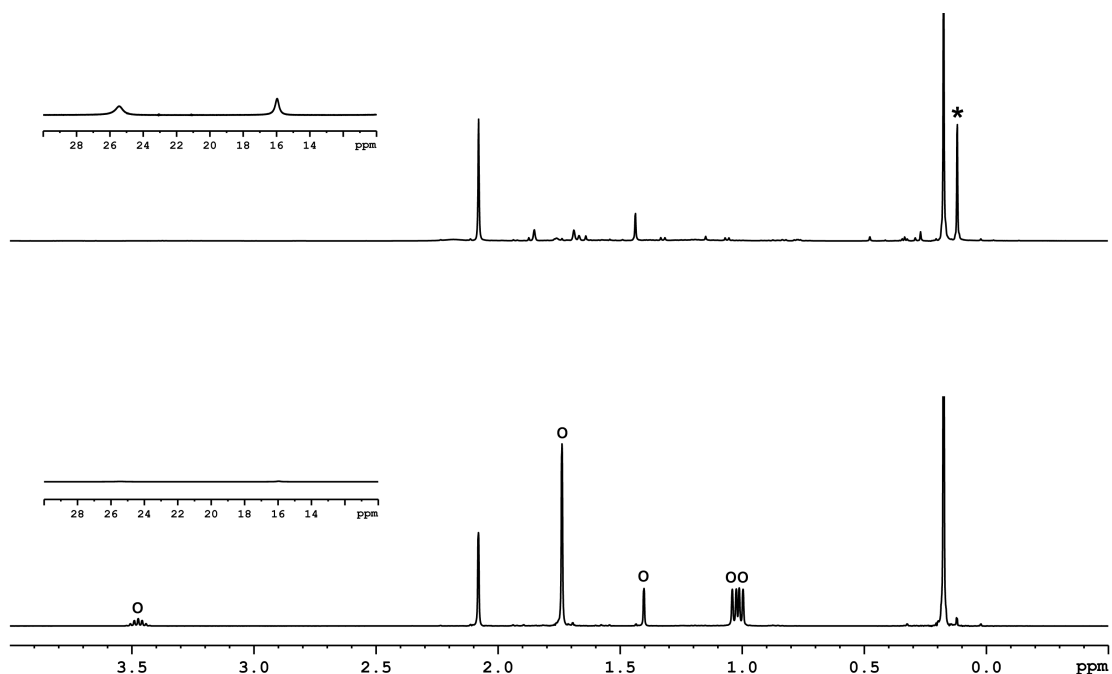
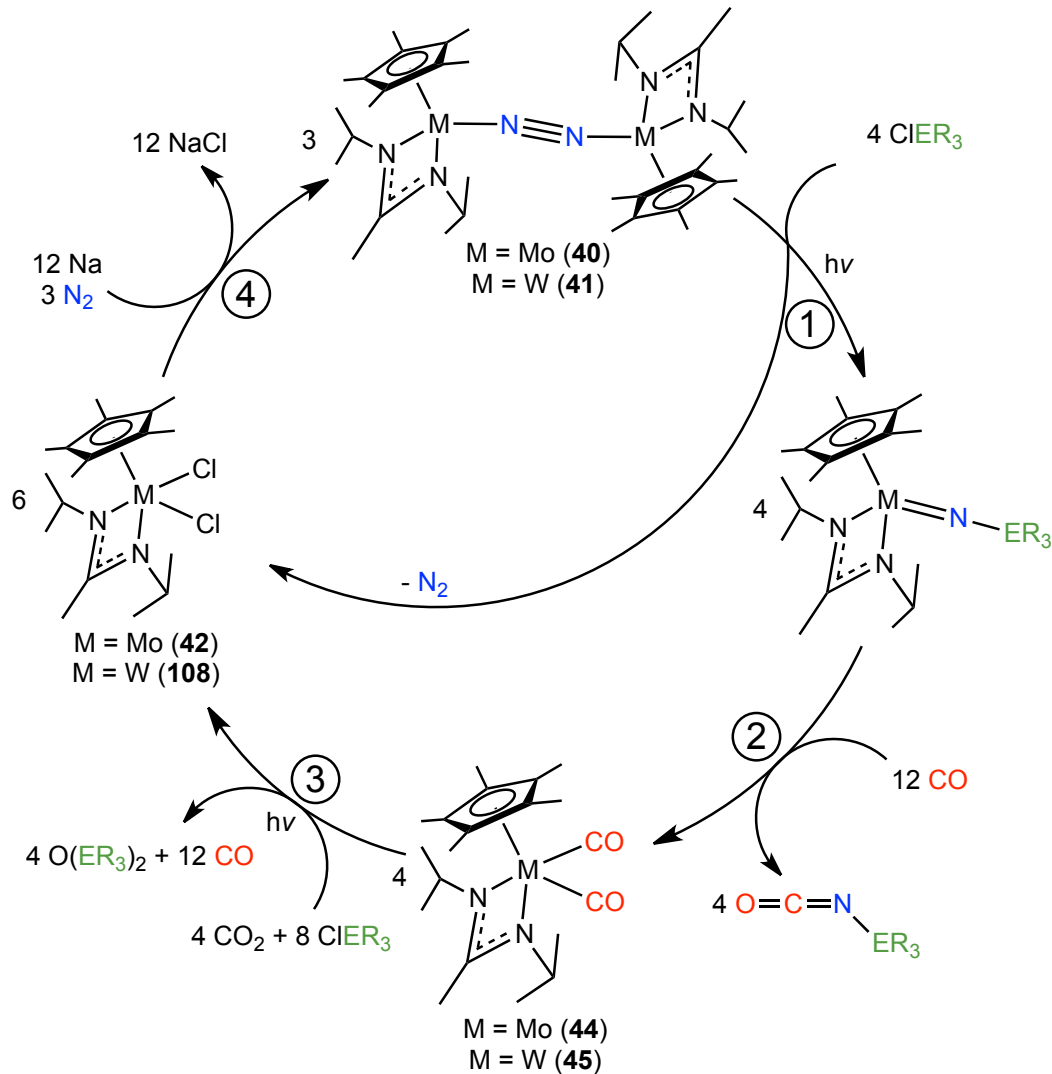


Figure 39. ^1H (400 MHz, benzene- d_6 , 25 °C) NMR spectra demonstrating the photolytic reaction of compound **44** with excess TMSCl and CO_2 (10 psi) after 0 h (bottom) and 20 h (top) with inset showing downfield paramagnetic resonances for compound **42**. Labeled resonances are compound **44** (o) and HMDSO (*). The unlabeled resonance at 2.08 ppm is durene internal standard.

4.3.3 Synthetic Cycle for N_2 Fixation

With every step in the desired synthetic cycle for N_2 fixation complete (Scheme 57), we next sought to determine the overall yield of the process from beginning to end. Rather than simply calculate the yields observed for each step, we instead began with a set amount of the ‘end-on-bridged’ dinitrogen compounds **40** and **41** and subjected them to the entire series of transformations depicted in Scheme 57, using TMSCl as the $-\text{ER}_3$ source. In this way, we hoped to gain a more realistic representation of the process’ efficacy.

Scheme 57



To begin, 3 mL of a benzene- d_6 solution consisting of the molybdenum ‘end-on-bridged’ N_2 complex **40** (19 mM), excess TMSCl (55 mM), and durene internal standard was prepared and transferred evenly between three Pyrex J Young NMR tubes. The solutions were photolyzed for 28 hours, at which point complete conversion to the molybdenum (IV) TMS imido and dichloride complexes (**111** and **42**, respectfully) was observed by 1H NMR. The headspace of each tube was then evacuated and charged with CO (10 psi), which lead to the production of TMS

isocyanate (49% based on initial concentration of **40**, 88% based on concentration of **111**) and the bis(carbonyl) compound **44** after two days at room temperature. Volatiles were then removed *in vacuo*, and fresh benzene-*d*₆ solutions of TMSCl (131 mM) were added to each tube. The headspaces were evacuated and charged with CO₂ (10 psi) and photolyzed for 20 hours, at which point paramagnetic **42** and HMDSO were observed by ¹H NMR. Compound **42** was isolated from this mixture and reduced with 3 equivalents of NaHg under N₂ atmosphere, which lead to the isolation of the starting material **40** in 44% yield after recrystallization (Figure 40). The analogous sequence of reactions was carried out with the tungsten derivative **41**, with the exception that Step 3 (Scheme 57) was performed step-wise. Specifically, the bis(carbonyl) compound **45** was photolyzed in the presence of CO₂ (10 psi) until complete conversion to the oxo compound **49** was observed by ¹H NMR. At this point, excess TMSCl was added, and the solution was heated to 80 °C for 18 hours to produce the dichloride compound **108**, which was then reduced under N₂ to provide the starting material **41** in 52% yield. Thus, for both molybdenum and tungsten, complete synthetic cycles for N₂ and CO₂ fixation to produce isocyanates and HMDSO have been achieved, and in both cases the starting material may be isolated in moderate yields.

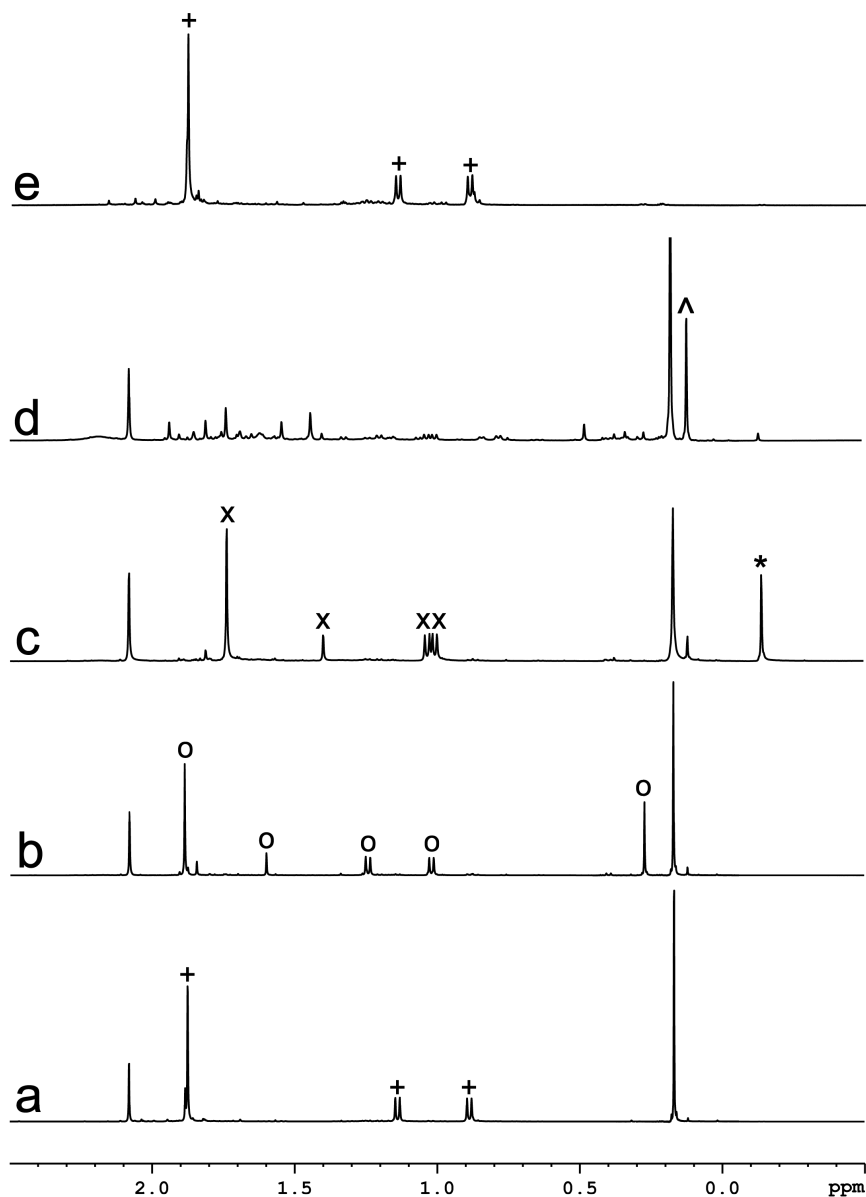
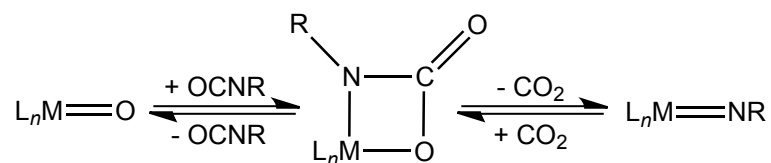


Figure 40. ^1H (400 MHz, benzene- d_6 , 25 $^\circ\text{C}$) NMR spectra demonstrating the synthetic cycle in Scheme 57 for $\text{M} = \text{Mo}$ and $-\text{ER}_3 = \text{TMS}$. (a) initial; (b) after complete conversion to compounds **111** and **42**; (c) after reaction with CO to produce compound **44** and TMS isocyanate; (d) after photolysis in the presence of CO_2 and TMSCl to produce compound **42** and HMDSO; (e) after reduction to regenerate **40**. Labeled resonances are **40** (+), **111** (o), **44** (x), TMS isocyanate (*), and HMDSO (^).

4.3.4 [2+2] Cycloadditions of CpAm Imido Complexes

Given the success of the newly developed cycles for tandem N₂/CO₂ fixation, we became interested in reducing the number of overall steps involved even further. Specifically, seeing as the N₂ derived imido complexes are sufficiently nucleophilic to react under mild conditions with CO, we wondered if they would react directly with CO₂ *via* [2+2] cycloaddition pathways to generate the terminal oxo complexes **48** and **49** and the corresponding isocyanates, thus eliminating the need to generate the bis(carbonyl) compounds **44** and **45** in the overall synthetic cycle.

Scheme 58

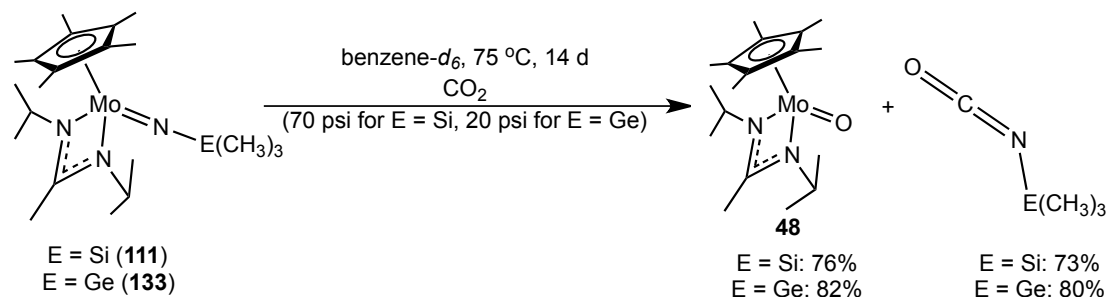


In general, such processes tend to occur in reverse. Specifically, it has been well established that terminal oxo compounds react with isocyanates to generate CO₂ and the corresponding imido compounds for tungsten,^{46,47} molybdenum,⁴⁸⁻⁵⁰ rhenium,⁵¹ and vanadium,⁵² as depicted in Scheme 58. Although the reaction exists in equilibrium, it generally proceeds to the right when performed in an open system, as CO₂ is slowly removed from the reaction as it diffuses out of solution. Several examples have appeared in the literature, however, which describe systems that favor the reverse reaction, however nearly all examples are confined to titanium. Specifically, Mountford demonstrated that the CpAm titanium *tert*-butyl imido complex Cp*[N(^{*i*}Pr)C(CH₃)N(^{*i*}Pr)]Ti[NC(CH₃)₃] (**131**) reacts with CO₂ at 25 °C to quickly produce the bridging oxo complex {Cp*[N(^{*i*}Pr)C(CH₃)N(^{*i*}Pr)]Ti}₂(μ-O)₂

(**132**) with concomitant production of *tert*-butyl isocyanate.⁵³ Changing the substituents of the imido ligand lead to the extension of this work to include proposed [2+2] cycloaddition reactions with various benzaldehydes and even dimethylformamide (DMF), along with more examples of CO₂ cycloaddition.^{54,55} Mindiola later reported that titanium imido complexes bearing 'nacnac' ligands may produce aryl isocyanates from reaction with CO₂,⁵⁶ and Anderson has demonstrated that 12 electron tris(pyridine) titanium imido complexes react with CO₂ to provide symmetrical ureas upon treatment with strong acid, a process which is believed to go through intermediate generation of isocyanates.⁵⁷ In addition to these examples, other reports for titanium compounds may be found in the literature, including one example for a group 5 compound (tantalum).⁵⁸⁻⁶⁰ Analogous chemistry with regard to group 6 metals has not yet been observed, although Schrock has reported spectroscopic evidence for the [2+2] cycloaddition of CO₂ to an anionic molybdenum (VI) imido species, however no generation of an isocyanate was detected.⁶¹ Mountford has reported similar reactivity with a cationic tungsten (VI) species, but this compound too did not yield any isocyanate.⁶²

In order to test whether or not our desired transformations were possible, the molybdenum imido complexes Cp*[N(^{*i*}Pr)C(CH₃)N(^{*i*}Pr)]Mo[N-E(CH₃)₃] [E = Si (**111**); E = Ge (**133**)]^{22,23} were reacted with CO₂ under near ambient conditions. Similar reactions were performed with the tungsten imido complex **112** as well, however initial results indicated that these transformations are much slower than those observed for molybdenum, therefore further investigations were not prioritized and are not presented here.

Scheme 59



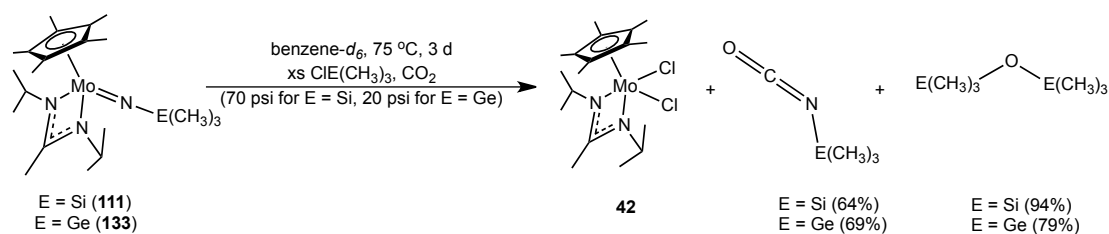
Upon treatment of the molybdenum TMS imido compound **111** with a modest pressure of CO_2 (20 psi) in benzene- d_6 solution, no reaction was detected by ^1H NMR after several days at 25 °C. Upon heating to 75 °C, however, slow generation of the terminal oxo complex **48** and TMS isocyanate was observed. After 26 days of reaction, complete consumption of the starting material was observed, and **48** and TMS isocyanate had been generated in 60% and 47% yield, respectively. Increasing the pressure of CO_2 within the reaction tube lead to an increase in the observed rate and yield; specifically, after 3 days of heating under 70 psi CO_2 , **48** and TMS isocyanate were observed in 16% and 15% yield, respectively. The reaction was then allowed to react for a total of 14 days at 75 °C, at which point complete consumption of the TMS imido compound **111** had occurred, and **48** and TMS isocyanate were present in 76% and 73% yield, respectively (Scheme 59).

The reactivity of the trimethylgermyl (TMG) imido complex **133** towards CO_2 was examined next (Scheme 59). Again, no reaction was observed at room temperature, however upon heating to 75 °C under 20 psi CO_2 in benzene- d_6 , faster conversion to compound **48** and TMG isocyanate was observed by ^1H NMR than in the case of compound **111**. After 2 days, these species were observed in 61% and 58% yield, respectively, and after extended reaction time (14 days total) were present

in 82% and 80% yield, thus demonstrating that the TMG substituted imido complex reacts significantly more quickly than the TMS derivative with CO₂ and under more reasonable pressures, and that the products are stable after prolonged heating in benzene-*d*₆ solution under CO₂ atmosphere.

[2+2] cycloaddition of CO₂ to an early transition metal imido is a rare occurrence, for which little precedent exists. More specifically, no such examples for group 6 metals have appeared in the literature to date. Likely, however, many have simply overlooked such reactions, as the reverse process is known to occur readily. The driving force for the transformations described here is likely the oxophilicity of the molybdenum compounds. Group 6 CpAm compounds have proven to be very oxophilic species,^{42,63} and the M-O bonds formed through the addition of CO₂ are believed to be stronger than the M-N bonds broken in the corresponding imido compounds. This belief is supported by the observation that the M-O bonds of compounds **48** and **49** are noticeably shorter than the M-N bonds in the TMS imido compounds for both tungsten and molybdenum, and the TMG imido compound for molybdenum [cf. for **48**, $d(\text{Mo-O}) = 1.7033(19) \text{ \AA}$; for **111**, $d(\text{Mo-N}) = 1.7428(12) \text{ \AA}$; for **133**, $d(\text{Mo-N}) = 1.751(2) \text{ \AA}$].^{22,23,42}

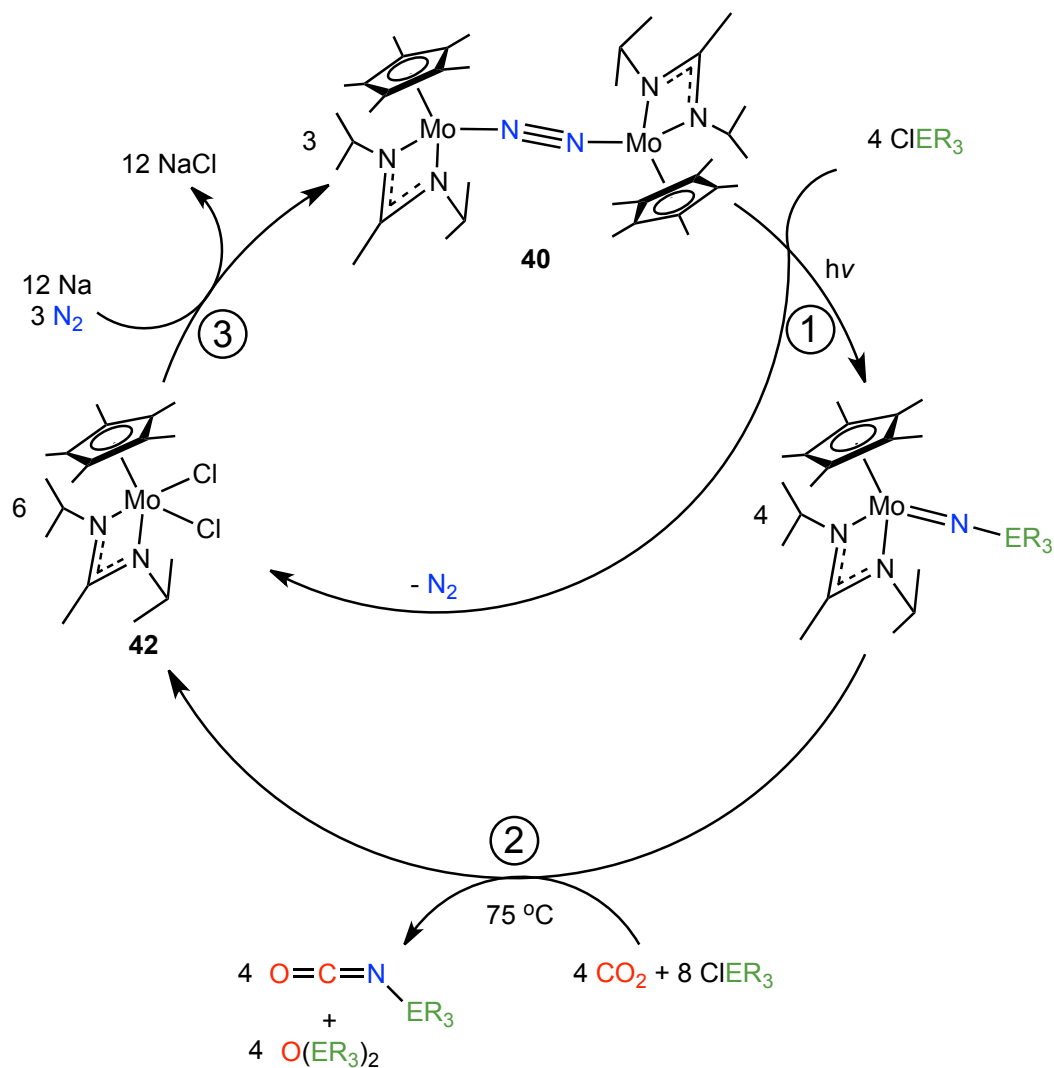
Scheme 60



In order to determine if the transformation from the imido compounds **111** and **133** to the dichloride complex **42** could occur in one step, the reactions described above were repeated in the presence of excess equivalents of Cl-E(CH₃)₃ (E = Si, Ge) (Scheme 60). Again, a higher pressure of CO₂ (70 psi) was employed for **111** than for **133** (20 psi). In both cases, complete consumption of the starting imido species was observed after 3 days at 75 °C, along with concomitant formation of the dichloride complex **42** (paramagnetic), and the corresponding isocyanates and ethereal products in good yields (Scheme 60). Likely, the reactions proceed with notably faster rates in the presence of Cl-E(CH₃)₃ because as the molybdenum oxo compound **48** is formed it is immediately consumed. Thus, any equilibrium which would otherwise be established upon formation of **48** is diminished, because **48** is not allowed to remain in solution long enough to reach an equilibrium concentration.

Most importantly, the observation that TMS and TMG isocyanate may be generated in high yields with concomitant formation of the dichloride complex **42** implies that the previously described synthetic cycle (Scheme 57) may be shortened, and that CO₂ reduction may occur *directly* with N₂ fixation (i.e. the use of CO is not required) (Scheme 61). In order to demonstrate this concept, a larger scale reaction was performed in which the ‘end-on-bridged’ N₂ compound **40** was photolyzed in the presence of excess TMGCl until complete conversion to **42** and **133** was observed by ¹H NMR. This mixture was then charged with CO₂ (20 psi) and heated to 75 °C for 3 days, at which point ¹H NMR revealed the production of TMG isocyanate in modest yield (36% with respect to initial concentration of **40**) along with paramagnetic **42**, which could be recovered in 82% yield as a pure, crystalline material. Thus, the

Scheme 61



group 6 CpAm complexes described herein present a rare case for the *simultaneous* fixation of both CO_2 and N_2 to produce a value added product within a complete synthetic cycle.^{64,65}

4.4 Conclusion

Several methods for the completion of the desired synthetic cycle for N_2 fixation have been explored. The first strategy examined was the attempted synthesis

of mono(carbonyl) complexes bearing labile ligands which we hoped would be displaced easily by N₂. In the case of dimethyl sulfide, C-S bond activation was found to occur, which lead to the formation of a tungsten η^2 -acyl complex, similar to those reported by Legzdins previously,²⁷ and methylation resulted in the regeneration and loss of dimethyl sulfide. Olefins were found to add to both molybdenum and tungsten to yield the desired compounds, however the generation of the ‘end-on-bridged’ dinitrogen compounds from these precursors was not successful in any meaningful way. Furthermore, in the case of tungsten, olefins with accessible α - or β -hydrogens lead to the production of decomposition products, which were able to be identified on the basis of NMR spectroscopy, and fully characterized in the case of *iso*-butene.

The discovery that the known terminal oxo compounds **48** and **49** are viable precursors for the regeneration of the ‘end-on-bridged’ N₂ compounds **40** and **41** was paramount to success in completing the desired synthetic cycle. Accordingly, it has been unequivocally established that these compounds may be used to produce a variety of isocyanates and subsequently be regenerated in moderate yields. Notably, the process couples two fundamental challenges posed to the chemical community, the fixation of CO₂ and N₂, in one process. The discoveries presented here have laid the foundation for future exploration into the operation of this synthetic cycle in a catalytic manner, likely invoking an electrochemical means for the final reduction step. Furthermore, investigations into the [2+2] cycloaddition reaction of CO₂ warrants further mechanistic studies. Specifically, a key hurdle to overcome will be the spectroscopic identification and, if possible, isolation of the transition state

species. Interrogation of the reaction kinetics by UV-vis and IR spectroscopies will be critical for such investigations.

4.5 References

- (1) Darwent, B. deB. *Bond DIssociation Energies in Simple Molecules*; NSRDS-NBS 31; National Bureau of Standards: Washington, D. C., 1970.
- (2) Laplaza, C. E.; Cummins, C. C. *Science* **1995**, *268*, 861.
- (3) Laplaza, C. E.; Johnson, M. J. A.; Peters, J. C.; Odom, A. L.; Kim, E.; Cummins, C. C.; George, G. N.; Pickering, I. J. *J. Am. Chem. Soc.* **1996**, *118*, 8623.
- (4) Kawaguchi, H.; Matsuo, T. *Angew. Chem. Int. Ed.* **2002**, *41*, 2792.
- (5) Clentsmith, G. K. B.; Bates, V. M. E.; Hitchcock, P. B.; Cloke, F. G. N. *J. Am. Chem. Soc.* **1999**, *121*, 10444.
- (6) Fryzuk, M. D.; Kozak, C. M.; Bowridge, M. R.; Patrick, B. O.; Rettig, S. J. *J. Am. Chem. Soc.* **2002**, *124*, 8389.
- (7) Grubel, K.; Brennessel, W. W.; Mercado, B. Q.; Holland, P. L. *J. Am. Chem. Soc.* **2014**, *136*, 16807.
- (8) Akagi, F.; Matsuo, T.; Kawaguchi, H. *Angew. Chem. Int. Ed.* **2007**, *46*, 8778.
- (9) Hirotsu, M.; Fontaine, P. P.; Epshteyn, A.; Zavalij, P. Y.; Sita, L. R. *J. Am. Chem. Soc.* **2007**, *129*, 9284.
- (10) Fontaine, P. P.; Yonke, B. L.; Zavalij, P. Y.; Sita, L. R. *J. Am. Chem. Soc.* **2010**, *132*, 12273.
- (11) Hirotsu, M.; Fontaine, P. P.; Zavalij, P. Y.; Sita, L. R. *J. Am. Chem. Soc.* **2007**, *129*, 12690.
- (12) Keane, A. J.; Yonke, B. L.; Hirotsu, M.; Zavalij, P. Y.; Sita, L. R. *J. Am. Chem. Soc.* **2014**, *136*, 9906.
- (13) Curley, J. J.; Sceats, E. L.; Cummins, C. C. *J. Am. Chem. Soc.* **2006**, *128*, 14036.
- (14) Fryzuk, M. D.; Johnson, S. A. *Coord. Chem. Rev.* **2000**, *200-202*, 379.
- (15) MacKay, B. A.; Fryzuk, M. D. *Chem. Rev.* **2004**, *104*, 385.
- (16) Solari, E.; Da Silva, C.; Iacono, B.; Hesschenbrouck, J.; Rizzoli, C.; Scopelliti, R.; Floriani, C. *Angew. Chem. Int. Ed.* **2001**, *40*, 3907.
- (17) Curley, J. J.; Cook, T. R.; Reece, S. Y.; Muller, P.; Cummins, C. C. *J. Am. Chem. Soc.* **2008**, *130*, 9394.
- (18) Kunkely, H.; Vogler, A. *Angew. Chem. Int. Ed.* **2010**, *49*, 1591.
- (19) MacLeod, K. C.; Vinyard, D. J.; Holland, P. L. *J. Am. Chem. Soc.* **2014**, *136*, 10226.
- (20) Miyazaki, T.; Tanaka, H.; Tanabe, Y.; Yuki, M.; Nakajima, K.; Yoshizawa, K.; Nishibayashi, Y. *Angew. Chem. Int. Ed.* **2014**, *53*, 11488.

- (21) Yonke, B. L. *Ph. D. Dissertation, University of Maryland* **2012**.
- (22) Yonke, B. L.; Reeds, J. P.; Fontaine, P. P.; Zavalij, P. Y.; Sita, L. R. *Organometallics* **2014**, *33*, 3239.
- (23) Keane, A. J. *Ph. D. Dissertation, University of Maryland* **2015**.
- (24) Adams, R. D.; Chodosh, D. F. *J. Am. Chem. Soc.* **1978**, *100*, 812.
- (25) Adams, R. D.; Blankenship, C.; Segmuller, B. E.; Shiralian, M. *J. Am. Chem. Soc.* **1983**, *105*, 4319.
- (26) Stein, C. A.; Taube, H. *J. Am. Chem. Soc.* **1978**, *100*, 336.
- (27) Debad, J. D.; Legzdins, P.; Batchelor, R. J.; Einstein, F. W. B. *Organometallics* **1993**, *12*, 2094.
- (28) Chatt, J.; Duncanson, L. A. *J. Chem. Soc.* **1953**, 2939.
- (29) Chatt, J.; Dilworth, J. R.; Richards, R. L. *Chem. Rev.* **1978**, *6*, 589.
- (30) Allen, F. H.; Kennard, O.; Watson, D. G.; Brammer, L.; Orpen, A. G.; Taylor, R. *J. Chem. Soc., Perkin Trans.* **1987**, S1.
- (31) Chiang, J. F.; Chiang, R.; Lu, K. C.; Sung, E.-M.; Harmony, M. D. *J. Mol. Structure.* **1977**, *41*, 67.
- (32) Craig, N. C.; Groner, P.; McKean, D. C. *J. Phys. Chem. A* **2006**, *110*, 7461.
- (33) Dyer, P. W.; Gibson, V. C.; Howard, J. A. K.; Whittle, B.; Wilson, C. *Polyhedron* **1995**, *14*, 103.
- (34) Marinescu, S. C.; King, A. J.; Schrock, R. R.; Singh, R.; Muller, P.; Takase, M. K. *Organometallics* **2010**, *29*, 6816.
- (35) Tsang, W. C. P.; Jamieson, J. Y.; Aeilts, S. L.; Hultzs, K. C.; Schrock, R. R.; Hoveyda, A. H. *Organometallics* **2004**, *23*, 1997.
- (36) Sharp, P. R. *Organometallics* **1984**, *3*, 1217.
- (37) Hanna, B. S.; MacIntosh, A. D.; Ahn, S.; Tyler, B. T.; Palmore, G. T. R.; Williard, P. G.; Bernskoetter, W. H. *Organometallics* **2014**, *33*, 3425.
- (38) Blomberg, M. R. A.; Siegbahn, P. E. M.; Svensson, M. *J. Phys. Chem.* **1992**, *96*, 9794.
- (39) Ning, Y.; Froese, R. D. J.; Margl, P.; Lee, E. L.; Nguyen, S. T.; Peterson, T. H.; Wagner, N.; Stern, C. L.; Sarjeant, A. A. *Organometallics* **2014**, *33*, 1120.
- (40) Chow, C.; Patrick, B. O.; Legzdins, P. *Organometallics* **2012**, *31*, 8159.
- (41) Ng, S. H. K.; Adams, C. S.; Hayton, T. W.; Legzdins, P.; Patrick, B. O. *J. Am. Chem. Soc.* **2003**, *125*, 15210.
- (42) Yonke, B. L.; Reeds, J. P.; Zavalij, P. Y.; Sita, L. R. *Angew. Chem. Int. Ed.* **2011**, *50*, 12342.
- (43) Luo, L.; Lanza, G.; Fragala, I. L.; Stern, C. L.; Marks, T. J. *J. Am. Chem. Soc.* **1998**, *120*, 3111.
- (44) Shin, J. H.; Savage, W.; Murphy, V. J.; Bonanno, J. B.; Churchill, D. G.; Parkin, G. *J. Chem. Soc., Dalton Trans.* **2001**, 1732.
- (45) Pilato, R. S.; Housmekerides, C. E.; Jernakoff, P.; Rubin, D.; Geoffroy, G. L.; Rheingold, A. L. *Organometallics* **1990**, *9*, 2333.

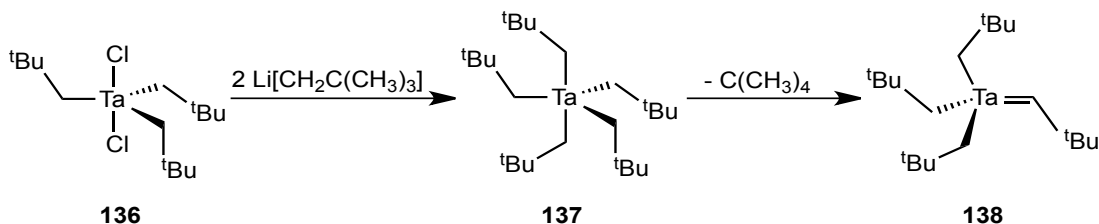
- (46) Johnson, L. K.; Virgil, S. C.; Grubbs, R. H. *J. Am. Chem. Soc.* **1990**, *112*, 5384.
- (47) Nielson, A. J.; Glenney, M. W.; Rickard, C. E. F.; Waters, J. M. *J. Chem. Soc., Dalton Trans.* **2000**, 4569.
- (48) Bryson, N.; Youinou, M.-T.; Osborn, J. A. *Organometallics* **1991**, *10*, 3389.
- (49) Ehrenfeld, D.; Kress, J.; Moore, B. D.; Osborn, J. A.; Schoettel, D. *J. Chem. Soc., Chem. Comm.* **1987**, 129.
- (50) Cross, W. B.; Anderson, J. C.; Wilson, C.; Blake, A. J. *Inorg. Chem.* **2006**, *45*, 4556.
- (51) Herrmann, W. A.; Weichselbaumer, G.; Paciello, R. A.; Fischer, R. A.; Herdtweck, E.; Okuda, J.; Marz, D. W. *Organometallics* **1990**, *9*, 489.
- (52) Devore, D. D.; Lichtenhan, J. D.; Takusagawa, F.; Maatta, E. A. *J. Am. Chem. Soc.* **1987**, *109*, 7408.
- (53) Guiducci, A. E.; Cowley, A. R.; Skinner, M. E. G.; Mountford, P. *J. Chem. Soc., Dalton Trans.* **2001**, 1392.
- (54) Groom, L. R.; Russell, A. F.; Schwarz, A. D.; Mountford, P. *Organometallics* **2014**, *33*, 1002.
- (55) Groom, L. R.; Schwarz, A. D.; Nova, A.; Clot, E.; Mountford, P. *Organometallics* **2013**, *32*, 7520.
- (56) Kilgore, U. J.; Basuli, F.; Huffman, J. C.; Mindiola, D. J. *Inorg. Chem.* **2006**, *45*, 487.
- (57) Anderson, J. C.; Bou-Moreno, R. *Org. Biomol. Chem.* **2012**, *10*, 1334.
- (58) Dunn, S. C.; Hazari, N.; Cowley, A. R.; Green, J. C.; Mountford, P. *Organometallics* **2006**, *25*, 1755.
- (59) Dubberley, S. R.; Friedrich, A.; Willman, D. A.; Mountford, P.; Radius, U. *Chem. Eur. J.* **2003**, *9*, 3634.
- (60) Royo, P.; Sanchez-Nieves J. *Organomet. Chem.* **2000**, 387, 61.
- (61) Tonzetich, Z. J.; Schrock, R. R.; Muller, P. *Organometallics* **2006**, *25*, 4301.
- (62) Ward, B. D.; Clot, E.; Dubberley, S. R.; Gade, L. H.; Mountford, P. *Chem. Comm.* **2002**, 2618.
- (63) Reeds, J. P.; Yonke, B. L.; Zavalij, P. Y.; Sita, L. R. *J. Am. Chem. Soc.* **2011**, *133*, 18602.
- (64) Bernskoetter, W. H.; Lobkovsky, E.; Chirik, P. J. *Angew. Chem. Int. Ed.* **2007**, *46*, 2858.
- (65) Knobloch, D. J.; Toomey, H. E.; Chirik, P. J. *J. Am. Chem. Soc.* **2008**, *130*, 4248.

Chapter 5: Synthesis, Stability, and Reactivity of Mid Valent Group 6 Alkyl, Alkylidene, and Alkylidyne Complexes

5.1 Introduction

The synthesis and reactivity of transition metal compounds containing metal-carbon multiple bonds has long attracted the attention of the chemical community. In particular, alkylidenes, which are compounds containing formal metal carbon double bonds, have gained significant fame for their role in olefin metathesis reactions, for which Schrock, Grubbs, and Chauvin shared the Nobel Prize in 2005.¹⁻⁴ Fischer first reported the synthesis of such a compound in 1964 by treatment of tungsten carbonyl $[\text{W}(\text{CO})_6]$ (**134**) with methyllithium, followed by addition of a cationic methylating agent, to yield $\{[(\text{CO})_5\text{W}[\text{C}(\text{OCH}_3)\text{CH}_3]\}$ (**135**).⁵ Several years later, Schrock prepared the first member of a different and distinct class of alkylidene complexes, which have since been named for him, through the addition of 2 equivalents of *neo*-pentyllithium to the tantalum (V) precursor $[(\text{CH}_3)_3\text{CCH}_2]_3\text{TaCl}_2$ (**136**), to generate the penta-*neo*-pentyl complex $[(\text{CH}_3)_3\text{CCH}_2]_5\text{Ta}$ (**137**), which then undergoes α -hydrogen abstraction to provide the alkylidene product $[(\text{CH}_3)_3\text{CCH}_2]_3\text{Ta}[\text{CHC}(\text{CH}_3)_3]$ (**138**) (Scheme 62).⁶

Scheme 62

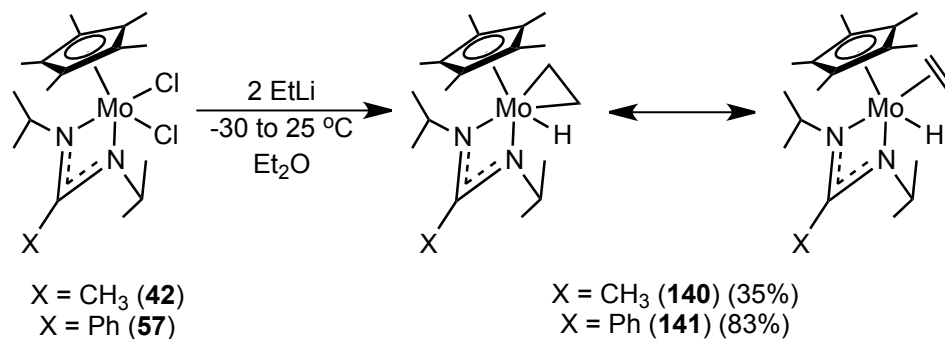


In regard group 6 chemistry since these foundational discoveries, an innumerable amount of high valent [i.e. M(VI)] Schrock-type alkylidene complexes have been synthesized and appeared in the literature. Most commonly, these compounds serve to catalyze olefin metathesis reactions, and the topic has been reviewed extensively.⁷⁻¹¹ What is far less common, however, is the preparation of group 6 alkylidene complexes in which the metal exists in a lower oxidation state. Legzdins has reported the synthesis of molybdenum (II) and tungsten (II) di-*neo*-pentyl species which are mildly stable in solution. Upon thermal activation, α -hydrogen abstraction yields very reactive 16 electron M(II) alkylidene complexes, which may be trapped in the presence of a coordinating ligand (e.g. trimethyl phosphine) or, more commonly, undergo a variety of C-H activation reactions.¹²⁻¹⁴ Within the scope of the CpAm ligand environment, Dr. Jonathan Reeds has previously prepared one molybdenum (IV) alkylidene complex, however could only do so in the presence of a carbonyl ligand to generate the (presumably) more stable 18 electron species $\text{Cp}^*[\text{N}(\text{iPr})\text{C}(\text{CH}_3)\text{N}(\text{iPr})]\text{Mo}(\text{CHCHCPh}_2)(\text{CO})$ (**139**).

Given the lack of reports regarding group 6 alkylidene complexes which exist in low to mid oxidation states with electron counts less than 18, we became interested in determining whether or not such species could exist when supported by the CpAm ligand framework. To explore this, the reactivity of the CpAm M(IV) dichloride complexes $\text{Cp}^*[\text{N}(\text{iPr})\text{C}(\text{CH}_3)\text{N}(\text{iPr})]\text{MCl}_2$ [M = Mo (**42**), M = W (**108**)] towards alkylating agents was explored, with the hope of generating dialkyl complexes which would then undergo α -hydrogen abstraction to provide the desired alkylidene products.

5.2 Molybdenum

Scheme 63



We first elected to explore the reaction of the dichloride compound **42** with two equivalents of ethyllithium. As shown in Scheme 63, treatment of **42** with ethyllithium at -30 °C in Et₂O followed by slow warming to room temperature lead to the isolation of the molybdenum ethene hydride complex Cp*[N(ⁱPr)C(CH₃)N(ⁱPr)]Mo(C₂H₄)(H) **140** in low yield. The presence of the hydride ligand was initially inferred from the high degree of asymmetry of the ethene ligand, as depicted in Figure 41a. Attempts to independently refine the hydrogen atom at the molybdenum center through XRD were unsuccessful, however, and its existence could not be confirmed by ¹H NMR spectroscopy given the paramagnetic nature of compound **140**.

Given the previously demonstrated success of the use of a phenyl group in the distal position of the amidinate ligand to provide molybdenum complexes that are highly crystalline, the reaction was repeated beginning from the dichloride compound **57** to provide the analogous ethene hydride species Cp*[N(ⁱPr)C(Ph)N(ⁱPr)]Mo(C₂H₄)(H) (**141**) in much higher yield. Gratifyingly,

compound **141** allowed for the unequivocal identification of a hydride ligand at the metal center by X-ray diffraction, and the structure is depicted in Figure 41b.

In the solid state, **140** and **141** display C-C bond lengths of the ethene ligand of 1.463(11) Å and 1.412(5) Å, respectively, noticeably longer than that in free

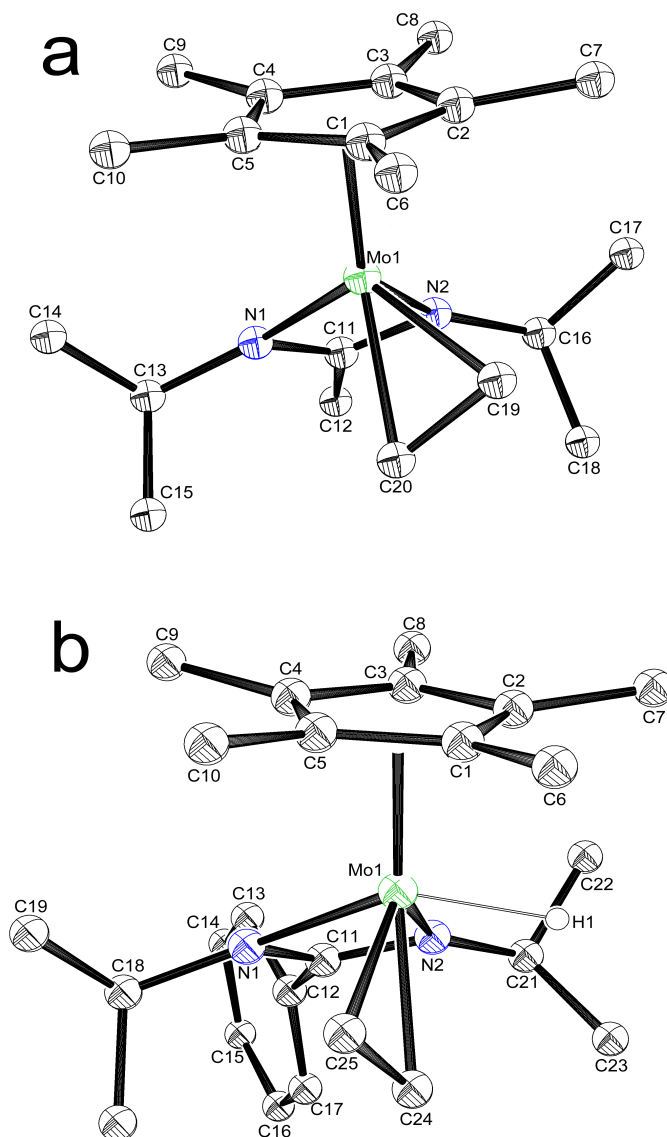
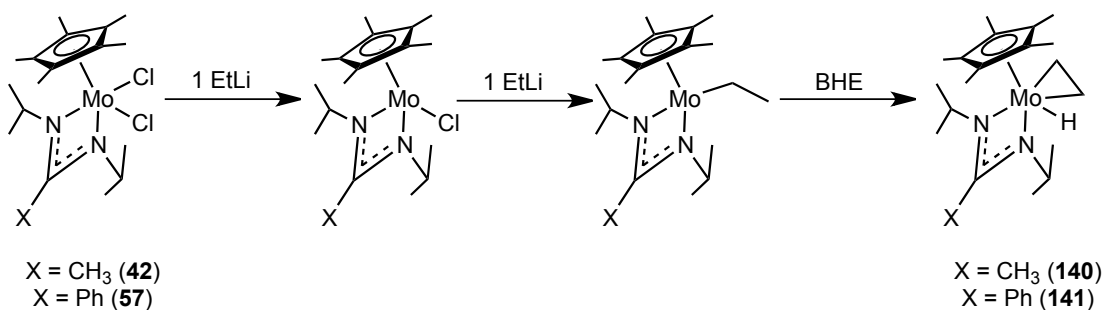


Figure 41. Molecular structures (30% thermal ellipsoids) of compounds **140** (a) and **141** (b). H atoms have been omitted for clarity except for H1 in **141** which is depicted as a small white sphere. Selected bond lengths (Å) for **140**: C19-C20 1.463(11), Mo1-C19 2.083(4), Mo1-C20 2.202(3); for **141**: C24-C25 1.412(5), Mo1-C24 2.161(3), Mo1-C25 2.196(3).

ethene (1.330 Å),¹⁵ indicative of significant π -backbonding from the molybdenum center to the π^* orbital of ethene. This is supported by a significant decrease in the sum of all angles about each carbon atom of the ethene ligand (e.g. 345.0° for C19 in **140**), indicating substantial deviation from the geometry expected for a trigonal planar olefin experiencing little to no π -backbonding of 360°. Accordingly, in both compounds **140** and **141**, the molybdenum can be regarded as lying close to the middle between the two extreme resonance structures of a metallocyclopropane type species in which the formal oxidation state of the metal is +5, and an olefin complex in which the formal oxidation state of the metal is +3 (depicted schematically in Scheme 63).¹⁶

We hypothesize that the formation of **140** and **141** proceeds through the rather simple mechanism depicted in Scheme 64. The first equivalent of ethyllithium serves to reduce the metal by one electron to form a molybdenum (III) monochloride intermediate, which then undergoes salt metathesis to provide a 15 electron molybdenum (III) ethyl species. From here, β -hydride elimination occurs to generate the final products **140** and **141**. Previously, we have reported that CpAm compounds of tantalum, titanium, zirconium, and hafnium bearing alkyl ligands with β -hydrogens

Scheme 64

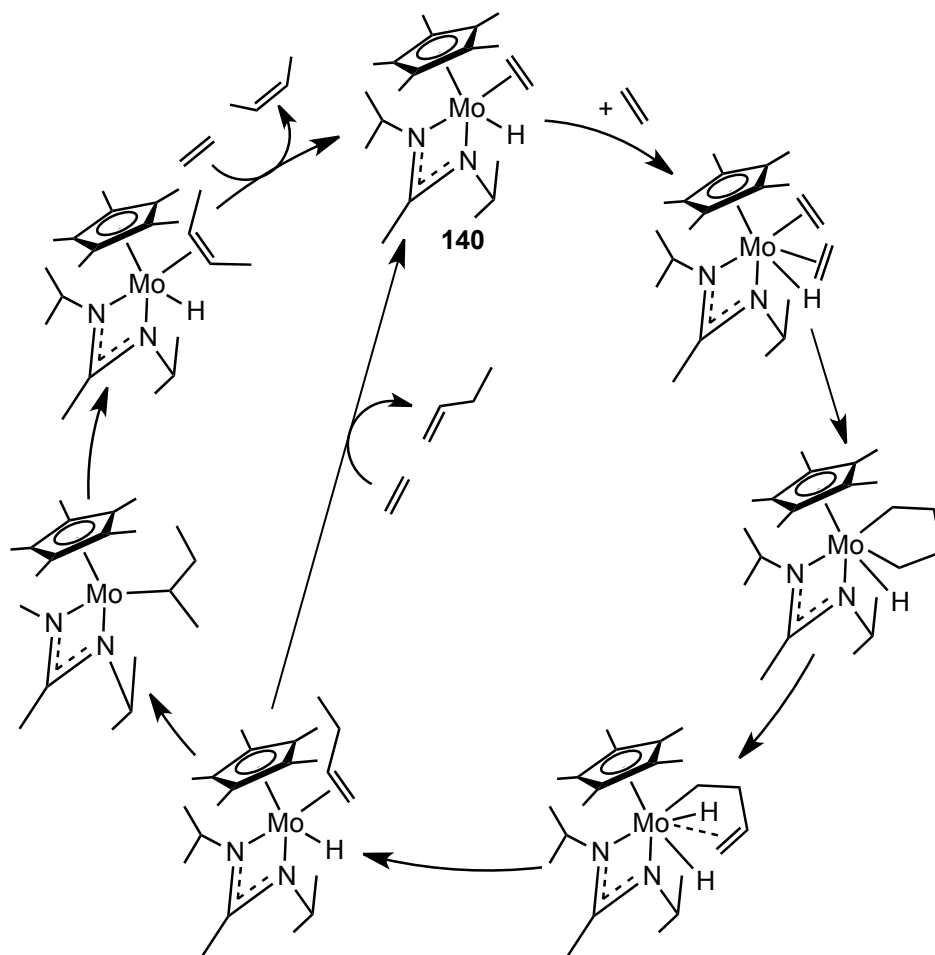


are immune to such decomposition pathways, even at elevated temperatures in some instances.¹⁷⁻²⁰ In these cases, however, the metal center is of five coordinate piano stool geometry (save titanium), whereas in the present case the molybdenum ethyl species are (presumably) four coordinate pseudo-tetrahedral, which may allow for the proper *syn*-coplanar geometry necessary to allow for β -hydride elimination to occur. On the other hand, the proposed molybdenum (III) ethyl intermediates are d^3 species, whereas those reported previously for group 4 and 5 compounds are either d^1 or d^0 complexes, which also likely contributes to their stability with regard to β -hydride elimination. Efforts were undertaken to circumvent the observed β -hydride elimination to obtain a four coordinate molybdenum (III) alkyl species. First, we switched to an alkylating agent that lacks β -hydrogens, benzyl magnesium chloride, however no molybdenum benzyl complex could be isolated. Furthermore, we employed alkylating agents that possess C_{β} -H bonds more resistant to β -hydride elimination,²¹ such as *iso*-butyl magnesium chloride, however in these cases β -hydride elimination was in fact observed, and the resulting bulky olefin was displaced by N_2 to provide the molybdenum (III) ‘end-on-bridged’ dinitrogen species $\{Cp^*[N(iPr)C(CH_3)N(iPr)]Mo(H)\}_2(\mu-\eta^1:\eta^1-N_2)$ (**142**).²²

Initially, no interesting reactivity was observed with these new ethene hydride species. Specifically, we were interested in inducing the microscopic reverse reaction of β -hydride elimination, olefin insertion, to regenerate the proposed molybdenum (III) ethyl intermediate, with the hopes of observing olefin oligomerization or, ideally, ethene trimerization, given the tremendous importance of this process.²³⁻²⁸ Heating a benzene- d_6 solution of compound **140** for several days under ethene or propene

atmosphere (10 psi) lead to no observable reaction nor the production of any higher α -olefins as judged by ^1H NMR. However, simply increasing the pressure of ethene in the reaction to 80 psi did in fact lead to the formation of a mixture of 1-butene and 2-butene after several days, with the latter appearing in noticeably higher concentration. No higher olefins (hexene, octane, etc.) nor oligomers were observed by ^1H NMR, and the use of a cocatalyst only lead to the slowing of the observed reaction rate. Presumably, rather than inducing olefin insertion into the Mo-H bond, ethene coordinates to the metal and forms a metallocyclopentane structure, which then undergoes β -hydride elimination followed by reductive elimination to produce a

Scheme 65

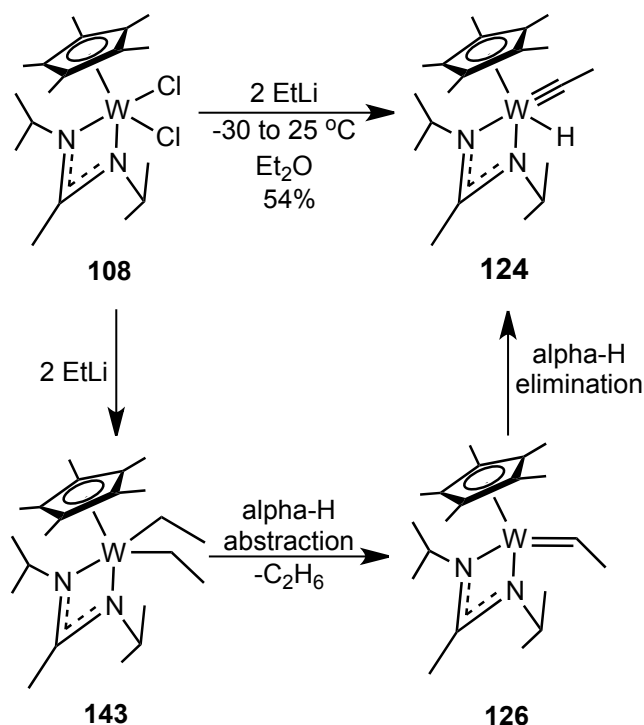


1-butene hydride species. The fact that 2-butene is observed in larger amounts than 1-butene suggests that the newly formed olefin ligand inserts into the Mo-H bond followed by another β -hydride elimination to finally produce 2-butene (Scheme 65). To test this hypothesis, the ‘end-on-bridged’ dinitrogen complex **40** was treated with ethene under identical conditions, and in this case 1-butene was the major isomer observed due to the lack of the initial hydride ligand at the molybdenum center which is essential for the metal mediated isomerization process.

5.3 Tungsten

Given the observation that the preparation of a molybdenum alkylidene through α -hydrogen abstraction may not be possible due to the fact that the first addition of alkylating agent serves only to reduce the metal, we next targeted the

Scheme 66



analogous reaction with tungsten. Accordingly, as shown in Scheme 66, the tungsten (IV) dichloride compound **108** was treated with two equivalents of ethyllithium under similar conditions, which lead to the isolation of the ethylidyne hydride species $\text{Cp}^*[\text{N}(\text{iPr})\text{C}(\text{CH}_3)\text{N}(\text{iPr})]\text{W}(\text{CCH}_3)(\text{H})$ (**124**) in moderate yield. In benzene- d_6 solution, compound **124** exhibits ‘ring-flipping’ of the amidinate ligand on the NMR timescale, as evidenced by broad peaks which suggest apparent C_s symmetry. Furthermore, a diagnostic resonance for the hydride ligand appears in the ^1H NMR spectrum at 6.77 ppm ($^1J_{\text{WH}} = 94$ Hz), nearly identical to the hydride resonance of compound **128**, and long range coupling for the protons of the ethylidyne ligand to ^{183}W ($^2J_{\text{WH}} = 9$ Hz) and the hydride ligand ($^3J_{\text{HH}} = 1$ Hz) was also observed. Single crystals were obtained for compound **124** and the solid state molecular structure is depicted in Figure 42.²⁹ The W1-C19 bond length of 1.7940(9) Å is in keeping with others reported for tungsten (VI) alkylidyne complexes.³⁰⁻³²

In regard to the mechanism through which compound **124** is produced, the most logical proposal is that the desired tungsten (IV) bis(ethyl) species **143** is generated through salt metathesis from the dichloride complex **108**. From here, α -hydrogen abstraction readily occurs to liberate ethane and produce the tungsten (IV) ethylidene complex **126**. Unfortunately, compound **126** likely is not stable, and α -hydrogen elimination occurs to yield the final product **124** (Scheme 66). Tungsten alkylidene complexes in which the metal is not in its highest oxidation state and have electron counts of less than 18 are known to be susceptible to such α -hydrogen elimination processes.^{33,34}

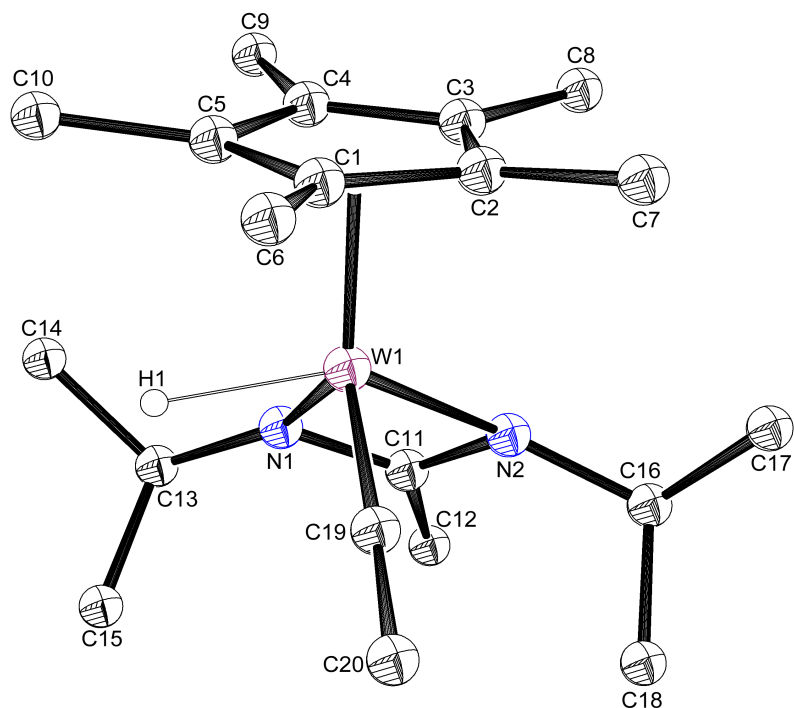
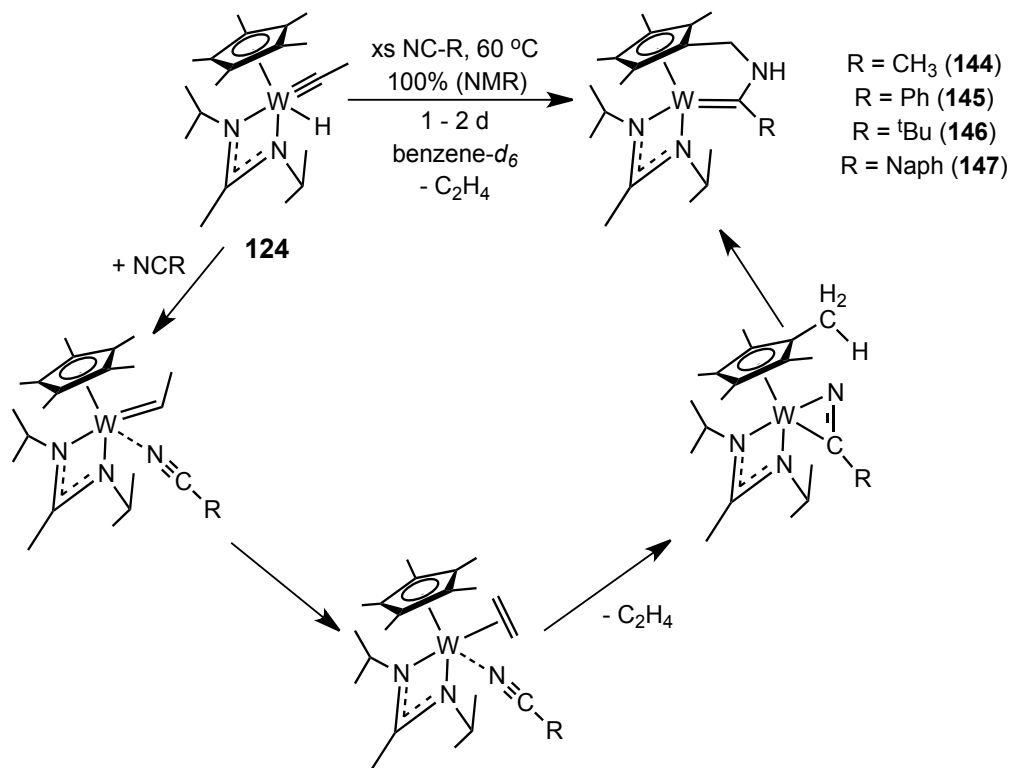


Figure 42. Molecular structure (30% thermal ellipsoids) of compound **124**. H atoms have been omitted for clarity except for H1 which is depicted as a small white sphere. Selected bond lengths (Å) and angles (°): W1-C19 1.7940(9), C19-C20 1.4790(15), W1-C19-C20 167.86(9).

The microscopic reverse of this undesired elimination reaction could not be observed to have occurred by heating in benzene- d_6 solution, even in the presence of olefins.³³ However, upon heating in the presence of various nitriles (NCR, R = CH₃, Ph, ^tBu, Naph) in benzene- d_6 solution, slow formation of new compounds of C_1 symmetry (designated **144** – **147**, respectively, Scheme 67) was observed by ¹H NMR, which were determined to be Fischer alkylidene complexes in which C-H bond activation of the Cp* ligand had occurred. The mechanism through which these new compounds form is believed to involve initial isomerization to a tungsten (IV) alkylidene upon coordination of a nitrile, followed by isomerization and elimination of ethene (observed by ¹H NMR), which occurs as the nitrile assumes an η^2 coordination mode, followed by C-H bond activation and formation of the new

alkylidene. When ^{13}C -labeled acetonitrile was employed ($\text{N}^{13}\text{CCH}_3$), the formation of the proposed new tungsten-carbon bond was confirmed by the observation of a

Scheme 67



new resonance in the $^{13}\text{C}\{^1\text{H}\}$ NMR spectrum at 83.2 ppm which displayed the expected coupling to the ^{183}W center ($^1J_{\text{WC}} = 35\text{ Hz}$). Unfortunately, these new species were extremely resistant to crystallization from all solvents employed, and thus confirmation of the structures through single crystal XRD could not be obtained.

5.4 Conclusion

For both tungsten and molybdenum, the targeted alkylidene complexes could not be isolated. Specifically, in the case of molybdenum, initial reduction of the metal center occurs to provide mono(chloride) species, which prevents the generation

of the desired bis(alkyl) complexes which we hoped would go on to generate alkylidene ligands through an α -hydrogen abstraction mechanism. In the case of tungsten, such a reaction was able to be observed, however the product was not immune to α -hydride elimination, which lead to the isolation of an ethylidyne hydride complex. Unfortunately, the only successful method for inducing the reverse reaction involved the liberation of ethene and the formation of new Fischer alkylidene complexes in which the alkylidene moiety is tethered to the Cp* ligand. These compounds could not be structurally characterized, despite extensive efforts. The instability of desired ethylidene intermediate complex **126** likely arises from the fact that α -hydrogens are known to possess significant amounts of positive charge in early transition metal complexes. Accordingly, the presence of a d² tungsten center in such close proximity to this α -hydrogen results in the rapid abstraction observed. Likely, as in the case of the molybdenum complex **139** described above, this decomposition within a d² group 6 compound may only be prevented by the presence of an additional ligand to increase the electron count to 18, however in doing so further reactivity could be inhibited.

5.5 References

- (1) All Nobel Prizes in Chemistry.
http://www.nobelprize.org/nobel_prizes/chemistry/laureates/ (accessed Jan. 15, 2015).
- (2) Schrock, R. R. *Angew. Chem. Int. Ed.* **2006**, 45, 3748-3759.
- (3) Grubbs, R. H. *Angew. Chem. Int. Ed.* **2006**, 45, 3760-3765.
- (4) Chauvin, Y. *Angew. Chem. Int. Ed.* **2006**, 45, 3740-3747.
- (5) Fischer, E. O.; Maasbol, A. *Angew. Chem. Int. Ed.* **1964**, 3, 580-581.
- (6) Schrock, R. R. *J. Am. Chem. Soc.* **1974**, 96, 6796-6797.
- (7) Schrock, R. R. *Acc. Chem. Res.* **2014**, 47, 2457-2466.

- (8) Schrock, R. R.; Hoveyda, A. H. *Angew. Chem. Int. Ed.* **2003**, *42*, 4592-4633.
- (9) Schrock, R. R. *Tetrahedron* **1999**, 8141-8153.
- (10) Schrock, R. R. *J. Mol. Catal. A: Chem.* **2004**, *213*, 21-30.
- (11) Schrock, R. R. *Chem. Rev.* **2009**, *109*, 3211-3226.
- (12) Chow, C.; Patrick, B. O.; Legzdins, P. *Organometallics* **2012**, *31*, 8159-8171.
- (13) Legzdins, P.; Veltheer, J. E. *Acc. Chem. Res.* **1993**, *26*, 41-48.
- (14) Blackmore, I. J.; Jin, X.; Legzdins, P. *Organometallics* **2005**, *24*, 4088-4098.
- (15) Craig, N. C.; Groner, P.; McKean, D. C. *J. Phys. Chem. A* **2006**, *110*, 7461-7469.
- (16) Chatt, J.; Duncanson, L. A. *J. Chem. Soc.* **1953**, 2939-2947.
- (17) Epshteyn, A.; Zavalij, P. Y.; Sita, L. R. *J. Am. Chem. Soc.* **2006**, *128*, 16052-16053.
- (18) Harney, M. B.; Keaton, R. J.; Fettingner, J. C.; Sita, L. R. *J. Am. Chem. Soc.* **2006**, *128*, 3420-3432.
- (19) Keaton, R. J.; Koterwas, L. A.; Fettingner, J. C.; Sita, L. R. *J. Am. Chem. Soc.* **2002**, *124*, 5932-5933.
- (20) Trunkely, E. F.; Epshteyn, A.; Zavalij, P. Y.; Sita, L. R. *Organometallics* **2010**, *29*, 6587-6593.
- (21) Negishi, E.; Nguyen, T.; Maye, J. P.; Choueiri, D.; Suzuki, N.; Takahashi, T. *Chem. Lett.* **1992**, *21*, 2367-2370.
- (22) Fontaine, P. P.; Yonke, B. L.; Zavalij, P. Y.; Sita, L. R. *J. Am. Chem. Soc.* **2010**, *132*, 12273-12285.
- (23) Deckers, P. J. W.; Hessen, B.; Teuben, J. H. *Angew. Chem. Int. Ed.* **2001**, *40*, 2516-2519.
- (24) Chen, Y.; Callens, E.; Abou-Hamad, E.; Merle, N.; White, A. J. P.; Taoufik, M.; Coperet, C.; Le Roux, E.; Basset, J.-M. *Angew. Chem. Int. Ed.* **2012**, *51*, 11886-11889.
- (25) Bollmann, A.; Blann, K.; Dixon, J. T.; Hess, F. M.; Killian, E.; Maumela, H.; McGuinness, D. S.; Morgan, D. H.; Neveling, A.; Otto, S.; Overett, M.; Slawin, A. M. Z.; Wasserscheid, P.; Kuhlmann, S. *J. Am. Chem. Soc.* **2004**, *126*, 14712-14713.
- (26) Andes, C.; Harkins, S. B.; Murtuza, S.; Oyler, K.; Sen, A. *J. Am. Chem. Soc.* **2001**, *123*, 7423-7424.
- (27) Arteaga-Muller, R.; Tsurugi, H.; Saito, T.; Yanagawa, M.; Oda, S.; Mashima, K. *J. Am. Chem. Soc.* **2009**, *131*, 5370-5371.
- (28) Sattler, A.; VanderVelde, D. G.; Labinger, J. A.; Bercaw, J. E. *J. Am. Chem. Soc.* **2014**, *136*, 10790-10800.
- (29) We wish to acknowledge the controbution of Dr. P. P. Fontaine, who provided crystals suitable for X-ray diffraction for compound **124**.
- (30) Schrock, R. R. *Acc. Chem. Res.* **1986**, *19*, 342-348.
- (31) Wu, X.; Daniliuc, C. G.; Hrib, C. G.; Tamm, M. *J. Organomet. Chem.* **2011**, *696*, 4147-4151.

- (32) Sarkar, S.; McGowan, K. P.; Kuppuswamy, S.; Ghiviriga, I.; Abboud, K. A.; Veige, A. S. *J. Am. Chem. Soc.* **2012**, *134*, 4509-4512.
- (33) Wengrovius, J. H.; Schrock, R. R.; Churchill, M. R.; Wasserman, H. J. *J. Am. Chem. Soc.* **1982**, *104*, 1739-1740.
- (34) Churchill, M. R.; Wasserman, H. J. *Inorg. Chem.* **1983**, *22*, 1574-1578.

Chapter 6: Summary and Outlook

The inclusion of small, highly abundant molecules into the synthesis of commodity chemicals is a challenge which will continue to grow in importance as the Earth's population and market demands continue to steadily increase and pressure to reduce the environmental impact of such processes intensifies. To this end, organometallic complexes have played, and will continue to play, a key role in catalyzing the production of such value added products. One of the most inviting aspects of the use of transition metals complexes for the activation of small molecules is their ability to activate and cleave strong multiple bonds under ambient conditions, however this typically results in the formation of equally strong metal-heteroatom bonds, which themselves too are inert. Therefore, future research must focus on fine-tuning metal species through the appropriate selection of ligands, such that they may sufficiently activate inert bonds under reasonable conditions, yet go on to react in a productive manner to produce a useful product.

In this regard, mid valent group 6 complexes supported by the CpAm ligand environment have proven quite effective, and have been detailed extensively in this thesis. It has been shown that M(IV) oxo complexes form under mild conditions through the activation of sulfoxides, and that these oxo complexes are reactive towards CO to allow for the photocatalytic OAT from sulfoxides to CO. In a similar fashion, several M(IV) imido complexes (in which the nitrogen atom is derived from N₂) react not only with CO but also the greenhouse gas CO₂ in an unprecedented manner (within group 6) to produce the M(IV) oxo complexes and isocyanates. The

unusual reactivity observed may be attributed to both the sterics and electronics of these CpAm compounds. The amidinate ligand offers a relatively small bite angle, which decreases steric demand of the supporting ligands around the metal-heteroatom bonds of interest and allows for the binding of multiple π -acids, which may be key for productive substrate oxidation. Furthermore, these systems operate either in a M(II)/M(IV) redox couple, or exclusively in the M(IV) oxidation state, which are more reduced than biological and biomimetic systems which have historically been very popular. These oxidation states may in fact be of great importance to explaining the observed reactions. In order to gain a better understanding of these complexes and truly assess the reasons for their reactivity, computational studies will be required. Furthermore, investigations into the mechanism and thermodynamics associated with these transformations have yet to be undertaken, but are currently a top priority for our group. Specifically, kinetics experiments will be performed in order to gain details regarding the reaction rates and mechanisms for the [2+1] cycloaddition of CO to the tungsten and molybdenum imido complexes available to our group, as well as the novel [2+2] cycloaddition of CO₂. Ideally, spectroscopic evidence for key intermediates for this latter reaction will be observed.

When extended to sulfur, molybdenum CpAm complexes were found to activate S₈, an incredibly inexpensive and abundant resource that has not yet been thoroughly explored as a reagent, in manners that avoid the formation of strong molybdenum-sulfur multiple bonds, therefore allowing for the facile catalytic synthesis of several sulfur containing small molecules under mild conditions. Aside from these processes utilizing a plentiful reagent in an environmentally sound

manner, what truly sets the technology reported in this thesis apart from that in other work in this field is the fact that these reactions proceed uninhibited when performed in the presence of other reactants, which has allowed for several ‘one-pot’ procedures which efficiently incorporate sulfur atoms, derived from plentiful S₈, or CO into valuable organic products. In doing so, these catalysts provide alternatives to the use of phosgene and thiophosgene to install carbonyl and thiocarbonyl groups into organic molecules, which are extremely hazardous reagents. It is typical to assume that organometallic complexes such as those described within this thesis are highly reactive, and the addition of Lewis basic (or other reactive) reagents will inhibit or prevent catalysis. Here, we have detailed several examples where this is not the case, and in doing so have circumvented the need to isolate and purify dangerous, difficult to handle products. We believe that this methodology should be able to be extended to many more catalytic systems, and hope to discover more processes within our group as well.

Lastly, a major goal for organometallic chemists is to transform small olefinic molecules, such as ethene, selectively into higher olefins under reasonable conditions. To this end, molybdenum complexes supported by the CpAm ligand environment are capable of selectively dimerizing ethene to either 1- or 2-butene, depending on the precatalyst employed. Although the sterics provided by the CpAm ligand set are sufficiently unencumbering to allow for the binding of multiple additional ligands, the reason why butenes are formed selectively by these compounds rather than hexenes is likely due to the fact that the metallocycloheptane intermediate which is necessary to form in the trimerization of ethene is unable to form due to the bulkiness of the

supporting ligand framework. Accordingly, the sterics of these molybdenum species should be able to be easily tuned to allow for the production of hexenes through the installation of smaller groups on either (or both) the cyclopentadienyl and amidinate ligands. Furthermore, such reduction in sterics may also allow for an increase in the rate of reaction between the molybdenum and tungsten imido complexes with CO and CO₂, and as such warrants investigation as well.

Appendix: Experimental Procedures

General Procedures. All manipulations with air and moisture sensitive compounds were carried out under N₂ or Ar atmospheres with standard Schlenk or glovebox techniques. Et₂O and THF were dried over Na/benzophenone and distilled under N₂ prior to use. Toluene and pentane were dried and deoxygenated by passage over activated alumina and GetterMax[®] 135 catalyst (purchased from Research Catalysts, Inc.) within a PureSolv solvent purification system manufactured by Innovative Technologies (model number PS-400-4-MD) and collected under N₂ prior to use. Benzene-*d*₆, toluene-*d*₈, and THF-*d*₈ were dried over Na/K alloy and isolated by vacuum-transfer prior to use, except when otherwise stated. Celite[™] was oven dried (150 °C for several days) before use in the glovebox. Cooling was performed in the internal freezer of a glovebox maintained at -30 °C. *tert*-Butyl isocyanide and all amines were purchased from Sigma-Aldrich and degassed by three “freeze-pump-thaw” cycles prior to use. *tert*-Butyl isothiocyanate, carbon disulfide, hexamethyldisiloxane, acetonitrile, *tert*-butylnitrile, and benzylnitrile were dried over CaH₂ and isolated by vacuum transfer prior to use. 2,6-Dimethylphenyl isocyanide, methyl triflate, activated manganese (IV) oxide, sulfur, ethyllithium, *iso*-butyl magnesium chloride, *n*-butyllithium, methyllithium, trimethylsilyl chloride, trimethylgermyl chloride, *N,N*-diisopropylcarbodiimide, and naphthalene-2-carbonitrile were used as received. All gaseous reagents were purchased from Sigma-Aldrich or Matheson and used as received. Chloroform-*d* and DMSO-*d*₆ were used as received. Liquid olefins were distilled from molten Na or Na/benzophenone under N₂

or vacuum prior to use. Sulfoxides and sulfides were distilled from CaH₂ under N₂ or vacuum. Methyl isocyanide, Cp*MoCl₄, and compounds **40**, **41**, **42**, **43**, **44**, **45**, **48**, **49**, **108**, **111**, **112**, **113**, **122**, and **133** were prepared according to the literature in similar yield and purity.¹⁻⁶ ¹H NMR spectra were recorded at 400 or 500 MHz. ¹³C NMR spectra were recorded at 125 MHz. ¹⁹F NMR spectra were recorded at 376 MHz and referenced externally to α,α,α-trifluorotoluene. Photolysis reactions were performed using a Rayonet[®] Photochemical Reactor containing a carousel of ultraviolet lamps (catalogue number: RPR-3500A) borrowed from Prof. P. DeShong. Elemental analyses were carried out by Midwest Microlab LLC.

Synthesis of Cp*Mo[N(ⁱPr)C(CH₃)N(ⁱPr)](O)₂ (54**).** MnO₂ (0.195 g, 2.24 mmol) was added to a solution of **40** (0.173 g, 0.22 mmol) in 10 mL toluene and stirred for 20 m. The solution was filtered through Celite, and additional MnO₂ (0.162 g, 1.87 mmol) was added and stirred for 3 hours. The solution was filtered through Celite, pumped down to dryness, and the resulting yellow oil was dissolved in minimal Et₂O and cooled to -30 °C, yielding **54** as yellow crystals (0.100 g, yield = 58%). ¹H NMR (400 MHz, benzene-*d*₆): 1.20 (12 H, d, *J* = 6.6 Hz), 1.51 (3H, s), 1.88 (15H, s), 3.61 (2H, sp, *J* = 6.6 Hz).

Synthesis of Cp*Mo[N(ⁱPr)C(Ph)N(ⁱPr)](O)₂ (55**).** MnO₂ (0.106 g, 1.21 mmol) was added to a solution of **56** (0.104 g, 0.12 mmol) in 10 mL toluene and stirred for 20 m. The solution was filtered, and additional MnO₂ (0.111 g, 1.27 mmol) was added and the solution was stirred for 30 m. The solution was filtered and additional MnO₂

(0.076 g, 0.87 mmol) was added and the solution was stirred for 20 m. The solution was filtered through Celite and volatiles were removed *in vacuo*. The crude material was dissolved in minimal Et₂O and cooled to -30 °C, yielding **55** as yellow crystals (0.058 g, yield = 56%). ¹H NMR (400 MHz, benzene-*d*₆): 1.24 (12H, d, *J* = 6.5 Hz), 1.95 (12H, s), 3.53 (2H, sp, *J* = 6.5 Hz), 7.02 (5H, br).

Synthesis of Cp*Mo[N(ⁱPr)C(Ph)N(ⁱPr)]Cl₂ (57**).** A solution of Cp*MoCl₄ (0.500 g, 1.34 mmol) in 100 mL Et₂O was cooled to -30 °C, at which point a solution of Li[N(ⁱPr)C(Ph)N(ⁱPr)] (0.722 g, 2.77 mmol) in 30 mL Et₂O, precooled to -30 °C, was added dropwise over a period of 5 min. The resulting solution was allowed to warm to room temperature and stirred overnight. The brown solution was then pumped down to dryness, extracted in toluene, filtered through Celite, and pumped down to dryness. The residue was recrystallized from toluene at -30 °C, and then washed with pentane (2 × 10 mL), furnishing brown crystals of **57** (0.527 g, yield = 78%). For **3**: Anal. Calcd. for C₂₃H₃₄Cl₂N₂Mo: C, 54.64; H, 6.78; N, 5.54; Found: C, 54.54; H, 6.74; N, 5.39. ¹H NMR (400 MHz, benzene-*d*₆): 2.5 (br), 6.4 (br), 9.1 (br), 11.8 (br), 13.6 (br), 20.5 (br).

Synthesis of {Cp*M[N(ⁱPr)C(Ph)N(ⁱPr)]}₂(μ-η¹:η¹-N₂) (56**).** In a dinitrogen filled glovebox, a 250 mL Schlenk flask charged with a solution of **57** (0.253 g, 0.50 mmol) in 20 mL THF was cooled to -30 °C, at which point 0.5% (w/w) of NaHg (6.932 g, 1.51 mmol) was added, and the solution was allowed to warm to room temperature. The reaction mixture was stirred for 2 h to yield an orange-brown colored solution, at

which time volatiles were removed *in vacuo* and the solid residue was extracted in pentane, filtered through Celite, and pumped down to dryness. The resulting solid was dissolved in a small amount of pentane and cooled to -30 °C to afford orange-brown crystals of **56** (0.098 g, yield = 44%). For **56**: Anal. Calcd. for C₄₆H₆₈N₆Mo₂: C, 61.58; H, 7.64; N, 9.37; Found: C, 61.74; H, 7.53; N, 9.39. ¹H NMR (400 MHz, benzene-*d*₆): 0.85 (12H, d, *J* = 6.3 Hz), 1.18 (12H, d, *J* = 6.3 Hz), 1.93 (30H, s), 3.45 (4H, sp, *J* = 6.3 Hz), 7.14 (8H, br), 7.98 (2H, br).

Synthesis of Cp*Mo[N(^{*i*}Pr)C(Ph)N(^{*i*}Pr)](CO)₂ (68**).** A solution of **56** (0.052 g, 0.06 mmol) in 5 mL toluene was prepared in a vial and transferred to a 50 mL storage tube equipped with a Teflon seal. The headspace was evacuated and charged with carbon monoxide (10 psi). The resulting dark red solution was then stirred overnight at room temperature. Volatiles were removed *in vacuo*, and the resulting red crystals were extracted in toluene, filtered through a pad of Celite, and pumped down to dryness. The resulting solid was then cooled to -30 °C in 3 mL pentane to afford red crystals of **68** (0.043 g, yield = 76%). For **68**: Anal. Calcd. for C₂₅H₃₄N₂O₂Mo: C, 61.20; H, 6.99; N, 5.71; Found: C, 61.30; H, 6.93; N, 5.68. ¹H NMR (400 MHz, benzene-*d*₆): 0.93 (6H, d, *J* = 6.4 Hz), 1.03 (6H, d, *J* = 6.4 Hz), 1.79 (15H, s), 3.41 (2H, sp, *J* = 6.4 Hz), 7.03 (5H, m). IR (KBr) ν_{C=O} = 1910 and 1810 cm⁻¹. ¹³C-Labeled-**68** was prepared by an identical procedure using ¹³C-labeled carbon monoxide. ¹³C{¹H} NMR (125.6 MHz, benzene-*d*₆): δ_{CO} = 269.2.

Synthesis of $\text{Cp}^*\text{Mo}[\text{N}(\text{iPr})\text{C}(\text{Ph})\text{N}(\text{iPr})](\text{CO})(\text{NCCH}_3)$ (70**).** A solution of **56** (0.033 g, 0.04 mmol) and acetonitrile (38 μL , 0.73 mmol) in 1 mL benzene- d_6 was transferred to a Pyrex J-Young NMR tube equipped with a Teflon seal. The headspace was evacuated and charged with carbon monoxide (2 psi). The mixture quickly turned red, and was allowed to react at room temperature for 1 h with periodic agitation, at which point the reaction was observed to be complete by ^1H NMR. Volatiles were then removed *in vacuo*. The resulting crude material was extracted in toluene, filtered through a pad of Celite, and pumped down to dryness. The residue was cooled to $-30\text{ }^\circ\text{C}$ in 5 mL pentane to afford orange crystals of **70** (0.027 g, yield = 72%). For **70**: Anal. Calcd. for $\text{C}_{26}\text{H}_{37}\text{N}_3\text{OMo}$: C, 62.00; H, 7.41; N, 8.35; Found: C, 62.20; H, 7.23; N, 8.39. ^1H NMR (400 MHz, benzene- d_6): 0.94 (3H, d, $J = 6.5\text{ Hz}$), 1.05 (3H, d, $J = 6.5\text{ Hz}$), 1.13 (3H, d, $J = 6.5\text{ Hz}$), 1.26 (3H, d, $J = 6.5\text{ Hz}$), 1.40 (3H, s), 1.82 (15H, s), 3.59 (1H, sp, $J = 6.5\text{ Hz}$), 3.67 (1H, sp, $J = 6.5\text{ Hz}$), 7.12 (3H, m), 7.28 (2H, m). IR (KBr) $\nu_{\text{C=O}} = 1767\text{ cm}^{-1}$. ^{13}C -Labeled-**70** was prepared by an identical procedure using ^{13}C -labeled carbon monoxide. $^{13}\text{C}\{^1\text{H}\}$ NMR (125.6 MHz, benzene- d_6): $\delta_{\text{CO}} = 281.7$.

Synthesis of $\text{Cp}^*\text{Mo}[\text{N}(\text{iPr})\text{C}(\text{Ph})\text{N}(\text{iPr})](\text{CO})(\eta^2\text{-S}_2)$ (71**) (from **56**).** A solution of **56** (0.040g, 0.04 mmol) and acetonitrile (40 μL , 0.77 mmol) in 0.6 mL benzene- d_6 was transferred to a Pyrex J Young NMR tube equipped with a Teflon seal. The headspace was evacuated and charged with carbon monoxide (3 psi). The tube was shaken periodically over the course of 2 h, at which point complete conversion to **70** was observed. Volatiles were removed *in vacuo*, and the resulting orange solid was

redissolved in 2 mL toluene and excess S₈ (0.023 g, 0.09 mmol) was added. The resulting mixture was agitated for 2 m, filtered through a pad of Celite, and pumped down to dryness. The resulting solid was dissolved in minimal toluene layered with pentane and cooled to -30 °C to afford orange crystals of **71** (0.028 g, yield = 56%). For **71**: Anal. Calcd. for C₂₄H₃₄N₂S₂OMo: C, 54.74; H, 6.51; N, 5.32; Found: C, 54.32; H, 6.64; N, 5.18. ¹H NMR (400 MHz, benzene-*d*₆): 0.73 (3H, d, *J* = 6.8 Hz), 0.75 (3H, d, *J* = 6.5 Hz), 1.21 (3H, d, *J* = 6.5 Hz), 1.28 (3H, d, *J* = 6.7 Hz), 1.65 (15H, s), 3.28 (1H, sp, *J* = 6.5 Hz), 3.55 (1H, sp, *J* = 6.8 Hz), 6.91 (1H, m), 7.03 (3H, m), 7.47 (1H, m). IR (KBr) ν_{C=O} = 1921 cm⁻¹.

Synthesis of Cp*Mo[N(ⁱPr)C(Ph)N(ⁱPr)](CO)(η²-S₂) (71**) (from **70**).** A solution of **70** (0.016 g, 0.03 mmol) and S₈ (0.008 g, 0.03 mmol) in 1 mL benzene-*d*₆ was transferred to a Pyrex J Young NMR tube equipped with a Teflon seal. ¹H NMR recorded immediately confirmed that the reaction was complete within minutes to produce **71**. Volatiles were removed *in vacuo* and the orange residue was extracted in toluene and filtered through a pad of Celite. The filtrate was pumped down to dryness to furnish orange crystals of **71** (0.012 g, yield = 74%). ¹³C-Labeled-**71** was prepared by an identical procedure using ¹³C-labeled-**70**. ¹³C{¹H} NMR (125.6 MHz, benzene-*d*₆): δ_{CO} = 246.9.

Synthesis of Cp*Mo[N(ⁱPr)C(Ph)N(ⁱPr)][κ-(*S,S*)S₂CO] (75**).** A solution of **71** (0.020 g, 0.04 mmol) in 1.2 mL benzene-*d*₆ was distributed between two Pyrex J Young tubes equipped with Teflon seals, and irradiated with UV light, with ¹H NMR

spectra recorded periodically, until 100% formation of **75** was observed (150 m). The solution was pumped down to dryness, extracted in toluene, filtered through Celite, and pumped down to dryness. The resulting residue was dissolved in minimal toluene layered with pentane and cooled to -30 °C to furnish orange crystals of **75** (0.013 g, yield = 66%). For **75**: Anal. Calcd. for C₂₄H₃₄N₂S₂OMo: C, 54.74; H, 6.51; N, 5.32; Found: C, 54.49; H, 6.48; N, 5.31. ¹H NMR (400 MHz, benzene-*d*₆): 0.85 (6H, d, *J* = 6.5 Hz), 1.22 (6H, d, *J* = 6.5 Hz), 1.75 (15H, s), 3.37 (2H, sp, 6.5 Hz), 6.76 (1H, m), 6.93 (2H, m), 7.03 (1H, d, *J* = 7.7 Hz), 7.11 (1H, d, *J* = 7.2 Hz). ¹³C{¹H} NMR (125.6 MHz, benzene-*d*₆): δ_{CO} = 205.5. IR (KBr) ν_{C=O} = 1673 cm⁻¹.

Synthesis of {Cp*Mo[N(^{*i*}Pr)C(Ph)N(^{*i*}Pr)]}₂(μ-S)₂ (77**).** In a 100 mL schlenk flask, a solution of **56** (0.042 g, 0.05 mmol) in 25 mL Et₂O was cooled to -30 °C. A slurry of S₈ (0.005 g, 0.02 mmol) in 15 mL Et₂O precooled to -30 °C was then added dropwise. The solution was allowed to warm to room temperature and stirred overnight. The resulting red solution was then pumped down to dryness. The resulting residue was extracted in pentane and filtered through a pad of Celite, and pumped down to dryness. The crude, red residue was dissolved in a minimal volume of pentane and cooled to -30 °C to afford red crystals of **77** (0.037 g, yield = 85 %). ¹H NMR (400 MHz, benzene-*d*₆): 0.96 (6H, d, *J* = 6.6 Hz), 1.07 (6H, d, *J* = 6.6 Hz), 1.82 (15H, s), 3.45 (2H, sp, *J* = 6.6 Hz), 7.02 (4H, m), 7.31 (1H, m).

NMR scale “On-Demand” Synthesis of 1,3-di(R) ureas. A representative procedure is given. To a solution of **68** (0.0038 g, 8 μmol) in 0.6 mL benzene-*d*₆ in a

J Young NMR tube equipped with a Teflon seal was added S₈ (0.0398 g, 155 μmol) and *n*-butyl amine (15 μL, 152 μmol). The headspace was evacuated and charged CO (10 psi). The solution was photolyzed for 18 h, at which point consumption of *n*-butyl amine was confirmed by ¹H NMR. Volatiles were removed *in vacuo* and the resulting crude material was filtered through silica gel with Et₂O to remove solids. The resulting crude material was pumped down to dryness, redissolved in chloroform-*d*, analyzed by ¹H and ¹³C{¹H} NMR, and compared against literature reports to confirm the proposed structure.

Preparative Scale “On-Demand” Synthesis of 1,3-di(R) ureas. A representative procedure is given. To a solution of **68** (0.0049 g, 10 μmol) in 2 mL toluene in a J Young NMR tube equipped with a Teflon seal was added S₈ (0.5231 g, 2.039 mmol) and *tert*-butyl amine (210 μL, 1.998 mmol). The headspace was evacuated and charged with CO (20 psi). The solution was photolyzed for 72 h, at which point volatiles were removed *in vacuo* and the resulting residue was extracted with dichloromethane, filtered through a plug of silica gel, and pumped down to dryness. The resulting solid was recrystallized from Et₂O to afford 1,3-di(*tert*-butyl) urea as off white crystals (0.052 g, yield = 29.6%). ¹H NMR (500 MHz, chloroform-*d*): 1.35 (18H, s). ¹³C{¹H} NMR (125.6 MHz, chloroform-*d*): 29.7, 50.4, 157.0. IR (KBr): 3344, 2960, 1636, 1560 cm⁻¹. ESI-MS: *m/z* 172.99 (M+H).

Synthesis of Cp*Mo[N(^{*i*}Pr)C(Ph)N(^{*i*}Pr)](CNCH₃)₂ (80**).** Methyl isocyanide (0.01 mL, 0.19 mmol) was added *via* microsyringe to a solution of **56** (0.038 g, 0.04 mmol)

in 3 mL of toluene at room temperature. The resulting red solution was stirred for 1 h, at which point volatiles were removed *in vacuo*. The resulting red solid was extracted in pentane and filtered through a pad of Celite, the volume was reduced *in vacuo*, and the resulting solution was cooled to -30 °C overnight furnishing red crystals of **80** (0.037 g, yield = 85%). For **80**: Anal. Calcd. for C₂₇H₄₀N₄Mo C, 62.76; N, 7.81; H, 10.85; Found C, 63.09; N, 7.57; H, 10.79. ¹H NMR (400 MHz, benzene-*d*₆): 1.07 (6H, d, *J* = 6.4 Hz), 1.15 (6H, d, *J* = 6.4 Hz), 1.95 (15H, s), 3.41 (6H, s), 3.55 (2H, sp, *J* = 6.4 Hz), 7.05 (2H, m), 7.16 (2H, m), 7.23 (1H, d, *J* = 7.4 Hz). IR (KBr) ν_{CN} = 2086, 1767 cm⁻¹.

Preparative Scale “On-Demand” Synthesis of 1-arylothiosemicarbazides. A representative procedure is given. S₈ (0.0666 g, 0.26 mmol), 2,6-dimethylphenyl isonitrile (0.033 g, 0.25 mmol), benzhydrazide (0.033 g, 0.25 mmol), and compound **80** (0.006 g, 0.01 mmol) were combined in 10 mL THF and heated to reflux for 18 h. Volatiles were removed *in vacuo*, and the resulting crude solid was extracted in ethyl acetate, washed with brine, filtered through a pad of silica gel and pumped down to dryness to furnish 1-benzoyl-4-(2,6-dimethylphenyl)thiosemicarbazide as an off white crystalline solid (0.049 g, yield = 67%). ¹H NMR (400 MHz, 25 °C. DMSO-*d*₆): 2.17 (6H, s), 7.05 (3H, m), 7.49 (2H, t, *J* = 7.4 Hz), 7.57 (1H, t, *J* = 7.4 Hz), 7.97 (2H, d, *J* = 7.4 Hz), 9.42 (1H, br), 9.58 (1H, br), 10.56 (1H, br). ¹³C{¹H} NMR (125 MHz, 25 °C. DMSO-*d*₆): 17.9, 126.6, 127.3, 127.9, 128.0, 131.6, 132.7, 136.5, 137.0, 166.1, 181.5. ESI-MS *m/z*: 300.11 (M+H).

Synthesis of $\text{Cp}^*\text{Mo}[\text{N}(\text{iPr})\text{C}(\text{Ph})\text{N}(\text{iPr})](\text{CN}^t\text{Bu})[\kappa\text{-(S,C)SCN}^t\text{Bu}]$ (84**).** To a solution of **81** (0.06 mmol generated *in situ*) in 2 mL toluene was added S_8 (0.014 g, 0.06 mmol) at room temperature. The resulting red solution was stirred for 10 m, at which point solids were removed by filtration through Celite, and volatiles were removed *in vacuo* to leave a red oil, which was analyzed by ^1H NMR (confirming it to be analogous to the catalyst resting state) before being cooled to $-30\text{ }^\circ\text{C}$ in toluene layered with pentane to yield single crystals of **85** suitable for X-ray analysis.

Synthesis of $\{\text{Cp}^*\text{Mo}[\text{N}(\text{iPr})\text{C}(\text{Ph})\text{N}(\text{iPr})]\}_2(\mu\text{-S})(\mu\text{-CS})$ (91**).** Carbon disulfide (0.08 mL, 0.13 mmol) was added to a solution of **56** (0.057 g, 0.06 mmol) in 10 mL toluene at room temperature. The mixture was stirred for 30 m to give a forest green solution, at which point volatiles were removed *in vacuo*. The residue extracted in pentane, pumped down to dryness, and then dissolved in minimal pentane and cooled to $-30\text{ }^\circ\text{C}$ to yield forest green crystals of **91** (0.046 g, yield = 76%). For **91**: Anal. Calcd for $\text{Mo}_2\text{C}_{47}\text{H}_{68}\text{N}_4\text{S}_2$ C, 59.72; H, 7.26; N, 5.93; Found C, 60.08; H, 7.45; N 5.89. ^1H NMR (400 MHz, benzene- d_6): 1.10 (6H, d, $J = 6.6$ Hz), 1.16 (3H, d, $J = 6.9$ Hz), 1.19 (6H, d, $J = 6.6$ Hz), 1.23 (3H, d, $J = 6.6$ Hz), 1.31 (3H, d, $J = 6.2$ Hz), 1.38 (3H, d, $J = 6.6$ Hz), 1.93 (15H, s), 2.08 (15H, s), 3.35 (1H, sp, $J = 6.6$ Hz), 3.61 (1H, sp, $J = 6.2$ Hz), 3.70 (1H, sp, $J = 6.2$ Hz), 4.28 (1H, sp, $J = 6.6$ Hz), 7.09 (7H, m), 7.25 (1H, d, $J = 6.7$ Hz), 7.29 (1H, d, $J = 7.3$ Hz), 7.48 (1H, d, $J = 6.7$ Hz). $^{13}\text{C}\{^1\text{H}\}$ NMR (125.6 MHz, benzene- d_6): $\delta_{\text{C=S}} = 387$.

Synthesis of $\text{Cp}^*\text{Mo}[\text{N}(\text{iPr})\text{C}(\text{Ph})\text{N}(\text{iPr})][\kappa\text{-(S,S)}\text{S}_2\text{CN}^t\text{Bu}]$ (93**).** To a solution of **56** (0.042 g, 0.05 mmol) in 10 mL toluene in a 100 mL Schlenk tube was added *tert*-butyl isothiocyanate (0.06 mL, 0.47 mmol). The tube was sealed and the solution was stirred at 65 °C for 3 d, at which point volatiles were removed *in vacuo*. The resulting orange/red oil was extracted in pentane, filtered through Celite, concentrated and cooled to -30 °C to yield orange/red crystals of **93** (0.028 g, yield = 52%). For **93**: Anal. Calcd. for $\text{C}_{28}\text{H}_{43}\text{N}_3\text{S}_2\text{Mo}$ C, 57.81; N, 7.23; H, 7.46; Found C, 58.17; N, 7.29; H, 7.39. ^1H NMR (400 MHz, benzene- d_6): 0.93 (3H, d, $J = 6.4$ Hz), 0.95 (3H, d, $J = 6.4$ Hz), 1.27 (3H, d, $J = 6.4$ Hz), 1.27 (3H, d, $J = 6.4$ Hz), 1.83 (15H, s), 1.84 (9H, s), 3.37 (1H, sp, $J = 6.4$ Hz), 3.38 (1H, sp, $J = 6.4$ Hz), 6.94 (4H, m), 7.11 (1H, m).

Synthesis of $\text{Cp}^*\text{Mo}[\text{N}(\text{iPr})\text{C}(\text{Ph})\text{N}(\text{iPr})][\kappa\text{-(S,S)}\text{S}_2\text{CN}(\text{CH}_3)^t\text{Bu}](\text{SO}_3\text{CF}_3)$ (94**).** Methyl triflate (0.01 mL, 0.08 mmol) was added to a solution of **93** (0.046 g, 0.08 mmol) in 5 mL pentane at room temperature and stirred for 15 m. The resulting orange powder was allowed to settle, at which point the supernatant was decanted. The resulting orange crystals were washed with pentane (2 X 10 mL), dissolved in benzene, and left at room temperature with slow diffusion of pentane into the solution to yield orange crystals of **94** (0.025 g, yield = 42%). For **94**: Anal. Calcd. for $\text{C}_{30}\text{H}_{46}\text{N}_3\text{S}_3\text{O}_3\text{F}_3\text{Mo}$ C, 48.33; N, 5.63; H, 6.22; Found C, 48.15; N, 5.59; H, 6.21. ^1H NMR (400 MHz, benzene- d_6): 0.80 (3H, d, $J = 6.7$ Hz), 0.83 (3H, d, $J = 6.7$ Hz), 0.95 (3H, d, $J = 6.7$ Hz), 1.02 (3H, d, $J = 6.7$ Hz), 1.61 (9H, s), 1.71 (15H, s), 3.33 (1H, sp, $J = 6.7$ Hz), 3.41 (1H, sp, 6.7 Hz), 3.65 (3H, s), 7.11 (2H, m), 7.22 (1H, d, J

= 7.7 Hz), 7.37 (1H, d, J = 8.1 Hz), 7.85 (1H, m). ^{19}F NMR (376 MHz, benzene- d_6): -78.5.

Synthesis of $\text{Cp}^*[\text{N}(\text{iPr})\text{C}(\text{CH}_3)\text{N}(\text{iPr})]\text{W}[\eta^2\text{-C}(\text{O})\text{CH}_3](\text{SCH}_3)$ (115**).** A solution of **45** (0.075 g, 0.15 mmol) and dimethyl sulfide (65 μL , 0.89 mmol) in 4 mL toluene was prepared and transferred to a Pyrex J-Young NMR tube equipped with a Teflon seal. The solution was photolyzed for 24 h, at which point volatiles were removed *in vacuo*, and the resulting orange/red oil was extracted in pentane, filtered through a pad of Celite, and pumped down to dryness. The crude material was dissolved in minimal Et_2O and cooled to $-30\text{ }^\circ\text{C}$ to furnish **115** as an orange crystalline material (0.047 g, yield = 59%). For **115**: Anal. Calcd. for $\text{C}_{21}\text{H}_{38}\text{N}_2\text{OSMo}$ C, 45.83; H, 6.96; N, 5.09; Found C, 45.82; H, 6.82; N, 5.06. ^1H NMR (400 MHz, benzene- d_6): 0.88 (3H, d, J = 7.2 Hz), 1.15 (3H, d, J = 7.2 Hz), 1.41 (3H, d, J = 6.5 Hz), 1.63 (3H, d, J = 6.5 Hz), 1.74 (3H, s), 1.91 (15H, s), 2.41 (3H, s), 2.43 (3H, s, J_{WH} = 2.8 Hz), 3.03 (1H, sp, J = 6.9 Hz), 4.13 (1H, sp, J = 6.9 Hz). ^{13}C -Labeled-**115** was prepared by an identical procedure using ^{13}C -labeled-**45**. $^{13}\text{C}\{^1\text{H}\}$ NMR (125.6 MHz, benzene- d_6): $\delta_{\text{C=O}}$ = 275.7, $^1J_{\text{WC}}$ = 72 Hz.

Synthesis of $\text{Cp}^*[\text{N}(\text{iPr})\text{C}(\text{CH}_3)\text{N}(\text{iPr})]\text{Mo}(\text{CO})(\text{C}_2\text{H}_4)$ (118**).** A solution of **122** (0.060 g, 0.14 mmol) in benzene- d_6 was prepared in a Pyrex J-Young NMR tube equipped with a Teflon seal. The headspace was evacuated and charged with ethene (15 psi), shaken vigorously, and allowed to react for 16 h, at which point complete consumption of **122** was observed by ^1H NMR. Volatiles were removed *in vacuo*, the

crude material was extracted in pentane and filtered through a pad of Celite, and pumped down to dryness. The resulting red crystals were dissolved in minimal pentane and cooled to -30 °C to furnish **118** as red crystals (0.043 g, yield = 75%). For **118**: Anal. Calcd. for C₂₁H₃₆N₂OMo C, 58.86; H, 8.43; N, 6.57; Found C, 58.87; H, 8.47; N, 6.54. ¹H NMR (400 MHz, benzene-*d*₆): 0.94 (3H, d, *J* = 6.9 Hz), 1.00 (3H, d, *J* = 6.9 Hz), 1.02 (1H, m), 1.10 (3H, d, *J* = 6.5 Hz), 1.26 (3H, d, *J* = 6.4 Hz), 1.31 (1H, m), 1.46 (3H, s), 1.64 (15H, s), 2.15 (1H, m), 3.07 (1H, sp, *J* = 6.9 Hz), 3.32 (1H, m), 3.61 (1H, sp, *J* = 6.4 Hz). IR (KBr) ν_{C=O} = 1867 cm⁻¹.

Synthesis of Cp*[N(ⁱPr)C(CH₃)N(ⁱPr)]Mo(CO)(C₇H₁₀) (119**).** A solution of **122** (0.035 g, 0.08 mmol) and norbornene (0.021 g, 0.22 mmol) in benzene-*d*₆ was prepared and transferred to a Pyrex J-Young NMR tube equipped with a Teflon seal. After 2 h complete consumption of **122** was observed by ¹H NMR. Volatiles were removed *in vacuo* and the crude material was extracted in pentane, filtered through a pad of Celite, and the filtrate was concentrated and cooled to -30 °C to furnish **119** as red/orange crystals (0.026 g, yield = 66%). For **119**: Anal. Calcd. for C₂₆H₄₂N₂OMo C, 63.14; H, 8.56; N, 5.66; Found C, 63.04; H, 8.55; N, 5.53. ¹H NMR (400 MHz, benzene-*d*₆): 0.89 (3H, d, *J* = 7.0 Hz), 0.99 (1H, d, *J* = 9.5 Hz), 1.04 (3H, d, *J* = 7.0 Hz), 1.14 (1H, m), 1.21 (3H, d, *J* = 6.3 Hz), 1.34 (3H, d, *J* = 6.3 Hz), 1.42 (2H, m), 1.50 (3H, s), 1.66 (15H, s), 1.87 (1H, d, *J* = 5.6 Hz), 2.04 (2H, m), 2.28 (1H, br), 2.35 (1H, d, *J* = 5.6 Hz), 3.14 (1H, sp, *J* = 7.0 Hz), 3.31 (1H, br), 3.70 (1H, sp, *J* = 6.3 Hz). IR (KBr) ν_{C=O} = 1859 cm⁻¹.

Synthesis of $\text{Cp}^*[\text{N}(\text{iPr})\text{C}(\text{CH}_3)\text{N}(\text{iPr})]\text{W}(\text{CO})(\text{C}_2\text{H}_4)$ (120**).** A solution of **45** (0.060 g, 0.12 mmol) in 1 mL benzene- d_6 was prepared in a Pyrex J-Young NMR tube equipped with a Teflon seal. The headspace was evacuated and charged with ethene (15 psi), at which point the tube was shaken vigorously and photolyzed for 16 h. The headspace was evacuated and charged with ethene again, and the solution was photolyzed for 9 h longer, at which point complete consumption of **45** was observed by ^1H NMR. Volatiles were removed *in vacuo*, the resulting crude material was extracted in pentane and filtered through a pad of Celite, and the filtrate was concentrated and cooled to $-30\text{ }^\circ\text{C}$ to furnish **120** as orange crystals (0.041 g, yield = 67%). For **120**: Anal. Calcd. for $\text{C}_{21}\text{H}_{36}\text{N}_2\text{OW}$ C, 48.85; H, 7.03; N, 5.42; Found C, 48.91; H, 6.67; N, 5.44. ^1H NMR (400 MHz, benzene- d_6): 0.95 (3H, d, $J = 6.7$ Hz), 0.98 (3H, d, $J = 6.9$ Hz), 0.99 (1H, m), 1.07 (3H, d, $J = 6.5$ Hz), 1.23 (3H, d, $J = 6.3$ Hz), 1.27 (1H, m), 1.41 (3H, s), 1.74 (15H, s), 1.84 (1H, m), 3.00 (1H, sp, $J = 6.8$ Hz), 3.01 (1H, m), 3.48 (1H, sp, $J = 6.3$ Hz). IR (KBr) $\nu_{\text{C=O}} = 1858\text{ cm}^{-1}$.

Synthesis of $\text{Cp}^*[\text{N}(\text{iPr})\text{C}(\text{CH}_3)\text{N}(\text{iPr})]\text{W}(\text{CO})(\text{C}_7\text{H}_{10})$ (121**).** A solution of **45** (0.052 g, 0.10 mmol) and norbornene (0.103 g, 1.10 mmol) in 1 mL benzene- d_6 was prepared and transferred to a Pyrex J-Young NMR tube equipped with a Teflon seal and photolyzed for 20 h, at which point complete consumption of **45** was observed by ^1H NMR. Volatiles were removed *in vacuo* and the crude material was extracted in pentane, filtered through a pad of Celite, and pumped down to dryness to furnish **121** as orange crystals (0.057 g, yield = 97%). For **121**: Anal. Calcd. for $\text{C}_{26}\text{H}_{42}\text{N}_2\text{OW}$ C, 53.61; H, 7.27; N, 4.81; Found C, 53.63; H, 7.00; N, 4.73. ^1H NMR (400 MHz,

benzene-*d*₆): 0.92 (3H, d, *J* = 6.8 Hz), 1.00 (3H, d, *J* = 6.8 Hz), 1.11 (1H, d, *J* = 9.8 Hz), 1.17 (3H, d, *J* = 6.6 Hz), 1.28 (3H, d, *J* = 6.6 Hz), 1.36 (1H, m), 1.46 (3H, s), 1.51 (2H, m), 1.75 (15H, s), 1.91 (1H, d, *J* = 6.5 Hz), 2.21 (2H, m), 2.28 (2H, m), 3.06 (1H, sp, *J* = 6.8 Hz), 3.24 (1H, br), 3.60 (1H, sp, *J* = 6.6 Hz). IR (KBr) $\nu_{\text{C=O}}$ = 1844 cm⁻¹.

Synthesis of Cp*[N(^{*i*}Pr)C(CH₃)N(^{*i*}Pr)]Mo(CO)(C₅H₈) (123). A solution of **122** (0.035 g, 0.08 mmol) and cyclopentene (35 μ L, 0.38 mmol) in 0.6 mL benzene-*d*₆ was prepared in a Pyrex J-Young NMR tube equipped with a Teflon seal and allowed to react for 2 h, at which point complete consumption of **122** was observed by ¹H NMR. Volatiles were removed *in vacuo* and the crude material was extracted in pentane and filtered through a pad of Celite. The filtrate was concentrated and cooled to -30 °C to furnish **123** as red crystals (0.020 g, yield = 54%). For **123**: Anal. Calcd. for C₂₄H₄₀N₂OMo C, 61.53; H, 8.60; N, 5.98; Found C, 61.21; H, 8.31; N, 6.09. ¹H NMR (400 MHz, benzene-*d*₆): 0.96 (3H, d, *J* = 6.8 Hz), 1.05 (3H, d, *J* = 6.8 Hz), 1.12 (3H, d, *J* = 6.5 Hz), 1.24 (3H, d, *J* = 6.4 Hz), 1.47 (3H, s), 1.65 (15H, s), 1.82 (2H, m), 1.98 (1H, m), 2.56 (1H, t, *J* = 5.4 Hz), 2.83 (2H, m), 3.18 (3H, m), 3.65 (1H, sp, *J* = 6.5 Hz). IR (KBr) $\nu_{\text{C=O}}$ = 1861 cm⁻¹.

Synthesis of Cp*[N(^{*i*}Pr)C(CH₃)N(^{*i*}Pr)]W(CCH₃)(H) (124). A solution of ethyllithium (0.45 mL, 1.47 M) was added dropwise to a solution of **108** (0.175 g, 0.33 mmol) in 75 mL Et₂O at -30°C. The resulting solution was allowed to warm to room temperature and stir overnight. The solution was then pumped down to

dryness, extracted in pentane, and filtered through Celite. The volume was reduced *in vacuo* and the solution was cooled to -30 °C to furnish dark yellow/brown crystals of **124** (0.086 g, yield = 54%). ¹H NMR (400 MHz, benzene-*d*₆): 1.20 (12H, br), 1.44 (3H, s), 2.10 (15H, s), 3.32 (3H, d, ³*J*_{HH} = 1.3 Hz, ²*J*_{WH} = 8.5 Hz), 3.46 (2H, br), 6.77 (1H, s, ¹*J*_{WH} = 93.6 Hz).

Synthesis of Cp*[N(ⁱPr)C(CH₃)N(ⁱPr)]W(H)(η³-C₄H₇) (127**).** A solution of **45** (0.047 g, 0.09 mmol) in 0.6 mL benzene-*d*₆ was prepared and transferred to a Pyrex J-Young NMR tube equipped with a Teflon seal. The headspace was evacuated and charged with *iso*-butene (15 psi) and the solution was photolyzed for 17 h. Again the headspace was evacuated and charged with *iso*-butene, and the solution was photolyzed for 20 h. This process was repeated once more, at which point nearly complete consumption of **45** was observed by ¹H NMR. Volatiles were removed *in vacuo* and the crude material was extracted in pentane, filtered through a pad of Celite, concentrated and cooled to -30 °C to furnish **127** as yellow crystals (0.032 g, yield = 68%). For **127**: Anal. Calcd. for C₂₂H₄₀N₂W C, 51.17; H, 7.81; N, 5.42; Found C, 50.64; H, 7.05; N, 5.03. ¹H NMR (400 MHz, benzene-*d*₆): -0.87 (1H, t, ³*J*_{HH} = 3.5 Hz, ¹*J*_{WH} = 54.7 Hz), 0.57 (1H, dd, *J* = 5.08 Hz, *J* = 1.8 Hz), 1.09 (3H, d, *J* = 6.9 Hz), 1.14 (3H, d, *J* = 6.9 Hz), 1.26 (3H, d, *J* = 6.7 Hz), 1.33 (3H, d, *J* = 6.9 Hz), 1.36 (1H, br), 1.47 (1H, d, *J* = 3.2 Hz), 1.59 (3H, s), 1.73 (15H, s), 2.36 (1H, dd, *J* = 5.2 Hz, *J* = 5.0 Hz), 3.05 (3H, s), 3.50 (1H, sp, *J* = 7.0 Hz), 3.68 (1H, sp, *J* = 6.8 Hz). ¹³C{¹H} NMR (125 MHz, benzene-*d*₆): 11.2, 21.1, 24.2, 25.2, 26.0, 26.7, 30.5, 45.7, 47.6, 52.8, 53.3, 79.0, 100.4, 165.3.

Synthesis of $\text{Cp}^*[\text{N}(\text{iPr})\text{C}(\text{CH}_3)\text{N}(\text{iPr})]\text{Mo}(\text{C}_2\text{H}_4)(\text{H})$ (140**).** A solution of ethyllithium (2.4 mL, 0.34 M) in benzene/cyclohexane (90/10) was added dropwise to a solution of **42** (0.184 g, 0.41 mmol) in 80 mL of Et_2O at $-30\text{ }^\circ\text{C}$. The resulting solution was allowed to warm to room temperature and stir overnight. The solution was then pumped down to dryness, extracted in pentane, and filtered through Celite. The volume was reduced *in vacuo*, and the solution was cooled to $-30\text{ }^\circ\text{C}$ to afford **140** as orange/brown crystals (0.055 g, yield = 33%). For **140**: Anal. Calcd. for $\text{C}_{20}\text{H}_{37}\text{MoN}_2$ C, 59.82; H, 9.29; N, 6.98; Found C, 59.59; H, 9.26; N, 6.69.

Synthesis of $\text{Cp}^*[\text{N}(\text{iPr})\text{C}(\text{Ph})\text{N}(\text{iPr})]\text{Mo}(\text{C}_2\text{H}_4)(\text{H})$ (141**).** A solution of ethyllithium (0.8 mL, 0.32 M) in benzene/cyclohexane (90/10) was added dropwise to a solution of **57** (0.062 g, 0.12 mmol) in 15 mL Et_2O at $-30\text{ }^\circ\text{C}$. The resulting solution was allowed to warm to room temperature and stir overnight. The solution was then pumped down to dryness, extracted in pentane, filtered through Celite, and pumped down to dryness. The resulting brown/red oil was dissolved in minimal pentane and cooled to $-30\text{ }^\circ\text{C}$ to afford **141** as orange/red crystals (0.047 g, yield = 83%). For **141**: Anal Calcd. for $\text{C}_{25}\text{H}_{39}\text{MoN}_2$ C, 64.76; H, 8.48; N, 6.05; Found C, 64.51; H, 8.41; N, 5.93.

Synthesis of **144 – **147**.** A representative procedure is given. Naphthalene-2-carbonitrile (0.018 g, 0.12 mmol) was added to a solution of **124** (0.041 g, 0.08 mmol) in 2 mL benzene- d_6 in a Pyrex NMR tube equipped with a Teflon seal, and

heated to 60 °C for 16 h, at which point complete consumption of **124** was observed by ¹H NMR. The solution was pumped down to dryness, extracted in pentane, filtered through Celite, and pumped down to dryness again to furnish **147** as an oil (0.049 g, yield = 96%). Recrystallization did not afford pure, crystalline material suitable for further characterization. ¹H NMR (400 MHz, benzene-*d*₆): 1.02 (3H, d, *J* = 6.3 Hz), 1.06 (3H, d, *J* = 6.3 Hz), 1.26 (3H, d, *J* = 6.3 Hz), 1.43 (3H, d, *J* = 6.3 Hz), 1.50 (3H, s), 1.53 (3H, s), 1.62 (3H, s), 2.59 (1H, dd, *J* = 7.3, 6.4 Hz), 2.91 (3H, s), 2.97 (3H, s), 3.11 (1H, dd, *J* = 8.3, 5.5 Hz), 3.39 (1H, sp, *J* = 6.3 Hz), 3.45 (1H, sp, *J* = 6.3 Hz), 5.42 (1H, t, *J* = 7.5 Hz), 7.26 (3H, comp), 7.66 (1H, d, *J* = 8.1 Hz), 7.70 (1H, s), 7.80 (1H, d, *J* = 8.1 Hz), 8.01 (1H, s).

References

- (1) Schuster, R. E.; Scott, J. E.; Casanova, J. *Org. Synth.* **1966**, *46*, 75.
- (2) Sal, P. G.; Jimenez, I.; Pedraz, T.; Royo, P.; Selles, A.; Vazquez de Miguel, V. *Inorg. Chim. Acta* **1998**, *273*, 270-278.
- (3) Yonke, B. L.; Reeds, J. P.; Zavalij, P. Y.; Sita, L. R. *Angew. Chem. Int. Ed.* **2011**, *50*, 12342-12346.
- (4) Fontaine, P. P.; Yonke, B. L.; Zavalij, P. Y.; Sita, L. R. *J Am Chem Soc* **2010**, *132*, 12273-12285.
- (5) Yonke, B. L.; Reeds, J. P.; Fontaine, P. P.; Zavalij, P. Y.; Sita, L. R. *Organometallics* **2014**, *33*, 3239-3242.
- (6) Keane, A. J. *Ph. D. Dissertation, University of Maryland*, **2015**.